C51.17/12:989/9

Tech Notes

September 1989

PB89-925909

PENNSYLVANIA STATE
UNIVERSITY

SEP 18 1989

DOCUMENTS COLLECTION
U.S. Depository Copy

NTIS

U.S. DEPARTMENT OF COMMERCE
National Technical Information Service
Center for the Utilization of Federal Technology

The Complete Guide to U.S. and State Government Business Help

For New and Growing Businesses

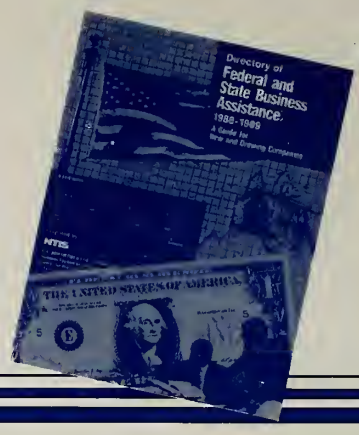

SECOND BIG EDITION!

Directory of Federal & State Business Assistance– A Guide for New and Growing Companies.

Your guide to sources of financing, technical information, planning and management know-how, procurement, and marketing assistance. Order this book today!

Describes 180 Federal and more than 500 State Programs

You get the information you need to directly contact hundreds of Federal and State sources of business assistance:

- Full summary of services offered
- Telephone number
- Mailing address
- Eligibility requirements (if any)

Take advantage of these programs designed to help U.S. businesses compete effectively in domestic and international markets.

Some of the programs listed:

Dept. of Commerce Export Licensing

Bureau of Labor Statistics Prices and Living Conditions Office

Federal Grant Data Center

Small Business Answer Desk

Florida Product Innovation Center

Iowa Small Business Loan Program

Michigan Biotechnology Institute

New York Direct Loan Program

You'll learn:

- How to get funding for your company's R&D
- Which states provide venture money
- How to take advantage of free export assistance
- What Federal and State contacts offer free management and procurement consulting
- Where to get mail lists of potential overseas business buyers
- Where to find evaluation of energy-related inventions or engineering help
- How to get help in selecting a site for your manufacturing plant
- Where to find customized economic impact statistics

and much more.

Federal Offices Want to Work with You

The 180 Federal entries selected for inclusion are arranged by agency. Discover sources of help in exporting, patent licensing, procurement, locating wage information, obtaining loan guarantees, finding marketing information, plus much more. A handy index lets you quickly locate just the Federal resources you need.

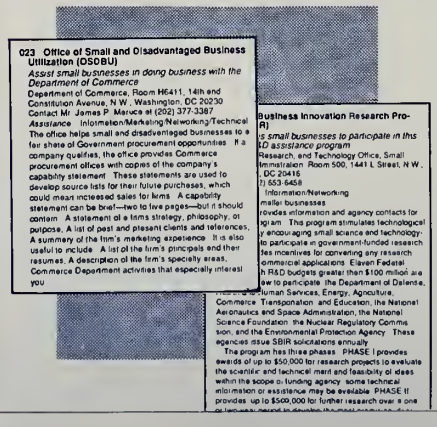
023 Office of Small and Disadvantaged Business Utilization (OSDBU)
Assist small businesses in doing business with the Department of Commerce
Department of Commerce, Room H6411, 14th and Constitution Avenue, N.W., Washington, DC 20230
Contact Mr. James P. Manico at (202) 377-3387
Assistance Information/Marketing/Networking/Technical
The office helps small and disadvantaged businesses to a fair share of Government procurement opportunities. If a company qualifies, the office provides Commerce procurement offices with copies of the company's capability statement. These statements are used to develop source lists for their future purchases, which could mean increased sales for firms. A capability statement can be brief—two to five pages—but it should contain: A statement of a firm's strategy, philosophy, or purpose. A list of past and present clients and references. A summary of the firm's marketing experience. It is also useful to include: A list of the firm's principals and their resumes. A description of the firm's specialty areas. Commerce Department activities that especially interest you

Business Innovation Research Pro-
(S)
s small businesses to participate in this
D assistance program
Research, and Technology Office, Small
Innistration Room 500, 1441 L Street, N.W.,
, DC 20416
) 653-6458
Information/Networking
maller businesses
rovides information and agency contacts for
gram. The program stimulates technological
encouraging small science and technology-
o participate in government-funded research
es incentives for converting any research
ommercial applications. Eleven Federal
R&D budgets greater than $100 million are
er to participate: the Department of Defense,
Human Services, Energy, Agriculture,
Commerce, Transportation, and Education, the National
Aeronautics and Space Administration, the National
Science Foundation, the Nuclear Regulatory Commis-
sion, and the Environmental Protection Agency. These
agencies issue SBIR solicitations annually.
The program has three phases. PHASE I provides
awards of up to $50,000 for research projects to evaluate
the scientific and technical merit and feasibility of ideas
within the scope of a funding agency. Some technical
information or assistance may be available. PHASE II
provides up to $500,000 for further research over a one

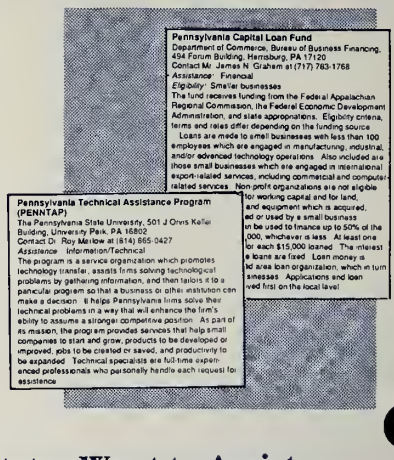
Pennsylvania Capital Loan Fund
Department of Commerce, Bureau of Business Financing, 494 Forum Building, Harrisburg, PA 17120
Contact Mr. James N. Graham at (717) 783-1768
Assistance Financial
Eligibility Smaller businesses
The fund receives funding from the Federal Appalachian Regional Commission, the Federal Economic Development Administration, and state appropriations. Eligibility criteria, terms and rates differ depending on the funding source.
Loans are made to small businesses with less than 100 employees which are engaged in manufacturing, industrial, and/or advanced technology operations. Also included are those small businesses which are engaged in international export-related services, including commercial and computer-related services. Non-profit organizations are not eligible.
for working capital and for land,
and equipment which is acquired,
ed or used by a small business
n be used to finance up to 50% of the
,000, whichever is less. At least one
lar each $15,000 loaned. The interest
e loans are fixed. Loan money is
ed area loan organizations, which in turn
sinesses. Applications and loan
ved first on the local level.

Pennsylvania Technical Assistance Program (PENNTAP)
The Pennsylvania State University, 501 J. Orvis Keller Building, University Park, PA 16802
Contact Dr. Roy Mellow at (814) 865-0427
Assistance Information/Technical
The program is a service organization which promotes technology transfer, assists firms solving technological problems by gathering information, and then tailors it to a particular program so that a business or other institution can make a decision. It helps Pennsylvania firms solve their technical problems in a way that will enhance the firm's ability to assume a stronger competitive position. As part of its mission, the program provides services that help small companies to start and grow, products to be developed or improved, jobs to be created or saved, and productivity to be expanded. Technical specialists are full-time experienced professionals who personally handle each request for assistance.

States Want to Assist Your Business

States know that strong businesses mean a strong economy. Services described include venture financing, planning help, product marketing, employee training, exporting assistance, site location, technology development, and technical and management information.

Every effort has been taken to make this Directory a valuable working resource to assist the growth of your company.

TO ORDER:

ASK FOR the ***Directory of Federal & State Business Assistance – A Guide for New and Growing Companies.*** (180 pp. ISBN 0-934213-10-0). Reference order number PB88-101977/ABH. The price is $29 plus $3 for handling.

CALL (703) 487-4650 and use your American Express, VISA, MasterCard, or NTIS deposit account.

Or send a check payable to the

National Technical Information Service
U.S. DEPARTMENT OF COMMERCE
Springfield, VA 22161.

Tech Notes

Highlighting Selected U.S. Government Technology & Resources

September 1989

Contents

Agriculture & Food 708

Computers 712

Electrotechnology 718

Energy 736

Engineering 740

Environmental Science & Technology 759

Manufacturing, Machinery & Tools 762

Materials 770

Medicine & Biology 790

Natural Resources Technology & Engineering 800

Physical Sciences 802

Transportation & Components 815

Published monthly by the National Technical Information Service (NTIS), Tech Notes bring together individual one- to two-page fact sheets prepared by Federal agencies, their laboratories, or contractors. These fact sheets highlight current Federal technology determined to have commercial or practical application. Topics cover new processes, materials, techniques, software, instrumentation, and resources.

Some of the current sources are the Department of the Navy, Department of the Army, NASA, Department of Energy, Environmental Protection Agency, Department of the Interior, and the Department of Agriculture.

Special assistance is provided by the Federal Laboratory Consortium.

Change of address or questions concerning subscriptions should be sent to:
Subscriptions Department
National Technical Information Service
Springfield, VA 22161
(703) 487-4630

Suggestions, comments, or questions concerning Tech Notes should be directed to:
Tech Notes Editor
Room 300B F
National Technical Information Service
Springfield, VA 22161
(703) 487-4805

How to Use Tech Notes

Every Tech Notes fact sheet lists a source for additional information. The source of this information may be a special support package from the originating agency, a personal contact, a licensing opportunity, or a backup report available from NTIS.

Each fact sheet also is perforated to allow for easy removal for those subscribers who may wish to keep a special fact sheet file or route to others in their organization

Sources of Further Backup Information

Below are two representative examples of how each Tech Note fact sheet provides you with a source of further information. In most cases, this information is provided directly by the agency or its laboratory.

However, there are cases where NTIS is the source for backup documentation. In these cases, use the order form at the end.

Examples:

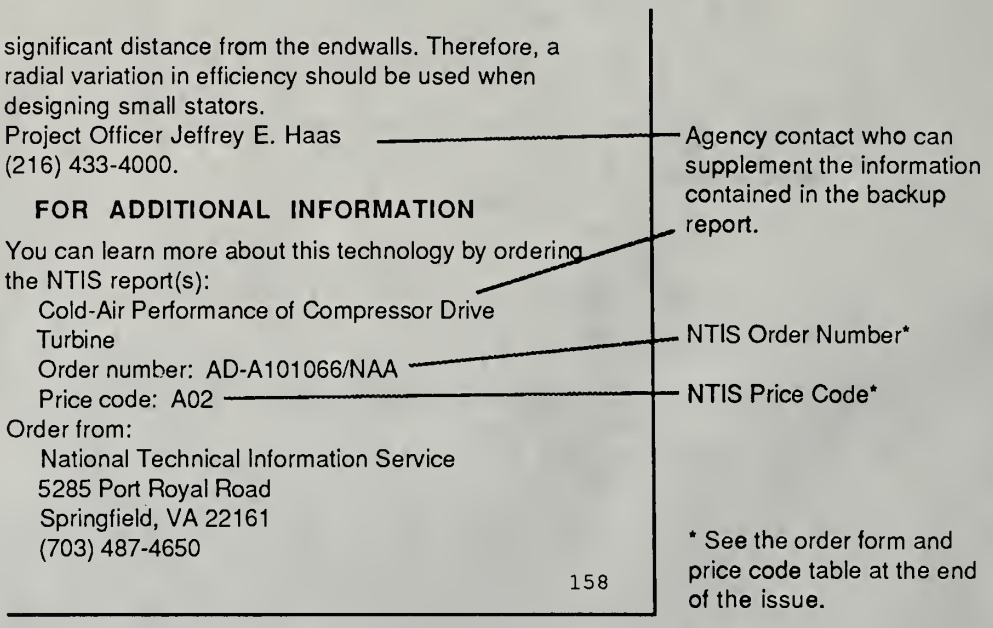
significant distance from the endwalls. Therefore, a radial variation in efficiency should be used when designing small stators.
Project Officer Jeffrey E. Haas
(216) 433-4000.
FOR ADDITIONAL INFORMATION
You can learn more about this technology by ordering the NTIS report(s):
Cold-Air Performance of Compressor Drive Turbine
Order number: AD-A101066/NAA
Price code: A02
Order from:
National Technical Information Service
5285 Port Royal Road
Springfield, VA 22161
(703) 487-4650
158
Agency contact who can supplement the information contained in the backup report.
NTIS Order Number*
NTIS Price Code*
* See the order form and price code table at the end of the issue.

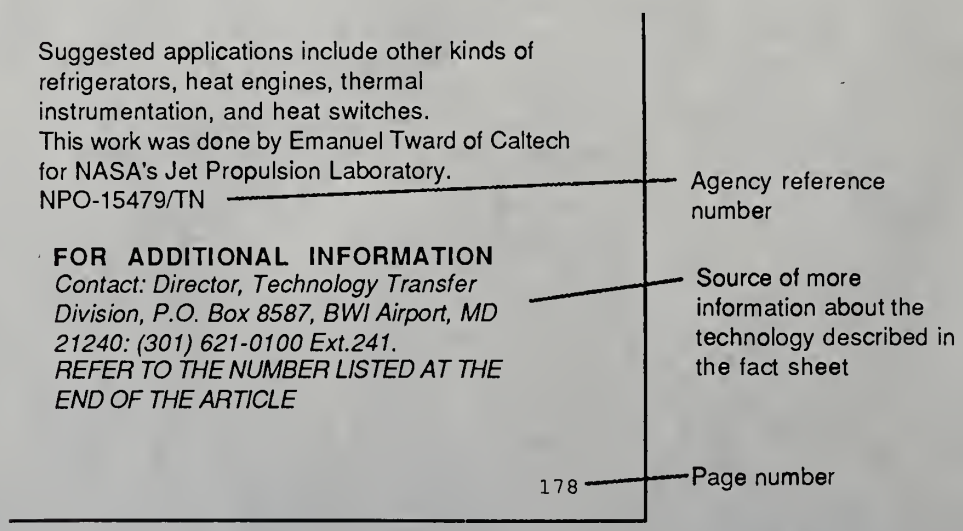
Suggested applications include other kinds of refrigerators, heat engines, thermal instrumentation, and heat switches.
This work was done by Emanuel Tward of Caltech for NASA's Jet Propulsion Laboratory.
NPO-15479/TN
FOR ADDITIONAL INFORMATION
Contact: Director, Technology Transfer Division, P.O. Box 8587, BWI Airport, MD 21240: (301) 621-0100 Ext.241.
REFER TO THE NUMBER LISTED AT THE END OF THE ARTICLE
178
Agency reference number
Source of more information about the technology described in the fact sheet
Page number

Tech Notes Title List for September 1989

Agriculture & Food

0708 Bacteria Zap Wheat Weeds (Licensing Opportunity)
0709 Bar Codes for Bees
0710 Fertilizer Applicator Helps Scientists Produce No-Till Corn
0711 Plant Sugar Reduces Salmonella in Poultry

Other Items of Interest

0759 Waste From Power Plants Conditions Soil
0761 Materials Aimed at Improving Pesticide, PCB Analyses

Computers

0712 Computer Interface for Hybrid Microcircuit Industry Under Development at NIST
0713 Cluster Finder: A Highly Parallel, Very Fast Trigger Processor

Software

0714 Common-Reliability Cumulative-Binomial Program—The point of equality between the reliability of the system and the common reliability of the components is found.
0715 Examining the Subroutine Structure of a VAX Image—A command program analyzes executable components of another program.
0716 Line-Editor Computer Program—Powerful editing tools are provided.
0717 Monitoring the Execution of a VAX Image—The time spent in each subroutine is displayed.

Other Items of Interest

0812 Keyboard Emulation for Computerized Instrumentation—Experimental parameters can be retrieved or re-entered at will.

Electrotechnology

0718 Compact Optical Correlator Developed
0719 Current Regulator for Sodium-Vapor Lamps—The operating current would be kept nearly constant as the lamp ages.
0720 Digital Controller for Acoustic Levitation—A computer controls sonic fields in three dimensions.
0721 Fabrication of Fiber-Optic Waveguide Coupler—Monitoring during fabrication enables control of the coupling between ports. (Licensing Opportunity)
0722 Design of Trellis Codes for Fading Channels—A new distance metric provides an additional degree of freedom design. (Licensing Opportunity)
0723 Inductively-Activated Short-Interval Timer—The absence of direct electrical contacts increases reliability. (Licensing Opportunity)
0724 Integrated-Circuit Broadband Infrared Sources—Microscopic devices consume less power, run hotter and are more reliable.
0725 Liquid-Crystal Optical Correlator—A liquid-crystal television screen serves as a spatial light modulator. (Licensing Opportunity)
0726 Low-Inductance Capacitor for Low Temperatures—A planer capacitor is made on an epoxy/fiberglass printed-circuit board.
0727 More on the Decoder-Error Probability of Reed-Solomon Codes—An explicit expression for the probability is derived.
0728 Optical Receivers with Rough Reflectors—A postdetection processor analyzes signals to reconstruct the transmitted message.
0729 Protection Against Brief Interruptions of Power—A rotating-machine system would bridge gaps of a few cycles in utility power.
0730 Spinner for Etching of Semiconductor Wafers—An ordinary electric-fan motor is adapted to a new use.

Software

0731 Electrostatic Discharge Susceptibility Data VZAP-2 Diskette Version

Testing & Instrumentation

0732 Waveguides and Fibers
0733 Chain of Test Contacts for Integrated Circuits—Microcircuit connections between probe pads yield data on the quality of fabrication. (Licensing Opportunity)
0734 Position-and-Direction Sensor for Light Beams—A beam from a spurious source could be detected.
0735 Timing Sampler for Delay Measurements—One chip contains delay chains and associated testing circuits. (Licensing Opportunity)

Other Items of Interest

0736 Automatic Monitoring Could Cut Costs of Emergency Power
0739 Multihundred-Kilowatt Rotary Electrical-Transfer Device—Roll rings decrease friction and electrical losses.
0803 Cladding for Transversely-Pumped Laser Rod—Pump power would be coupled in more effectively. (Licensing Opportunity)
0808 Measuring High-Temperature Superconductors
0816 Low-Cost Vertical Accelerometer for Aircraft—Self-aligning feature eliminates the need for costly attitude-rate sensors.

Energy

0736 Automatic Monitoring Could Cut Costs of Emergency Power
0737 Conversion of Gasoline-Powered Buses to Diesel-Powered Buses
0738 Lithium Battery (Licensing Opportunity)
0739 Multihundred-Kilowatt Rotary Electrical-Transfer Device—Roll rings decrease friction and electrical losses.

Engineering

0740 Chloride-Oxygen Leaching Technique Recovers Metals from Complex Sulfide Ores

0741 Integrity Factor Approach to Mine Pillar Stability Evaluation and Design

0742 Sprayfans Combined with Reverse Sprays Ventilate 40-Foot Cuts

0743 Navy Tests Composite Propeller Shaft

0744 Compact Right-Angle Connector—Part of a stack of adaptive fittings is eliminated.

0745 Correlation Analysis of Vibration Data From Rotary Pumps—Fourier coefficients describing vibrations are constructed from files of FFT pump-response data.

0746 Endjoints for Structural Elements—Struts are joined easily and rapidly to make frames. (Licensing Opportunity)

0747 Inspection in Overhead Spaces Containing Asbestos—A simple method saves time and effort.

0748 Ultraclean Radiant Furnace—Cooling of the walls minimizes contamination from outgassing.

0749 Variable-Volume Container—The container expands and contracts according to changes in volume of its solid contents.

Testing & Instrumentation

0750 Filmless X-Ray Inspection Methods—Speeds Aircraft Inspection Onboard Carriers

0751 Monitoring Foundation Response to Subsidence Using a Tiltmeter

0752 New Process Produces Lead from Galena Concentrates Without Pollution

0753 Ultralow-Frequency Through-the-Earth Electromagnetic Fire Warning Alarm System for Underground Mines (Licensing Opportunity)

0754 Techniques for Measuring Stress and Strain

0755 Flight Balance for Skin-Friction Measurements—The force of a tangential airstream is determined by a null-position servomechanism. (Licensing Opportunity)

0756 Measuring Bearing Wear Via Weight Loss—Dimensional changes are estimated from areas, weight losses, and densities.

0757 Miniature Flow-Direction/Pitot-Static Pressure Probes—Probes measure the directions and pressures of hypersonic flows at temperatures up to 500° F.

0758 Nondestructive Inspection of Foam and Multilayer Insulations—Electromagnetic and electrostatic sensors probe hidden surfaces and layers.

Other Items of Interest

0760 Asbestos Management Guide is Available—How to manage asbestos-containing materials until materials are removed

0766 Self-Aligning Robotic End Effector and Receptacle—Congruent surfaces provide alignment for gripping, installation, and removal.

0817 Computing Flutter Boundaries—This program calculates aeroelastic responses of mistuned airfoils.

0818 Using EMATs For Rail Car Wheel Inspection

Environmental Science & Technology

0759 Waste From Power Plants Conditions Soil

0760 Asbestos Management Guide is Available—How to manage asbestos-containing materials until materials are removed

Testing & Instrumentation

0761 Materials Aimed at Improving Pesticide, PCB Analyses

Other Items of Interest

0752 New Process Produces Lead from Galena Concentrates Without Pollution

0792 Alaskan Coastal Biological Data

Manufacturing, Machinery & Tools

0762 Adaptive Control of Remote Manipulator—A reference trajectory is tracked without modeling robot dynamics. (Licensing Opportunity)

0763 Discrete-Time Model-Reference Adaptive Control—The command-generator tracker concept is exploited in the discrete-time setting.

0764 Lightweight Restraint for Coupling Flanges—A cable-and-pulley mechanism allows limited motion. (Licensing Opportunity)

0765 Miniature Centrifugal Compressor—A small machine compresses neon for cooling to temperatures as low as 30K.

0766 Self-Aligning Robotic End Effector and Receptacle—Congruent surfaces provide alignment for gripping, installation, and removal.

0767 New Device Achieves Faster, More Uniform Metal Coating

0768 New Solder Joint Inspection System

Testing & Instrumentation

0769 Non-Destructive Laser/Thermal and Acoustic Microscopy Techniques for TAB Technology

Other Items of Interest

0720 Digital Controller for Acoustic Levitation—A computer controls sonic fields in three dimensions.

0806 Impedance Probe "Fine-Tunes" Electroplating Solutions

Materials

0770 Damage Tolerance and Durability of Rapidly-Solidified Aluminum-Base Powder Metallurgy Alloys

0771 SCC of Tungsten Alloy Penetrators

0772 Welding of Rapidly-Solidified Aluminum-Base Powder Metallurgy Alloys

0773 Low-Alloy Steel Calibration Standard Available

0774 Program on HIPing of Metal Powders Established
0775 Standard Reference Material Report Contains Microsphere Experiments
0776 David Taylor Research Center Researches New Anticorrosion Coating—Technique called electrochemical impedance spectroscopy
0777 Thermal Mechanical Processing to Control Grain Size
0778 Additives Lower Pickup of Moisture by Polyimides—Positron-annihilation tests show increased densities. (Licensing Opportunity)
0779 Alumina-Enhanced Thermal Barrier—Improved fibrous refractory composite material raises the temperature limit. (Licensing Opportunity)
0780 Annealing Increases Stability of Iridium Thermocouples—An improved heat treatment also increases ductility.
0781 Better PFAE's from Direct Fluorination—The process yields stable and effective lubricants under proper conditions.
0782 Calculating Dynamic Shear Moduli of Polymers—A nonlinear mathematical model replaces oversimplified linear and Prony-series models. (Licensing Opportunity)
0783 CdO Pretreatment for Graphite Lubricant Films—Sputtered films decrease friction and increase endurance.
0784 Effects of Aging on Embrittlement by Hydrogen—Concentration of hydrogen at grain boundaries determines the mode of fracture.
0785 Degradation of Carbon/Phenolic Composites by NaOH—NaOH degrades both the carbon and the phenolic components of carbon/phenolic laminates.
0786 Orientating Superconductive Crystals for High Current Density—Uniaxial stress would promote rearrangement of oxygen atoms in a favorable direction.
0787 Variable-Energy Ion Beams for Modification of Surfaces—Ions at low energy react chemically with silicon without damaging it. (Licensing Opportunity)

Testing & Instrumentation

0788 Measurement of Composition in Transparent Model Alloy—Noninvasive measurements are taken by Fourier-transform infrared spectroscopy
0789 Acoustical Imaging of Defects in Ceramics—Ultrasound is superior to x rays in the detection of microporosity.

Other Items of Interest

0743 Navy Tests Composite Propeller Shaft
0758 Nondestructive Inspection of Foam and Multilayer Insulations—Electromagnetic and electrostatic sensors probe hidden surfaces and layers.
0767 New Device Achieves Faster, More Uniform Metal Coating
0806 Impedance Probe "Fine-Tunes" Electroplating Solutions

Medicine & Biology

0790 Host Immune Response Causes Anemia of Malaria
0791 Navy Combats Hypothermia
0792 Alaskan Coastal Biological Data
0793 National Magnetic Resonance Facility at Madison
0794 Cryopreservation of Murine Germplasm
0795 Institute of Laboratory Animal Resources
0796 MIT Cell Culture Center
0797 University Resource in Laboratory Animal Medicine
0798 Directional Hearing Aid—The approximate directions of sounds are indicated visually. (Licensing Opportunity)

Testing & Instrumentation

0799 New Developments Available to Test Marine Plankton Light Emissions—Test chamber uses an integrating sphere to collect light

Other Items of Interest

0761 Materials Aimed at Improving Pesticide, PCB Analyses

Natural Resources Technology & Engineering

0800 Formula Predicts the Spontaneous Combustion Potential of Bituminous Coals
0801 High-Altitude Turbulence for Supersonic Airplanes—Characteristics and associated meteorological features are discussed.

Other Items of Interest

0799 New Developments Available to Test Marine Plankton Light Emissions—Test chamber uses an integrating sphere to collect light

Physical Sciences

0802 Heat, Alkali, Convert Crops to Chemicals (Licensing Opportunity)
0803 Cladding for Transversely-Pumped Laser Rod—Pump power would be coupled in more effectively. (Licensing Opportunity)
0804 Metal Oxide/Zeolite Combination Absorbs H_2S—A regenerable absorber cleans up how gas streams. (Licensing Opportunity)
0805 Theory of a Pyrotechnically Driven Device—Predictions and measurements of operation are presented.

Testing & Instrumentation

0806 Impedance Probe "Fine-Tunes" Electroplating Solutions
0807 Piezoelectric Polymer Forms Inexpensive Accelerometer
0808 Measuring High-Temperature Superconductors
0809 Eight-Channel Spectrometer—Photodetector signals are multiplexed for digitization and recording. (Licensing Opportunity)

Physical Sciences (Cont.)

0810 Delay-Line Anode for Microchannel-Plate Spectrometer—A zigzag pattern enables the location of incident pulses in two dimensions.

0811 Electron/Ion-Scattering Apparatus—Electron and ion beams are merged, then separated for analysis (Licensing Opportunity)

0812 Keyboard Emulation for Computerized Instrumentation—Experimental parameters can be retrieved or re-entered at will.

0813 Measurement of Molecular Mobilities of Polymers—Time-resolved electron-spin resonance (ESR) offers 667 times the sensitivity of conventional ESR.

0814 Modified Technique for Chemisorption Measurements—A greater number of smaller adsorbate volumes yields more-accurate measurements.

Other Items of Interest

0738 Lithium Battery (Licensing Opportunity)

0749 Variable-Volume Container—The container expands and contracts according to changes in volume of its solid contents.

0761 Materials Aimed at Improving Pesticide, PCB Analyses

0765 Miniature Centrifugal Compressor—A small machine compresses neon for cooling to temperatures as low as 30K.

0778 Additives Lower Pickup of Moisture by Polyimides—Positron-annihilation tests show increased densities. (Licensing Opportunity)

0781 Better PFAE's from Direct Fluorination—The process yields stable and effective lubricants under proper conditions.

0786 Orientating Superconductive Crystals for High Current Density—Uniaxial stress would promote rearrangement of oxygen atoms in a favorable direction.

0787 Variable-Energy Ion Beams for Modification of Surfaces—Ions at low energy react chemically with silicon without damaging it. (Licensing Opportunity)

Transportation & Components

0815 Tire Footprint Affects Hydroplaning on Wet Pavement—Higher aspect ratio of the tire footprint requires slower speed for safer driving on wet roads.

0816 Low-Cost Vertical Accelerometer for Aircraft—Self-aligning feature eliminates the need for costly attitude-rate sensors.

Software

0817 Computing Flutter Boundaries—This program calculates aeroelastic responses of mistuned airfoils.

Testing & Instrumentation

0818 Using EMATs For Rail Car Wheel Inspection

Other Items of Interest

0750 Filmless X-Ray Inspection Methods—Speeds Aircraft Inspection Onboard Carriers

0755 Flight Balance for Skin-Friction Measurements—The force of a tangential airstream is determined by a null-position servomechanism. (Licensing Opportunity)

Agriculture & Food

0708 Bacteria Zap Wheat Weeds (Licensing Opportunity)

0709 Bar Codes for Bees

0710 Fertilizer Applicator Helps Scientists Produce No-Till Corn

0711 Plant Sugar Reduces Salmonella in Poultry

Other Items of Interest

0759 Waste From Power Plants Conditions Soil

0761 Materials Aimed at Improving Pesticide, PCB Analyses

Research Technology
Agricultural Research Service
U.S. Department of Agriculture

Bacteria Zap Wheat Weeds

Weeds like downy brome, growing in the midst of winter wheat and other cereal grains, may soon be biologically controlled.

These weeds, which cost growers at least $375 million a year, cut winter wheat yields up to 45 percent by competing with crops for moisture, space, and nutrients. They've been spreading in recent years because conservation tillage systems, in which straw and other residues from the previous year's crops are left on the soil surface to slow erosion, make these weeds more difficult to control than with conventional tillage systems, where residues are plowed under.

ARS scientists found that certain strains of naturally occurring soil bacteria, in the genus *Pseudomonas*, can selectively kill or slow the growth of downy brome (also known as cheatgrass) and other weedy grasses in wheat, barley, oats, rye, and triticale.

"Since we do not have a herbicide for downy brome in wheat, this biocontrol method comes at the right time," says microbiologist Lloyd F. Elliott, who until recently was located at ARS' Land Management and Water Conservation unit in Pullman, Washington.

This may be the first time scientists have devised a way to get microorganisms to grow in the field and inhibit only the roots of weeds.

According to Elliott's coworker at Pullman, soil microbiologist Ann C. Kennedy, these bacteria are most effective in late fall and early spring when temperatures are low. By reducing the growth of downy brome roots early in the growing season, the bacteria allow the cereal crop to compete more effectively, thus reducing the negative impact of the weed on crop yield.

The pseudomonads are sprayed on the soil surface or residues where they begin to multiply and colonize the growing roots of downy brome.

"Once in the root zone, the pseudomonad bacteria produce toxins that interfere with the weeds' growth, often killing them," says Kennedy. "Those weeds that survive the winter may die or be so weakened they can't compete with the grain crop."

She says spraying the soil surface with pseudomonads before planting can boost yields of winter wheat as much as 35 percent.

Early test results indicate a single application of the bacterium can eliminate over 50 percent of the weeds, says Kennedy, but actual control will have to be verified in future field tests.

More than 2 years of field tests will be run to ensure the bacterium suppresses only the weeds. If it does, farmers may get the green light to apply these environmentally safe bacteria to their fields.

For technical information, contact Ann C. Kennedy, USDA-ARS Land Management and Water Conservation, Room 215, Johnson Hall, Washington State University, Pullman, WA 99164-6421; (509) 335-1552. For patent information, contact Office of Federal Patent Licensing, Center for the Utilization of Federal Technology, Room 304, NTIS, Springfield, VA 22161 (703) 487-4738 Patent Application Serial No. 07,207,592, "Method for Screening Bacteria and Application Thereof for Field Control of the Weed Downy Brome."

FOR ADDITIONAL INFORMATION: Inquiries concerning rights for commercial use of this invention should be addressed to: Office of Federal Patent Licensing, Center for the Utilization of Federal Technology, Room 304, NTIS, Springfield, VA 22161; (703) 487-4738. Refer to Patent Application 07,207,592/TN.

Bar Codes for Bees

Bees in Tucson are sporting a few extra stripes these days—bar codes like those found on packaged foods and other merchandise.

They are the world's smallest bar codes. Nine stripes, less than one-tenth an inch long, are glued to the tiny hairs on bees' backs at the Agricultural Research Service's Carl Hayden Bee Research Center in Tucson, Arizona. An electronic bar-code reader at the doorway of the beehive records each bee's exit and entrance.

Scientists hope the system will reveal such things as how hard honey bees work collecting pollen and nectar, the number of trips each bee makes, the length of time each spends foraging, and how resistant bees are to pesticides.

"Keeping track of individual bees used to be almost impossible because they all look alike," says entomologist Stephen L. Buchmann. "We couldn't easily monitor bees' leaving and returning to their hives. Now we're keeping a dossier on each tagged bee to record its activity over a long period."

The research findings, kept on a computer for easy analysis, might yield new clues to selecting healthier and more productive bees as parents for future generations of honey bees. Without the electronically read bar codes, research on the often mysterious behavior of honey bees takes an enormous amount of time and excessive handling of bees.

Buchmann got the idea of using bar codes from visits to the local supermarket. Bar codes are found on most packaged foods to keep tabs on product costs and to monitor inventory. In the 1960's, ARS helped pioneer commer-

DAVID RING

Weighing less than 20-millionths of an ounce, the bar code glued to this worker bee lets researchers automatically monitor the bee's passage through the hive entrance as it goes for nectar and pollen.

cial application of bar codes for supermarket use.

Buchmann's challenge was to reduce the postage-stamp-size, or larger, bar codes to a small rectangle less than the width of a bee's back. He succeeded by lowering the typical number of bars from as many as 55 to 9 because he only needed to keep tabs on 100 bees at a time. Standard bar codes can differentiate more than a million items.

Previously, Buchmann marked bees with dyes and paints that often wore off. Other systems required painting a white dot on bees' backs, then hand-painting a number over it after the dot dried.

Not only was this time-consuming, it also involved much handling of the bees, which upset their normal behavior and flawed research findings.

Buchmann says, "Our bar-code paper and glue weighs about one-twentieth as much as the nectar and pollen carried on each foraging trip away from their hives. So the bees behave normally, unaware of what's on their backs."

Buchmann is working with Sprague Ackley, a researcher with INTERMEC Corp. of Lynnwood, Washington, developers of bar codes and scanning equipment.

FOR ADDITIONAL INFORMATION: To discuss this effort further, contact Stephen L. Buchmann, USDA-ARS Carl Hayden Bee Research Center, 2000 East Allen Road, Tuscon, AZ 85719 (602)629-6327.

Research Technology
Agricultural Research Service
U.S. Department of Agriculture

Fertilizer Applicator Helps Scientists Produce No-Till Corn

The point-injector applicator, made by a firm in Iowa, pumps a solution of ammonium nitrate and urea through rolling spokes that penetrate about 4 inches into the soil. Putting fertilizer near the roots, instead of on the surface, keeps rainstorms from washing it away. And the point-injector treats roots gently, unlike conventional applicators that "knife" fertilizer into the soil. With the new applicator, farmers can apply nitrogen according to plant needs several times during the growing season. This will reduce nutrient losses from evaporation and chemical breakdown of nitrogen. In a 2-year test, researchers injected fertilizer into soil at a rate of 156 pounds of nitrogen per acre. Yields averaged about 7 bushels per acre higher than when the same amount of nitrogen was knifed in deep bands beside the corn rows.

FOR ADDITIONAL INFORMATION: Soil and Water Conservation Research, Ames, IA. Thomas S. Colvin, (515) 294-5724.

Research Technology
Agricultural Research Service
U.S. Department of Agriculture

Plant Sugar Reduces Salmonella in Poultry

A sugar produced naturally by a Mediterranean plant could reduce the chances of *Salmonella* bacteria contaminating poultry. D-mannose, produced by the *Fraxinus ornus* plant, reduces by at least 90 percent the ability of *Salmonella typhimurium* bacteria to settle in broilers' intestines. The bacteria pass harmlessly from the birds' bodies. Scientists dosed 120 broiler chicks with 100 million *Salmonella* bacteria when they were 3 days old and then gave half the chicks 2.5 percent D-mannose in their drinking water for 10 days. At 50 days of age, the time when broilers typically go to market, only one of the 60 birds that received the D-mannose had *Salmonella* bacteria, while 6 of the birds on plain water were infected. Studies in which larger groups of birds received mannose treatment, but were examined earlier than 50 days of age, showed equally significant reductions in *Salmonella*. Humans can get salmonellosis by eating improperly prepared chicken that is contaminated by the bacteria; symptoms include nausea, vomiting and diarrhea. D-mannose is available commercially in the United States, and a sister compound, mannitol, has been used for many years as a stabilizer and preservative in pharmaceutical products.

FOR ADDITIONAL INFORMATION: Veterinary Toxicology Research, College Station, TX, John R. DeLoach, (409) 260-9484.

Computers

0712 Computer Interface for Hybrid Microcircuit Industry Under Development at NIST

0713 Cluster Finder: A Highly Parallel, Very Fast Trigger Processor

Software

0714 Common-Reliability Cumulative-Binomial Program—The point of equality between the reliability of the system and the common reliability of the components is found.

0715 Examining the Subroutine Structure of a VAX Image—A command program analyzes executable components of another program.

0716 Line-Editor Computer Program—Powerful editing tools are provided.

0717 Monitoring the Execution of a VAX Image—The time spent in each subroutine is displayed.

Other Items of Interest

0812 Keyboard Emulation for Computerized Instrumentation—Experimental parameters can be retrieved or re-entered at will.

Navy Manufacturing Technology

Automated Manufacturing Research Facility

National Institute of Standards & Technology
Formerly the National Bureau of Standards (NBS)
U.S. Department of Commerce, Gaithersburg, MD 20899

Computer Interface for Hybrid Microcircuit Industry Under Development at NIST

NIST and the Naval Ocean Systems Center (NOSC) have begun a program to develop a standardized interface to link hybrid microelectronics manufacturing equipment with a local computer which controls equipment operations. NOSC's participation in the effort is based on defense industry needs brought to light during its Integrated Facility for Automated Hybrid Microcircuit Manufacturing (IFAHMM) Program. The NOSC follow-on program, Microelectronics Computer Integrated Manufacturing (MICROCIM), will implement the interface.

Efforts are underway to incorporate computer integrated manufacturing (CIM) strategies into the hybrid microelectronics manufacturing industry. The progress of these efforts can be enhanced with the introduction of a robust and adaptable interface between manufacturing equipment and the computers being used to control that equipment.

Traditionally, the equipment-to-controller interface has been accomplished by developing a custom program for each model of equipment. This method is both expensive and time consuming.

NIST and NOSC held the Low-Level Design Workshop in San Francisco April 12 and 13 to continue development of the specification for the interface. The Office of Continuing Education for the College of Engineering at the University of North Carolina, Charlotte joined in sponsoring the workshop.

The specification addresses the same level of interface targeted by the Manufacturing Automation Protocol (MAP), Technical and Office Protocol (TOP), and Semiconductor Equipment Manufacturer's Institute Equipment Communications Standard (SECS) standards. Not all hybrid manufacturing equipment suppliers and integrators have embraced these standards. Some maintain that they do not meet the specific requirments of the hybrid industry and others are not willing to commit to any one standard while disagreements continue. In the meantime, some equipment suppliers are developing their own physical and messaging interface specifications leading to further integration difficulties.

The interface specification being developed by NIST and NOSC will require minimal investment by industry, converge with national standards, and assure compatibility with existing factory network technologies. It draws on networking experience gained in the AMRF and will provide a vehicle to help industry transition from the perceived standards chaos of today to a more stable standards future.

Additional workshops will be held to continue development of the specification. A prototype release of the specification will be available in less than a year and a public demonstration is planned for the NIST Automation Program Open House scheduled for November. The completed interface specification will be available in the spring of 1990.

For Additional Information:

To discuss this effort further, contact:
Fred Rybczynski
AMRF Project
Building 220—Room A-127
National Institute of Standards & Technology
Gaithersburg, MD 20899
(301) 975-3540

Fermi National Accelerator Laboratory

The Cluster Finder: A Highly Parallel, Very Fast Trigger Processor

The Cluster Finder is a highly parallel, very fast trigger processing system which operates on the analog signals derived from a 400-channel lead-glass hodoscope generating a factor of 1-in-10,000 to 100,000 elimination of unwanted events. To accomplish this task, a large amount of channel-specific processing is used in conjunction with central pattern recognition to process up to a 15 MHz event rate.

The system has three parts: a channel-level processor, a pattern-recognition section, and a charge-digitization part.

The Cluster Finder's noise rejection rate, fast rise time of 80 ns, and wide dynamic range (30,000 to 1) represent an advance on existing technology.

The Fermilab Office of Research and Technology Application foresees commercial application of the Cluster Finder in the areas of processing information from lead-glass hodoscopes in particle physics experiments and in medical imaging such as that used in whole-body positron emmission tomography.

For Additional Information:

Office of Research and Technology Applications
Fermi National Accelerator Laboratory
P.O. Box 500
MS 208
Batavia, IL 60510
(312) 840-3333

Refer to FAA-288/TN

NASA Tech Brief
National Aeronautics and Space Administration

Common-Reliability Cumulative-Binomial Program

The point of equality between the reliability of the system and the common reliability of the components is found.

The cumulative-binomial computer program, CROSSER, is one of a set of three programs that calculate cumulative binomial probability distributions for arbitrary inputs. The three programs, CROSSER, CUMBIN (NPO-17555), and NEWTONP (NPO-17556), can be used independently of one another. CROSSER can be used by statisticians and users of statistical procedures, test planners, designers, and numerical analysts. The program has been used for calculations of reliability and availability.

CROSSER calculates the point at which the reliability of a *k*-out-of-*n* system equals the common reliability of the *n* components. It is designed to work well with all integer values $0 < k < n$. To run the program, the user simply runs the executable version and inserts the information requested by the program. The program is not designed to reject incorrect inputs, so the user must take care to make sure that the inputs are correct. Once all input data have been entered, the program calculates and lists the result. It also lists the number of iterations of Newton's method required to calculate the answer within a given error.

The CROSSER program is written in C. It was developed on an IBM AT computer with a numeric coprocessor using Microsoft C 5.0. Because the source code is written by use of standard C structures and functions, it should compile correctly with most C compilers. The format of the program is interactive. It has been implemented under DOS 3.2 and has a memory requirement of 26K. CROSSER was developed in 1988.

This program was written by Ernest M. Scheuer and Paul N. Bowerman of Caltech for **NASA's Jet Propulsion Laboratory**.
NPO-17557/TN

FOR ADDITIONAL INFORMATION

CONTACT:
COSMIC®
112 Barrow Hall
University of Georgia
Athens, GA 30620
(404) 542-3265

Examining the Subroutine Structure of a VAX Image

A command program analyzes executable components of another program.

SCANEXE is a command program for the DEC VAX computer used to scan a VMS run-time image and print information about the routines it uses. Optionally, SCANEXE lists each routine, with its entry point, and how many times it is called, if at all. Information on the progress of the program can be printed at the user's option as it analyzes the various executable components.

SCANEXE relies on "debug" records that are included by default in ".EXE" files. However, if an image is linked with the "/NOTRACEBACK" option (as are all system programs), then it cannot provide the necessary information. SCANEXE counts only the number of times it finds a statement calling each routine, which is not necessarily the same as the number of times that the routine would be called if the program were run.

SCANEXE is written in C (83 percent), FORTRAN 77 (13 percent), and Assembler (4 percent) for batch execution on the DEC VAX computer under VMS 4.X. It has a central-memory requirement of 61,952 bytes. The program was released in 1988.

This program was written by Peter J. Scott of Caltech for **NASA's Jet Propulsion Laboratory**. *NPO-17298/TN*

FOR ADDITIONAL INFORMATION

CONTACT:
COSMIC®
112 Barrow Hall
University of Georgia
Athens, GA 30602
(404) 542-3265

Line-Editor Computer Program

Powerful editing tools are provided.

The ZED editing program for the DEC VAX computer is a simple, yet powerful line editor for text, program source code, and nonbinary data. Line editors can be superior to screen editors in some cases; for example, executing complex multiple or conditional commands or editing via slow modem lines. ZED excels in the processing of text by use of procedure files. For example, such procedures can reformat a file of addresses or remove all in-line comments from a FORTRAN program.

In addition to command files, ZED also features versatile search qualifiers, global changes, conditionals, online help, hexadecimal mode, space compression, looping, logical combinations of search strings, journaling, visible control characters, and automatic detabbing.

The ZED editor was originally developed at Cambridge University in London and has been repeatedly enhanced since 1976. Users of the Cambridge implementation have devised such elaborate ZED procedures as chess games, calculators, and programs for evaluating π. This implementation of ZED maintains almost all the characteristics of the Cambridge editor.

A complete ZED manual is included on the tape. ZED is written entirely in C for either batch or interactive execution on the DEC VAX computer under VMS 4.X and requires 80,896 bytes of memory. The program was released in 1988.

This program was written by Peter J. Scott of Caltech for **NASA's Jet Propulsion Laboratory**. *NPO-17300/TN*

FOR ADDITIONAL INFORMATION

CONTACT:
COSMIC®
112 Barrow Hall
University of Georgia
Athens, GA 30602
(404) 542-3265

Monitoring the Execution of a VAX Image

The time spent in each subroutine is displayed.

The computer program PROCSCAN was developed to monitor the profile of an executable image during execution. The purpose is to identify the routines in which a program is spending most of its time. Thus, PROCSCAN can be a very useful first step in the optimization of a program.

PROCSCAN samples the program counter of the executing image and compares its value to a table of entry-point addresses to determine which subroutine is executing. The table of subroutines in the image is generated by the program SCANEXE (NPO-17298), which is included with this program, but is also available from COSMIC as a separate package. The output from PROCSCAN is a sorted histogram of subroutines versus time spent in each subroutine.

Because of the number of data collected, it is not possible to sample the program counter every time it changes, so the data represent a proportionate sampling of where the program is spending its time. During a few minutes of operation of a central processing unit, a fairly accurate picture can be formed. If a program has been linked with the /NOTRACEBACK qualifier, or it calls routines contained within a sharable library, then PROCSCAN will not function.

The program is written in C (77 percent), Assembler (13 percent), and FORTRAN 77 (10 percent) for execution on a VAX 11/780 computer opérating under VMS 4.X with a central-memory requirement of 33,280 bytes. The program was developed in 1987.

This program was written by Peter J. Scott of Caltech for **NASA's Jet Propulsion Laboratory**. *NPO-17297*

FOR ADDITIONAL INFORMATION

CONTACT:
COSMIC®
112 Barrow Hall
University of Georgia
Athens, GA 30602
(404) 542-3265

Electrotechnology

0718 Compact Optical Correlator Developed

0719 Current Regulator for Sodium-Vapor Lamps—The operating current would be kept nearly constant as the lamp ages.

0720 Digital Controller for Acoustic Levitation—A computer controls sonic fields in three dimensions.

0721 Fabrication of Fiber-Optic Waveguide Coupler (Licensing Opportunity)

0722 Design of Trellis Codes for Fading Channels (Licensing Opportunity)

0723 Inductively-Activated Short-Interval Timer—The absence of direct electrical contacts increases reliability. (Licensing Opportunity)

0724 Integrated-Circuit Broadband Infrared Sources—Microscopic devices consume less power, run hotter and are more reliable.

0725 Liquid-Crystal Optical Correlator—A liquid-crystal television screen serves as a spatial light modulator. (Licensing Opportunity)

0726 Low-Inductance Capacitor for Low Temperatures—A planer capacitor is made on an epoxy/fiberglass printed-circuit board.

0727 More on the Decoder-Error Probability of Reed-Solomon Codes

0728 Optical Receivers with Rough Reflectors—A postdetection processor analyzes signals to reconstruct the transmitted message.

0729 Protection Against Brief Interruptions of Power—A rotating-machine system would bridge gaps of a few cycles in utility power.

0730 Spinner for Etching of Semiconductor Wafers—An ordinary electric-fan motor is adapted to a new use.

Software

0731 Electrostatic Discharge Susceptibility Data VZAP-2 Diskette Version

Testing & Instrumentation

0732 Waveguides and Fibers

0733 Chain of Test Contacts for Integrated Circuits (Licensing Opportunity)

0734 Position-and-Direction Sensor for Light Beams—A beam from a spurious source could be detected.

0735 Timing Sampler for Delay Measurements (Licensing Opportunity)

Other Items of Interest

0736 Automatic Monitoring Could Cut Costs of Emergency Power

0739 Multihundred-Kilowatt Rotary Electrical-Transfer Device—Roll rings decrease friction and electrical losses.

0803 Cladding for Transversely-Pumped Laser Rod—Pump power would be coupled in more effectively. (Licensing Opportunity)

0808 Measuring High-Temperature Superconductors

0816 Low-Cost Vertical Accelerometer for Aircraft—Self-aligning feature eliminates the need for costly attitude-rate sensors.

U.S. Army Fact Sheet

Compact Optical Correlator Developed

Research developed a compact coherent optical correlator and a matched filter maker system. The correlator performs two-dimensional correlation of the input scene against images stored in the filters for the purpose of image recognition. The input scene enters the correlator via an imaging lens in real time while the filters are prerecorded on photographic plates that can be inserted into the correlator. In case of a match, a bright correlation spot appears at the output plane that is detected by a miniature television camera and is converted into a standard composite video signal. The spot position indicates the location of the object in the input scene. The output signal can be displayed and observed on any TV monitor or can be used as the input to other follow-on processors or control systems in fully automated applications.

The operating and performance requirements for the system were: 1) address 30 separate filter positions, 2) fit within a 15 cm diameter cylinder approximately 30 cm long, 3) operate over a 10(to the 4th exponential power): 1 scene brightness range, corresponding to a range from bright sunlight to a dark, overcast sky, 4) operate in real time, 5) fabricate filters within a 30 minute time period. These requirements went well beyond what had been done previously and required the solution of a number of technical problems and innovative approaches. An image intensifier in conjunction with attenuators increased the brightness range over which the correlator operates. Specially fabricated holographic optical elements combined the functions of several standard optical elements reducing the correlator size. An ultraprecise plate holder was fabricated to precisely reposition prerecorded filters in the correlator.

Details of the correlator package are given along with the filter maker system and design considerations and choices. Fabrication of a specialized holographic optical element essential to the correlator is described.

FOR ADDITIONAL INFORMATION: A copy of the report is available from NTIS, Springfield, VA 22161; (703) 487-4600.

NTIS order number: AD-A200 769/NAC

Price code: A05

NASA Tech Brief
National Aeronautics and Space Administration
NASA's Jet Propulsion Laboratory, Pasadena, California

Current Regulator for Sodium-Vapor Lamps

The operating current would be kept nearly constant as the lamp ages.

A proposed regulating circuit would maintain a nearly-constant alternating current in a sodium-vapor lamp. The regulator is necessary because, as the lamp ages, the potential drop across the lamp at the specified operating current decreases from about 150 to about 90 V. The regulator is part of a dc-to-ac inverter circuit that might be used to supply power to a street lamp from a battery charged by a solar-cell array.

As shown in the figure, power from a solar-cell array or battery is fed to a dc-to-ac inverter, the frequency of which is determined by a voltage-controlled oscillator. The inverter output is supplied to the lamp through a current-limiting inductor. Because the reactance of the inductor is proportional to the frequency, the lamp current can be increased or decreased by respectively decreasing or increasing the frequency.

The lamp current is sensed by a current transformer, the output of which is fed to one input of an error amplifier. The other input is a reference voltage corresponding to the specified lamp current. When the lamp current differs from the specified value, the current-transformer output differs from the reference voltage. The voltage comparator, therefore, emits a voltage proportional to the current error.

The error voltage is fed to the oscillator as a frequency-control signal, thereby changing the oscillator frequency and the lamp current by an amount that nearly cancels the current error. For a lamp-voltage variation of 150 to 90 V, this circuit can maintain the lamp current within 1 percent of the desired value.

This work was done by Colonel W. T. McLyman of Caltech for **NASA's Jet Propulsion Laboratory** *NPO-16702/TN*

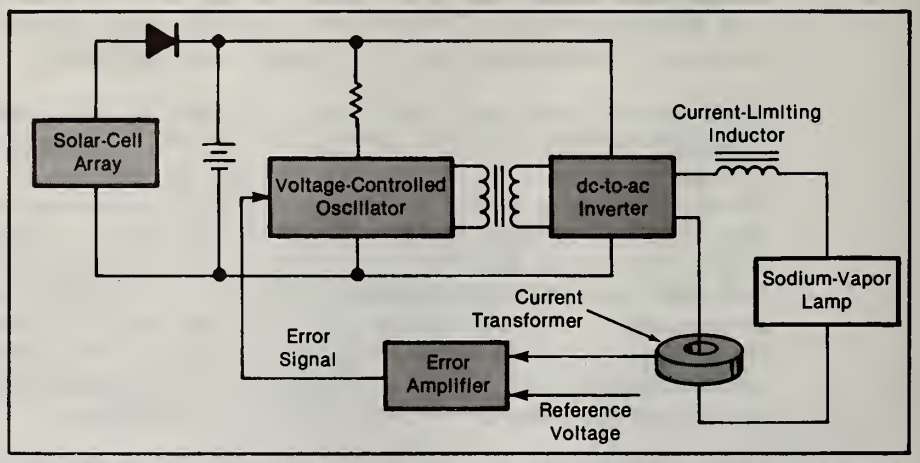

The **Regulated Lamp Power Supply** would maintain a nearly-constant lamp current over a wide range of lamp voltage drops. The inverter frequency would be varied to control the current via the frequency dependence of the reactance of the current-limiting inductor.

NASA Tech Brief
National Aeronautics and Space Administration
NASA's Jet Propulsion Laboratory, Pasadena, California

Digital Controller for Acoustic Levitation

A computer controls sonic fields in three dimensions.

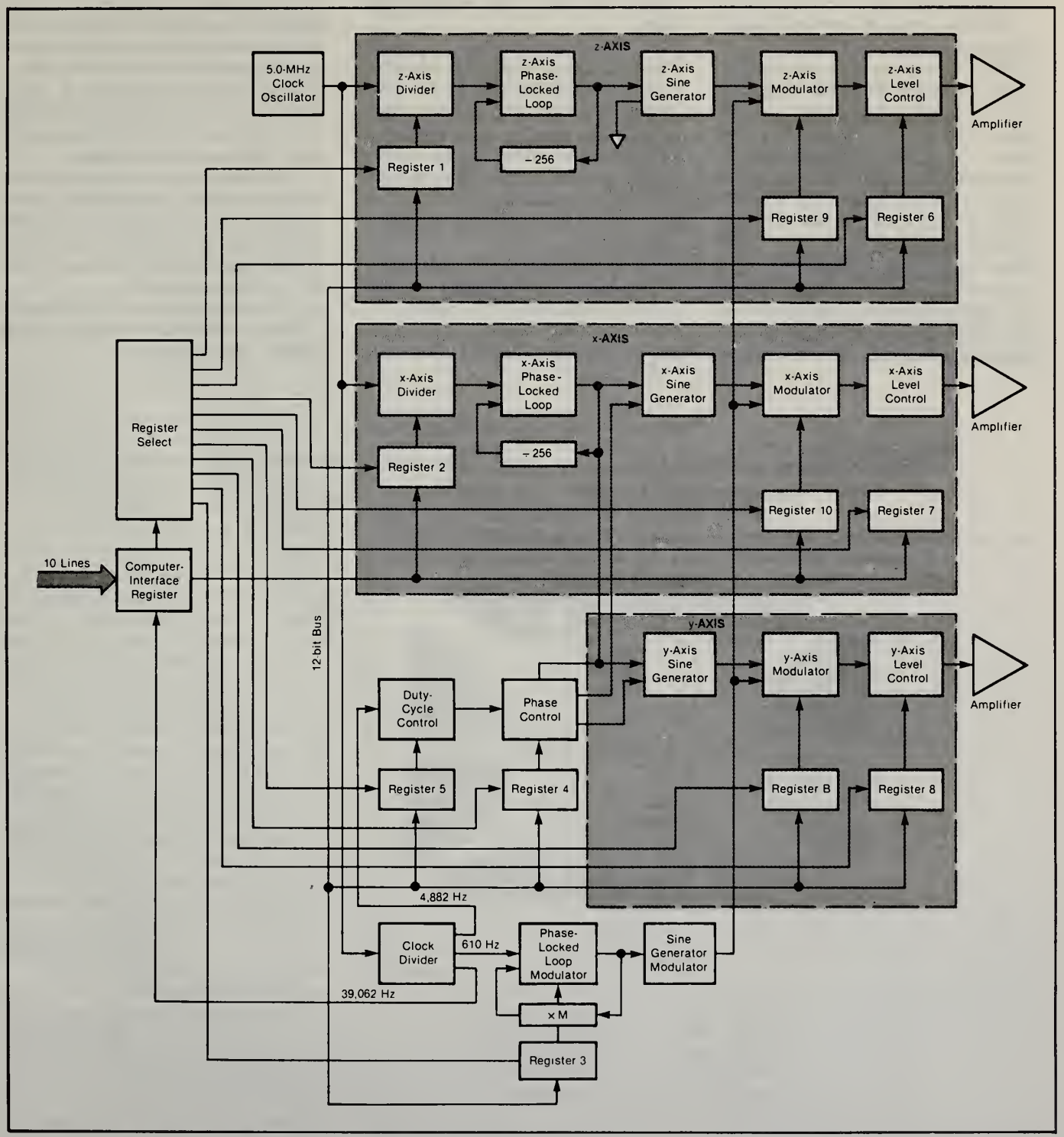

A **Computer Sends Instructions** to a computer-interface register, which distributes them to various registers in the acoustic controller. The channels for the z and x axes use three registers each, and the channel for the y axis uses two. The functions of three additional registers are shared by the channels.

An acoustic driver digitally controls sound fields along three axes. It allows the computerized acoustic levitation and manipulation of small objects for such purposes as containerless processing and nuclear-fusion power experiments. It may also be used for controlling the motion of vibration-testing tables in three dimensions.

The driver produces three mutually orthogonal sine waves, maintaining precise relationships among their frequencies, phases, and amplitudes. The driver outputs are independently determined by digital signals from 11 function registers (see figure). The registers are parallel-input, parallel-output storage devices, connected to receive control signals from a twelfth register, the computer-interface register. A computer sends data to the computer-interface register over 10 input lines.

In the z-axis channel, register 1 controls a frequency divider that operates on the 5-MHz clock signal. In combination with a phase-locked loop and a sine-wave generator, the divider produces a carrier wave. Under control of register 9, the degree of modulation of the carrier wave is established. The modulated carrier is fed to a level controller, where the output level amplitude is set according to the data in register 6. After amplification, this audio signal is fed to the z-axis acoustic transducer.

In the x-axis channel, registers 2, 10, and 7 do the frequency, modulation, and amplitude control, respectively. In the y-axis channel, the output of the x-axis phase-locked loop is fed to the sine-wave generator. This ensures that the frequencies of the x and y axes are identical. The degree of modulation and amplitude are controlled just as in the z and x channels, by registers 11 and 8.

For all channels, the modulating frequency is controlled by the data in register 3. This register feeds the modulators in each of the channels synchronously. It can vary the modulating frequency from about 0.05 to 12 Hz and integral multiples thereof up to 1,000 Hz.

A phase-control circuit receives instructions from register 4. This circuit produces a pulse that starts the x and y sine-wave generators on their sine-wave cycles. It thus fixes the phase relationship of the x and y channels. The phase-control circuit receives its clock pulses from the x-axis phase-locked loop so that its function is synchronized with the x and y carriers.

When activated by register 5, a duty-cycle controller commands the phase-control circuit to reverse. This reverses the sine waves on the x and y axes.

The driver produces its outputs at frequencies ranging from 620 to 10,000 Hz, depending on the choice of equipment. The frequency of a given equipment selection can be varied over a 1-octave range by the computer software.

This work was done by D. Kent Tarver of Caltech for **NASA's Jet Propulsion Laboratory**. *NPO-16623/TN*

FOR ADDITIONAL INFORMATION: *Contact: Director, Technology Transfer Division, P.O. Box 8757, BWI Airport, MD 21240; (301) 621-0100 Ext. 241*
REFER TO THE NUMBER LISTED AT THE END OF THIS ARTICLE

NASA Tech Brief
National Aeronautics and Space Administration
NASA's Jet Propulsion Laboratory, Pasadena, California

Licensing Opportunity

Fabrication of Fiber-Optic Waveguide Coupler

Monitoring during fabrication enables control of the coupling between ports.

A technique for making four-port, single-mode fiber-optic waveguide couplers requires no critically-precise fabrication operations or open-loop processes. Waveguide couplers are analogous to beam-splitter prisms (see Figure 1). They are essential in many applications that require the coherent separation or combination of two waves; for example, for interferometric purposes.

This and earlier coupler designs are based on the placement of two similar weakly-guiding fiber-optic waveguides adjacent to each other. A wave launched in one guide dies out simultaneously with the growth of a similar wave in the other guide. This coupling occurs because the optical waves extend beyond the guiding cores in weakly guiding fibers. The interaction length required for the transfer of half the power at a wavelength of 830 nm is approximately 15 mm for waveguide cores of 5 μm in diameter, center-to-center spacing of 13 μm, and a difference of 0.003 between the indices of refraction of the core and the cladding.

To begin the fabrication of the coupler, most of the cladding layer of a short portion near the midlength of each of two optical fibers is etched away. The diameter of the fibers is monitored during etching by observing the Fraunhofer diffraction pattern produced by illuminating the fibers with a laser beam. To hold the fibers in a plane, the etched portions of the two fibers are stretched taut over two fibers of 125 μm in diameter lying on a microscope slide (see Figure 2). The outer ends of the fibers are held in position by paraffin. The plane of the slide is then held vertically, and small weights, which can be made from short pieces of fiber, are hung on the upper fiber to bring it into contact with the lower fiber along a short length.

An arc-welding process is used to fuse the remaining cladding of the two fibers. As the welding proceeds, the degree of coupling is monitored by injecting laser light into one of the fibers and monitoring the light emerging from the far ends of both fibers. Because the objective is to obtain a low-temperature fusion of the cladding without distorting the cores of the fibers, a low welding current of about 10 mA is used. When the output signals reach the desired

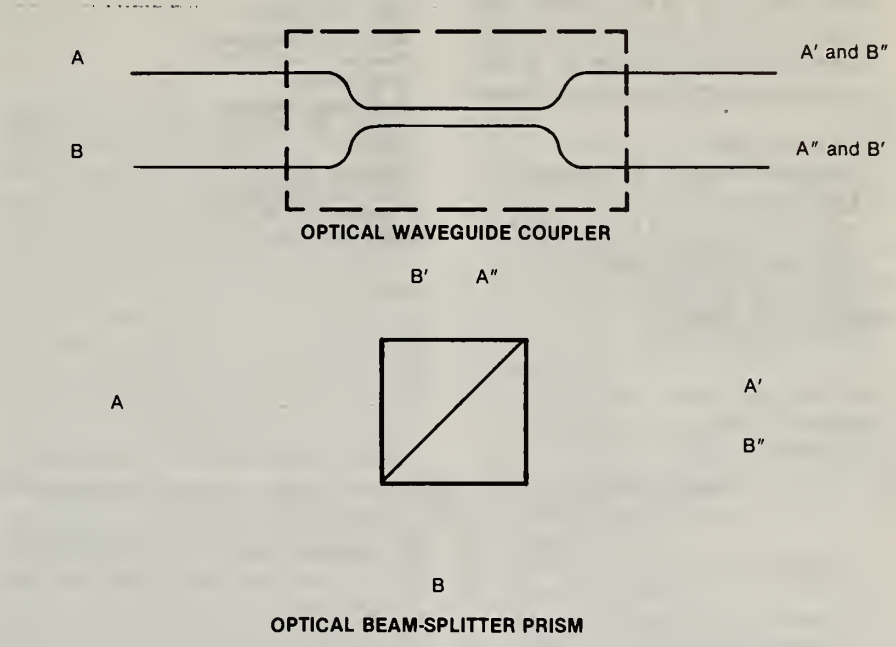

Figure 1. An **Optical Waveguide Coupler** is analogous to an optical beam-splitter prism.

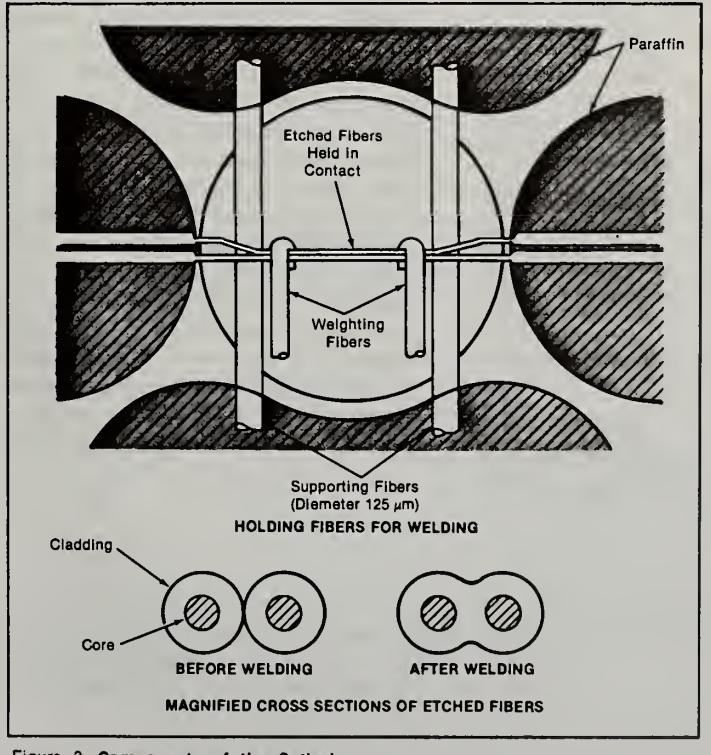

Figure 2. **Components of the Optical Waveguide Coupler** are held by paraffin on a microscope slide while the remaining cladding of the two optical fibers is fused together by arc welding.

ratio, welding is stopped.

This work was done by Willis Goss, Mark D. Nelson, and John M. McLauchlan of Caltech for **NASA's Jet Propulsion Laboratory**.

Title to this invention, covered by U.S. Patent No. 4523810, has been waived under the provisions of the National Aeronautics and Space Act [42 U.S.C. 2457(f)]. Inquiries concerning licenses for its commercial development should be addressed to

Edward Ansell
Director of Patents and Licensing
Mail Stop 301-6
California Institute of Technology
1201 East California Boulevard
Pasadena, CA 91125
Refer to NPO-15630/TN

Jet Propulsion Lab.
NASA Resident Office
Technology Utilization Officer: Gordon S. Chapman
Mail Stop 180-801
4800 Oak Grove Drive
Pasadena, CA 91109
(818) 354-4849
Patent Counsel: Paul F. McCaul
Mail Code 180-801
4800 Oak Grove Drive
Pasadena, CA 91109
(818) 354-2734
Technology Utilization Mgr. for JPL: Norman L. Chalfin
Mail Stop 156-211
4800 Oak Grove Drive
Pasadena, CA 91109
(818) 354-2240

FOR ADDITIONAL INFORMATION: *Contact: Director, Technology Transfer Division, P.O. Box 8757, BWI Airport, MD 21240; (301) 621-0100 Ext. 241*
REFER TO THE NUMBER LISTED AT THE END OF THIS ARTICLE

NASA Tech Brief
National Aeronautics and Space Administration

Licensing Opportunity

Design of Trellis Codes for Fading Channels

A new distance metric provides an additional degree of freedom in design.

A report develops the theoretical basis for the design of trellis codes that perform optimally when used in multiple trellis-coded modulation on Rician fading communication channels. These codes perform better than do codes designed to be optimal on nonfading channels with only additive white Gaussian noise (AWGN). The design of the improved codes is based on a new distance measure suitable for fading channels. (Here "distance" denotes a measure of separation in an abstract space in the theory of codes rather than in ordinary three-dimensional space.)

The authors look more carefully than before into the properties of the trellis-coded modulation that enter into the various expressions for average bit-error probability, then use these properties as design criteria for conventional and multiple trellis codes operating over a fading channel. It has been well established in the literature that the maximization of the free Euclidean distance (d_{free}) is the appropriate optimum-design criterion for an AWGN channel. However, for a Rician fading channel with interleaving and deinterleaving, the authors show that the asymptotic performance of trellis-coded modulation at a high signal-to-noise ratio (SNR) is dominated by several other factors that depend on the value of the Rician parameter K. [K is the ratio of direct plus specular power (coherent components) to diffuse power (noncoherent component).]

In particular, at small values of K (where the channel tends toward Rayleigh fading), the primary design criteria for high SNR become (1) a newly defined length of the shortest error-event path and (2) the product of branch distances along that path, with d_{free} a secondary consideration. Thus, at low values of K, the longer the shortest error-event path and the larger the product of the branch distances along that path, the better the code performs, even though d_{free} does not reach its optimum value for an AWGN channel. As K increases, the relative significance of these primary and secondary considerations shifts until K reaches infinity (AWGN), in which case optimum performance is once again achieved by a trellis code designed to maximize d_{free}

To demonstrate the foregoing analytically, the authors first take previously derived upper bounds on the average error-probability performance in the presence of fading and investigate their asymptotic behavior as the SNR grows large. The comparison of these results for the different cases (coherent versus differentially coherent detection and the presence versus the absence of information on the state of the channel) reveal some striking similarities with regard to the way in which certain properties of the trellis-code design affect the rate of descent of the average probability of error with the average SNR. The authors then show that when these properties are used as a motivation for the design of a good code, multiple trellis-coded modulation, wherein more than one channel symbol is assigned to each trellis branch, is a natural choice. Indeed, multiple trellis-coded modulation can achieve a performance on the fading channel superior to that of conventional (single channel symbol per trellis branch) trellis-coded modulation of the same throughput and number of trellis states.

This work was done by Marvin K. Simon and Dariush Divsalar of Caltech for **NASA's Jet Propulsion Laboratory**. *"The Design of Trellis Codes for Fading Channels,"*

In accordance with Public Law 96-517, the contractor has elected to retain title to this invention. Inquiries concerning rights for its commercial use should be addressed to

Edward Ansell
Director of Patents and Licensing
Mail Stop 301-6
California Institute of Technology
1201 East California Boulevard
Pasadena, CA 91125
Refer to NPO-17356/TN

Jet Propulsion Lab.
NASA Resident Office
Technology Utilization Officer: Gordon S. Chapman
Mail Stop 180-801
4800 Oak Grove Drive
Pasadena, CA 91109
(818) 354-4849
Patent Counsel: Paul F. McCaul
Mail Code 180-801
4800 Oak Grove Drive
Pasadena, CA 91109
(818) 354-2734
Technology Utilization Mgr. for JPL: Norman L. Chalfin
Mail Stop 156-211
4800 Oak Grove Drive
Pasadena, CA 91109
(818) 354-2240

FOR ADDITIONAL INFORMATION: *Contact: Director, Technology Transfer Division, P.O. Box 8757, BWI Airport, MD 21240; (301) 621-0100 Ext. 241*
REFER TO THE NUMBER LISTED AT THE END OF THIS ARTICLE

NASA Tech Brief
National Aeronautics and Space Administration
NASA's Jet Propulsion Laboratory, Pasadena, California

Licensing Opportunity

Inductively-Activated Short-Interval Timer

The absence of direct electrical contacts increases reliability.

A timing circuit in a pneumatically launched projectile triggers an explosive charge in the projectile at a specified delay after the launch. Both power and control signals are coupled inductively to the timer from the stationary launcher circuitry (see figure). This eliminates the need for direct electrical contacts, which are unreliable and which can generate sparks that trigger the explosive accidentally. Inductive coupling also provides higher reliability in field operation than contacts do. The underlying concept could be useful in such other safety-related applications as remotely or automatically controlling the flow of bottled flammable gas.

Initially, a driver in the launcher operates in a flyback-transformer mode at a repetition rate between 20 and 120 kHz to charge the main storage capacitor, C_1, to about 8 V. The smaller filter capacitor, C_2, is charged to about 5 V. The capacitors supply power to the signal-processing logic circuits through voltage and current regulators.

The energy to fire the explosive squib is taken from C_1. Power for the regulators is drawn from C_1 through the squib at a low current (less than the firing current), as a means of continually testing whether the current path through the squib remains intact. If it is not intact, C_1 is discharged to prevent accidental detonation in the event of subsequent unplanned reconnection.

The signals that control the delay are coded by the frequency of the pulses applied from the launcher. Under normal circumstances, only the reset and delay-setting frequencies need to be applied. Another frequency code orders a shutdown for safety, and the lack of frequency signifies the launch and the start of the delay. All frequencies and timings within the circuit are determined with reference to its 32.768-kHz crystal oscillator.

Initially, the reset code (120 kHz) is applied for a minimum of 0.5 s. Because this is the highest frequency used, it charges the storage capacitor at the maximum possible rate. It also provides time for the crystal oscillator to stabilize and turns the circuits on in a known reset state.

Next, the delay-setting frequency is applied for a minimum of 0.26 s and is maintained until shortly after the launch. The nominal frequency range for setting the delay is 32 to 99 kHz, corresponding to a delay of 24 to 8 s. Logic circuits in the timing section execute a formula for delay that decreases with increasing frequency.

The safe-shutdown frequency can range between 16 and 24 kHz and is nominally 20 kHz. This signal need be present for only 5 ms. Then the energy in C_1 is discharged through the same coil on the board that is used to receive the initial charging pulses so that the discharge can be detected for test purposes by inductive coupling back to the external driving coil.

This invention is owned by NASA, and a patent application has been filed. Inquiries concerning nonexclusive or exclusive license for its commercial development should be addressed to the Patent Counsel, NASA Resident Office-JPL

This work was done by Gordon A. Wiker and George H. Wells, Jr., of Caltech for **NASA's Jet Propulsion Laboratory**.

Refer to NPO-16882/TN

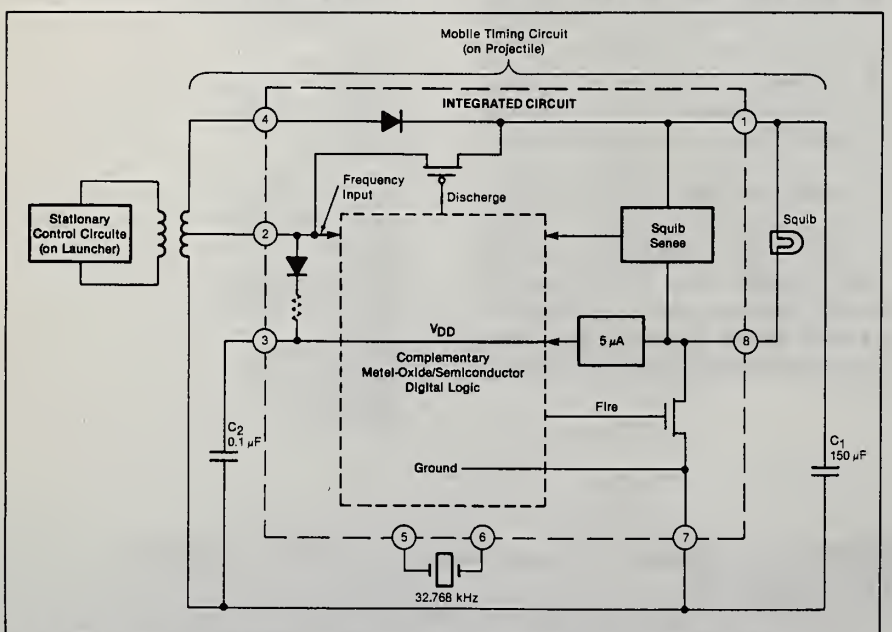

Frequency-Coded Power and Control Signals are coupled inductively through the airgap between coils on the launcher and on the circuit board of the projectile.

Jet Propulsion Lab.
NASA Resident Office
Technology Utilization Officer: Gordon S. Chapman
Mail Stop 180-801
4800 Oak Grove Drive
Pasadena, CA 91109
(818) 354-4849
Patent Counsel: Paul F. McCaul
Mail Code 180-801
4800 Oak Grove Drive
Pasadena, CA 91109
(818) 354-2734
Technology Utilization Mgr. for JPL: Norman L. Chalfin
Mail Stop 156-211
4800 Oak Grove Drive
Pasadena, CA 91109
(818) 354-2240

FOR ADDITIONAL INFORMATION: *Contact: Director, Technology Transfer Division, P.O. Box 8757, BWI Airport, MD 21240; (301) 621-0100 Ext. 241*
REFER TO THE NUMBER LISTED AT THE END OF THIS ARTICLE

NASA Tech Brief
National Aeronautics and Space Administration
Goddard Space Flight Center, Greenbelt, Maryland

Integrated-Circuit Broadband Infrared Sources

Microscopic devices consume less power, run hotter, and are more reliable.

Simple, compact, lightweight, rapidly-responding reference sources of broadband infrared radiation have been made available by integrated-circuit technology. These devices are intended primarily for use in the calibration of remote-sensing infrared instruments. The new devices should eventually replace conventional infrared sources, which are relatively massive and complicated, dissipate excessive power, and respond too slowly. The new devices should also replace the present generation of miniature infrared sources, which are expensive and delicate and have both unduly-low maximum operating temperatures and reduced reliability when operating near those maximum temperatures.

The new devices are essentially microscopic resistors that consist of beams of polycrystalline silicon. The resistors are heated by electrical current to make them glow in the desired range of wavelengths. They can operate in air or vacuum. The voltage applied to each resistor is adjusted to obtain the desired operating temperature, current, or power dissipation. (Measurements have shown that the current-vs.-voltage curve is fairly linear.)

A device can be made or used alone or as part of a flat-panel or complicated multi-element array of reference sources. A device or array is fabricated as follows:

1. A silicon substrate is oxidized to a depth of 10,000 Å.
2. A film of polycrystalline silicon 8,000 to 10,000 Å thick is deposited on the oxide.
3. The polycrystalline silicon is doped with boron to obtain a resistance of 50 to 100 Ω/□.
4. The polycrystalline silicon is etched to form the pattern of resistor strips and contact areas (e.g., as shown in the upper part of the figure).
5. The oxide is stripped from the exposed areas of the wafer and from under the beam(s), leaving only the oxide under the contact areas.
6. A thin film of aluminum is evaporated onto the entire wafer.
7. The pattern of contact pads is masked, and the aluminum is etched to leave only the portion in the contact areas.
8. The aluminum is alloyed to form the contacts.

A typical completed device is shown in the lower part of the figure.

The self-passivating nature of the polycrystalline silicon adds to the reliability of the devices. The maximum operating temperature is over 1,000 K, as compared to the maximum of 600 K in prior devices. The power dissipation is only one-fourth that of the prior devices.

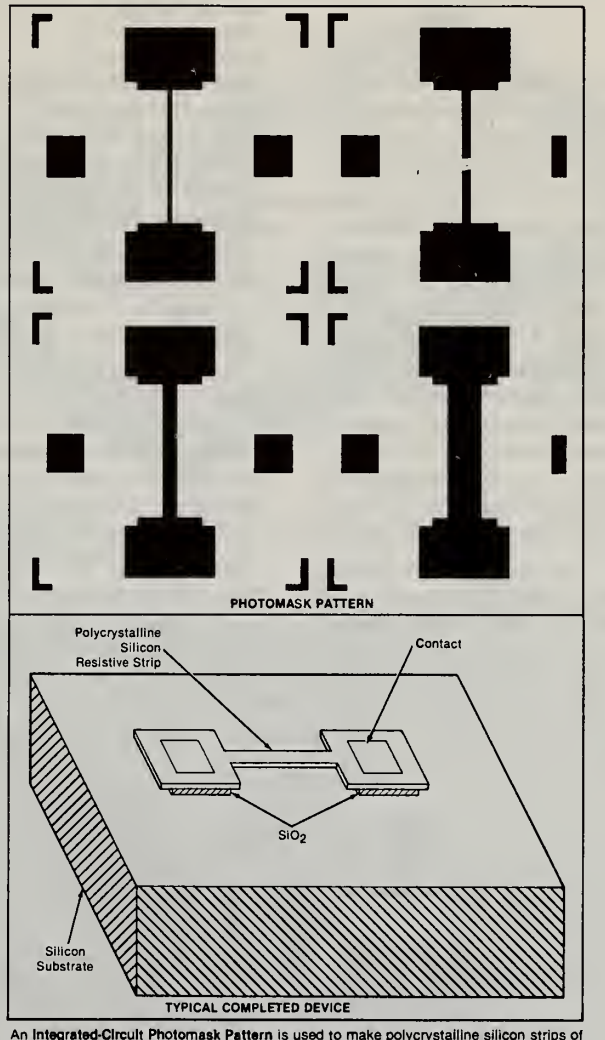

An **Integrated-Circuit Photomask Pattern** is used to make polycrystalline silicon strips of various widths and, therefore, of various electrical resistances and infrared characteristics. The strips are used as "glow-bar" resistors to calibrate infrared-sensing instruments.

This work was done by G. Lamb, M. Jhabvala, and A. Burgess of **Goddard Space Flight Center.** *GSC-13085/TN*

FOR ADDITIONAL INFORMATION: *Contact: Director, Technology Transfer Division, P.O. Box 8757, BWI Airport, MD 21240; (301) 621-0100 Ext. 241*
REFER TO THE NUMBER LISTED AT THE END OF THIS ARTICLE

NASA Tech Brief
National Aeronautics and Space Administration
NASA's Jet Propulsion Laboratory, Pasadena, California

Licensing Opportunity

Liquid-Crystal Optical Correlator

A liquid-crystal television screen serves as a spatial light modulator.

An optical correlator uses a commercially-available liquid-crystal television (LCTV) screen as a spatial light modulator. Correlations with this device can be done at video frame rates, making such operations as bar-code recognition possible at a reasonable cost. With further development, such a correlator may be useful in automation, robotic vision, and optical image processing. As higher resolution LCTV's are developed, the resolvability of such correlators will increase, the cost of this improvement being borne by the consumer television market.

The correlator is shown in the figure. An input video signal generated by a computer, video camera, or television receiver is sent to the LCTV screen. A collimated laser beam is incident upon the screen. Each LCTV picture element consists of two parallel polarizers with a polarizing liquid crystal in between that is oriented by an impressed electric field. The light transmission through each picture element ranges from about 0 to a maximum value depending on the bias applied.

Thus, the video modulation applied to each picture element determines the amount of laser light that passes through it. As a result, the collimated beam is spatially modulated so that a cross section of the beam looks like the television image.

The light transmitted through the screen passes through a lens focused on the Fourier-transform plane. A reference light beam, split off by a beam splitter after collimation, is focused by a long-focal-length correlation lens and reflected onto the correlation plane beyond the Fourier-transform plane. A Fresnel-zone plate of the pattern with which it is desired to correlate is formed at the Fourier-transform plane. In the initial experiments, the pattern was a computer-generated Ronchi ruling and was recorded at the Fourier-transform plane with a thermoplastic recording camera. In a more sophisticated version, spatial filtering was added to remove the grid patterns of the LCTV screen.

When an image is subsequently impressed on the screen, the light pattern on the correlation plane shows the correlation between the present image and the one represented on the zone plate. A detector array, photographic film, or other medium may be used to record the correlation pattern.

This work was done by Hua-Kuang Liu of Caltech for **NASA's Jet Propulsion Laboratory**. *For further information, Circle 143 on the TSP Request Card.*

In accordance with Public Law 96-517, the contractor has elected to retain title to this invention. Inquiries concerning rights for its commercial use should be addressed to

Edward Ansell
Director of Patents and Licensing
Mail Stop 301-6
California Institute of Technology
1207 East California Boulevard
Pasadena, CA 91125

Refer to NPO-16750, volume and number of this NASA Tech Briefs *issue, and the page number.*

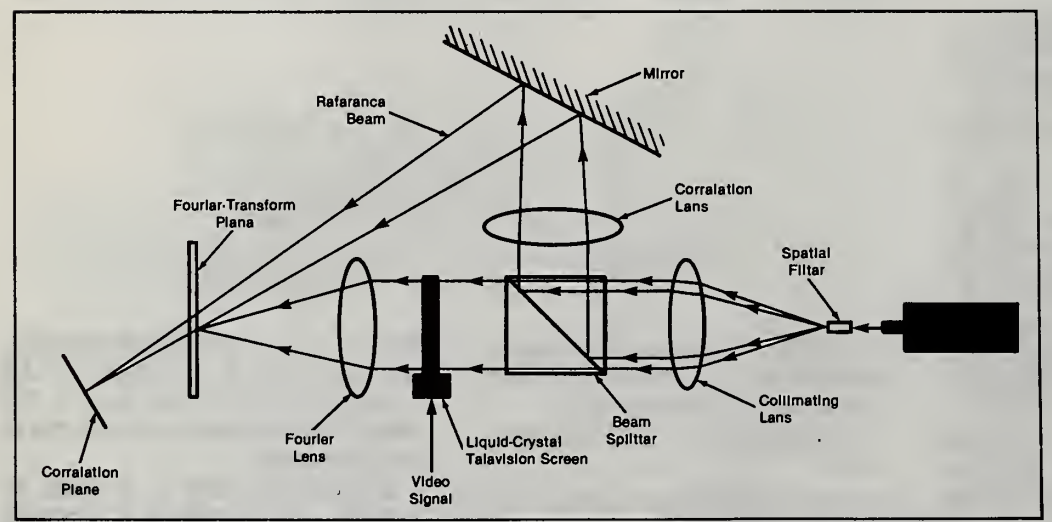

In the **Optical Correlator,** the liquid-crystal television screen serves as a transmitting spatial light modulator. The correlation between the pattern on the screen and the pattern represented on a zone plate at the Fourier-transform plane appears as a pattern on the correlation plane.

Jet Propulsion Lab.
NASA Resident Office
Technology Utilization Officer: Gordon S. Chapman
Mail Stop 180-801
4800 Oak Grove Drive
Pasadena, CA 91109
(818) 354-4849
Patent Counsel: Paul F. McCaul
Mail Code 180-801
4800 Oak Grove Drive
Pasadena, CA 91109
(818) 354-2734
Technology Utilization Mgr. for JPL: Norman L. Chalfin
Mail Stop 156-211
4800 Oak Grove Drive
Pasadena, CA 91109
(818) 354-2240

FOR ADDITIONAL INFORMATION: *Contact: Director, Technology Transfer Division, P.O. Box 8757, BWI Airport, MD 21240; (301) 621-0100 Ext. 241*
REFER TO THE NUMBER LISTED AT THE END OF THIS ARTICLE

NASA Tech Brief
National Aeronautics and Space Administration
Langley Research Center, Hampton, Virginia

Low-Inductance Capacitor for Low Temperatures

A planar capacitor is made on an epoxy/fiberglass printed-circuit board.

A test at the National Transonic Facility (NTF) requiring the use of a shadowgraph system dictated that the light source be mounted on the wall of the test section within the cryogenic environment of the plenum of the tunnel. The light source of the shadowgraph, which includes a high-pressure, 75-W xenon arc lamp, was modified to allow all high-voltage triggering components to be mounted inside an aluminum lamp housing. When the entire assembly was tested in operation in an environmental chamber at temperatures down to −160 °C, the high-voltage capacitor in the assembly did not survive the extreme cold: differential contraction of the internal parts of the capacitor caused the unit to fail. Subsequent tests of replacement oil-filled and ceramic high-voltage capacitors yielded the same results, and a limited search for capacitors of similar voltage rating that could tolerate the extreme cold was unsuccessful.

It was decided to design, fabricate, and test a suitable capacitor at the facility. The desired properties included tolerance of a wide range of temperature, low inductance, high breakdown potential, low series equivalent resistance, and ease of manufacture. A planar design using G-10 (or equivalent) epoxy/fiberglass double-sided printed-circuit-board material was selected. The planar design and flat copper plates ensured low inductance and low series resistance. The planar construction minimized the effects of thermal contraction, and the epoxy/fiberglass substrate ensured a high breakdown voltage.

Tests indicated that a capacitor between 600 and 700 pF would be adequate to produce reliable starting of the lamp. A board 0.032 in. (0.81 mm) thick, 9.5 cm by 16.5 cm, was etched with 0.75-cm borders to yield a conductor area of 8 cm by 15 cm (see Figure 1), with a measured capacitance of 650 pF. With the dielectric strength of the epoxy/fiberglass material rated at 510 volts per mil (2×10^7 V/m) the board possesses a dielectric strength of over 16,000 V, which is more than adequate for this application.

The capacitor was mounted in the lamp housing (see Figure 2), and the complete unit was repeatedly cycled between room

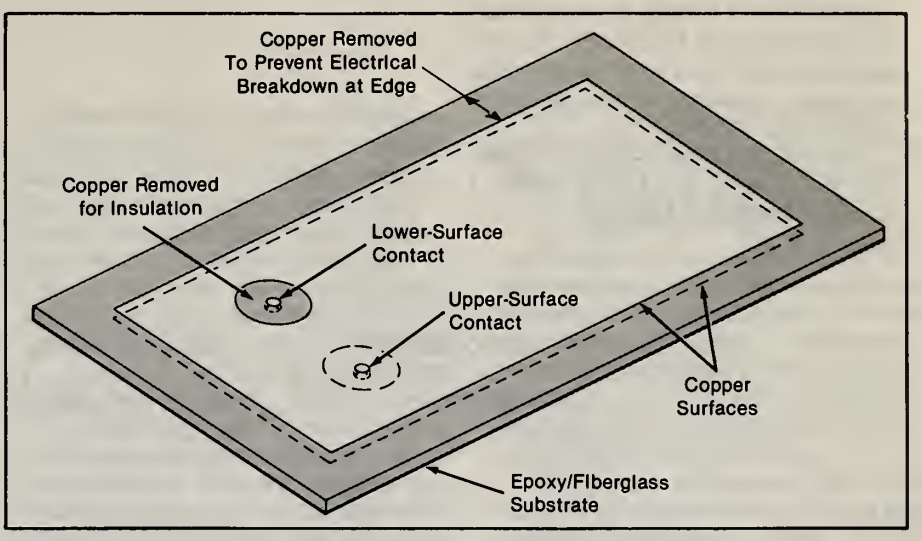

Figure 1. **Etched Circular Areas** insulate contacts on the planar capacitor fabricated from printed-circuit-board material.

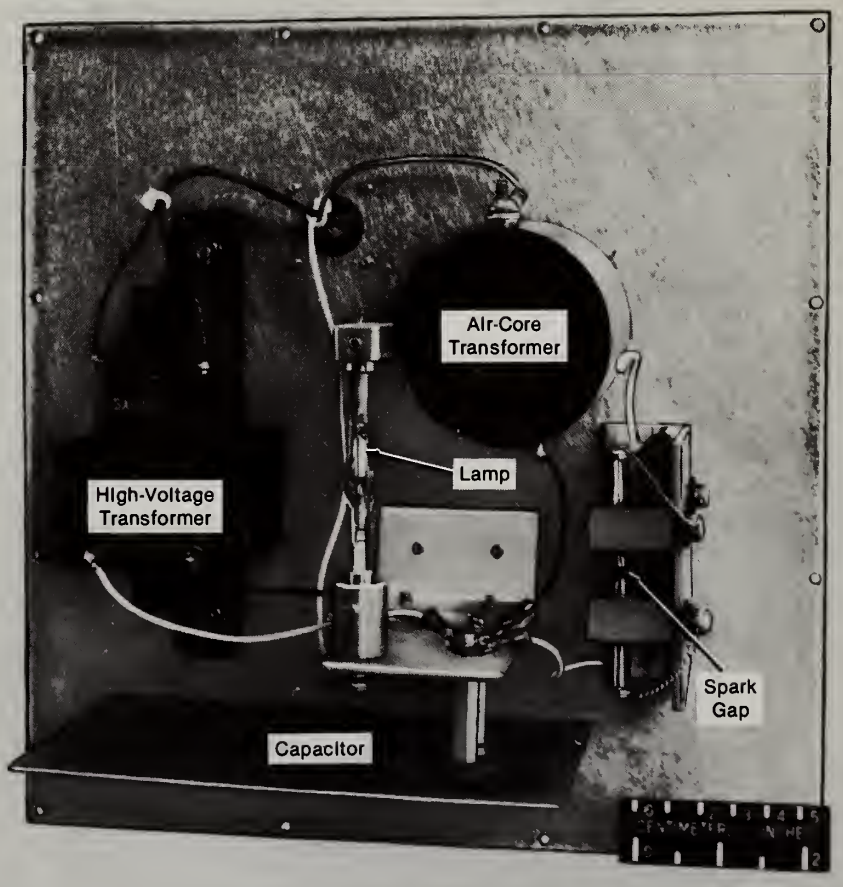

Figure 2. This **View From the Rear of the Lamp Housing** shows the placement of components, including the new capacitor.

temperature and −160 °C. The lamp was started, and the operation was verified at each change in temperature of 20 °C. The complete shadowgraph system was installed in the plenum chamber of the NTF and functioned without failure.

The design is simple, and this type of capacitor should be easy for any printed-circuit-board facility to fabricate. The design is suitable for any small-capacitance, high-voltage capacitor, whether operating at low or high temperature.

This work was done by David B. Rhodes, Stephen B. Jones, and John M. Franke of **Langley Research Center.**

LAR-13714 /TN

FOR ADDITIONAL INFORMATION: *Contact: Director, Technology Transfer Division, P.O. Box 8757, BWI Airport, MD 21240; (301) 621-0100 Ext. 241*

REFER TO THE NUMBER LISTED AT THE END OF THIS ARTICLE

NASA Tech Brief
National Aeronautics and
Space Administration

More on the Decoder-Error Probability of Reed-Solomon Codes

An explicit expression for the probability of error is derived.

A paper extends the theory of the decoder-error probability for linear maximum-distance separable (MDS) codes. This general class of error-correcting codes includes the Reed-Solomon codes, which are important in communications with distant spacecraft, in military communications, and in the compact-disk recording industry. Advancing beyond previous theoretical developments that placed upper bounds on decoder-error probabilities, the author derives an exact formula for the probability $P_E(u)$ that the decoder will make an error when u code symbols are in error.

In this paper, by using the principle of inclusion and exclusion, the formula for the number of code words of Hamming weight u in a linear MDS code is derived. This idea is extended to derive a more-complicated general formula for the number of decodable code words of Hamming weight u. Some combinatorial theorems are then invoked to obtain a simplified weight-distribution formula. The formula is then used to calculate the numbers of decodable words in a (4,2) MDS code over GF(5) with $t = 1$ and in a (6,3) MDS code over GF(4) with $t = 1$ (where t = the number of errors that the code can correct).

By assuming that the decoder is a bounded-distance decoder and that all error patterns of Hamming weight u are equally probable, the exact decoder-error probability $P_E(u)$ is derived using the weight-distribution formula of the number of decodable words. It was shown in an earlier paper that $P_E(u)$ is the ratio of the number of decodable words of Hamming weight u to the number of words of Hamming weight u in the whole vector space.

At this point, the author introduces Q, the probability that a completely-random error pattern will cause a decoder error. It is shown that as u becomes large, $P_E(u)$ approaches Q — more specifically, that the upper bound on $|P_E(u)/Q - 1|$ decreases nearly exponentially with u as u increases. The paper concludes with the important examples of $P_E(u)$'s of the (255,223) NASA code and the (31,15) JTIDS code.

This work was done by Kar-Ming Cheung of Caltech for **NASA's Jet Propulsion Laboratory**. *"More on the Decoder Error Probability for Reed-Solomon Codes."*
NPO-17467/TN

FOR ADDITIONAL INFORMATION: *Contact: Director, Technology Transfer Division, P.O. Box 8757, BWI Airport, MD 21240; (301) 621-0100 Ext. 241*
REFER TO THE NUMBER LISTED AT THE END OF THIS ARTICLE

NASA Tech Brief
National Aeronautics and Space Administration
NASA's Jet Propulsion Laboratory, Pasadena, California

Optical Receivers With Rough Reflectors

A postdetection processor analyzes signals to reconstruct the transmitted message.

A proposed receiver for optical communications would use a rough reflector instead of the diffraction-limited reflector customarily thought to be necessary for such systems. The rough reflector would collect and focus the optical signal. The other receiver components include a narrow-passband optical filter to reject out-of-band background radiation, a spatial filter to limit the receiver field of view, an optical-detector array (typically two concentric detectors), and a postdetection processor to reconstruct the transmitted message (see figure).

In price and performance, rough-reflector receivers are expected to be competitive with receivers using diffraction-limited optics, when large-aperture reflectors are required and background noise is not too high. A diffraction-limited reflector provides the greatest protection against background noise because the receiver field of view can be minimized. However, a large diffraction-limited reflector is difficult and costly to construct.

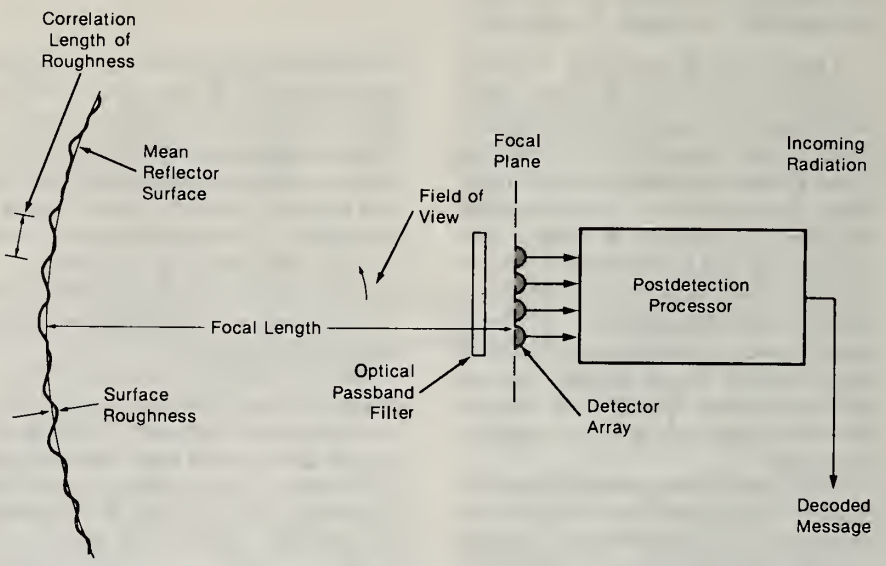

An **Optical Receiver With a Rough Reflector** rely on spectral filtering, spatial filtering, and postdetection signal processing to achieve performance nearly equivalent to that of a receiver with a diffraction-limited reflector.

The error probabilities for a receiver employing a rough reflector depend on the average signal and background counts, which in turn depend on the reflector rms (root mean square) surface deviation (surface roughness), the average correlation length of the surface deviation, the reflector aperture, and the receiver field of view. The error probabilities must be optimized to achieve the best performance as the other parameters are changed. In the absence of background radiation, only one detector is required, and the only drawback in using a rough reflector is that the larger field of view required for a given performance level increases the chance that signal sources other than the intended one might enter the field of view.

The degradation, induced by noise, in the performance of a rough reflector can be viewed as a loss of effective collecting aperture. The effective diameter can be expressed as the diameter of a diffraction-limited reflector of equivalent performance. For a rough reflector having an aperture diameter of 20 m, a surface roughness of 2 μm, and a correlation length of 1.4 μm in a receiver operating at a symbol error probability of 10^{-5}, the effective aperture diameter decreases to 10 m as the background noise increases from 0 to 0.1 counts per picosteradian.

For a signal with a circularly-symmetric intensity distribution emanating from a pointlike source, the receiver can be optimized by partitioning the field of view into two concentric regions, each of which contains an independent detector. In addition to the background noise, one detector is designed to receive a significant portion of the signal in the central diffraction ring, while the other is included to receive a significant portion of the signal scattered out of the central diffraction ring. The output signal is computed using a decision function involving weighted sums of the two detector signals.

This work was done by Victor A. Vilnrotter of Caltech for **NASA's Jet Propulsion Laboratory**. *NPO-16664/TN*

FOR ADDITIONAL INFORMATION: *Contact: Director, Technology Transfer Division, P.O. Box 8757, BWI Airport, MD 21240; (301) 621-0100 Ext. 241*
REFER TO THE NUMBER LISTED AT THE END OF THIS ARTICLE

NASA Tech Brief
National Aeronautics and Space Administration
NASA's Jet Propulsion Laboratory, Pasadena, California

Protection Against Brief Interruptions of Power

A rotating-machine system would bridge gaps of a few cycles in utility power.

A proposed rotating standby power system would compensate for brief interruptions in the commercial power supply. The system would furnish a few cycles of alternating current from its stored rotational energy. It would protect equipment vulnerable to brief losses of power; for example, it would prevent computers from erroneously suppressing or adding bits to the data being handled at the moment of a power failure.

Although "uninterruptible" power supplies make up for low power-main voltages by employing synchronous inverters across the mains and provide power as long as their batteries hold out, they are expensive. The proposed rotary standby system may be more economical when interruptions last no more than a few cycles.

The standby system could include a synchronous motor, alternator, or condenser. It would operate in synchronism with the power-main voltage. It would run on energy furnished by the mains, which also supply the load composed of computers, air-conditioning, lighting, and other equipment.

The synchronous machine would have to be large enough to drive the load for the maximum expected duration of an interruption in power without slowing down appreciably. The proper size would be determined from the total energy needed by the load during the longest expected outage, the energy stored in the rotating mass of the machine, and the speed-versus-voltage characteristics of the unpowered but loaded machine.

So that the entire system that includes the machine presents a favorable power factor to the utility lines, its phase angle would be adjusted by standard power-factor controllers. The adjustment would lower electricity bills by reducing — or even canceling — the reactive volt-amperes drawn by the load. However, the phase angle between the line and the machine should not be made so large that it produces a large phase shift when the line drops out and the machine takes over. Such a shift could disturb some types of power supplies, especially in single-phase applications.

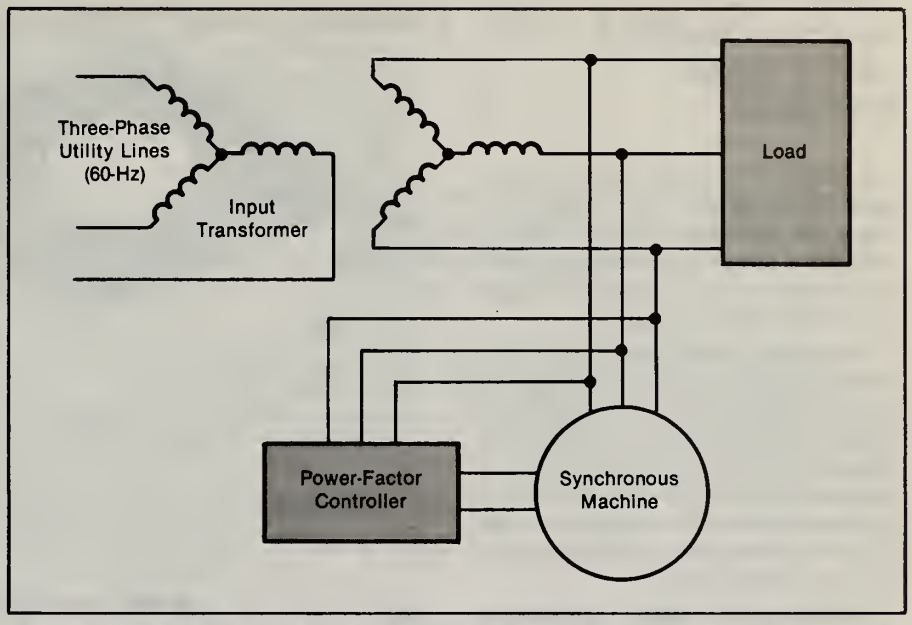

A **Synchronous Machine Idles** on power from a three-phase utility line. If the utility power ceases, the synchronous machine supplies power to the load for a few cycles.

To demonstrate the concept, tests were run on a 15-kW, 18.7-kVA generator connected as a synchronous condenser and standby power source. The unit was operated with and without a flywheel attached. The time in 60-Hz alternating-current cycles was measured from the instant the line power was interrupted until the generator voltage dropped to 422 V (88 percent of its rated output). With the flywheel, that time proved to be ample for brief outages, with a worst-case value of 2.2 cycles under full load at unity power factor.

This work was done by Theodore A. Casad of Caltech for **NASA's Jet Propulsion Laboratory**. *NPO-16768/TN*

FOR ADDITIONAL INFORMATION: *Contact: Director, Technology Transfer Division, P.O. Box 8757, BWI Airport, MD 21240; (301) 621-0100 Ext. 241*
REFER TO THE NUMBER LISTED AT THE END OF THIS ARTICLE

NASA Tech Brief
National Aeronautics and Space Administration
NASA's Jet Propulsion Laboratory, Pasadena, California

Spinner for Etching of Semiconductor Wafers

An ordinary electric-fan motor is adapted to a new use.

A simple, inexpensive apparatus (see figure) coats semiconductor wafers uniformly with hydrofluoric acid for etching. The apparatus is made in part from a small commercial electric-fan motor. It features a bowl that collects the acid.

The blades, 3 to 4 in. (7.6 to 10.2 cm) in diameter, are removed from the fan assembly. A cylindrical Teflon (or equivalent) supporting platform, 2 in. (5.1 cm) in diameter, is mounted on the hub of the motor. The acid-collecting bowl is made from two polyethylene beakers. The smaller one, 2 in. (5.1 cm) in diameter, is fused inside the 4 in. (10.2 cm) diameter beaker.

A silicon wafer is placed on the platform and centered on the axis; then the motor is switched on. As the wafer spins, drops of hydrofluoric acid are applied from a syringe. Centrifugal force spreads the acid across the wafer in a fairly uniform sheet. The wall of the bowl catches the drops of acid as they fly off the edge of the wafer. The unit operates at a speed of 3,600 r/min.

This work was done by Frank Lombardi of Caltech for **NASA's Jet Propulsion Laboratory**. *For further information, Circle 105 on the TSP Request Card.*
NPO-16912

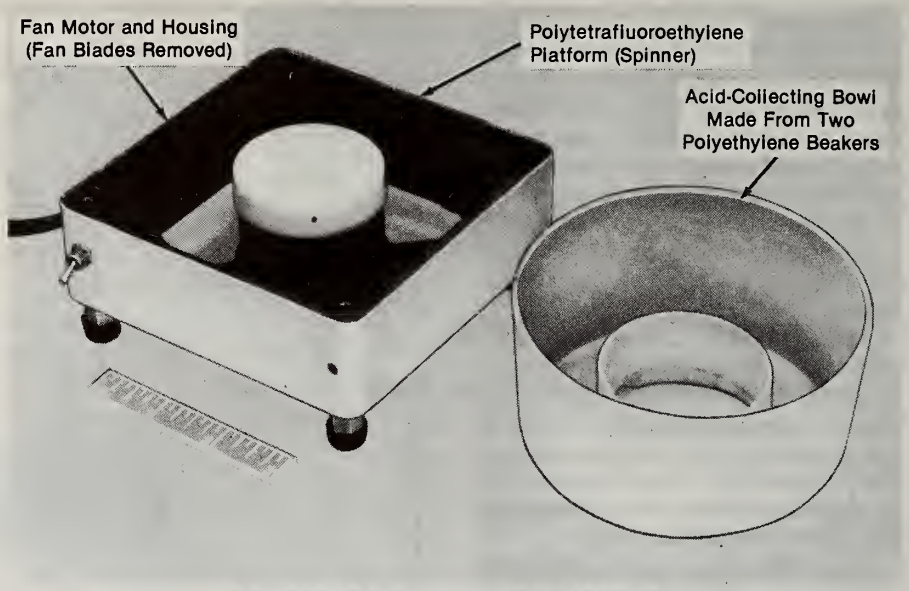
Fan Motor and Housing (Fan Blades Removed)
Polytetrafluoroethylene Platform (Spinner)
Acid-Collecting Bowl Made From Two Polyethylene Beakers

SPINNER ASSEMBLY WITH VESSEL REMOVED

VESSEL INSTALLED OVER SPINNER

The **Fan Motor and Housing** form the basis of a device that etches semiconductor wafers. A bowl collects the used etchant.

FOR ADDITIONAL INFORMATION: *Contact: Director, Technology Transfer Division, P.O. Box 8757, BWI Airport, MD 21240; (301) 621-0100 Ext. 241*
REFER TO THE NUMBER LISTED AT THE END OF THIS ARTICLE

Technology Assessment
U.S. Air Force

Electrostatic Discharge Susceptibility Data VZAP-2 Diskette Version

The Reliability Analysis Center is announcing the diskette version of the new RAC publication, VZAP-2, "Electrostatic Discharge Susceptibility Data." The diskette version of VZAP-2 is intended to complement the hardcopy version.

VZAP-2 contains a list of integrated circuits, discrete semiconductors and passive devices, compiled by the Reliability Analysis Center, which have been assigned an ESD susceptibility classification based on MIL-STD-1686A classification guidelines and actual test data.

The software package contains the data used to generate the VZAP-2 document in a database which is accompanied by a data access program and a user manual. The user accessprogram allows the user to retrieve VZAP-2 data by specifying a search criteria consisting of any combination of the contained information, such as partnumber, manufacturer or device type.

The package is designed to operate on an IBM PC/XT®, PC/AT® or equivalent, operating under DOS 2.10 or later. Hardware requirements are 384K of RAM and a Fixed Disk. The data file requires 1.8M of disk space while the access program requires 250K.

The cost for the diskette version is $185.00. Non-U.S. orders, add $15.00 for shipping and handling.

For Additional Information, contact:

Reliability Analysis Center
P.O. Box 4700
Rome, NY 13440-8200
(315) 330-4151

NIST Technology Update

National Institute of Standards & Technology
(Formerly the National Bureau of Standards)
U.S. Department of Commerce, Gaithersburg, MD 20899

Waveguides and Fibers

NIST continues to expand its capabilities for making optical measurements to support the communications industry. Two recent reports deal with fiber and waveguide measurements. The first Group Index and Time Delay Measurements of a Standard Reference Fiber (NBSIR 88-3091), discusses optical means for precision length measurements of single-mode optical fibers at a wavelength of 1300 nanometers. With this method a 7-kilometer fiber can be measured to within 2 meters. Reference test fibers with well-characterized length and transmission properties are used by NIST to verify distance measuring accuracy and attenuation accuracy of optical time-domain reflectometers. The second report, System for Measuring Optical Waveguide intensity Profiles (NBSIR 88-3092), discusses a computer-controlled system for measuring the intensity profile of optical waveguides. Knowledge of the intensity profile indicates the shape of the waveguide and therefore the degree to which light can be coupled to the guide from an optical fiber.

FOR ADDITIONAL INFORMATION: Both reports are available from Jo Emery, Division 104, NIST, Boulder, Colo. 80303; telephone: 303/497-3237.

NASA Tech Brief
National Aeronautics and Space Administration
NASA's Jet Propulsion Laboratory, Pasadena, California

Licensing Opportunity

Chain of Test Contacts for Integrated Circuits

Microcircuit connections between probe pads yield data on the quality of fabrication.

A test structure that forms a chain of "cross" contacts can be fabricated together with large-scale integrated circuits. If necessary, a number of such chains can be incorporated at suitable locations in an integrated-circuit wafer for determination of the fabrication yield of the contacts.

The test structure (see figure) includes a first and a second layer of metal (or heavily doped semiconductor) arranged in thin, meandering strips ending in terminal pads for electrical probing. The strips overlap in cross-like intersections where contacts are made between the layers through "vias" in the intermediate insulating layer. Current is injected at the ends of the chain, i.e. through pads No. 2 and 23. Voltages are measured between pads No. 1 and 4, 3 and 5, etc., up to No. 21 and 24. The ratio of the voltages to the current is a good measure of the ("interfacial") contact resistance, although some parasitic resistance is added by the requirement that the strips must be wider than the contact to allow for misalignment. Progressing along the chain, the cross contacts are designated alternately as "odd" and "even" for convenience in discerning the effects of misalignment on the resistances of the contacts.

In a conventional two-terminal contact chain, one can measure only the total resistance of all the contacts in the chain. If the number of contacts is large, measurements of a number of chains yield only limited statistical data about the quality of fabrication, and the measurement of one chain can be insensitive to unacceptably high resistance in one or a few contacts. However, in the new structure, the resistances of individual contacts can be determined: In addition to making it possible to identify local defects, it enables the generation of statistical distributions of contact resistances for the prediction of the "parametric" contact yield of the fabrication process.

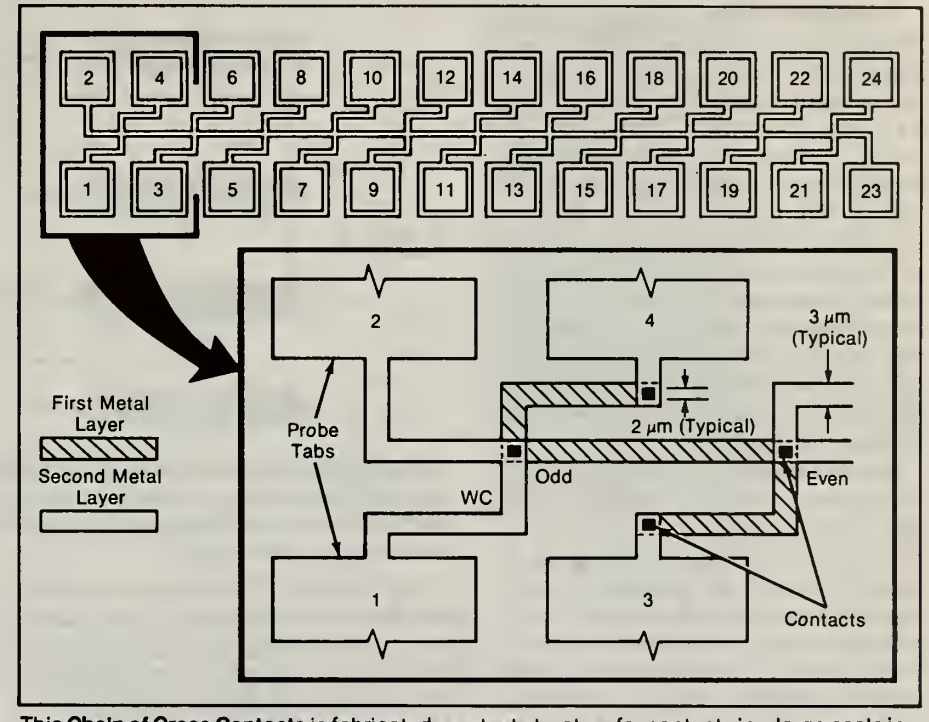

This **Chain of Cross Contacts** is fabricated as a test structure for contacts in a large-scale integrated circuit. Four-point resistances are measured to obtain statistical data on the quality of contact fabrication.

Two prototype wafers contained 40 test structures like the one shown in the figure. The contact resistances of each wafer had bimodal distributions — one mode for the even contacts and another mode for the odd contacts. This bimodality was attributed to a misalignment of the odd contacts that was observed under a microscope. However, if one plots the contact conductance G (i.e., the inverse of the resistance) on normal probability paper, then both modes extrapolate to similar probabilities Y_o at $G = 0$. The average Y_o is a convenient measure of the parametric contact yield.

This work was done by Udo Lieneweg of Caltech for **NASA's Jet Propulsion Laboratory.**

This invention has been patented by NASA (U.S. Patent No. 4,725,773). Inquiries concerning nonexclusive or exclusive license for its commercial development should be addressed to the Patent Counsel, NASA Resident Office-JPL Refer to NPO-16784/TN

Jet Propulsion Lab.
NASA Resident Office
Technology Utilization Officer: Gordon S. Chapman
Mail Stop 180-801
4800 Oak Grove Drive
Pasadena, CA 91109
(818) 354-4849
Patent Counsel:
Paul F. McCaul
Mail Code 180-801
4800 Oak Grove Drive
Pasadena, CA 91109
(818) 354-2734
Technology Utilization Mgr. for JPL: Norman L. Chalfin
Mail Stop 156-211
4800 Oak Grove Drive
Pasadena, CA 91109
(818) 354-2240

FOR ADDITIONAL INFORMATION: *Contact: Director, Technology Transfer Division, P.O. Box 8757, BWI Airport, MD 21240; (301) 621-0100 Ext. 241*
REFER TO THE NUMBER LISTED AT THE END OF THIS ARTICLE

NASA Tech Brief
National Aeronautics and Space Administration
Marshall Space Flight Center, Alabama

Position-and-Direction Sensor for Light Beams

A beam from a spurious source could be detected.

A proposed optoelectronic sensor would measure both the position and the direction of incidence of a laser beam or other narrow beam of light. A conventional sensor used to measure the direction of incidence contains one position-sensitive photodetector or a linear array of photodetectors. The measured position of incidence of the beam on the array, in combination with an assumption as to the point of origin, is used to infer the direction of incidence. However, when the assumption is incorrect (for example, when stray light strikes the detector), then the position of incidence is no longer a true measure of the direction of incidence.

The new sensor would be part of a robotic welding system in which a laser beam is reflected from the pool of molten metal and monitored by a lateral-position sensor. In this system, it is necessary to distinguish between the true reflected beam and spurious light and to measure the direction of the true reflected beam. To provide an unambiguous measurement of both the lateral position and the direction of the incident beam, the proposed sensor would include two position-sensitive photodetectors or linear arrays of photodetectors.

This incident beam of light would strike detector 1 at position x_1 and detector 2 at position x_2, as shown in the figure. Provided that the plane of incidence coincides with the plane of the figure, x_1 and x_2 can be expressed as slightly complicated functions of the angle of incidence (ϕ), the lateral position of incidence (y), the angle of the beam splitter (α), the length of the detectors (M), the longitudinal distance between the detectors (L), and the index of refraction (n) of the glass or other prism material.

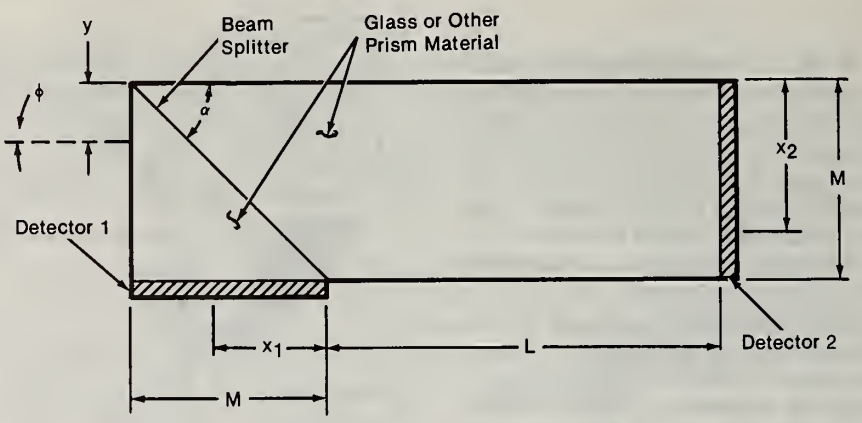

The Position-and-Direction Sensor would split an incident beam of light into two beams and measure their positions of incidence x_1 and x_2. The position y and direction ϕ of the incident beam can be calculated from x_1 and x_2. The sensor could be made as a rigid unit that would be resistant to misalignment.

Because α, L, M, and n are fixed and known in advance, the equations can be solved for the desired quantities ϕ and y in terms of the measured positions of incidence x_1 and x_2. The position outputs of the photodetectors could be digitized and processed continuously to obtain real-time indications of the lateral position and direction of the beam of light.

This work was done by Matthew A. Smith of Rockwell International Corp. for **Marshall Space Flight Center.**
MFS-29275/TN

FOR ADDITIONAL INFORMATION: *Contact: Director, Technology Transfer Division, P.O. Box 8757, BWI Airport, MD 21240; (301) 621-0100 Ext. 241*
REFER TO THE NUMBER LISTED AT THE END OF THIS ARTICLE

NASA Tech Brief
National Aeronautics and Space Administration
NASA's Jet Propulsion Laboratory, Pasadena, California

Licensing Opportunity

Timing Sampler for Delay Measurements

One chip contains delay chains and associated testing circuits.

An integrated circuit called a timing sampler is used to measure delays in complementary metal oxide/silicon logic gates, as part of the system described in the preceding article. The circuit chip contains chains of inverters and metal traces having the minimum parasitic delays (delay chains), circuits to compare pulse timings, and an output multiplexer (see Figure 1). The timing sampler enables delay measurements for both positive and negative logic-level transitions by use of a variety of circuit geometries representing tentative practical designs.

There are 128 delay chains, eight of which are metal traces. Each of the remaining 120 chains is a series of 40 inverters. The chains differ in the sizes and shapes of the transistors in the inverters and in the inverter loadings: The n-channel (pulldown) transistors have widths of 3, 4.5, 6, 9, and 12 μm. The p-channel (pullup) resistors and the pulldown transistors have the same lengths, the values being 3, 6, 9, and 12 μm. The ratios of the widths of the pullup transistors to those of the pulldown transistors are 1, 1.5, and 2. In 60 of the delay chains, loads are connected to the out-

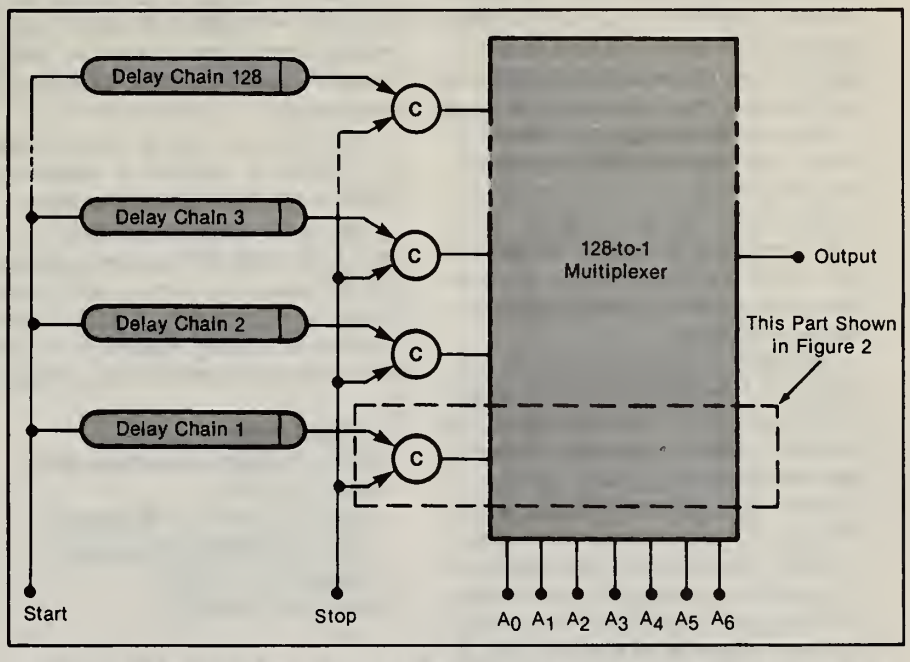

Figure 1. The **Timing Sampler** is an integrated circuit that includes metal traces and inverter chains to be tested for signal-propagation delays. The circuit chip also includes timing comparators (C-elements) and a computer-controlled multiplexer that connects the C-element outputs to the computer one at a time.

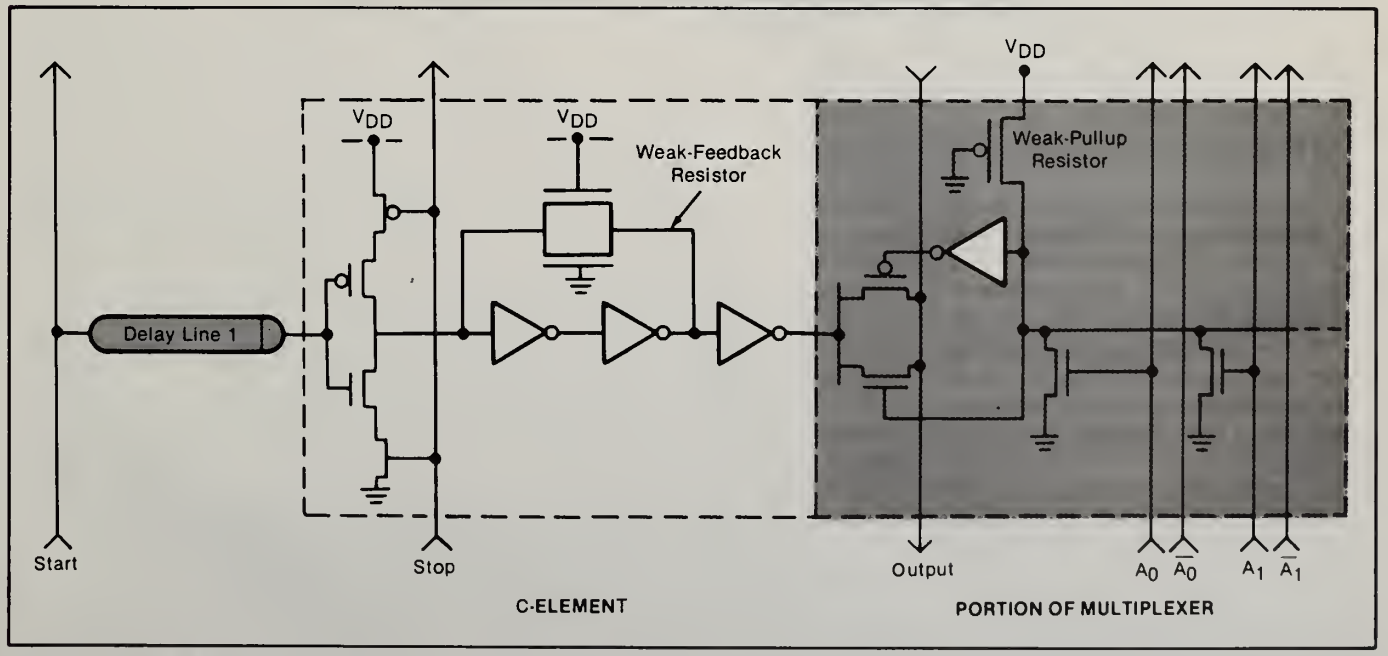

Figure 2. A **C-Element** is a bistable circuit with hysteresis. It is used as a timing comparator because its output depends on whether the "start" or the "stop" pulse arrives first.

put of every other inverter to simulate a fanout of two for each inverter pair. The input ends of all the delay chains are connected to a common input "start" line.

At the output end of each delay chain is a bistable circuit called a "C-element" (see Figure 2), which has two input terminals and one output. A C-element of this type is constructed with the output of a three-input majority circuit connected back to one input. One C-element input is connected to a common input "stop" line; the other input is connected to the output of the last inverter in the chain. The latter input is specially designed to provide the same load to the last inverter as that connected to the other inverters in the chain, so that the delay of the last inverter is the same as those of the preceding inverters. (Delay is a function of loading.)

The output of each C-element is connected to a 128-to-1 multiplexer, the output of which is the timing-sampler output. The C-element exhibits hysteresis: Its output logic state becomes zero when both inputs are zero, or one when both inputs are one; otherwise, the output remains in its previous state. The output transitions depend on which of the two input signals arrives first: the "stop" pulse or the "start" pulse, which has been delayed by propagation through the delay chain.

The timing sampler is used with other equipment that adjusts the interval between the "start" and "stop" pulses until both pulses arrive at the C-element input at the same time, as indicated by the C-element output signal. In a series of such measurements, an experimental timing sampler performed as expected. When correlated with the circuit geometries, the measurements showed that the inverter delay is inversely proportional to the transistor width.

This work was done by Brent R. Blaes and Martin G. Buehler of Caltech for **NASA's Jet Propulsion Laboratory**.

Title to this invention, covered by U.S Patent No. 4,688,947 has been waived under the provisions of the National Aeronautics and Space Act [42 U.S.C. 2457(f)]. Inquiries concerning licenses for its commercial development should be addressed to

Edward Ansell
Director of Patents and Licensing
Mail Stop 301-6
California Institute of Technology
1207 East California Boulevard
Pasadena, CA 91125

Refer to NPO-16645/TN

Jet Propulsion Lab.
NASA Resident Office
Technology Utilization Officer: Gordon S. Chapman
Mail Stop 180-801
4800 Oak Grove Drive
Pasadena, CA 91109
(818) 354-4849
Patent Counsel: Paul F. McCaul
Mail Code 180-801
4800 Oak Grove Drive
Pasadena, CA 91109
(818) 354-2734
Technology Utilization Mgr. for JPL: Norman L. Chalfin
Mail Stop 156-211
4800 Oak Grove Drive
Pasadena, CA 91109
(818) 354-2240

FOR ADDITIONAL INFORMATION: *Contact: Director, Technology Transfer Division, P.O. Box 8757, BWI Airport, MD 21240; (301) 621-0100 Ext. 241*
REFER TO THE NUMBER LISTED AT THE END OF THIS ARTICLE

Energy

0736 Automatic Monitoring Could Cut Costs of Emergency Power

0737 Conversion of Gasoline-Powered Buses to Diesel-Powered Buses

0738 Lithium Battery (Licensing Opportunity)

0739 Multihundred-Kilowatt Rotary Electrical-Transfer Device—Roll rings decrease friction and electrical losses.

Sandia National Laboratory

Automatic Monitoring Could Cut Costs of Emergency Power

Sandia National Laboratories has developed a system that could reduce the need for additional backup power equipment by automatically monitoring the starting ability of emergency diesel generators. Researchers believe the system, designed for commercial nuclear power plants, also would be cost effective for large facilities such as hospitals and universities.

The monitoring system was developed for the U.S. Department of Energy as part of an effort to extend the lives of nuclear power plants. The project focuses on predicting performance of equipment as a means of reducing equipment surveillance testing, maintenance, and malfunctions.

The Nuclear Regulatory Commission (NRC), which is responsible for ensuring safety in civilian uses of nuclear materials, requires a plant to shut down if a minimum number of its emergency generators are not operable. The generators range in size from hundreds of kilowatts to almost 10 megawatts and can cost as much as $30 million.

Analyses have shown that some nuclear plants may be required to install additional diesel generators to meet NRC specifications for reliable backup power. However, an engine monitoring system could reduce the need for additional units. It also could extend the lives of a plant's existing generators by reducing the frequency of engine-taxing startup tests. The NRC currently requires nuclear power plants to conduct these tests monthly by starting a generator's engine and running it under load for 24 hours.

"That introduces a lot of wear and tear on the engine," says Hugh Bundy, who is conducting the project at Sandia.

The Sandia monitoring system uses direct sensing and computer analyses to evaluate engine starting ability. It was developed by Sandia's Advanced Nuclear Power Technology Division under the supervision of David D. Carlson. Much of the work was done by Tim DeBey, who is now with the U.S. Department of Interior in Denver, Colo. Bundy took over the project after DeBey left Sandia.

Bundy estimates that the complete monitoring system could be installed for less than $10,000. In many cases, he says, equipment already used to monitor operating engines could be used, further reducing the cost of the system.

The Sandia researchers identified three main types of engine starting problems: unsuccessful or sluggish cranking, nondelivery of fuel to the cylinders, and failures in starting controls such as governors, relays, and solenoids. The system developed at Sandia addresses all of these areas. Sensors mounted in the engine monitor cranking speed, fuel delivery, and operation of speed governors. Performances of other starting controls are inferred by computer analyses of the sensed data.

In order to acquire these data, the engine must turn over as it would in an actual starting operation. This could be done by applying a start signal to the engine and either preventing fuel from reaching the cylinders or preventing the engine from reaching a cranking speed sufficient for ignition. But both of these methods are unacceptable because they could cause future problems with the engine.

Instead, the system monitors performance by applying a start signal of approximately 0.1 second to the engine controls. This very short signal is sufficient to cause the engine to rotate approximately 90 degrees in about 3 seconds. Data picked up by the sensors are plotted on the computer screen during the test and analyzed to see if the engine is operating properly.

The automated prototype system is capable of performing engine tests at intervals from 1 hour to 99 hours. All data collected during these tests is stored and available for transfer to other computers.

The system has been tested with a diesel engine used for emergency power generation at Sandia. Researchers have been consistently able to detect such problems as sluggish governor operation, sluggish air solenoid valve operation, air in fuel lines, blocked fuel lines, low starting air pressure, improper switch settings, closed air valves, failed relays, and failures to reset trip switches.

Meanwhile, no engine problems have been caused by the monitoring through 500 test cycles. Researchers report that the engine actually appears to benefit from the monitoring process since the more frequent cycling of the components reduces moisture accumulation and oxidation.

The engine used in the test has a direct air injection starting system, which causes the engine to rotate by injecting compressed air into the cylinders. Sandia also plans testing engines using the other two common types of starter systems - electric and air turbine starter motors.

FOR ADDITIONAL INFORMATION: Public Information Division, Code 3161, Department of Energy, Sandia National Laboratories, Albuquerque, NM 87185-5800; (505)844-4207. Refer to announcement 24, No. 5.

NCEL
Techdata Sheet

NAVAL CIVIL ENGINEERING LABORATORY
PORT HUENEME, CALIFORNIA 93043

Conversion of Gasoline-Powered Buses to Diesel-Powered Buses

PWC, San Diego operates a fleet of 39 passenger buses ranging in age from 2 to 13 years old. They are in the process of converting thirteen 1980-81 International buses to run on diesel instead of gasoline. Seven of these buses have had their 392-cubic-inch gasoline engines replaced with Navistar (formally International) 6.9-liter diesel engines and have been running for a year. The conversions are done by a contractor. The statistics on the conversions are:

- The conversion costs $10,000. This includes the engine, new accessories, a new radiator, new bearings and labor. Navistar provides a complete conversion kit designed for S series Navistar buses.

- The conversion takes 2 to 3 weeks.

- Mileage increases from 3 mpg for gasoline to 10 mpg for diesel.

- Driver acceptance of the diesel buses is very positive. The converted diesel buses at PWC, San Diego are driven twice as much as the gasoline buses. Drivers prefer the diesel buses because they have more power and are more reliable. The diesel buses are also preferred for long trips.

- The downtime for the gasoline buses is 6 to 7%, while the downtime for the diesel buses is 3%.

- Maintenance of a diesel converted bus is 25% that of a similar age gasoline bus that has already gone through several engines.

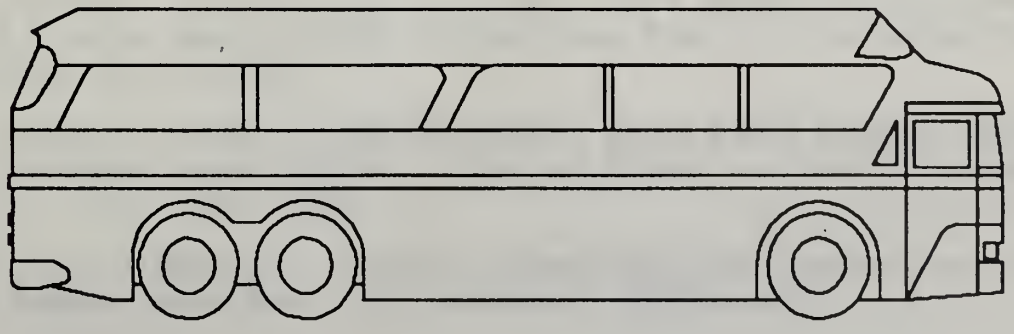

- FY88 budgeting costs are 74 cents per gallon for gasoline and 60 cents per gallon for diesel.

- A new diesel bus costs approximately $30,000.

The program has been extremely successful. The buses at PWC, San Diego average 30,000 miles per year. The fuel cost for a gasoline bus is $7,400/year as compared with $1,800/year for a diesel bus at present fuel rates. Because of the increased fuel savings and decreased maintenance costs, the conversion is paid for within one year. The life of the bus is also extended 5 to 6 years. This is a very practical alternative to purchasing a new bus.

For Additional Information:

To discuss this effort further, contact:

Jerry Dummer
Code L03C
Facilities Engineering Support Office
Naval Civil Engineering Laboratory
Port Hueneme, CA 93043
(805) 982-4070

Refer to Techdata sheet 89-02/TN

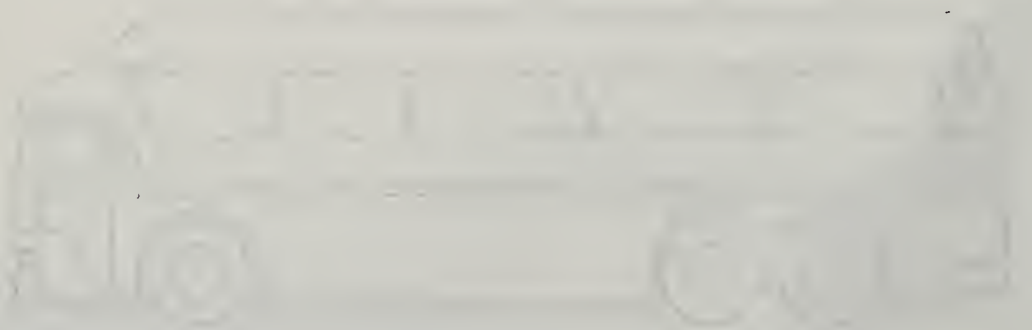

U.S. Navy Fact Sheet

Licensing Opportunity

Lithium Battery

Since the early sixties, there has been a great deal of research and development work seeking the "ideal lithium battery." The effort has centered on achieving high energy and power density. Two oxysulfur cathode systems, Li/SO2 and Li/SOCl2, assumed importance during the seventies. They have proven to be very successful in yielding high energy density with excellent discharge characteristics. However, safety problems persisted with these systems. Under some conditions, they are prone to fires and explosions with the venting of toxic gases. The objective of NSWC's task was to investigate various alternatives to current lithium systems that are of equal energy density, but would be much safer and less toxic.

One approach to finding alternative oxidants is to explore fluorochlorocarbons whose properties include low toxicity and/or a relatively low shock sensitivity toward lithium. This seems a likely choice since many halocarbons have high calculated free energies for their reaction with lithium.

A wide range of commercially available halocarbon liquids has been characterized as potential cathode materials for safer Li batteries. The most promising halocarbon identified in the investigation is 1,1,2,2,-tetrachloroethane, CHCl2CHCl2 (TCE), whose catalyzed voltages were 2.3-2.4V at 1mA.cm -2 and 2.0-2.1V at 5mA.cm-2.

Discharges performed on Li/CHCl2CHCl2-THF,1M LiAsF6 cells where the amount of electrolyte was limited, indicated that capacities equivalent to 1.5M LiAlCl4-SOCl2 cell could be achieved when the halocarbon/THF ratio equaled 69/31 volume %.

It is further noted that lithium halocarbon cells should be considerably safer than many existing lithium systems. Although CHCl2CHCl2 is carcinogenic, it is certainly less noxious and less acutely toxic than SO2 and various sulfur oxychlorides. This is an advantage if a cell should vent in an enclosed space. In addition, the lack of sulfur is considered to be an advantage since under certain conditions sulfur may act with lithium producing thermal runaway conditions.

A resulting product provides for a new non-aqueous high energy lithium battery. The properties of this lithium battery design are: safe storage, does not ignite or explode, does not vent toxic gases, and has a high output voltage and a high storage capacity.

Descriptive Literature:

a. "New Liquid Cathodes for Lithium Batteries," Part A, Halocarbons, K. M. O'Neill, S. D. James, and P. H. Smith, Technical Report TR84-178, Naval Surface Warfare Center, White Oak, MD

b. "A Survey of Halogen - Containing Liquids as Lithium Battery Cathodes," Part I Uncatalized Systems, and Part II: Catalyzed Systems, Journal of Electrochemistry, 13b, 1625, 1631 (1989).

FOR ADDITIONAL INFORMATION: Robert Heindenreich, Naval Surface Warfare Center, 10901 New Hampshire Avenue, Silver Spring, MD 20903-5000; (202)394-4332.

NASA Tech Brief
National Aeronautics and
Space Administration
Lewis Research Center, Cleveland, Ohio

Multihundred-Kilowatt Rotary Electrical-Transfer Device

Roll rings decrease friction and electrical losses.

A roll-ring electrical-power-transfer device is capable of transferring high power (hundreds of kilowatts) through a rotating connection. This roll-ring assembly can transfer up to 500 V at 200 A per circuit, either dc or ac to frequencies of 20 kHz. The roll-ring assembly (see figure) has eight power circuits. An outstanding feature of this design is very low power loss — only 16 W per circuit while transferring 100 kW.

At present, slip rings are the most commonly used devices for transmitting power across a rotating joint. Slip rings can transfer only limited amounts of power. The roll-ring device eliminates sliding friction by using rolling contacts. This allows the unit to rotate with very little torque. The elimination of sliding friction makes possible the transfer of very large amounts of power per circuit with very low losses.

The roll ring has the potential to be one of the major components of the Space Station or any other space program where large amounts of power are required. It is the only known device that can transfer large currents (200 A) per circuit at high voltages (500 V, dc or ac) with very low losses. The roll-ring assembly will allow the Space Station to grow to larger power levels. Also, any terrestrial application requiring power to transfer through a rotating joint with low losses could use the roll-ring technology. It can be used in air or vacuum with no design changes.

This work was done by Peter Jacobson of Sperry Flight Systems for **Lewis Research Center**. *LEW-14269/TN*

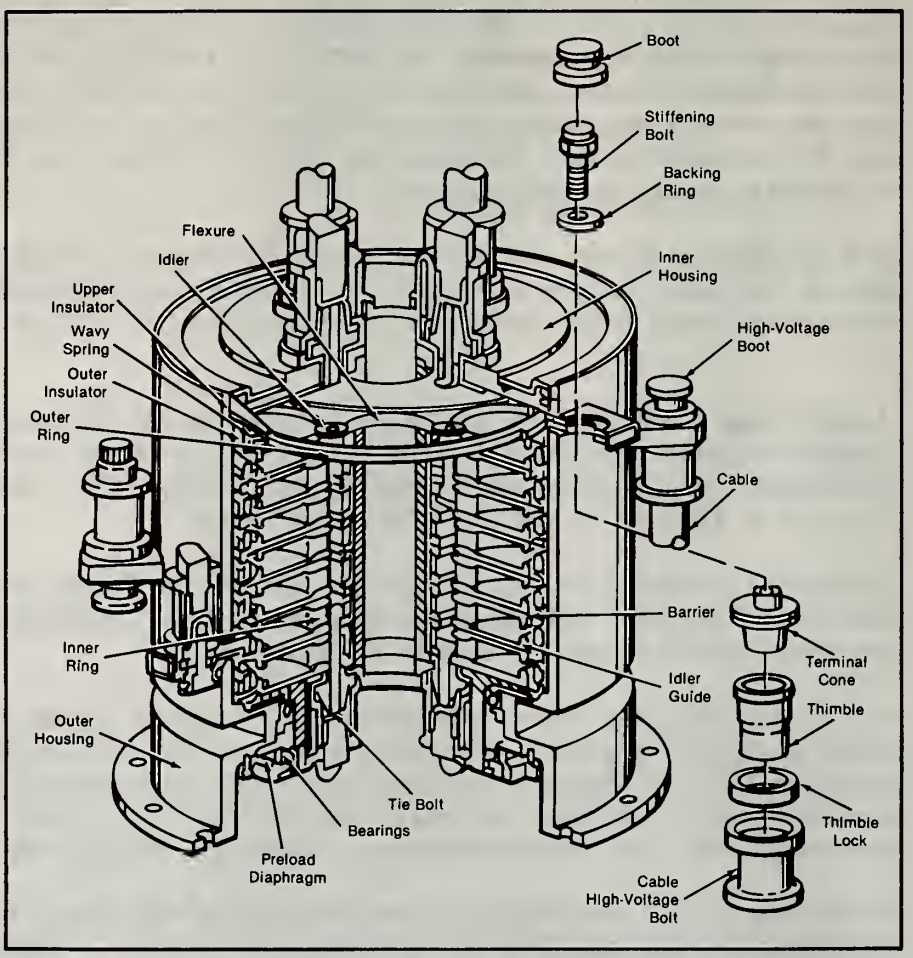

The **Roll-Ring Assembly** uses rolling contacts to transfer electrical power between the rotor and the stator. This eight-circuit assembly dissipates only 16 W while transferring 100 kW.

FOR ADDITIONAL INFORMATION: *Contact: Director, Technology Transfer Division, P.O. Box 8757, BWI Airport, MD 21240; (301) 621-0100 Ext. 241*
REFER TO THE NUMBER LISTED AT THE END OF THIS ARTICLE

Engineering

0740 Chloride-Oxygen Leaching Technique Recovers Metals from Complex Sulfide Ores

0741 Integrity Factor Approach to Mine Pillar Stability Evaluation and Design

0742 Sprayfans Combined with Reverse Sprays Ventilate 40-Foot Cuts

0743 Navy Tests Composite Propeller Shaft

0744 Compact Right-Angle Connector—Part of a stack of adaptive fittings is eliminated.

0745 Correlation Analysis of Vibration Data From Rotary Pumps

0746 Endjoints for Structural Elements—Struts are joined easily and rapidly to make frames. (Licensing Opportunity)

0747 Inspection in Overhead Spaces Containing Asbestos—A simple method saves time and effort.

0748 Ultraclean Radiant Furnace—Cooling of the walls minimizes contamination from outgassing.

0749 Variable-Volume Container—The container expands and contracts according to changes in volume of its solid contents.

Testing & Instrumentation

0750 Filmless X-Ray Inspection Methods—Speeds Aircraft Inspection Onboard Carriers

0751 Monitoring Foundation Response to Subsidence Using a Tiltmeter

0752 New Process Produces Lead from Galena Concentrates Without Pollution

0753 Ultralow-Frequency Through-the-Earth Electromagnetic Fire Warning Alarm System for Underground Mines (Licensing Opportunity)

0754 Techniques for Measuring Stress and Strain

0755 Flight Balance for Skin-Friction Measurements

0756 Measuring Bearing Wear Via Weight Loss—Dimensional changes are estimated from areas, weight losses, and densities.

0757 Miniature Flow-Direction/Pitot-Static Pressure Probes

0758 Nondestructive Inspection of Foam and Multilayer Insulations

Other Items of Interest

0760 Asbestos Management Guide is Available—How to manage asbestos-containing materials until materials are removed

0766 Self-Aligning Robotic End Effector and Receptacle—Congruent surfaces provide alignment for gripping, installation, and removal.

0817 Computing Flutter Boundaries—This program calculates aeroelastic responses of mistuned airfoils.

0818 Using EMATs For Rail Car Wheel Inspection

Technology News

From the Bureau of Mines, United States Department of the Interior

Chloride-Oxygen Leaching Technique Recovers Metals from Complex Sulfide Ores

Objective

Develop a means of recovering metal values from complex sulfide concentrates which improves upon conventional smeltering and hydrometallurgical techniques while eliminating environmental problems with waste residues and emissions traditionally associated with conventional processes.

Background

Complex sulfide ores are significant sources of copper, nickel, cobalt, lead, zinc, gold, and silver. However, current smelting technology is incapable of successfully treating such ore concentrates because of their complex mineralization. In addition, current oxygen pressure leaching technology cannot treat these complex concentrates without using some means to remove iron, arsenic, and antimony from wastes. This is is a costly and time-consuming step.

The Bureau of Mines has developed a technique called chloride-oxygen leaching which is ideally suited to recovering metal values from complex sulfide ores as well as other feed materials such as oxides and scrap metals. This processing technique has proven very effective in extracting such metals as copper, lead, zinc, nickel, cobalt, mercury, bismuth, cadmium, and precious metals from a wide variety of feed materials while eliminating unstable or toxic waste residue.

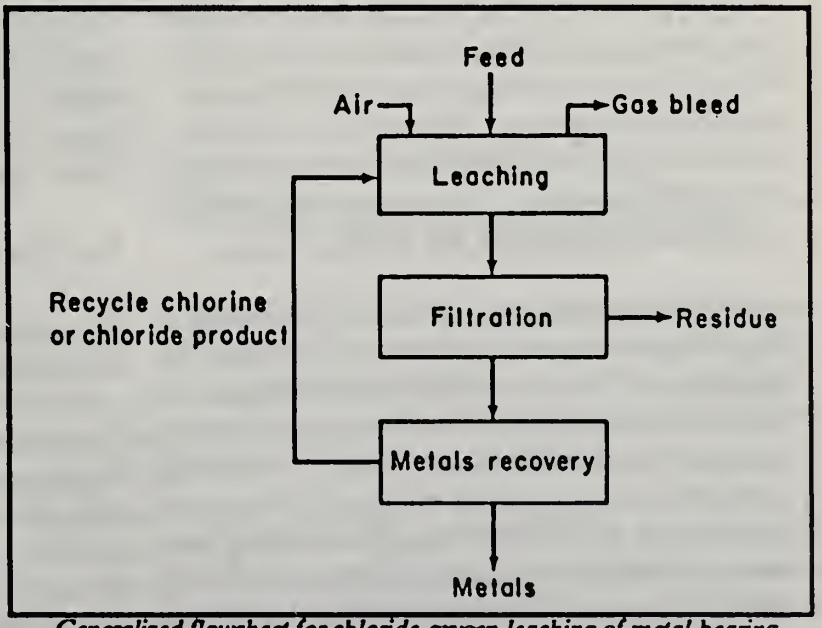

Generalized flowsheet for chloride-oxygen leaching of metal-bearing products.

Chloride-Oxygen Leaching

During chloride-oxygen leaching, valuable metals are solubilized while worthless or toxic impurities are rejected as an extremely stable leaching residue. Leaching and separation of valuable metals from waste products are made in one step within a leaching reactor. Leaching occurs quickly under relatively mild conditions due to a very efficient aeration design of this reactor. The leaching reactor is operated at temperatures between 100° and 120°C under 50 psig of oxygen or compressed air. It is equipped with a high shear gas-solids contacting mechanism. The chloride content within the reactor charge is controlled so that there is only enough chloride to meet the counter ion requirements of the valuable metals. Leaching conditions are adjusted so that no free acid is present after leaching. These conditions cause the waste elements to hydrolyze and completely precipitate from the leaching solution.

Chloride-oxygen leaching has distinct advantages over existing technologies. For one, chloride-oxygen leaching is superior to conventional pressure leaching systems due to the extremely aggressive nature of the leach which allows it to be applied to many minerals, dusts or finely divided scrap. Intense aeration combined with the strong complexing power of chloride provides efficient leaching under very mild pressure oxidation conditions. Even gold has been solubilized in the chloride-oxygen system as long as metals like copper or iron are in their highest oxidation states during the leach.

Another key advantage of the chloride-oxygen leaching technique is that it rejects impurities by hydrolysis. Toxic or worthless elements such as chromium, iron, arsenic, antimony, and aluminum, are removed to below 1 mg/L concentration levels as very stable complex compounds. Because of this, chloride-oxygen leaching may be appropriate for use as a means of profitably cleaning up environmental problems involving heavy metal contaminants as well as a quick and effective means of leaching complex concentrates.

Test Results

The chloride-oxygen leaching technique has been demonstrated to be effective on over 95 percent of over 100 ore concentrates tested. It has been used successfully during laboratory tests to remove metals from grinding sludges, smelter and steel plant flue dusts, cementation products, precious metal ores, and even finely divided superalloy scrap. Minipilot demonstrations were made on high silver complex copper sulfide concentrate, lead concentrate, zinc concentrate, and lead smelter matte. The process is being evaluated on a pilot-scale to treat an arsenic-bearing copper smelter flue dust.

Patent Status

The U.S. Department of the Interior holds several patents on the chloride-oxygen leaching process. These patents include U.S. Patent No. 4,410,496, "Recovery of Metal Values from Complex Sulfides"; U.S. Patent No. 4,053,308, "Recovery of Copper and Silver from Sulfide Concentrates"; and U.S. Patent No. 3,981,962, "Decomposition Leach of Sulfide Ores with Chlorine and Oxygen." For information about these patents or on patent licenses, please write to the Bureau of Mines, Office of Technology Transfer, 2401 E Street, N.W., Mailstop 6201, Washington, DC 20241.

For More Information

For answers to technical questions or for more information about this research, please contact:

Thomas G. Carnahan
Bureau of Mines
Reno Research Center
1605 Evans Avenue
Reno, NV 89512
Tel: (702) 784-5391

Technology News

From the Bureau of Mines, United States Department of the Interior

Integrity Factor Approach to Mine Pillar Stability Evaluation and Design

Objective

Develop a new method for coal mine pillar stability evaluation and design based on pillar load measurements.

Approach

A novel approach to chain pillar stability evaluation and design for longwall coal mining panels has been developed by the Bureau of Mines. The evaluation approach uses an INTEGRITY FACTOR as the criterion for stability. Hydraulic borehole pressure cells developed by the Bureau are used to measure stresses in a pillar for stability evaluation. The results are used to improve the pillar design.

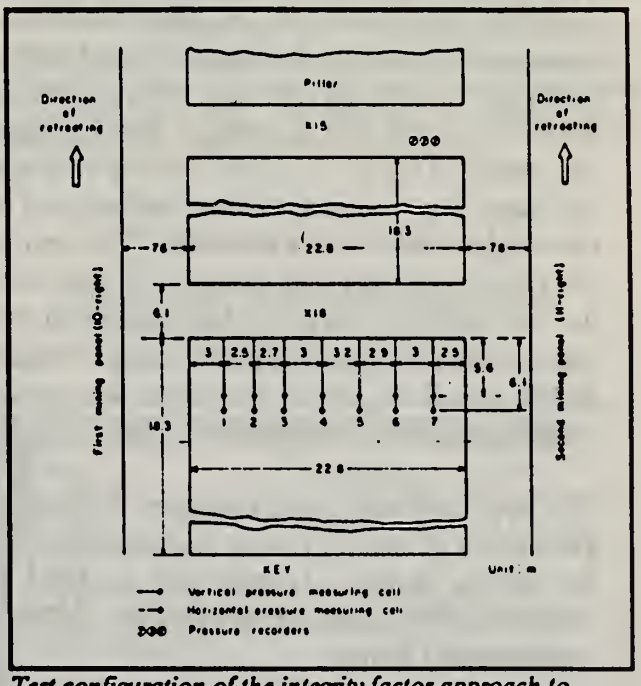

Test configuration of the integrity factor approach to evaluate mine pillar design and stability.

How It Works

Integrity factor is defined as the ratio of the total strength integrated across the critical dimension of the pillar to the total load integrated across the same critical dimension. The pillar strength is calculated from the triaxial compressive strength of the coal determined from laboratory tests using the horizontal stresses measured in situ as confining pressures. The pillar load is calculated from the vertical stresses measured in situ. The biaxial stresses in the pillar are measured by installing two pressure cells in a horiztonal drill hole; one cell is oriented vertically and the other horizontally.

The INTEGRITY FACTORS determined at different stages of the longwall mining process are used to evaluate the long-term stability of chain pillars over their useful life-span. An integrity factor greater than 1 is considered to be

a stable condition, whereas an integrity factor equal to or smaller than 1 is considered to indicate an unstable condition. The chain pillar design is then modified, if necessary, to assure pillar stability during the expected useful life-span based on results of the evaluation.

Test Results

Tests were conducted in a coal mine with approximately 500 m of cover over its retreat longwall mining panels. The longwall panels were developed with a two-entry gateroad system with 22.8-m-wide chain pillars. Seven horizontal holes were drilled into a chain pillar at approximately 3-m intervals across its width. Two borehole pressure cells were installed in each hole: one oriented to measure the vertical stress and one oriented to measure the horizontal stress. Based on the continuous measurement of vertical and horizontal pillar stresses, the transient integrity factors corresponding to different face positions during the longwall retreating process were evaluated. The test results indicated that this chain pillar was stable during the entire period of the first-panel mining, because the minimum value of its integrity factor was 2.55, which exceeded the critical value of 1.

This approach can also be adapted for stability evaluation of barrier pillars and room-and-pillar mining panels. It may also be used for coalburst prediction and prevention studies in underground mines.

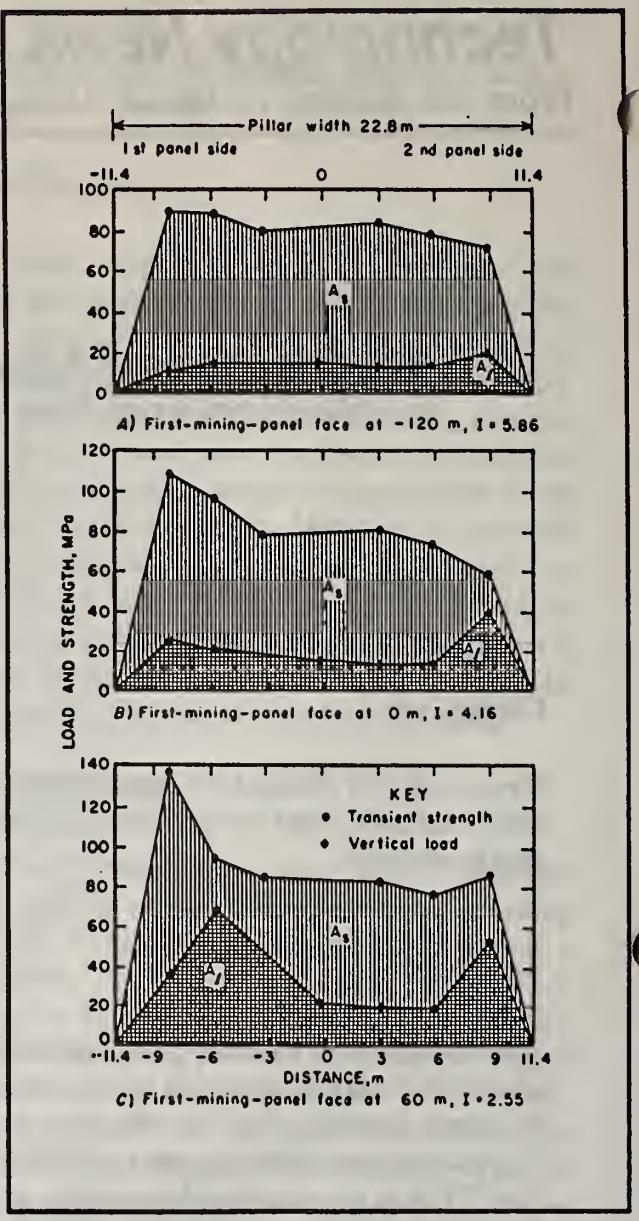

Strength and loading profiles are constructed using this approach, and the transient integrity factors at respective milestone stages of mining are evaluated.

For More Information

Several papers on this subject have been published and presented by the Bureau of Mines at national and international symposia. For information on how to obtain copies of these papers or for answers to technical questions, please contact the Bureau's principal investigator for this research:

Dr. Paul H. Lu
Denver Research Center
U.S. Bureau of Mines
Bldg. 20, Denver Federal Center
Denver, CO 80225
(303) 236-0745

Technology News

From the Bureau of Mines, United States Department of the Interior

Sprayfans Combined with Reverse Sprays Ventilate 40-Foot Cuts

Objective

Provide exhaust face ventilation to remotely-controlled continuous mining machines making extended advances without exposing workers to unsupported roof.

Approach

Modify the sprayfan to move additional air to and from the coal mine face. Unmodified, sprayfans are capable of ventilating the face with 20-foot brattice setbacks. Additional sprays on the rear of the mining machine allow setbacks to be extended up to 40 feet.

How It Works

Remotely-controlled continuous mining machines and automated temporary roof support systems have opened the door to extended cuts in room-and-pillar mining. Cuts of up to 40 feet are possible between place changes and this can significantly increase coal mine productivity. However, the application of these new developments has been limited by the lack of adequate face ventilation technology. The Bureau of Mines has evaluated a new face ventilation system for extended advances up to 40 feet. The new system uses the sprayfan system along with additional forward and reverse pointing sprays. Specifically, the water sprays work in several ways (see the figure):

1. The sprays along the left, intake side of the machine push the intake air along the side of the machine and into the off- curtain corner. This prevents a short circuit of air to the return.
2. The angled front sprays then push face dust and methane across the face and toward the return side of the machine.
3. Finally, a reverse spray on the right rear of the machine boosts air toward the curtain mouth. This prevents the contaminated air from circulating over the top of the machine back to the face.

System Description

Water sprays move air through momentum transfer from the water droplet to the air. To move the most air, hollow cone sprays with an unobstructed free throw are best. Extensive laboratory and field tests show the following locations, spray types and spray angles (from machine centerline) give the best ventilation results:

1. Point 12 front top boom sprays 30° toward the curtain side of the machine and up 10°.
2. If the cutting head extends past the boom width, add 4 sprays, 2 on each side pointed at the cutting head for dust control.

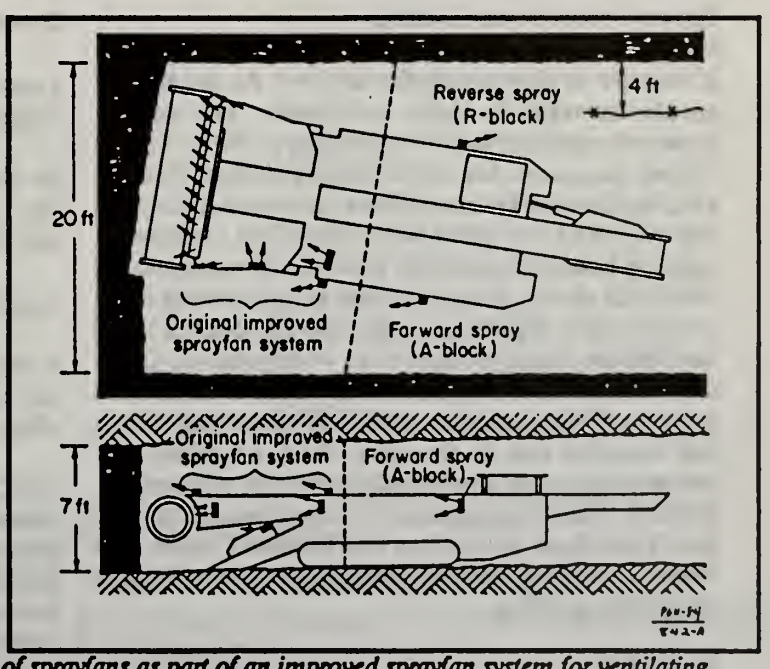

Orientation of sprayfans as part of an improved sprayfan system for ventilating extended advances up to 40 feet.

3. Just outby the hinge point, add 4 sprays on the off angled out 10°, go on the side of the machine. One should be angled up 5°, and the other down 5°. Two sprays mount on top of the machine and are angled up 10°. One should point 0° toward the face, and the other 40° to ward the curtain side. If roof eight is sufficient, elevate this spray 4 to 6.inches above the top surface of the machine.
4. Add 2 sprays on the upper edge of the shovel for under-boom coverage. Orient these sprays 90° and 50° from the face, toward the return. Under boom sprays are important for dust control.
5. Just inby the off-curtain rear of the machine add 2 sprays. Angle them 10° out, one up 5°. See A-block in the figure.
6. At the rear of the machine, closest to the exhaust curtain, add 2 sprays pointing away from the face. Both of these sprays are adjusted 30° out and 0° elevated. See R-block in the figure.
7. The sprays in 5 and 6 above are valved separately. They are activated only after the curtain is past the rear bumper of the machine.
8. A second mirror image system is used if the ventilation curtain is needed on alternating sides of the machine. NOTE: *Make sure both systems are plumbed separately and will not operate simultaneously.*

System Operation and Testing

Successful operation of this system depends on the balance of primary air flow to sprayfan air flow. An unbalanced system can result in higher dust levels. The simplest balance method is to vary the water spray pressure. To help balance the system, first set the primary air flow. Next use a BC dry chemical fire extinguisher (do not use ABC types) and release a burst on the intake side of the machine. A properly balanced system will show the air moving to the off-curtain corner, crossing the face and proceeding to the curtain mouth. Significant circulation of air over the top of the machine means you need more water pressure. Circulation behind the mining machine is indicative of too much pressure. If the circulation paths look correct and there is still excessive dust in the entry, check for intake dust contamination, dust from the flight conveyor or diesel particulates. The sweeping action of the sprayfan results in less dust knockdown at the face and increased return dust levels. Additional water volume under the boom helps to reduce this problem.

Results

Several mines are using this system to ventilate cuts up to 40 feet. Face Ventilation Effectiveness (FVE) factors were determined through tracer gas studies. These results show that the ventilation effectiveness of this system exceeds that of a comparable 10-foot exhaust system and conventional water sprays for all mining positions and setbacks up to 40 feet from the face.

Some mines have obtained MSHA variances for 40-foot exhaust curtain setbacks, others for 30 feet using a 10-foot extensible section. At setbacks over 40 feet, the underground tests show that shuttle car movements disrupt the airflow patterns and result in less effective ventilation. Curtain-type ventilation works better than tubing. None of these mines have significant methane gas to control.

Idle faces are poorly ventilated using exhaust systems and further curtain setbacks can aggravate this situation. One method to successfully ventilate an idle face is to wing the exhaust curtain across the entry to create a blowing jet. Sprayfans are inexpensive to build and can be easily installed as a retrofit to old machines or factory installed on new machines.

Patent Status

The Department of the Interior is not applying for a patent of this technology.

For More Information

Four reports are available for additional information about the sprayfan system. They are:

1. "Exhaust Ventilation of Deep Cuts Using a Continuous Mining Machine," BuMines RI 8992, 1985.
2. "Extended Advance Ventilation Systems," a paper presented at the 2nd U.S. Mine Ventilation Symposium, Reno, NV, Sept. 1985.
3. "Improved Diffuser and Sprayfan Systems for Ventilation of Coal Mine Working Faces," Contract No. JO113010, Foster-Miller Inc., NTIS PB 86-168440, July 1985.
4. "Deep Cut Mine Face Ventilation," Contract No. HO348039, Foster-Miller, Inc., January 1988.

A copy of each report or more technical information may be obtained by writing to the technical project officer for this research:

Jon C. Volkwein
Bureau of Mines
Pittsburgh Research Center
P.O. Box 18070
Cochrans Mill Road
Pittsburgh, PA 15236
or telephone him at (412) 892-6689

NAVY
Domestic Technology Transfer Fact Sheet

Navy Tests Composite Propeller Shaft

Under an exploratory development program sponsored by the Office of Naval Technology, the David Taylor Research Center, Bethesda and Annapolis, Maryland, has developed a fiber-reinforced plastic propeller shaft. Conventional steel propulsion shafts are highly conductive paths for transmitting both noises and magnetic signals to the water environment. When detected by underwater sensors, these signals and noises provide an identifing signature of the ship's characteristics and capabilities. In addition to magnetic signals, the shaft line currents produce corrosion and deterioration in critical shaft line components leading to high maintenance costs.

The new shaft concept utilizes a Navy-developed, laminated design composed of graphite and glass fibers in an epoxy resin matrix. Compared to current metal shaft systems, the composite system is projected to eliminate the magnetic signatures and corrosion associated with shaft line currents, while significantly reducing machinery noise transmission. In addition, the composite shaft will be at least 25 percent cheaper, 50 percent lighter, and considerably less costly to maintain than a comparable metal shaft.

A prototype composite shaft system has been demonstrated for more than 3,500 hours of operation of a Navy patrol vessel. After four years of service under all possible maneuvering conditions, the composite shaft has shown no degradation of strength of material characteristics in the sea water environment.

A full-scale, 500,000 horsepower shaft section has been manufactured and is scheduled for land-based testing before at-sea deployment on a SACRAMENTO-class ship under an advanced development program.

For Additional Information:

Backup material on this effort is available from:

Navy Domestic Technology Fact Sheet Reader Reply Service
Code E211
Naval Surface Weapons Center
Dahlgren, VA 22448-5000
(703) 663-8921

Refer to 131003/TN

NASA Tech Brief
National Aeronautics and Space Administration
Lyndon B. Johnson Space Center, Houston, Texas

Compact Right-Angle Connector

Part of a stack of adaptive fittings is eliminated.

A new right-angle connector between a hose and a "quick-disconnect" coupler is smaller and simpler than its predecessor. It employs fewer parts and is therefore cheaper and less likely to leak.

The new connector (see figure) consists of only two major parts:

1. A cast stainless-steel tube elbow with machined sealing surfaces for the mating parts, and
2. A nut that provides sealing torque and is permanently attached to the elbow with a lockwire.

In contrast, the old connector included a double-swivel-nut elbow and, therefore, needed a tube coupling and a large hex union to adapt to the hose assembly. Both the old and new connectors accommodate an in-line filter.

The new connector is unusual in that it has both an internally threaded tube on its solid end and a 37° flare-type tube fitting inside the swiveling end. Elbows with this combination of ends are not stock items.

This work was done by Salvador L. Barajas and Vonde E. Pierson of Rockwell International Corp. for **Johnson Space Center**.

MSC-20697/TN

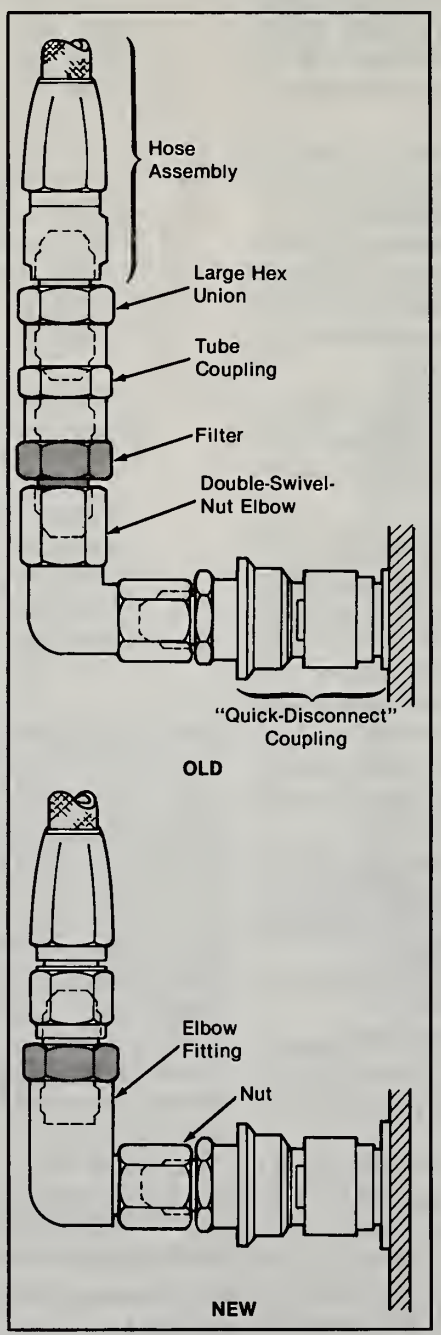

The **New Right-Angle Connector** has about half the volume and weight of the old connector. Flared-tube sealing and boss-tube sealing are combined in the new elbow.

FOR ADDITIONAL INFORMATION: *Contact: Director, Technology Transfer Division, P.O. Box 8757, BWI Airport, MD 21240; (301) 621-0100 Ext. 241*
REFER TO THE NUMBER LISTED AT THE END OF THIS ARTICLE

NASA Tech Brief
National Aeronautics and Space Administration
Marshall Space Flight Center, Alabama

Correlation Analysis of Vibration Data From Rotary Pumps

Fourier coefficients describing vibrations are constructed from files of FFT pump-response data.

A proposed correlation technique represents vibration data from rotary pumps in a compact form convenient for storage in a data base. The analysis determines the coefficients of a Fourier series representing the typical response of a pump for one revolution of the pump shaft. Changes in the harmonic spectrum of the pump may indicate changes in performance caused by internal wear, rubbing of seals, and the like.

Such an analysis could be performed by averaging data in a time series for a number of shaft rotations to eliminate random contributions, then representing the averaged data by a Fourier series. However, that approach would require significant development and would be an expensive addition to the standard evaluation of data. The proposed correlation method is preferable if the dynamic data have already been stored as frames of fast-Fourier-transform (FFT) data, rather than as time series, and if one of the data tracks contains a timing signal or other similar signal with a clear once-per-revolution character that can be used both to determine the rotation period and as a phase reference for the rotation of the pump.

In the proposed technique, a set of reference harmonics would be generated based on the timing signal. The phase of each harmonic would be an integral multiple of that of the fundamental. The harmonic spectrum would be very sparse, comprising a real and an imaginary value at each integral multiple of the frequency of rotation of the pump. A simple algorithm would generate the real and imaginary values from the fundamental-frequency real and imaginary values.

The cross-correlation of the reference harmonic spectrum with the Fourier-transform data would provide the coherence spectrum, which, when multiplied by the data-channel power spectrum, would provide the powers at the harmonic frequencies. This spectrum can be carried as far as necessary to cover the range of frequencies included in the Fourier-transform data.

This work was done by James R. Fenwick of Rockwell International Corp. for **Marshall Space Flight Center**. *No further documentation is available.* *MFS-29401/TN*

FOR ADDITIONAL INFORMATION: *Contact: Director, Technology Transfer Division, P.O. Box 8757, BWI Airport, MD 21240; (301) 621-0100 Ext. 241*
REFER TO THE NUMBER LISTED AT THE END OF THIS ARTICLE

NASA Tech Brief
National Aeronautics and Space Administration
Langley Research Center, Hampton, Virginia

Licensing Opportunity

Endjoints for Structural Elements

Struts are joined easily and rapidly to make frames.

An endjoint and connecting-node system has been designed for use in the erection of frames. The design (see figure) includes an approximately spherical node with flat facets and tapped holes positioned at 45° to one another to provide for 18 bolted strut connections equally spaced over its surface. The design also includes fittings for attaching the nodes to strut elements.

The strut connection is constructed to facilitate rapid assembly or disassembly of the frame. The joint system utilizes internal latch mechanisms housed in the struts. A strut connection can be made quickly and simply by positioning the two mating fittings together and rotating the cammed ring to lock them into place.

The system is structurally sound and simple to operate. All nodes and struts are interchangeable. Nodes and struts can be attached to form cubic cell structures to produce beams, platforms, towers, or combinations of these. In addition to the 18 flat facets with tapped holes, the node contains 8 additional tapped holes at the cubic diagonal locations, which may be used to attach payloads either within or outside previously assembled cubic cell structures.

Although intended as an endjoint system for space-station construction, this design is suitable for use in the construction of other space structures and such terrestrial skeletal frameworks as antenna-reflector supports, roof structures for large buildings, lookout towers, radio-transmitter towers, powerline pylons, and scaffolds.

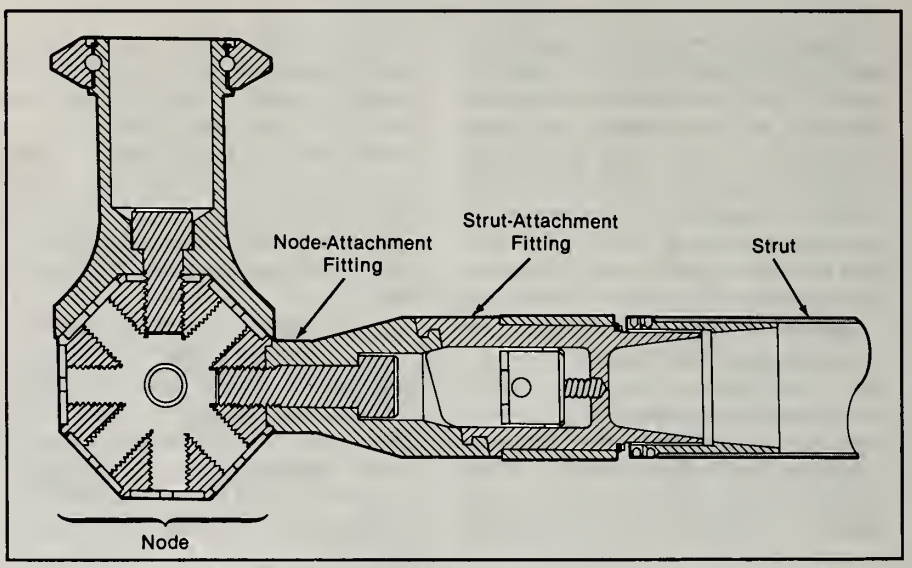

A **Node With Tapped Holes** can be attached rapidly to as many as 18 struts.

This work was done by Harold G. Bush and Martin M. Mikulas of **Langley Research Center** *and Richard E. Wallsom of PRC Kentron, Inc. No further documentation is available.*

This invention is owned by NASA, and a patent application has been filed. Inquiries concerning nonexclusive or exclusive license for its commercial development should be addressed to the Patent Counsel, Langley Research Center [see page 22]. Refer to LAR-13584.

Langley Research Ctr.
Technology Utilization Officer: John Samos
Mail Stop 139A
Hampton, VA 23665
(804) 864-2484
Patent Counsel:
George F. Helfrich
Mail Code 279
Hampton, VA 23665
(804) 864-3523

FOR ADDITIONAL INFORMATION: *Contact: Director, Technology Transfer Division, P.O. Box 8757, BWI Airport, MD 21240; (301) 621-0100 Ext. 241*
REFER TO THE NUMBER LISTED AT THE END OF THIS ARTICLE

NASA Tech Brief
National Aeronautics and Space Administration
Lyndon B. Johnson Space Center, Houston, Texas

Inspection in Overhead Spaces Containing Asbestos

A simple method saves time and effort.

A procedure for inspection in spaces above dropped ceilings that contain asbestos saves time and effort without sacrificing safety. The conventional inspection method requires elaborate and time-consuming preparation and cleanup: People have to leave the immediate area, and the floor and furniture have to be covered with sheets of plastic. Wearing a respirator, the inspector examines the space above the ceiling. Finally, the room is vacuum-cleaned, the plastic sheets are discarded, and the inspector's tools, equipment, and respirator are cleaned.

With the new method, the only items of safety equipment needed are a glove bag, a storage bag, and a roll of adhesive tape. The inspector first tapes the glove bag tightly to the support grid around the ceiling tile to be removed. With hands in the gloves, the inspector lifts the tile gently and places it aside (see figure). Extending head and shoulders into the bag, the inspector examines the space above the ceiling with the help of a flashlight. (A lightweight, collapsible frame could be used to hold up and spread out the bag so that the inspector could maneuver more easily in the confined space.)

After the examination, the inspector replaces the tile, lowers the glove bag, ties it up close to the ceiling, and tapes the storage bag (labeled "For Asbestos") to the ceiling around the glove bag. Finally, the inspector pulls the glove bag loose, drops it into the storage bag, ties the storage bag closed, and discards the storage bag appropriately.

This work was done by Jacque Bell, George Hartwick, and Jerry Hutcherson of Pan Am World Services, Inc., for **Johnson Space Center**. *No further documentation is available.*
MSC-21362/TN

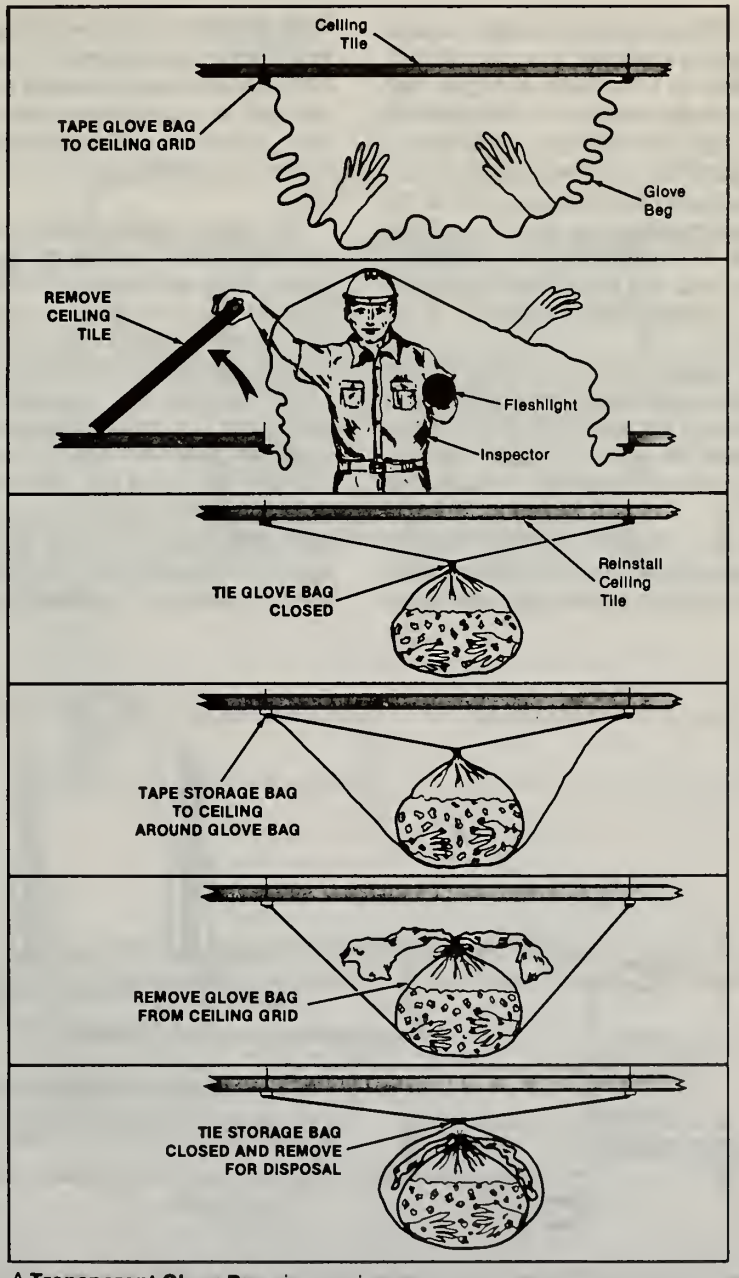
Ceiling Tile
TAPE GLOVE BAG TO CEILING GRID
Glove Bag
REMOVE CEILING TILE
Flashlight
Inspector
Reinstall Ceiling Tile
TIE GLOVE BAG CLOSED
TAPE STORAGE BAG TO CEILING AROUND GLOVE BAG
REMOVE GLOVE BAG FROM CEILING GRID
TIE STORAGE BAG CLOSED AND REMOVE FOR DISPOSAL

A **Transparent Glove Bag** gives an inspector a clear view of the space above a dropped ceiling and prevents asbestos from contaminating the area below.

FOR ADDITIONAL INFORMATION: *Contact: Director, Technology Transfer Division, P.O. Box 8757, BWI Airport, MD 21240; (301) 621-0100 Ext. 241*
REFER TO THE NUMBER LISTED AT THE END OF THIS ARTICLE

NASA Tech Brief
National Aeronautics and Space Administration
Marshall Space Flight Center, Alabama

Ultraclean Radiant Furnace

Cooling of the walls minimizes contamination from outgassing.

A relatively-inexpensive radiant furnace can bring a specimen in a controlled atmosphere to a temperature higher than was previously attainable — nearly as high as the maximum operating temperature of the heating element. The heating element can be made of a refractory material like tungsten, molybdenum, graphite, or silicon carbide, or could consist of a plasma or electric arcs. The furnace distributes heat fairly uniformly over the surface of the specimen.

The heating element is kept in its own protective environment, distinct from that surrounding the specimen. The wall that surrounds the specimen is kept substantially cooler than the heating element or the specimen.

The furnace includes three coaxial tubes (see figure). The outer tube is sealed at its ends to the intermediate tube, forming a closed chamber filled with a gas that protects the heating element — for a tungsten element, a good choice is a halogenated gas. In advanced versions of the furnace, the outer tube could be designed to reflect or reradiate heat onto the specimen.

The intermediate tube surrounds the inner tube, which contains the specimen. These tubes are made of a transparent material like fused quartz or sapphire so that maximum energy reaches the specimen. Coolant flows through the space between the inner and intermediate tubes. The coolant maintains them at or below room temperature, despite the intense radiation. The vapor pressure of the inner tube is therefore kept extremely low, and as a result, the atmosphere of the inner tube is not contaminated by vapor from the wall. Processes of extremely high purity can therefore be carried out in the specimen.

In a prototype of the furnace, a specimen in an inner tube with an inner diameter of 6 mm was heated electrically via a coil of tungsten/3-percent rhenium ribbon. Although the available power was limited, the temperature of the specimen reached 1,885 K. The temperature of the coolant at the outlet was 748 K — believed to be substantially higher than the average temperature of the wall of the inner tube. In a fully developed version of the furnace, it should be possible to heat a sample to 3,000 K in about 10 seconds.

This work was done by David W. Blair of Princeton Scientific Enterprises for **Marshall Space Flight Center.**

MFS-26070/TN

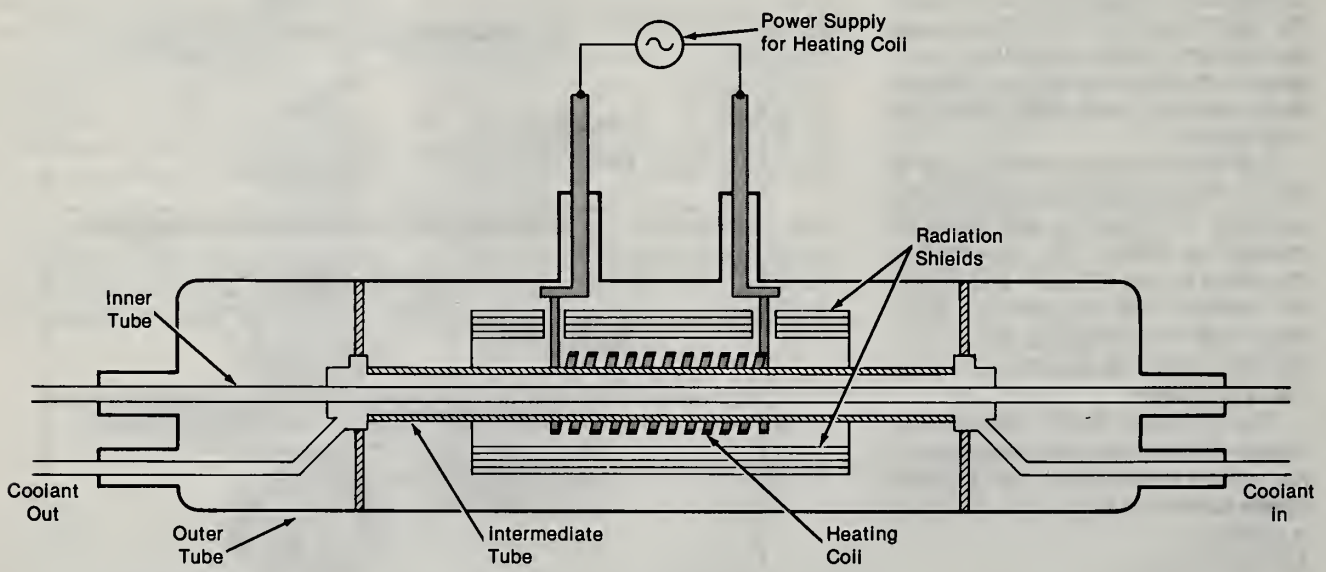

A **Tube Within a Tube Within a Tube,** the furnace provides separate environments for the heating element and the specimen. Coolant flowing between the intermediate and inner tubes keeps the temperature of the inner tube low, despite the extremely high temperature of the specimen within it.

FOR ADDITIONAL INFORMATION: *Contact: Director, Technology Transfer Division, P.O. Box 8757, BWI Airport, MD 21240; (301) 621-0100 Ext. 241*
REFER TO THE NUMBER LISTED AT THE END OF THIS ARTICLE

NASA Tech Brief
National Aeronautics and Space Administration
Lyndon B. Johnson Space Center, Houston, Texas

Variable-Volume Container

The container expands and contracts according to changes in volume of its solid contents.

A container holds a bed of beads securely while accommodating sizable changes in volume and allowing gases to flow through the bed. The container was developed for an air-purifying system in which carbon dioxide is removed by solid amine beads.

The beads absorb CO_2 as the air flows over them. When they become saturated with CO_2, steam is passed over the beads to regenerate them. However, the beads swell as their moisture content increases. The volume of a bed increases by about 17 percent during regeneration and decreases by the same amount afterward. Simply using a container large enough to hold the expanded beads may not be acceptable. Under some conditions, dry beads would then be packed too loosely, and the air would not flow uniformly over them.

Accordingly, the container was designed to expand and contract with the beads. A metal bellows serves as the sidewall of the container, and metal-felt plates are placed at the ends (see figure). The bellows elongates as its contents expand. When the contents contract, springs return the bellows to its original length.

This work was done by A. K. Colling, T. A. Nallette, and F. Sansevero of United Technologies Corp. for **Johnson Space Center**. *No further documentation is available.*
MSC-21355/TN

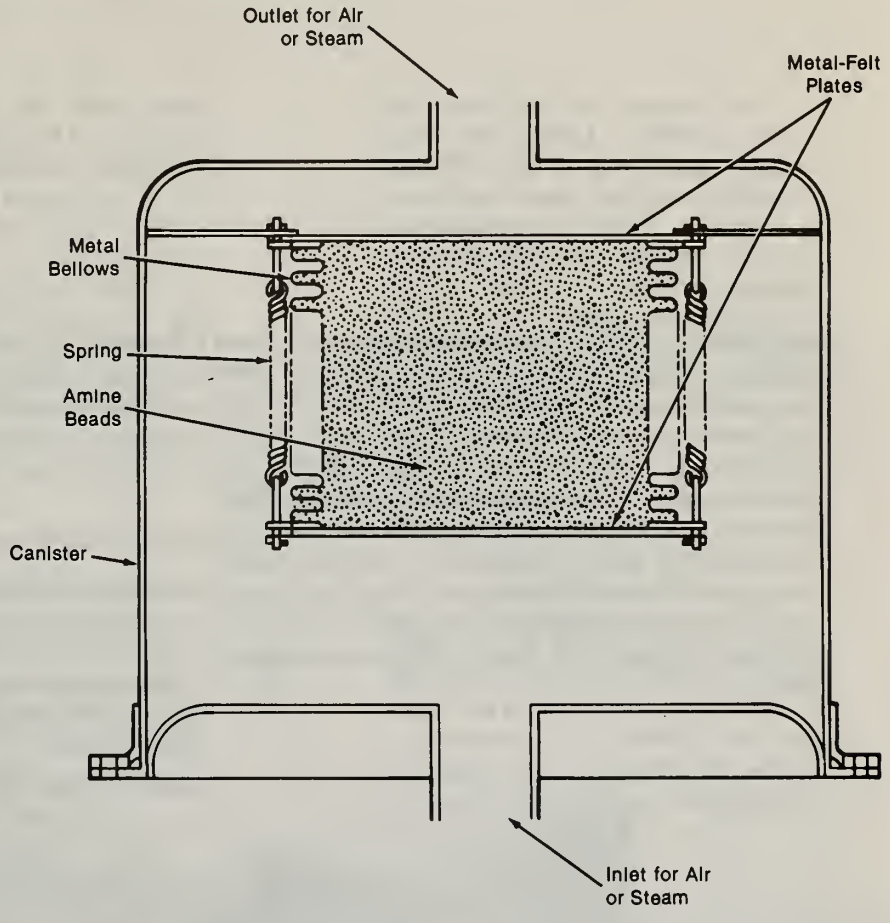

Expanding Beads create pressure in the container so that its bellows elongates, thereby increasing the volume. Springs return the bellows to its original length when the beads shrink.

NAVY
Domestic Technology Transfer Fact Sheet

Filmless X-Ray Inspection Methods
Speeds Aircraft Inspection Onboard Carriers

The Naval Air Engineering Center (NAEC), Lakehurst, New Jersey, sponsored by the Office of Naval Technology, has developed a filmless X-ray technique to inspect aircraft onboard aircraft carriers. Under the exploratory development program, NAEC scientists have tested the new, computer-aided, nondestructive inspection device.

New aircraft design includes highly stressed components and new materials that present new challenges to nondestructive inspections of components for material defects or failures.

Present inspections, which employ conventional X-ray techniques, require facilities and skills to process the film and considerable time-delay to develop a hard-copy image for examination. In addition, inspections must be done while the aircraft is on the elevator to prevent radiation hazards to personnel. This results in a temporary loss of the elevator's primary mission--to move aircraft.

The filmless technique uses a digital computer memory that can be stored on video tape. Stored images, enhanced by advanced software, can either be viewed on a monitor or be printed on a high-resolution graphics printer.

For Additional Information:

Backup material on this effort is available from:

Navy Domestic Technology Fact Sheet Reader Reply Service
Code E211
Naval Surface Weapons Center
Dahlgren, VA 22448-5000
(703) 663-8921

Refer to 140402/TN

Technology News

From the Bureau of Mines, United States Department of the Interior

Monitoring Foundation Response to Subsidence Using a Tiltmeter

Objective

Determine how subsidence resulting from underground coal mining affects surface structures, and evaluate the usefulness of the tiltmeter for monitoring foundation movement.

Approach

The Bureau of Mines is studying foundation response to mine subsidence in order to determine how subsidence-induced ground movements affect foundations in place directly above the mine. These investigations are essential if economic mitigation and repair techniques are to be made. In addition, commercially available tiltmeters are being evaluated for use as a cost-effective monitoring technique. To study foundation response and to evaluate the tiltmeter system, full-scale model foundations were constructed, instrumented, and monitored for three years. Vertical and horizontal displacements, tilt magnitudes and directions, and observed damages were recorded. Displacements were compared with measured tilt to determine if the tiltmeter was tracking foundation response to subsidence. The Bureau developed a computer software package to aid in the reduction and analysis of the tiltmeter data.

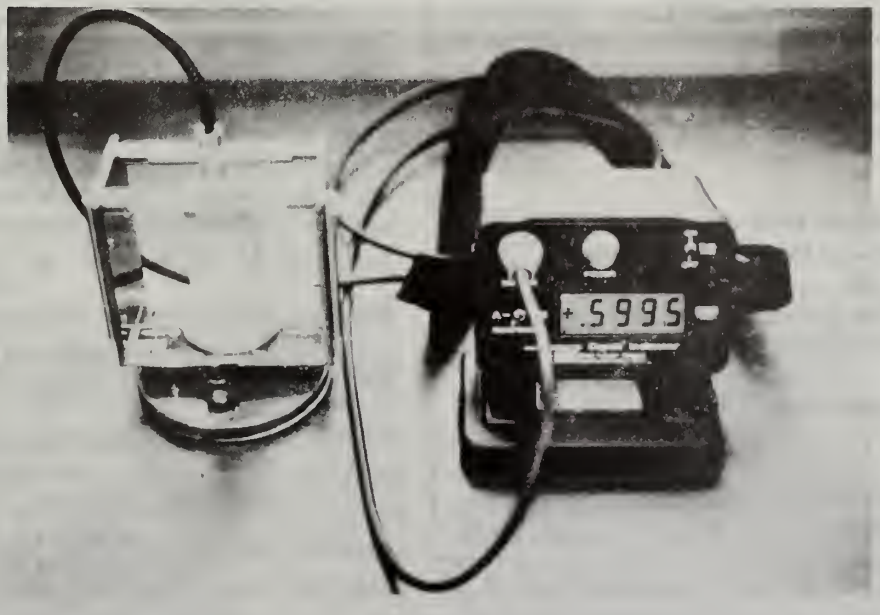

Portable tiltmeter system evaluated by the Bureau for monitoring foundation response to subsidence.

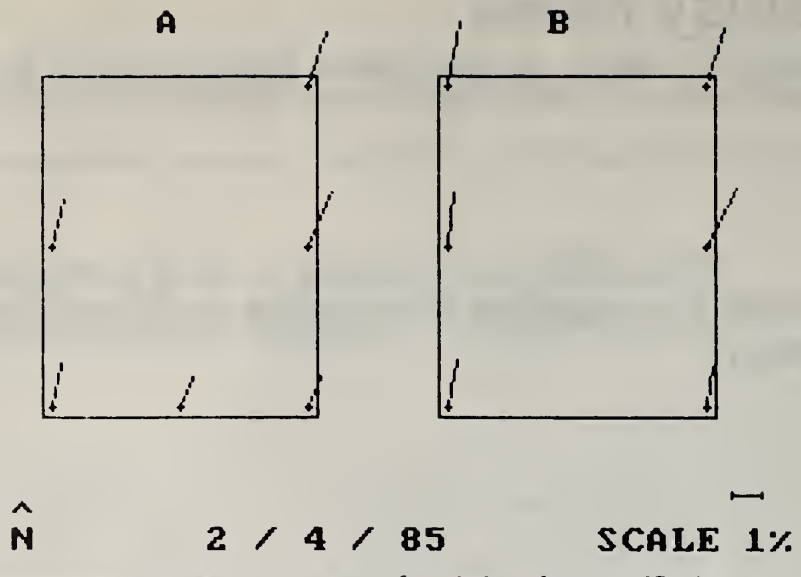

Tilt shown as scaled vectors on two foundations for a specific date.

How the Tiltmeter Works

The tiltmeter system consists of a portable sensor, digital indicator and tiltplates. The sensor has a single closed-loop, servo-accelerometer for detecting the angle of inclination of the sensor base plate. The smallest change in tilt angle that can be detected is 0.1mm/m. To minimize errors, readings are obtained by aligning the sensor on the tiltplate in all four directions. Thus, tilts are obtained in all four directions as a function of the sine of the angle that the tiltplate makes with the horizontal. The maximum tilt and tilt direction can be calculated from these readings.

Computer Program Features

To facilitate data reduction, a menu-driven, interactive computer program was written that executes the tedious tilt calculation suggested by the tiltmeter manufacturer. The computer program offers several advantages and benefits:

(1) It allows the user to build or modify files containing tiltmeter readings taken from the field.

(2) It calculates tilt angle and tilt direction from the input data and stores the information in files.

(3) It reduces tabular output of field data and calculated data.

(4) It displays graphs of scaled vectors showing magnitude and direction of tilt relative to time and position of the tiltplate on the structure.

The program is written in BASIC language using low-resolution graphics and will run on most personal computers.

Summary

The tiltmeter is simple to use and was proven to accurately track the magnitude and direction of foundation response to mine subsidence.. Excellent correlation between tilt and subsidence was obtained during Bureau studies and showed that the tiltmeter is measuring the correct foundation movements. Measuring tilts revealed that the foundations experienced differential tilt, or curvature. This allows the tiltmeter to be used for assessing strain, because differential tilt or curvature is an indication of the amount of strain imposed on a structure.

For More Information

The tiltmeters and their use for monitoring foundations are described in two papers. One is entitled "Measurement and Analysis of Foundation Tilt Resulting From Mine Subsidence in Southern Illinois," by Larry R. Powell, Theodore L. Triplett, and Ronald E. Yarbrough, and the other is titled "Foundation Response to Subsidence Induced by High Extraction Mining in Southern Illinois," by Theodore L. Triplett, Ronald E. Yarbrough, and Larry R. Powell.

For more details, including information on how to obtain a copy of the computer program or the papers described above, please contact the principal researchers:

Rebecca J. Ford (612) 725-4573
or
Larry R. Powell (612) 725-4577
or write to:
U.S. Bureau of Mines
Twin Cities Research Center
5629 Minnehaha Avenue South
Minneapolis, Minnesota 55417

Technology News

From the Bureau of Mines, United States Department of the Interior

New Process Produces Lead from Galena Concentrates Without Pollution

Objective

Provide an environmentally compatible means of producing lead from galena concentrates that replaces the current high-temperature pyrometallurgical primary lead smelting process and supplies pure lead metal within present and proposed Environmental Protection Agency (EPA) and Occupational Safety and Health Administration (OSHA) lead emission standards.

Approach

The U.S. Bureau of Mines developed an energy efficient and pollution-free leach-electrowinning method for use in recovering pure lead metal and byproducts from lead sulfide concentrates.

How It Works

The present method for smelting lead sulfide concentrates to produce lead is a pyrometallurgical smelting method that requires temperatures as high as 1,400°C. Such smelting methods result in high lead and sulfur dioxide emissions. These high-temperature smelting operations will be unable to meet proposed emission standards. Unless new technology is developed or some compromise is reached, such operations could be forced to close. The U.S. Bureau of Mines developed a lead recovery process that promises to provide a pollution-free alternative to high-emission smelting methods. Using the Bureau's new process, galena concentrates are leached directly under oxidative conditions in waste fluosilicic acid at tem-

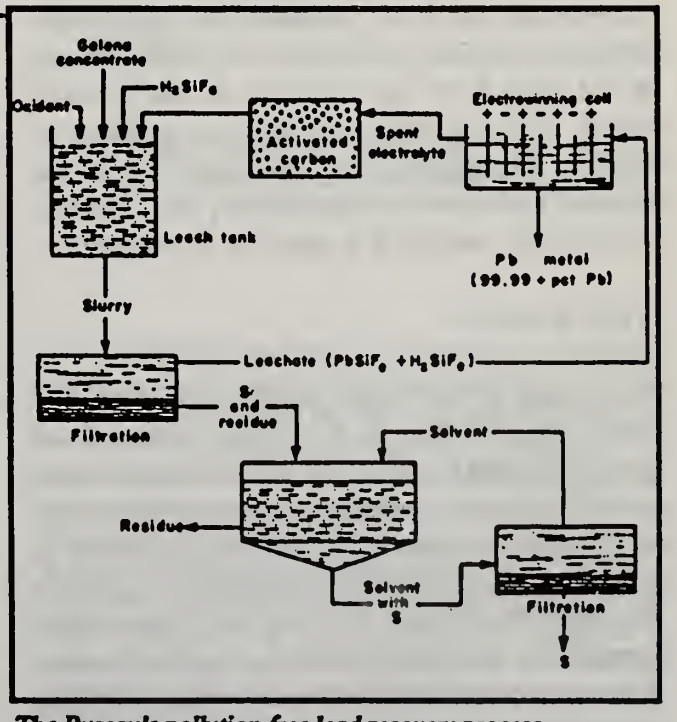

The Bureau's pollution-free lead recovery process.

peratures less than 120°C. This solubilizes the lead and produces a residue containing elemental sulfur and other metal values. Pure lead metal (99.99 pct) is recovered from the leach solution by electrowinning using inert anodes and lead cathode starting sheets. To prevent lead dioxide formation at the anodes during the electrowinning step, phosphorus is added to the fluosilicic acid electrolyte. The amount of energy consumed during the entire process is an efficient 800 kilowatt hours per ton of lead produced.

The new method produces lead metal pure enough for any application; conventional smelting methods produce a pure lead product only after extensive refining to remove antimony and other impurities. The refining method used by smelting operations can result in further lead emission problems.

Another advantage of the Bureau's recovery process is that the leach-electrowinning method converts sulfur in the lead sulfide concentrates to elemental sulfur. Existing smelting methods produce sulfur dioxide, some of which is captured and converted to sulfuric acid. Of the two conversion products, elemental sulfur is more desirable because it is of more value per ton and is the best form for shipping at the greatest value. Sulfuric acid is three times as heavy as sulfur. In addition, the leach residue of the Bureau's process contains silver, zinc, copper, and cobalt, making it a valuable byproduct.

Test Results

Successful 1-liter scale bench tests were followed by leaching in a 100-liter tank. Lead extraction was 96 pct when galena concentrates were leached in recycled waste fluosilicic acid using hydrogen peroxide and lead dioxide as oxidants. After solid-liquid separation to obtain the lead-fluosilicate solution and the residue containing elemental sulfur, pure lead metal was electrowon in a 20-liter cell containing four titanium anodes coated with lead dioxide and three pure lead cathodes. Approximately 99 pct of the elemental sulfur was separated from the leach residue with tetrachloroethylene and kerosene at 115°C.

The fixed capital cost of a plant designed to recover 300 tons of lead per day has been estimated to be about $36 million, based on third-quarter 1985 equipment costs. Net operating costs are estimated to be about $0.22 per pound of lead. With the August 1988 market price of lead at $0.36 per pound, the potential return on investment of $0.14 per pound makes this process economically attractive.

Patent Status

The U.S. Department of the Interior does hold several patents on this process. These include U.S. patents 4,159,231, 4,272,340, and 4,500,398. For additional information about these patents or on patent licensing, please contact the Bureau of Mines, Office of Technology Transfer, M.S. 6201, 2401 E Street, NW., Washington, DC 20241.

For More Information

Additional information about this process can be obtained from U.S. Bureau of Mines Report of Investigations (RI) 9055, "Hydrometallurgical Process for Producing Lead and Elemental Sulfur From Galena Concentrates." A free single copy of this report can be had by contacting the Bureau's Publication Distribution Section, P.O. Box 18070, Cochrans Mill Road, Pittsburgh, PA 15236. For answers to technical questions or other information, please contact the principal investigator for this work:

Agnes Y. Lee
U.S. Bureau of Mines
Rolla Research Center
1300 Bishop Avenue
P.O. Box 280
Rolla, MO 65401
Tel: (314) 364-3169

Technology News

From the Bureau of Mines, United States Department of the Interior

Licensing Opportunity

Ultralow-Frequency Through-the-Earth Electromagnetic Fire Warning Alarm System for Underground Mines

Objective

Provide a rapid, reliable means of warning underground miners of a fire or other emergency.

Approach

An ultralow-frequency electromagnetic signaling system was designed, breadboarded, and tested at various underground mines.

How It Works

Current fire warning systems for underground mines, such as stench, audible alarms, and messengers, are slow, unreliable, and seldom achieve total mine coverage. An ultralow-frequency electromagnetic fire warning alarm system with true through-the-earth signaling capabilities was developed to solve these problems. The system was originally designed for high-back room-and-pillar mines where stench systems are unusable due to the low velocity of mine air flow. However, the system has an application to all underground mines.

The system is comprised of two basic elements: a transmitter and a receiver. The transmitter consists of a signal generator, an audio-range amplifier, and a large loop transmitting antenna. The receiver consists of a small tuned ferrite-core antenna and a micro- receiver module. In the event of a mine emergency, the transmitter is used to establish a very large electromagnetic field throughout the mine's workings. The ferrite-core of the receiving antenna is capable of capturing and concentrating this magnetic flux, generating a tiny current in the receiver antenna windings. This tiny current is then filtered and amplified in the micro-receiverr module, activating a relay which triggers the fire warning signal. The properties of ultralow-frequency electromagnetic transmission through rock have long been known, and are the basis for a previous Bureau development, the trapped miner location and communication system. However, unlike previous systems, the receiving antenna for the new fire warning alarm system is small enough to be carried about by miners without interfering with normal work activities. The ferrite-core antenna used in this system is 3/8 in dia. by 7 in long. Both it and the micro-receiver module will easily fit into a modified cap lamp battery case, thereby providing a convienient means for both carrying and powering the system (see photograph). Attachment to the miner's cap lamp also enables an effective emergency warning signal. Rather than using audible or visual alarms which might not be noticed by busy miners using noisy equipment, the new system causes the miner's cap lamp to blink. The miner then acknowledges the warning by pushing a button on the cap lamp to stop the blinking.

The ultralow-frequency electromagnetic fire warning system fits into a modified cap lamp battery case.

The system is simple in design, flexible in application, and inexpensive in construction. The basic components are "low tech" and readily available from a number of commercial suppliers. The transmitting antenna can be arrayed on the surface or underground, to suit local conditions. The receiver can be configured for attachment to the cap lamp battery as described above, or for attachment directly onto mining equipment. For example, if miners remove their cap lamps while operating LHD's or haulage trucks, the receivers could be mounted directly onto those vehicles and wired into their electrical systems to blink the headlights and tail lights or to activate a strobe. The system is safe because its ultralow-frequency signal is not capable of initiating electric blasting caps. Finally, system costs are quite reasonable. The transmitting antenna consists of multiple turns of insulated #10 copper wire and the signal generator and audio-range amplifier can be obtained for under $5,000. The micro-receiver module can be assembled commercially in small quantities for about $40. If produced commercially in large quantities, the cost would drop considerably. The ferrite-core antennas are about $4 a piece in small quantities and less in large quantities.

Test Results

The system was tested at three underground mines. The first test evaluated the basic concept and was performed at a sandstone mine having about 50 ft of overburden consisting of limestone, sandstone, and glacial till. Using a 100 ft dia loop transmitting antenna made up of 6 turns of #10 copper wire arrayed on the surface and a transmitter power output of about 2 W, the receiver showed the capability of detecting the field underground over an area about 10 times the area of the transmitting antenna.

In an attempt to evaluate the system under "worst case" conditions, follow-up testing was performed at mines having less favorable overburden characteristics. Since signal attenuation is proportional to both through-the-earth transmission distance and rock conductivity, testing was performed over greater distances and in rock having higher conductivity. The second test was performed at an underground iron mine having overburden containing high amounts of iron with correspondingly high conductivity Using an underground transmitting antenna made up of 10 turns of #10 and #12 copper wire approximately 100 ft in dia and transmitting at 50W, the signal was detected through over 2,500 ft of rock. The third test was performed at an underground zinc mine overlain by about 1,200 ft of highly conductive water-saturated saprolite. Using a surface transmitting antenna made up of 10 turns of #10 and #12 copper wire in a 100 ft dia loop and transmitting at 50W, the signal was detected at the bottom of the mine approximately 1,850 ft from the transmitter.

Patent Status

The Bureau of Mines is applying for a patent on the ultralow-frequency electromagnetic fire warning system. For further information about patent licensing procedures, contact the Bureau's Office of Technology Transfer, M.S. 6201, 2401 E St., NW, Washington, DC 20241 or call (202) 634-1223.

For More Information

This research is described in the paper "Fire Detection and Warning in Noncoal Mines." A single free copy of this paper can be obtained by contacting the project's principal investigator:

Mr. Kenneth Hjelmstad
Twin Cities Research Center
Bureau of Mines
5629 Minnehaha Avenue South
Minneapolis, MN 55417
Telephone (612) 725-4632

NIST Technology Update

National Institute of Standards & Technology
(Formerly the National Bureau of Standards)
U.S. Department of Commerce, Gaithersburg, MD 20899

Techniques for Measuring Stress and Strain

NIST scientists have developed a computer-controlled, optical technique for measuring deformations in materials. The system, which utilizes a laser, video cameras, and still photography, measures all three components of strain as well as rigid body rotations. The system can measure strains at 16,000 locations in a 2.5-inch square grid in about 5 hours. It currently is being used to study the initiation and growth of cracks in composite panels in conjunction with the Ford Motor Company.

FOR ADDITIONAL INFORMATION: Several papers are available from Jo Emery, NIST, Division 104, Boulder, Colo. 80303; (303)497-3237.

NASA Tech Brief
National Aeronautics and Space Administration
Langley Research Center, Hampton, Virginia

Licensing Opportunity

Flight Balance for Skin-Friction Measurements

The force of a tangential airstream is determined by a null-position servomechanism.

A skin-friction balance (flight balance) for use in flight on an aircraft fuselage incorporates a type-one, closed-loop control to make direct skin-friction force measurements. A curved surface element 2 in. (5.08 cm) in diameter is used to sense the tangential force of an airstream passed over it. A linear electromagnetic force motor exerts a restoring force that nulls the position of the sensing element. The applied skin-friction force is measured by sensing the amount of current through the motor necessary to maintain the null position. The full-scale range of the balance is adjustable from 0.1 to 1.0 g weight/cm^2 (9.8 to 98 Pa), and the overall size is approximately 8 by 5 by 5 in. (20.3 by 12.7 by 12.7 cm).

The flight balance, an electromechanical servomechanism, is a modified version of a design previously developed at NASA Langley Research Center. The unit is rugged, accurate, reliable, and easy to operate. These features are achieved through the use of an oscillating double four-bar mechanism, which enables accurate skin-friction measurements in the presence of an offcenter normal force and rectilinear vibrations in the background. The insensitivity of the balance to background rectilinear vibrations and its ability to sustain large transient loads during takeoffs and landings make it most attractive for flight testing.

Two identical units were fabricated and used on a jet aircraft to make skin-friction measurements in flight. The results indicated that both balances functioned satisfactorily and that data taken from the balances in tests with similar profiles conducted on different days were duplicated within 5 percent.

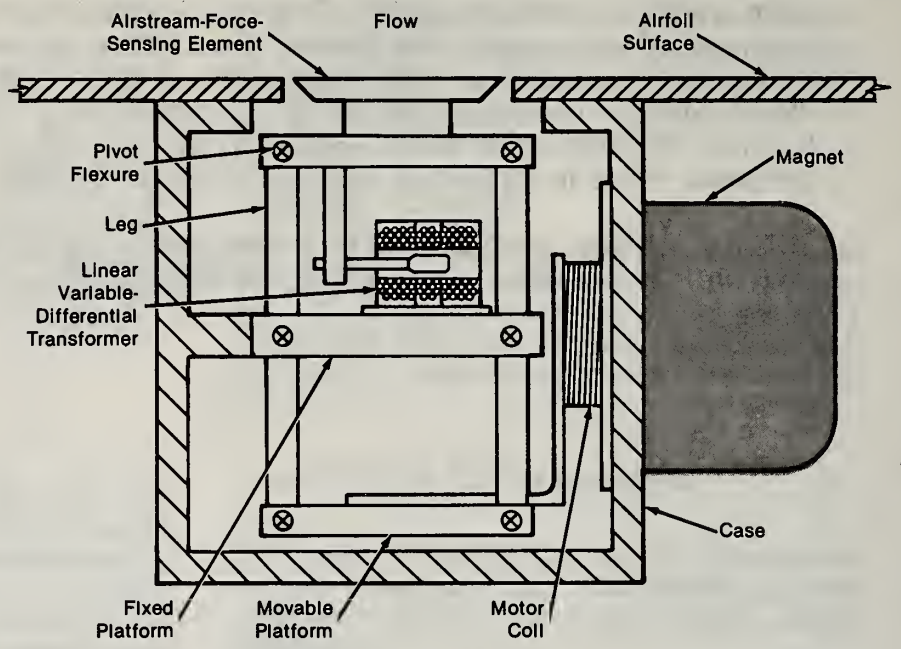

The Electromechanical Servomechanism restores the airstream-force-sensing element to the null position.

This work was done by Ping Tcheng and Frank H. Supplee, Jr., of **Langley Research Center**.

This invention is owned by NASA, and a patent application has been filed. Inquiries concerning nonexclusive or exclusive license for its commercial development should be addressed to the Patent Counsel, Langley Research Center
Refer to LAR-13710/TN

Langley Research Ctr.
Technology Utilization Officer: John Samos
Mail Stop 139A
Hampton, VA 23665
(804) 864-2484
Patent Counsel:
George F. Helfrich
Mail Code 279
Hampton, VA 23665
(804) 864-3523

FOR ADDITIONAL INFORMATION: *Contact: Director, Technology Transfer Division, P.O. Box 8757, BWI Airport, MD 21240; (301) 621-0100 Ext. 241*
REFER TO THE NUMBER LISTED AT THE END OF THIS ARTICLE

NASA Tech Brief
National Aeronautics and Space Administration
Marshall Space Flight Center, Alabama

Measuring Bearing Wear Via Weight Loss

Dimensional changes are estimated from areas, weight losses, and densities.

Wear in the critical parts of bearings can be measured via the amounts of weight lost during use. First used on the balls, races, and cage of a bearing in a turbopump of the Space Shuttle main engine, the weight-loss measurement technique is clearly applicable in general to bearings made of nonporous materials.

Previously, weight-loss measurements had not been attempted because of the belief that sufficient accuracy and repeatability could not be achieved. However, preliminary experience has shown that in comparison with measurements of dimensions, the weight-loss measurements are easier, faster, more precise, and less likely to damage the measured parts. The weight-loss measurements can be performed in clean rooms and under the constraint of extreme cleanliness for compatibility with liquid oxygen.

The technique requires an analytical balance that has a resolution of 10^{-4} g. Before use, the inner race(s), outer race, and cage are weighed individually, and the balls are weighed as a set. If the bearing is to be lubricated with a dry film, these components are weighed both before and after coating.

After use, the components are weighed again. If the bearing is lubricated with a dry film, the components are weighed both before and after the film is stripped off.

The approximate thickness of material worn off a component can be estimated as the loss of mass divided by the product of the density of the material and the area of the component. The accuracy and repeatability of the technique are sufficient to resolve a loss of about 1 mg of material: On a bearing ball of typical size, this would signify a decrease of less than 10^{-6} in. ($\sim 2.5 \times 10^{-8}$ m) in diameter.

This work was done by John E. Keba and Richard S. Moore of Rockwell International Corp. for **Marshall Space Flight Center**. *No further documentation is available.*
MFS-29438/TN

FOR ADDITIONAL INFORMATION: *Contact: Director, Technology Transfer Division, P.O. Box 8757, BWI Airport, MD 21240; (301) 621-0100 Ext. 241*
REFER TO THE NUMBER LISTED AT THE END OF THIS ARTICLE

NASA Tech Brief
National Aeronautics and Space Administration
Langley Research Center, Hampton, Virginia

Miniature Flow-Direction/Pitot-Static Pressure Probes

Probes measure the directions and pressures of hypersonic flows at temperatures up to 500°F.

Precision flow-direction/pitot-static pressure probes, ranging from 0.035 to 0.090 inch (0.89 to 2.29 mm) in outside diameter, have been successfully fabricated and calibrated for use in the Langley 20-inch Mach 6 Tunnel. The probes will simultaneously measure the flow direction and the static and pitot pressures in flow fields about configurations in hypersonic flow at temperatures up to 500 °F (260 °C).

The probe design incorporates a combination of a "pyramid" flow-direction probe, which has four raked-back tubes 90 ° apart around a flat-face tube and a pitot-static pressure probe. The latter consists of a central tube inside an encasing tube that has 4 equally spaced static-pressure orifices with outside diameters of 0.01 inch (0.25 mm), 10 or more tube diameters downstream of the nose. An equal distance was allowed behind the orifices, between them and the wedge-shaped "gooseneck," to avoid feedback from the wedge pressure field. The probe was made as small as possible to minimize intrusive interference. The center tube was beveled internally at 60 ° to reduce its sensitivity to the angularity of the flow.

The probe with the 0.035-inch (0.89-mm) outside diameter had the minimum size that could accommodate a bundle of five pieces of the smallest available tubing [0.008-inch (0.20-mm) outside diameter] together with the four alignment spacers. The other sizes (see figure) were constructed because the "pressure-settling" time varied inversely with the probe size and could be prohibitively long at the smallest probe sizes. The progressively increasing probe sizes ensure that the best compromise between the probe size and "pressure-settling" time, relative to the operating time limits of the tunnel, can be made.

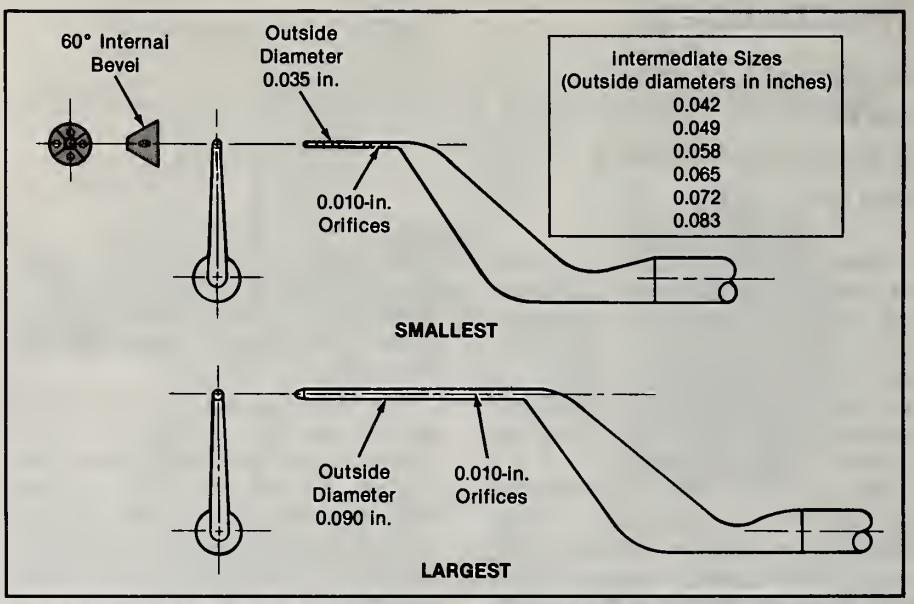

The **Outer Tube Serves as the Housing** for the static ports and as a casing for five inner tubes that are used to measure the direction and pitot pressure of the flow.

For calibration, the probes were mounted in a calibration fixture and pitched through ±20° and sideslipped through ±8 °. Because of instrumentation and mounting problems, complete calibrations were obtained only for those probes having outside diameters of 0.090 inch (2.29 mm) and 0.083 inch (2.10 mm). A partial calibration of the 0.042-inch-(1.07-mm-) outside-diameter probe was obtained. A least-squares fit to the calibration data is within ±1 ° and, in most cases, within ±0.5 °. The calibrations of the two larger probes were nearly coincident, and calibration of the smaller probe had the same slope as that of the larger probes. This leads to the conclusion that all of the probes, regardless of size, would have the same calibration slope, and that a single equation (wherein the pressure-difference parameters for each probe at 0 ° pitch and sideslip would be input constants) could be used to determine the flow angles from the flow measurements of any of the probes.

This work was done by George C. Ashby, Jr., David S. Coombs, John W. Eves, Howard E. Price and Peter Vasquez of **Langley Research Center**. *LAR-13643/TN*

FOR ADDITIONAL INFORMATION: *Contact: Director, Technology Transfer Division, P.O. Box 8757, BWI Airport, MD 21240; (301) 621-0100 Ext. 241*
REFER TO THE NUMBER LISTED AT THE END OF THIS ARTICLE

NASA Tech Brief
National Aeronautics and Space Administration
Marshall Space Flight Center, Alabama

Nondestructive Inspection of Foam and Multilayer Insulations

Electromagnetic and electrostatic sensors probe hidden surfaces and layers.

Techniques and equipment undergoing development will enable the nondestructive inspection of sprayed-on foam and multilayer reflecting thermal insulations on metallic substrates. Intended originally for the testing of thermal-protection systems on spacecraft, this technology also could be applied in factories and laboratories; for example, to inspect insulation on cryogenic tanks and pipes.

The prototype equipment (see Figure 1) can measure the overall thickness of foam insulation or the overall thickness, thickness between individual reflecting layers, locations of gaps, and/or amount of corrosion of multilayer reflecting insulation. The properties of the insulation are calculated from the responses to excitations applied to the insulation via inductive and capacitive sensors mounted in a common probe head (see Figure 2). In an inductive measurement, eddy currents are generated in the metallic layer of interest to sense the location of the layer or the size and/or location of a discontinuity, The eddy currents affect the complex impedance of the probe coil, which can be measured and processed along with ancillary calibration data to infer the quantity of interest.

For example, the complex impedance of one of the coils when excited at a frequency of 10 kHz is a known function of the distance of the coil from the metallic substrate and can, therefore, be used to infer the thickness of the insulation. The 10-kHz frequency was selected because it makes the measurement relatively insensitive to thin intervening reflecting layers and can, therefore, be used on both types of insulation. Because inductive measurements at 200 kHz are sensitive to the reflecting layers, they are used to measure gaps in multilayer reflective insulation.

The capacitive electrodes at the end of the probe head are excited at 1 MHz to serve as a proximity sensor. The capacitance between the electrodes is affected by the distance to the nearest conductive surface and/or the presence of dielectric material. The capacitance is measured to detect contact with foam insulation, to measure the thickness of foam insulation, or to measure the distance to the outer-

Figure 1. The **Prototype Equipment** includes a probe head, several electronic modules that take measurements via electromagnetic and electrostatic sensors in the probe head, a small computer to store and process the signals from the modules, and a printer.

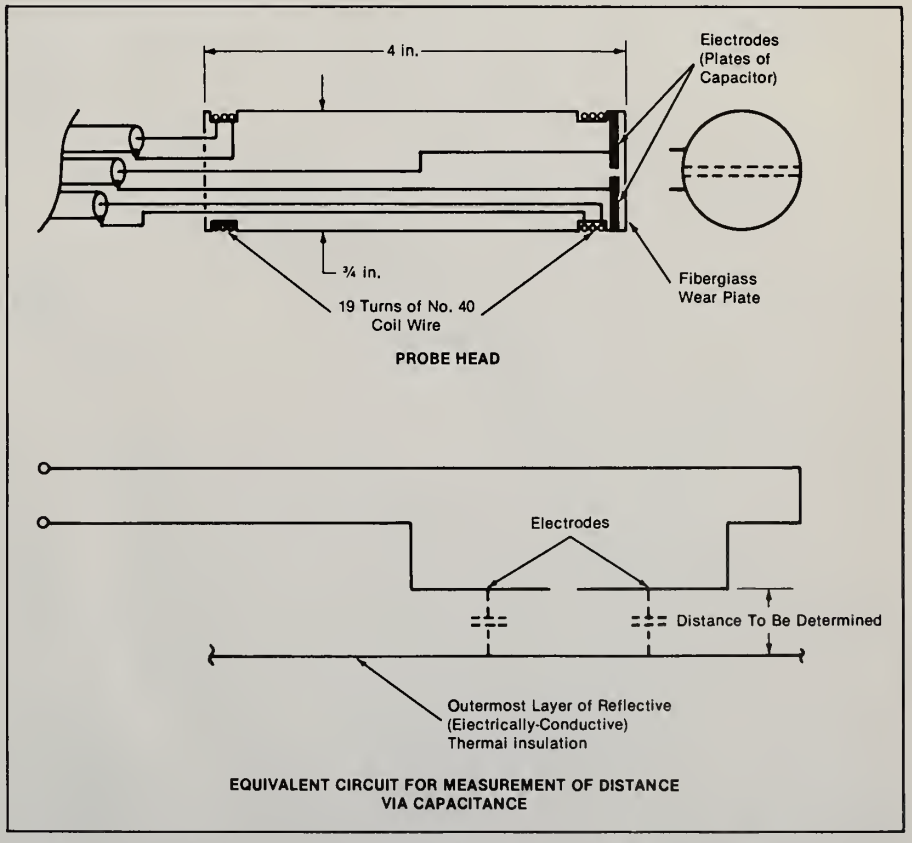
4 in.
Electrodes (Plates of Capacitor)
¾ in.
19 Turns of No. 40 Coil Wire
Fibergiass Wear Plate
PROBE HEAD
Electrodes
Distance To Be Determined
Outermost Layer of Reflective (Electrically-Conductive) Thermal Insulation
EQUIVALENT CIRCUIT FOR MEASUREMENT OF DISTANCE VIA CAPACITANCE

Figure 2. The **Probe Head** of Figure 1 contains two inductors and two plates of a capacitor. These elements are excited at various frequencies to obtain the various measurements. For example, a simple measurement of capacitance and the known properties of the equivalent circuit shown below can be used to determine the distance from the probe to the outermost layer of multilayer reflective insulation.

most layer of multilayer reflective insulation.

If contact tabs from the individual reflecting layers are brought out at the edge of multilayer insulation, the capacitances between layers can be measured to infer the distances between layers and the overall thickness. The capacitance between the metal coats on the two surfaces of the plastic sheet in each layer can also be measured. This capacitance can be compared with the value measured immediately after manufacture to determine the amount lost due to loss of the reflective coating through corrosion.

Also tested, but not included in the capabilities of the prototype, are an acoustical technique and a technique of real-time holographic interferometry combined with thermal probing to detect poor adhesion between foam insulation and a substrate. The ability of the acoustical technique to yield quantitative determinations of the degree of adhesion is limited. The holographic technique is more promising in this regard and is more likely to be included in subsequent versions of the testing equipment.

This work was done by Dennis R. Krause, Robert J. Bauman, and Thomas J. Davis of Spectron Development Laboratories, Inc., for **Marshall Space Flight Center**.

MFS-27199/TN

FOR ADDITIONAL INFORMATION: *Contact: Director, Technology Transfer Division, P.O. Box 8757, BWI Airport, MD 21240; (301) 621-0100 Ext. 241*

REFER TO THE NUMBER LISTED AT THE END OF THIS ARTICLE

Environmental Science & Technology

0759 Waste From Power Plants Conditions Soil

0760 Asbestos Management Guide is Available—How to manage asbestos-containing materials until materials are removed

Testing & Instrumentation

0761 Materials Aimed at Improving Pesticide, PCB Analyses

Other Items of Interest

0752 New Process Produces Lead from Galena Concentrates Without Pollution

0792 Alaskan Coastal Biological Data

Research Technology
Agricultural Research Service
U.S. Department of Agriculture

Waste From Power Plants Conditions Soil

Coal-burning plants that generate electricity must remove acid-forming oxides of sulfur and nitrogen from smokestack gases. If released into the air, these gases can contribute to the formation of acid rain, says a U.S. Department of Agriculture scientist.

According to soil scientist William L. Stout, the most promising removal system proposed and tested so far is a process known as atmospheric fluidized bed combustion. Byproducts from this pollution-controlling method of burning coal are environmentally safe to use as a soil conditioner for reclaimed strip mines and for farms that grow several forage and food crops.

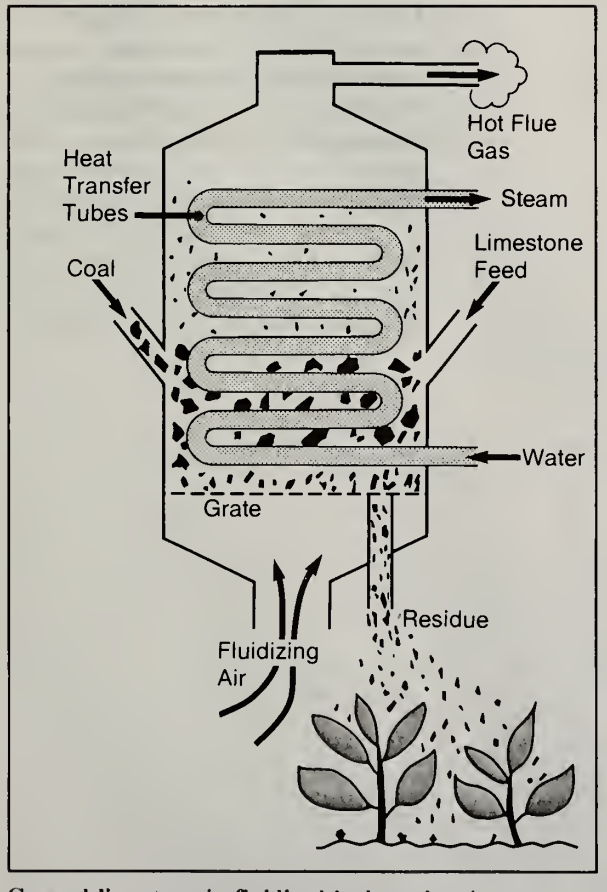

Ground limestone in fluidized bed combustion chamber removes sulfur and other potential contaminants from flue gases.

This finding is according to a 10-year study by USDA's Agricultural Research Service in cooperation with state experiment stations in Alabama, Virginia, and West Virginia.

In this system, crushed coal and finely ground limestone are suspended or fluidized by jets of air and burned at a controlled rate and temperature. Sulfur from the coal reacts with calcium in the limestone to form gypsum, calcium oxide, and some oxides of metals.

The whitish, granular residue contains essential plant nutrients such as sulfur, calcium, magnesium, potassium, phosphorus, iron, molybdenum, boron, copper, and zinc, as well as some toxic heavy metals such as cadmium.

"But crop plants are far less likely to take up heavy metals from fluidized bed residues than from sewage sludge containing them," Stout says. That was confirmed, he adds, in tests done on reclaimed surface mines, orchards, food crops, and pastures.

"We found no excessive buildup of harmful substances in soil or plants," he says. "Cows and sheep did not get toxic quantities from forage. Neither did pigs fed corn, wheat, soybeans, fruit, and vegetables."

Fluidized bed combustion produces about 2,000 tons of residue a day at a 1,000-megawatt power plant—enough for a typical application of residue on 500 acres, according to Stout. All farm uses of the residue must be approved by the appropriate regulatory agencies, he cautions.

Stout says that the tests show that the residue is best used as a liming agent to lower soil acidity. Its gypsum content

gives the residue an advantage over lime: It unites near-microscopic particles of clay to form granules. The spaces between the granules give roots better access to water and fertilizer.

The residue could also be used in roadbeds and as an aggregate in cement and building blocks.

Chemist James L. Hern, formerly with ARS at its Appalachian Soil and Water Conservation Research Laboratory in Beckley, West Virginia, notes that the residue is highly caustic and can severely injure unprotected skin, lungs, and eyes. When handling the substance, people must observe the federal safety guidelines.

According to ARS' Carl Carlson (retired), fluidized bed combustion may also promise an efficient way to dispose of trash in the future. "Many municipalities are already hard-pressed for landfill sites," he says. "Technology gained from the present studies could be used to develop electricity-generating plants that burn garbage without polluting the air. This might put an end to ocean dumping of wastes."

The researchers published recommendations for the safe application of the residue in a manual for power plant managers, consultants, and government agencies in August 1988, says one of its co-authors, soil scientist Ronald F. Korcak of the ARS Fruit Laboratory, Beltsville, Maryland.

The studies were supported by the U.S. Department of Energy and the Tennessee Valley Authority National Fertilizer Development Center.

William L. Stout is in the USDA-ARS Regional Pasture Research Laboratory, Curtin Rd., University Park, PA 16802 (814) 863-0947. Ronald F. Korcak is in the USDA-ARS Fruit Laboratory, Bldg. 004, Beltsville Agricultural Research Center, Beltsville, MD 20705 (301) 344-4650. ✦

The Manual for Applying Fluidized Bed Combustion Residue to Agricultural Lands (ARS-74) may be purchased from the National Technical Information Service, 5285 Port Royal Road, Springfield, VA 22161, (703) 487-4600. Cost is $13.95 each plus $3.00 handling.

NAVY
Domestic Technology Transfer Fact Sheet

Asbestos Management Guide is Available

How to manage asbestos-containing materials until materials are removed

Managing asbestos-containing materials (ACM) is necessary until those materials are removed. Major elements of a sound ACM management program include

- Alerting workers and building occupants to the location of ACM in their work spaces
- Implementing initial and periodic cleaning
- Training custodial, maintenance, and service personnel in proper cleaning and maintenance
- Establishing preventive measures to minimize ACM disturbances during routine operations, minor building maintenance, and repair and renovation projects
- Monitoring the conditions of the ACM to determine any increased potential for producing airborne fibers

The Naval Engineering and Environmental Support Activity (NEESA), Port Hueneme, California, has developed an Operations and Maintenance Guide Plan to provide the basics for assuring that effective programs are established in a timely manner once asbestos conditions have been identified.

For Additional Information:

Backup material on this effort is available from:

Navy Domestic Technology Fact Sheet Reader Reply Service
Code E211
Naval Surface Weapons Center
Dahlgren, VA 22448-5000
(703) 663-8921

Refer to 140302/TN

NIST Technology Update

National Institute of Standards & Technology
(Formerly the National Bureau of Standards)
U.S. Department of Commerce, Gaithersburg, MD 20899

Materials Aimed at Improving Pesticide, PCB Analyses

Scientists seeking to develop or validate the accuracy of analytical methods for measuring selected pesticides, polychlorinated biphenyls (PCBs), and alpha-tocopherol (a form of vitamin E) in fish and other fatty food products should find a new standard reference material (SRM) useful. The SRM contains certified concentrations of six chlorinated pesticides (hexachlorobenzene, alpha-HCH, trans-chlordane, cis-chlordane, trans-nonachlor, and dieldrin), five individual PCBs, and the nutrient alpha-tocopherol in cod liver oil. In addition to containing the certified components, the SRM also has noncertified concentrations of six dioxin compounds and a related compound, octachlorodibenzofuran.

FOR ADDITIONAL INFORMATION: The new material, SRM 1588, Organics in Cod Liver Oil, is available for $199 per set of five sealed vials from the Office of Standard Reference Materials, NIST, B311 Chemistry Bldg., Gaithersburg, Md. 20899; telephone: (301)975-6776.

Manufacturing, Machinery & Tools

0762 Adaptive Control of Remote Manipulator—A reference trajectory is tracked without modeling robot dynamics. (Licensing Opportunity)

0763 Discrete-Time Model-Reference Adaptive Control—The command-generator tracker concept is exploited in the discrete-time setting.

0764 Lightweight Restraint for Coupling Flanges—A cable-and-pulley mechanism allows limited motion. (Licensing Opportunity)

0765 Miniature Centrifugal Compressor—A small machine compresses neon for cocling to temperatures as low as 30K.

0766 Self-Aligning Robotic End Effector and Receptacle—Congruent surfaces provide alignment for gripping, installation, and removal.

0767 New Device Achieves Faster, More Uniform Metal Coating

0768 New Solder Joint Inspection System

Testing & Instrumentation

0769 Non-Destructive Laser/Thermal and Acoustic Microscopy Techniques for TAB Technology

Other Items of Interest

0720 Digital Controller for Acoustic Levitation—A computer controls sonic fields in three dimensions.

0806 Impedance Probe "Fine-Tunes" Electroplating Solutions

NASA Tech Brief
National Aeronautics and Space Administration

Licensing Opportunity

NASA's Jet Propulsion Laboratory, Pasadena, California

Adaptive Control of Remote Manipulator

A reference trajectory is tracked without modeling robot dynamics.

A robotic control system (see figure) causes a remote manipulator to follow closely a reference trajectory in a Cartesian reference frame in the work space, without resort to a computationally intensive mathematical model of robot dynamics and without knowledge of the robot and load parameters. The system, derived from linear multivariable theory, uses relatively simple feedforward and feedback controllers with model-reference adaptive control.

The system requires measurements of the position and velocity of the end effector of the manipulator. These can be obtained directly from optical sensors or by calculation using the known kinematic relationships between the measured manipulator-joint angles and the end-effector position.

In deriving the control equations, the coupled nonlinear differential equations of the robot dynamics and kinematics are first expressed in general form, then linearized by the calculation of perturbations about a specified operating point in the Cartesian coordinates of the end effector. The resulting mathematical model is a linear multivariable system of order 2n (where n = the number of independent spatial coordinates of the manipulator) that expresses the relationship between the increments of the n actuator control voltages (inputs) and the increments of the n coordinates of end-effector trajectory (outputs).

The problem then becomes one of making the end-effector trajectory increments track the reference-trajectory increments: this requires independent feedback and feedforward controllers. The feedback controller provides a stable closed-loop system with poles at desired locations in the Laplace-transform complex-frequency domain and ensures that initial tracking errors decrease asymptotically to zero with time. For this purpose, it suffices to apply position and velocity feedback through n × n position- and velocity-feedback gain matrices.

The feedforward controller causes the actual position to track the reference position. The incremental feedforward controller is chosen to be the minimal-order inverse of the end-effector transfer function. The total control law combines the trajec-

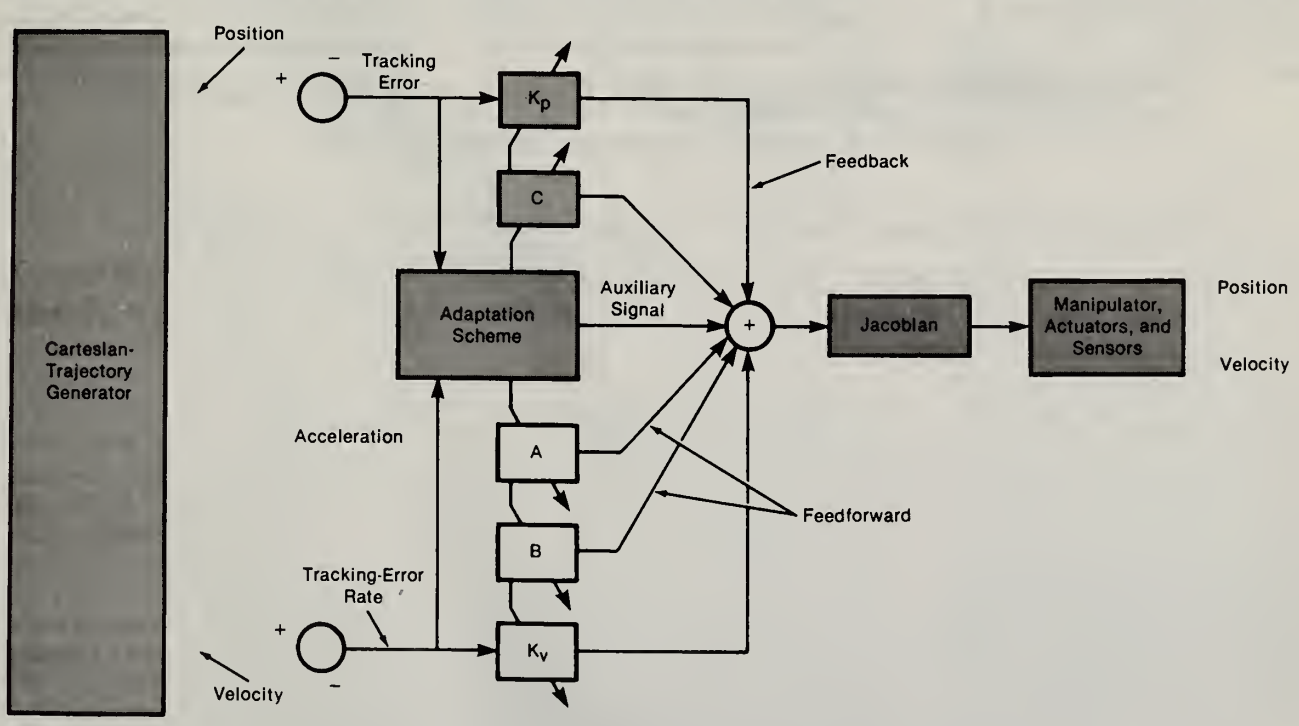

Note: K_p, C, A, B, and K_v are Controller-Gain Matrices

The Adaptive Control System, using feedforward of the desired trajectory and feedback of the actual manipulator position and velocity, causes the manipulator to track a reference trajectory. The system is insensitive to changes in the robot and load parameters and requires less computation and memory than do other control systems of similar capability.

tory and actuator-voltage increments with the values of the actuator voltages and positions at the nominal operating point.

The gains of the controllers and the operating-point term in the total control law are varied continuously to adapt to variations in the coefficients of the robot model due to changes in the operating point. The adaptation laws, derived by the Lyapunov method, do not require the knowledge of any robot parameters or of the payload and are based entirely on the reference trajectory and the tracking error, both of which are available. Thus, the adaptive controller treats the robot as a "black box."

This work was done by Homayoun Seraji of Caltech for **NASA's Jet Propulsion Laboratory**.

In accordance with Public Law 96-517, the contractor has elected to retain title to this invention. Inquiries concerning rights for its commercial use should be addressed to

Edward Ansell,
Director of Patents and Licensing
Mail Stop 301-6
California Institute of Technology
1207 East California Boulevard
Pasadena, CA 91125

Refer to NPO-16922/TN

Jet Propulsion Lab.
NASA Resident Office
Technology Utilization Officer: Gordon S. Chapman
Mail Stop 180-801
4800 Oak Grove Drive
Pasadena, CA 91109
(818) 354-4849
Patent Counsel: Paul F. McCaul
Mail Code 180-801
4800 Oak Grove Drive
Pasadena, CA 91109
(818) 354-2734
Technology Utilization Mgr. for JPL: Norman L. Chalfin
Mail Stop 156-211
4800 Oak Grove Drive
Pasadena, CA 91109
(818) 354-2240

FOR ADDITIONAL INFORMATION: *Contact: Director, Technology Transfer Division, P.O. Box 8757, BWI Airport, MD 21240; (301) 621-0100 Ext. 241*
REFER TO THE NUMBER LISTED AT THE END OF THIS ARTICLE

NASA Tech Brief
National Aeronautics and Space Administration

Discrete-Time Model-Reference Adaptive Control

The command-generator tracker concept is exploited in the discrete-time setting.

A paper discusses the stability of digital model-reference adaptive control (MRAC) of a robotic system or plant that operates at discrete time steps. The command-generator tracker (CGT) concept, originally proposed for continuous-time systems, is applied in the discrete-time setting, enabling the relaxation of some restrictive assumptions that guarantee the stability of the system controlled according to the resulting algorithm.

The mathematical development begins with the representation of the plant in deterministic-autoregressive-moving-average form. The CGT condition on inputs and outputs is invoked. Then the error-equation dynamics are stated and incorporated to obtain a nonadaptive model-reference control law. Finally, the indirect MRAC law is derived, and the main theorem regarding stability is proved.

The use of the CGT concept is novel in discrete-time MRAC in that matching of the model is addressed in terms of the output signals rather than the transfer functions. The CGT condition enables the formulation of the error equation in terms of the parameters of the plant. The indirect adaptive-control method of estimating first the unknown parameters and using them in, for example, the pole-placement algorithm can then be applied to the error equation. This scheme affords a small reference model via the CGT condition and casts away the minimum-phase requirement by virtue of the adaptive placement of poles.

There is a price, however. If the CGT condition must hold for an arbitrary model input signal, then the plant is necessarily of minimum phase. If it is not of minimum phase, then the resulting control algorithm, in its present form, applies only to single-input/single-output finite-dimensional systems. The tradeoff between the class of model input signals and the class of systems that can be considered may be a practical and desirable one in many situations. Likely applications include systems in which sensors and actuators are not placed together.

This work was done by John T. Wen and Deirdre R. Meldrum of Caltech and Mark J. Balas of Rensselaer Polytechnic Institute for **NASA's Jet Propulsion Laboratory**. *"Discrete Time Model Reference Adaptive Control Using CGT Concept." NPO-17062/TN*

FOR ADDITIONAL INFORMATION: *Contact: Director, Technology Transfer Division, P.O. Box 8757, BWI Airport, MD 21240; (301) 621-0100 Ext. 241*
REFER TO THE NUMBER LISTED AT THE END OF THIS ARTICLE

NASA Tech Brief
National Aeronautics and Space Administration
Lyndon B. Johnson Space Center, Houston, Texas

Licensing Opportunity

Lightweight Restraint for Coupling Flanges

A cable-and-pulley mechanism allows limited motion.

The end flanges of a flexible coupling system are restrained against excessive rotation or axial separation by an inexpensive, lightweight mechanism based on cables and pulleys. Intended to replace a cumbersome set of gimbals on a pair of spacecraft-coupling rings, the restraining mechanism can be adapted to cable, duct, hose, or passageway couplings between vehicles, or to other applications in which angular and positional misalignments must be restricted to moderate specified values.

A continuous cable is threaded alternately through pulleys dispersed about the circumference of the two flanges (see figure). In a redundant scheme, two or more independent pulley-and-cable sets would be used so that at least one could continue to provide restraint if the others break. Instead of having a continuous cable (or cables), the cable ends can be anchored near each other on one of the flanges.

When the flanges are pulled axially away from each other, the cable stretches taut, preventing further separation. If one flange then tilts with respect to the other, the cable runs through the pulleys to allow increased axial separation on one side and decreased axial separation on the other side, while the axial distance between the centers of both flanges remains the same.

The mechanism restricts torsional rotations: when the cable is taut, further turning pulls the flanges together along the axis, eventually bringing them hard against each other. In a similar manner, the mechanism can also restrict lateral misalignment. However, to prevent damage to the cables by the edges of the pulleys, it is probably better to restrict lateral misalignment by means of hard stops.

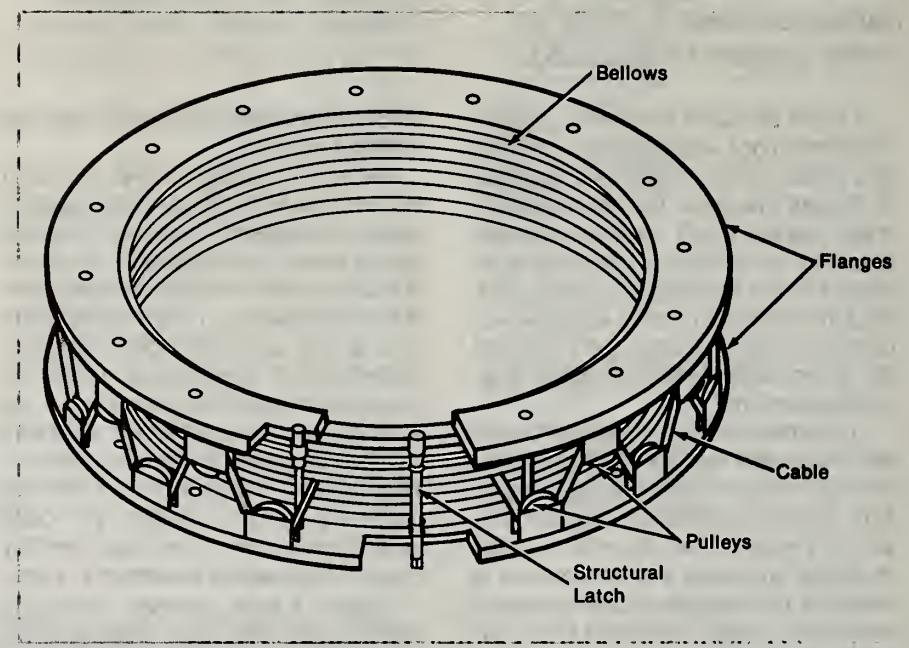

The Total Misalignment of Two End Flanges is limited to the amount of slack available in the cable-and-pulley mechanism. When the cable is taut, the further axial separation of the flange centers is restrained, but small tilts are accommodated by the running of the cable through the pulleys.

This work was done by Willie D. Whitaker of McDonnell Douglas Corp. for **Johnson Space Center.**

This invention is owned by NASA, and a patent application has been filed. Inquiries concerning nonexclusive or exclusive license for its commercial development should be addressed to the Patent Counsel, Johnson Space Center
Refer to MSC-21211/TN

Lyndon B. Johnson Space Center
Technology Utilization Officer: Dean C. Glenn
Mail Code IC-4
Houston, TX 77058
(713) 483-3809
Patent Counsel:
Edward K. Fein
Mail Code AL3
Houston, TX 77058
(713) 483-4871

FOR ADDITIONAL INFORMATION: *Contact: Director, Technology Transfer Division, P.O. Box 8757, BWI Airport, MD 21240; (301) 621-0100 Ext. 241*
REFER TO THE NUMBER LISTED AT THE END OF THIS ARTICLE

NASA Tech Brief
National Aeronautics and Space Administration
Goddard Space Flight Center, Greenbelt, Maryland

Miniature Centrifugal Compressor

A small machine compresses neon for cooling to temperatures as low as 30 K.

A miniature turbocompressor undergoing development is designed for reliability and long life. A cryogenic system that includes the compressor, a turboexpander, and heat exchanger will provide 5 W of refrigeration at 70 K from 150 W input power. The design speed of the machine is 510,000 rpm.

The compressor (see figure) has gas-lubricated journal bearings and a magnetic thrust bearing. When the compressor is running, there is no bearing contact and thus no wear. Wear can occur only when the machine is starting or stopping — before the bearings lift off and after they set down, and this wear can be relatively insignificant.

The solid rotor contains narrow axial grooves that direct the magnetic flux toward the axis. The flux is therefore surrounded by a relatively-large cross-sectional area of steel to carry the circulating electric current. This reduces the effective electrical resistance and increases the efficiency of the motor.

The motor stator does not contain salient pole teeth on its inside diameter because such teeth would generate eddy currents on the surface of the solid rotor. Instead, it contains internal bores for the windings. The windings are stranded copper wire insulated with polytetrafluoroethylene. The wire is threaded through circular holes in the bores of the stator; the heat generated in the wires is carried away by conduction through the stator.

The stator consists of layers of a low-loss magnetic nickel/iron alloy, with a layer of copper at every seventh layer. The copper, which has a thermal conductivity more than 30 times as great as that of the magnetic alloy, aids in the removal of heat from the windings. Cooling water circulates through a jacket around the stator to remove heat from the motor housing.

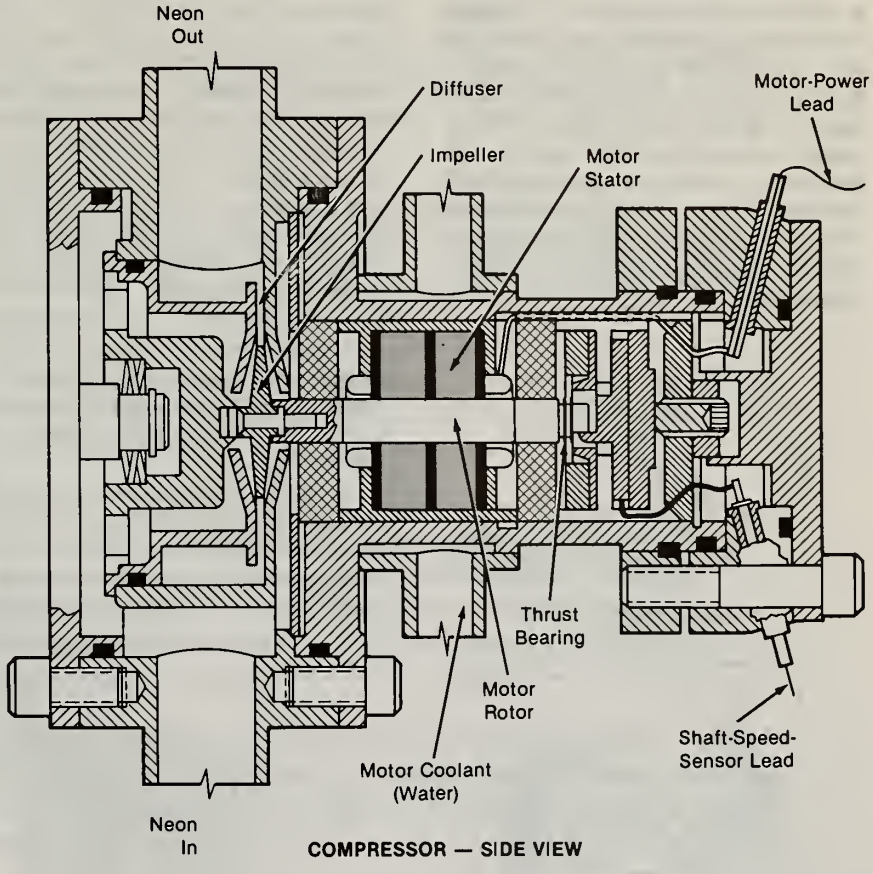

COMPRESSOR — SIDE VIEW

Neon Working Fluid Flows Symmetrically on both sides of the impeller. At the opposite end of the turbine shaft, a capacitance sensor measures rotational speed by detecting the passage of a flat surface on the shaft. The shaft has a mass of only a few grams. It exhibits little vibration because the gas bearings damp oscillations.

The impeller in the compressor is double-sided and symmetrical: This shape results in a far smaller axial thrust than would be generated by a single-sided impeller. The small remaining axial thrust can be handled by a magnetic thrust bearing instead of by the gas thrust bearing that would otherwise be needed. The magnetic bearing is expected to absorb less power than a comparable gas bearing, and thus to improve the efficiency of the compressor.

This work was done by Herbert Sixsmith of Creare Inc. for **Goddard Space Flight Center** *GSC-13093/TN*

FOR ADDITIONAL INFORMATION: *Contact: Director, Technology Transfer Division, P.O. Box 8757, BWI Airport, MD 21240; (301) 621-0100 Ext. 241*
REFER TO THE NUMBER LISTED AT THE END OF THIS ARTICLE

NASA Tech Brief
National Aeronautics and Space Administration
Goddard Space Flight Center, Greenbelt, Maryland

Self-Aligning Robotic End Effector and Receptacle

Congruent surfaces provide alignment for gripping, installation, and removal.

An industrial-robot hand (end effector) and a mating receptacle include congruent male and female conical and V-shaped surfaces for positive alignment. The receptacle is part of an object to be removed from a fixed position, transported, and installed in another fixed position — for example, during an assembly process. The end effector grasps the receptacle firmly for transport, and a tool in the end effector loosens or tightens a mounting screw in the object during removal or installation, respectively.

The robot hand, which is at the end of a remote manipulator, is observed via television and guided by manual joystick control to approximate alignment within about 0.5 in. (13 mm) of the receptacle. An automatic electronic "feeling" system then takes control and quickly performs the precise final alignment similarly to the way in which a human technician aligns and pushes together mating parts. When the mating conical surfaces first make contact (see Figure 1), the control system responds to signals from force and torque sensors in the end effector by moving the end effector slightly sideways to reduce the contact forces and torques to zero. As the end effector moves farther into the receptacle, contact is made and broken repeatedly in this manner.

The end effector is also rotated about its conical axis, and contact forces and torques are used to detect the alignment of the V-shaped surfaces. When the end effector and the receptacle are pushed all the way together and all mating surfaces are precisely aligned after the final contact/repositioning cycle, the force/torque system senses only an axial contact force. The contact/repositioning cycles are so brief that to a human observer the alignment process appears to be a smooth motion.

The end effector includes parallel gripping jaws equipped with lifting pins, which are inserted in opposing holes on the receptacle once alignment is achieved (see Figure 2). While the receptacle is thus gripped, the object can be moved about or held fixed while an allen wrench or similar tool engages a mating recess in the head of the mounting screw. A remotely controlled motor in the end effector turns the tool to tighten or loosen the screw.

This work was done by Glen J. VanSant and Eugene G. Gibbs of RCA Corp. for **Goddard Space Flight Center.**
GSC-13152/TN

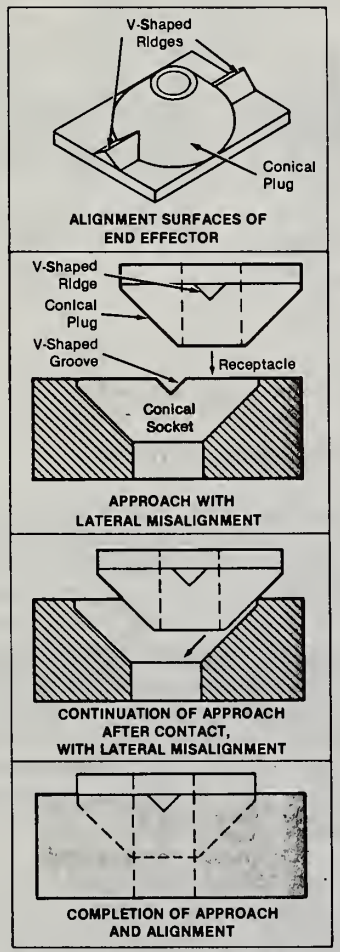

Figure 1. **The Surfaces of the End Effector and Receptacle** are keyed to each other for automatic alignment.

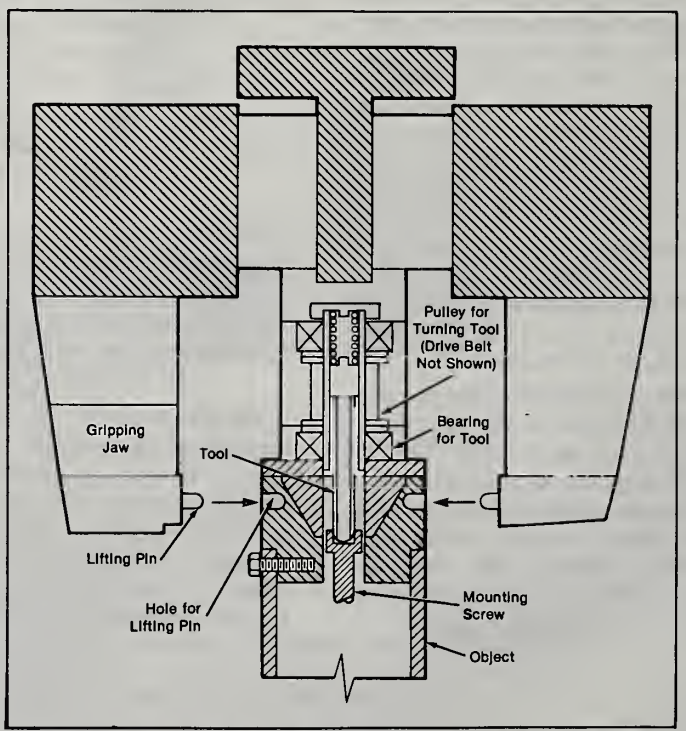

Figure 2. **Lifting Pins Are Inserted** in the receptacle to lock the end effector and receptacle together. The tool can then turn the mounting screw, and the end effector can lift the object.

FOR ADDITIONAL INFORMATION: *Contact: Director, Technology Transfer Division, P.O. Box 8757, BWI Airport, MD 21240; (301) 621-0100 Ext. 241*
REFER TO THE NUMBER LISTED AT THE END OF THIS ARTICLE

Sandia National Laboratory

New Device Achieves Faster, More Uniform Metal Coating

A new device offering greater speed and uniformity in metal plating through ion beam sputtering has been developed by Donald J. Sharp of Sandia National Laboratories. As a result, the U.S. Department of Energy (DOE) has been awarded a patent (NO.4,757.922) in Sharp's name.

The technique of ion beam sputtering directs highly energized ions of inert gases (argon, neon, xenon) at a target material such as copper or aluminum. Atoms of the metal are thereby dislodged as ions and deposited as a thin film on a nearby negatively charged surface.

Current technologies for sputtering material off the target and onto a substrate suffer from a lack of uniformity in deposition. Sharp's device addresses this problem by using a hollow cylindrical target. Most ion sputtering devices use a flat target.

The cylindrical target geometry offers several advantages: ions strike the target material at a glance, kicking up more debris than they do when hitting the target head-on, thereby resulting in faster deposition; the positively biased ion bombardment at one end of the negatively biased cylinder produces a steady beam of metal for plating flat substrates like silicon wafer; by introducing ion beams from both ends of the cylinder it is possible to plate spherical or odd-shaped objects suspended inside.

"This invention was inspired by the need to put down a uniform coating on the micro-balloons used in Sandia's PBFA (Particle Beam Fusion Accelerator)," Sharp explains. There are small spheres which, when filled with deuterium or tritium, eventually will serve as targets for advanced experiments with PBFA.

Sharp's new ion sputtering device proved to be inappropriate for the micro-balloons, but the technology appears promising for applications where a very high rate of sputtered deposition is important, or in situations where it is desirable to clean the substrate immediately before plating. Examples of the latter would include contaminated or oxidized metallic surfaces.

With the target cylinder at ground potential and the substrate biased negatively, the positively biased ion beam will pass through the center of the cylinder and strike the substrate. This will clean the substrate with ion bombardment immediately before plating begins, simply by switching a negative charge of approximately 2 k V back over to the cylinder. Deposition can then take place on a freshly cleaned substrate, ensuring optimum adhesion.

"By raising or lowering the cylinder voltage, we can cause the ion beam to intercept the target early or late, or to go on through the cylinder," Sharp points out. "This means that voltage provides a mechanism for controlling the trajectory, or spread, of sputtered material.

Most conventional ion sputtering devices aim the ion beam directly at the target. As Sharp describes it, each ion hits the target like a meteor colliding with the moon's surface, embedding itself in the material and kicking up debris.

"The trick to our device is to have the particles come in at an acute angle," Sharp notes. "These 'artificial micrometeorites' eject more debris when the impact occurs at such a glancing angle, as compared with a particle striking a material head-on."

As the inert-gas ions plow tangentially into the target, they dislodge a tiny plume of atoms from the sputtered material. These too become ions once they have lost one or more electrons, and therefore are available as contributors to the plating process.

Since plating occurs within the cylinder (centrally or near one end), the system is not suitable for covering large areas. The laboratory model at Sandia, for example, is limited to use with items measuring less than four inches since its cylinder diameter is four inches.

Sharp is in Sandia's Interfacial Chemistry and Coating Research Division.

FOR ADDITIONAL INFORMATION: Public Information Division, Code 3161, Department of Energy, Sandia National Laboratories, Albuquerque, NM 87185-5800; (505) 844-4207. Refer to announcement 24, No. 4.

NAVY Manufacturing Technology Program

New Solder Joint Inspection System

Solder joint quality has been evaluated for years using carefully developed visual criteria. These criteria include detailed instructions for the optimum observation and analysis of those joint parameters, such as wetting angles, which most accurately predict field performance. However, human visual observation is generally considered to be unreliable due to its subjective, non-quantitative and inconsistent nature.

Recognizing these limitations, the U.S. Navy's Electronics Manufacturing Productivity Facility (EMPF) in Ridgecrest, CA and IBM's System Integration Division, Owego, NY set, as a major objective of the CCAPS (Circuit Card Assembly and Processing System) program, the goal of developing a superior solution to the multi-billion dollar solder quality problem. A thorough investigation of existing and potential solder joint inspection approaches led to RVSI, a world leader in three-dimensional machine vision.

Significant breakthroughs in both high resolution, 3-D non-contact machine vision and expert system software resulted in a system which can automatically and consistently judge solder joint quality using established visual criteria.

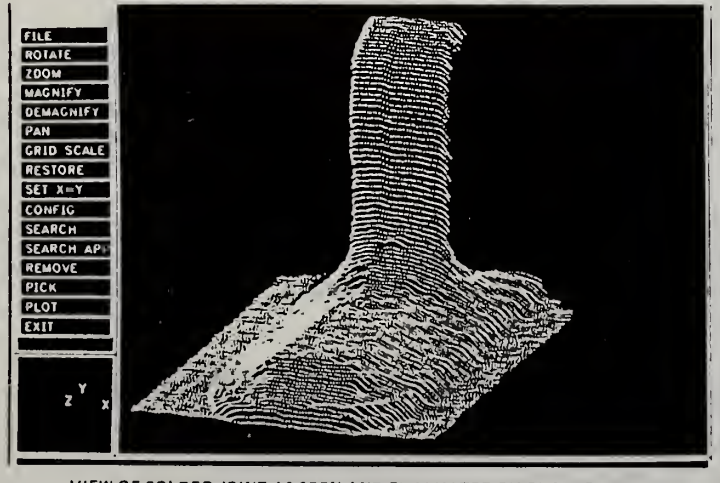

VIEW OF SOLDER JOINT AS SEEN AND EVALUATED BY RVSI HR-2000

The RVSI HR-2000, uses precise structured laser light scanning and optical triangulation techniques to obtain an extremely detailed 3-D geometric map of each solder joint. The thousands of independent x, y, z measurements gathered for each joint are processed by a sophisticated rule based software system, which draws upon the accumulated knowledge of joint quality experts and uses established, time-tested visual inspection criteria.

Process control, always desired but effectively impossible in the subjective world of human visual observation, is expected to be the greatest benefit to high reliability military electronics suppliers. The quantitative measurements taken by the machine provide the ability to spot process trends, before any defective boards are manufactured.

The automated approach draws on the same visual criteria being used today in military specifications such as MIL-STD-2000. The major difference is that the quantification of these criteria has removed the subjectivity from the evaluation process.

The CCAPS investment in solder joint inspection is expected to pay immediate dividends through a dramatic reduction in needless rework, fewer field failures, higher first-pass yields, labor savings and the introduction of true statistical process control in soldering.

For Additional Information:

For more information about the BMP program, please contact:

Best Manufacturing Practices Program
Office of the Assistant Secretary of
the Navy (Shipbuilding and Lobistics)
Mr. Ernie Renner, RM&QA-PA
Washington, DC 20360-5000
(202) 692-1146/0121

Non-Destructive Laser/Thermal and Acoustic Microscopy Techniques for TAB Technology

There has been a two year study underway as a dual contract award by Rome Air Development Center (RBRE) to develop a nondestructive test for metallurgical tape bonds formed by Tape Automated Bonding (TAB). The two contractors involved were: Vanzetti Systems, Stoughton, MA and Sonoscan Inc., Bensenville, IL. All technical work has now been completed.

The Vanzetti organization has had a laser/thermal inspection system for TAB bonds in operation since mid-`86 which can reveal lifted and deformed leads. However, in VLSI design the lead widths for TAB bonds can be as small as 2 mils. Under the contract funding Vanzetti was able to extend the present inspection methods to these smaller sizes. With further modification their system is able to analyze package bonds in the area range of thirty square mils to fifteen square mils. With the high speed and batch analysis of these bonds and increased sensitivity, it is possible to distinguish acceptable metallurgical bonds from rejectable bonds. Examples of rejectable bonds are: cold joints, voids and entrapped foreign material. The analytical technique was demonstrated on a minimum of four hundred metallurgical bonds and these bonds on the chip include both perimeter and area array bonds. All of the rejected bonds were also verified by destructive analysis.

Sonoscan has developed a non-destructive test utilizing real-time Scanning Laser Acoustic Microscopy (SLAM) to determine the quality of TAB bonds. In developing the test, Inner Lead Bonds (ILB) and Outer Lead Bonds (OLB) were individually documented acoustically and then pull tested for verification. Optical and metallurgical examination of the pulled leads and bond sites revealed inadequacies in the conventional pull test methods when applied to TAB, thus emphasizing the pressing need for more reliable evaluation techniques for TAB bond integrity. Acoustic microscopy appears to be able to supply this need.

Acoustic microscopy is the term applied to high resolution, high frequency ultrasonic inspection techniques which produce images of features beneath the surface of a sample. Because ultrasonic energy requires continuity of materials to propagate, internal defects such as voids, delamitations and cracks interfere with the transmission and/or reflection of ultrasound signals. Since air is a very poor conductor of ultrasound, gaps within or between samples are easily visualized by the localized changes in the ultrasound.

A matrix of samples having a range of bond qualities was obtained by both contractors and these samples were used to establish evaluation parameters. New test methods are proposed for inclusion in MIL-STD-883. For further information contact, P. Speicher, RADC/RBRE, Griffiss AFB, NY 13440-5700, (315) 330-4055.

FOR ADDITIONAL INFORMATION: Contact Reliability Analysis Center, P.O. Box 4700, Rome, NY 13440-8200; (315) 330-4151.

Materials

0770 Damage Tolerance and Durability of Rapidly-Solidified Aluminum-Base Powder Metallurgy Alloys

0771 SCC of Tungsten Alloy Penetrators

0772 Welding of Rapidly-Solidified Aluminum-Base Powder Metallurgy Alloys

0773 Low-Alloy Steel Calibration Standard Available

0774 Program on HIPing of Metal Powders Established

0775 Standard Reference Material Report Contains Microsphere Experiments

0776 David Taylor Research Center Researches New Anticorrosion Coating—Technique called electrochemical impedance spectroscopy

0777 Thermal Mechanical Processing to Control Grain Size

0778 Additives Lower Pickup of Moisture by Polyimides—Positron-annihilation tests show increased densities. (Licensing Opportunity)

0779 Alumina-Enhanced Thermal Barrier—Improved fibrous refractory composite material raises the temperature limit. (Licensing Opportunity)

0780 Annealing Increases Stability of Iridium Thermocouples—An improved heat treatment also increases ductility.

0781 Better PFAE's from Direct Fluorination—The process yields stable and effective lubricants under proper conditions.

0782 Calculating Dynamic Shear Moduli of Polymers (Licensing Opportunity)

0783 CdO Pretreatment for Graphite Lubricant Films—Sputtered films decrease friction and increase endurance.

0784 Effects of Aging on Embrittlement by Hydrogen—Concentration of hydrogen at grain boundaries determines the mode of fracture.

0785 Degradation of Carbon/Phenolic Composites by NaOH

0786 Orientating Superconductive Crystals for High Current Density

0787 Variable-Energy Ion Beams for Modification of Surfaces (Licensing Opportunity)

Testing & Instrumentation

0788 Measurement of Composition in Transparent Model Alloy—Noninvasive measurements are taken by Fourier-transform infrared spectroscopy

0789 Acoustical Imaging of Defects in Ceramics—Ultrasound is superior to x rays in the detection of microporosity.

Other Items of Interest

0743 Navy Tests Composite Propeller Shaft

0758 Nondestructive Inspection of Foam and Multilayer Insulations—Electromagnetic and electrostatic sensors probe hidden surfaces.

0767 New Device Achieves Faster, More Uniform Metal Coating

0806 Impedance Probe "Fine-Tunes" Electroplating Solutions

U.S. Air Force Fact Sheet

Damage Tolerance and Durability of Rapidly-Solidified Aluminum-Base Powder Metallurgy Alloys

A series of tests were conducted at the General Dynamics Fort Worth Division for the Air Force Wright Aeronautical Laboratories to compare the damage tolerance and durability of rapidly-solidified powder metallurgy alloys with presently used high strength aluminum-base ingot metallurgy alloys. Five different materials were included in this study; tensile and fracture toughness properties of these materials are described in Table 1. CW67 and 7091 are fine grained, highly alloyed Al-Zn-Mg-Cu alloys produced by powder metallurgy methods. CW67 was procured in the extruded form while 7091 was procured both as extrusions and as near-net-shape forgings. 2124 and 7475 alloys were procured as ingot-fabricated plate.

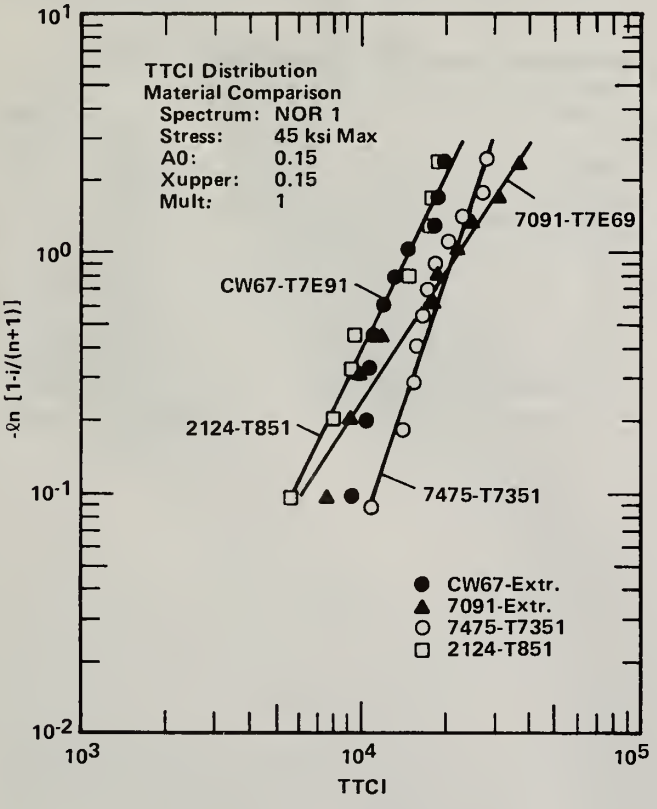

Figure 1. Time to Crack Initiation (TTCI) Comparisons for Four Aluminum Alloys (NOR 1 Spectrum)

Table 1. Mechanical Properties of Longitudinal Orientation

Material	Yield Strength, ksi	Tensile Strength, ksi	Elongation, percent	Fracture Toughness, ksi $\sqrt{in.}$
2124-T851	64	71	9	29
7475-T7351	63	73	14	48
7091-T7E69	75	83	14	36
7091-FORG.	73	80	15	–
CW67-T7E91	86	90	12	50

Two types of spectrum load fatigue tests were carried out to compare the damage tolerance of the five materials. One of these involved principally tension-compression loading, the other principally tension-tension loading. The results of the various fatigue tests were presented in detail in the summary report, and several graphs were provided in which time-to-failure, crack-growth-rate, or time-to-crack-initiation of the different materials were compared. A typical example, one based on the tension-tension spectrum load test results, is shown in Figure 1.

It was concluded from an analysis of the results of the various fatigue studies that powder metallurgy extrusions and forgings provided potential improvements in structural performance and reliability as compared to ingot metallurgy 2124 and 7475. It was also noted that 7091 extrusions appeared slightly superior to 7091 forgings, although the reason for this difference was not obvious. The type of loading also affected the relative performance of the different materials. For example, 7091 showed a greater advantage over 2124 when comparing results from tension-compression spectrum tests than from tension-tension spectrum tests.

FOR ADDITIONAL INFORMATION: A copy of the report is available from NTIS, Springfield, VA 22161; (703) 487-4600.

NTIS order number: ADA 199336/NAC

Price code: A08

U.S. Army Fact Sheet

SCC of Tungsten Alloy Penetrators

The stress-corrosion cracking (SCC) behavior of sintered tungsten alloy kinetic energy penetrators for military applications has been investigated at the U.S. Army Armament Research, Development, and Engineering Center.[6] Precracked cantilever bend specimens were immersed in 3.5 percent NaCl solution, and then were sustained loaded and exposed a maximum of 500 hours in 95 percent RH air. Fracture toughness (K_{Ic}) and stress-corrosion cracking threshold stress intensity (K_{Iscc}) values for the four alloys tested are summarized below:

Alloy, w/o	Stress Intensity, MPa $\sqrt{m}$ K_{Ic}	K_{Iscc}
95W-1.5Fe-3.5Ni	59.5	53.6
90W-5Fe-5Ni	54.5	45.2
90W-7.5Ni-2.5Cu	64.0	43.6
97W-0.7Fe-1.6Ni-0.5Cu-0.1Co	49.5	32.6

Note that all candidate alloys exhibited SCC, but that the 95W-1.5Fe-3.5Ni alloy was least susceptible.

FOR ADDITIONAL INFORMATION: A report is available from NTIS, Springfield VA 22161; (703)487-4600.

NTIS order number: ADA 203201/NAC

Price code: A03

U.S. Army Fact Sheet

Welding of Rapidly-Solidified Aluminum-Base Powder Metallurgy Alloys

Work supported at the Ohio State University Research Foundation by the Army Research Office during the past 3 years is summarized in a report issued in April 1988. Two types of advanced aluminum base alloys of considerable current interest were investigated in that program. The first were Al-Fe-X alloys designed for applications requiring high strength at high temperatures; the second were Al-Li-X alloys with attractive combinations of strength, density, and elastic modulus at room temperature.

The Al-Fe-X alloys proved the easier to join successfully. Procedures which were applied to the various alloys included electron-beam welding, capacitor-discharge welding, inertia-friction welding, and diffusion bonding. The primary requirement to achieve a satisfactory bond using one of the two fusion welding procedures (electron-beam welding or capacitor-discharge welding) was to obtain rapid solidification through the freezing range so as to recreate the fine intermetallic dispersion originally present in the alloy. For electron beam welding procedures to be useful, it was also essential that the hydrogen content of the alloys be low. If not, porosity was excessive. Inertia-friction welding resulted in a minimum disruption of the microstructure initially present in the alloys to be joined, and could also be used to join high-hydrogen materials. Diffusion bonding could be accomplished, but required careful selection of bonding procedures to avoid particle growth and/or porosity formation at the bond line as a result of the Kirkendall Effect. A silver interlayer was used to facilitate diffusion bonding.

Less study was devoted to studies of the joining of Al-Li-X alloys than to the joining of Al-Fe-X alloys. In general, fusion welding procedures were incapable of providing acceptable welds in the lithium-containing alloys due to high hydrogen contents. It was suggested that inertia-friction welding was more likely to prove successful in joining Al-Li-X produced from rapidly solidified powder, but it does not appear from the information provided in the report that such procedures were tried.

Four publications that have appeared, or will appear in the future, in the technical literature were included in an Appendix to the Summary Report. Those publications provide significantly more detail regarding the results achieved in the study than is included in the body of the Summary Report.

FOR ADDITIONAL INFORMATION: A copy of the report is available from NTIS, Springfield, VA 22161; (703) 487-4600.

NTIS order number: ADA 194677/NAC

Price code: A06

NIST Technology Update

National Institute of Standards & Technology
(Formerly the National Bureau of Standards)
U.S. Department of Commerce, Gaithersburg, MD 20899

Low-Alloy Steel Calibration Standard Available

A new standard for checking and calibrating oxygen and nitrogen analyzers in the steel industry has been developed under a cooperative program between the American Society for Testing and Materials (ASTM) and NIST. Information on the concentrations of these gases is important to the properties of steel because they contribute markedly to steel brittleness and therefore to the strength and durability of steels. Standard Reference Material (SRM) 1754, Oxygen and Nitrogen in Low-Alloy Steel, AISI 4320, is in rod form, 0.95 cm x 0.95 cm x 10.2 cm (3/8" x 3/8" x 4"). The new SRM was certified through the NIST/ASTM Research Associate Program involving nine industrial laboratories.

FOR ADDITIONAL INFORMATION: SRM 1754 is available for $119 per unit of 1 rod from the Office of Standard Reference Materials, NIST, B311 Chemistry Bldg., Gaithersburg, MD 20899; (301)975-6776.

NIST Technology Update

National Institute of Standards & Technology
(Formerly the National Bureau of Standards)
U.S. Department of Commerce, Gaithersburg, MD 20899

Program on HIPing of Metal Powders Established

The hot isostatic pressing (HIPing), or consolidation of rapidly solidified metal powders into near-net, or close-to-final, shapes, may be a very reliable way to make parts out of advanced alloys such as titanium aluminide. A team of scientists and engineers from industry, universities, and government are working to develop the measurement and control tools needed to automate the HIPing process. The collaborative effort is jointly sponsored by NIST and the Defense Advanced Research Projects Agency (DARPA). For titanium-aluminide alloys, rapidly solidified powders are sealed in a canister or mold and placed inside a furnace. The materials is heated to approximately 1100 degrees Celsius and compressed into solid shapes by hydrostatic pressures up to 200 megapascals, or 30,000 pounds per square inch. Under the collaborative effort, researchers are developing sensors, process models, and an "expert" computer system to automate the entire production cycle from raw powders to finished parts.

FOR ADDITIONAL INFORMATION: For information on the cooperative HIPing program, contact: Dr. Robert J. Schaefer, NIST, A153 Materials Bldg., Gaithersburg, Md. 20899; (301)975-6162.

NIST Technology Update

National Institute of Standards & Technology
(Formerly the National Bureau of Standards)
U.S. Department of Commerce, Gaithersburg, MD 20899

Standard Reference Material Report Contains Microsphere Experiments

A series of microscope experiments for students is described in a NIST report on the construction, preparation, and recommended uses of Standard Reference Material (SRM) 1965, Microsphere Slide, 10-Micrometer Polystyrene Spheres. The SRM is a microscope slide with the first commercial product made in space - the 10-micrometer polystyrene spheres - deposited on it. The SRM is an education tool as well as a standard to calibrate microscopes for small particle measurements. The spheres are arranged in two types of groupings. One is an "unordered" arrangement, resembling strings of beads. The other grouping is an "ordered" two-dimensional hexagonal array for use as a microlength standard and to act as a "stage" micrometer.

FOR ADDITIONAL INFORMATION: Copies of Description of the SRM 1965 Microsphere Slide SRM 1965 are available for $105 from the Office of Standard Reference Materials, NIST, B311 Chemistry Bldg., Gaithersburg, MD 20899; telephone: 301/975-6776. A copy of the report is available from NTIS, Springfield, VA 22161; (703)487-4600.

NTIS order number: PB 89153704/NAC
Price code: A04-1595

NAVY
Domestic Technology Transfer Fact Sheet

David Taylor Research Center Researches New Anticorrosion Coating

Technique called electrochemical impedance spectroscopy

To improve the Navy's capabilities for lifetime prediction of coating performance, the David Taylor Research Center (DTRC), Bethesda, Maryland, is using an electrochemical impedance method. A new electrochemical technique correlates with the long-term corrosion performance of Navy coatings for ships. The technique, called electrochemical impedance spectroscopy (EIS), is nondestructive, and involves applying a very low amplitude alternating voltage to a piece of coated steel, then measuring the current required. By applying the signal over a wide range of frequencies, the electrical behavior of the coating can be separated from the electrochemical behavior of the underlying steel.

Panels coated with a variety of coatings were exposed in seawater for more than two years. Coating performance was analyzed visually using an ASTM rating system. Some EIS measurement parameters were found to correlate well with the visual assessments of coating performance and could detect coating deterioration long before it became apparent visually. As a result, researchers at DTRC expect to reduce life-cycle costs resulting from corrosion.

For Additional Information:

Backup material on this effort is available from:

Navy Domestic Technology Fact Sheet Reader Reply Service
Code E211
Naval Surface Weapons Center
Dahlgren, VA 22448-5000
(703) 663-8921

Refer to 140304/TN

U.S. Navy Fact Sheet

Thermal Mechanical Processing to Control Grain Size

Studies have been conducted at the Naval Air Development Center to determine whether intermediate thermal mechanical processing can be used to produce a fine grain size in 2020 aluminum alloy, an aluminum copper alloy containing alloying additions of lithium, cadmium, and manganese. The objective of this work was to improve the fracture toughness of 2020-T6.

Three variables were examined to determine their effects on grain size: the microstructure of the alloy prior to thermal mechanical processing, the amount of cold (or warm) reduction, and the recrystallization conditions. By appropriate selection of those variables, it was possible to reduce the grain size from 400 μm to 10 μm.

The amount of cold rolling proved to be the most significant variable. It was not possible to achieve recrystallization, at least within the range of initial microstructures and recrystallization treatments examined, unless the alloy was cold rolled more than 40 percent reduction in thickness. Cracking occurred at slightly less than 50 percent reduction. Recrystallization conditions were second in importance. Recrystallization at too low a temperature did not result in recrystallization whereas grain growth was excessive at very high temperatures. Recrystallization at 900 to 940 F for a time period approaching 3 hours proved successful. Initial microstructure was least important although only two were examined, either solution heat treated (water quenched) or fully annealed. The latter treatment was considered slightly superior, apparently as a consequence of a retarding effect of coarse precipitates on grain growth.

No information was reported on the effects of the fine, recrystallized strain structure that was produced by intermediate thermal mechanical processing on fracture toughness, or other mechanical properties of the alloy after final heat treatment.

FOR ADDITIONAL INFORMATION: A copy of the report is available from NTIS, Springfield, VA 22161; 487-4600.

NTIS order number: ADA 199249/NAC
Price code: A03

NASA Tech Brief
National Aeronautics and Space Administration
Langley Research Center, Hampton, Virginia

Licensing Opportunity

Additives Lower Pickup of Moisture by Polyimides

Positron-annihilation tests show increased densities.

A series of new polyimide-processing additives decrease the free volume and the pickup of moisture in a new 422 copolyimide. The physical properties of several copolyimides synthesized from linear BDSDA/ODA/MPD (see table) homopolymers have been investigated previously, by positron-annihilation spectroscopy, with results indicating that the copolyimides have a unique transition molecular structure characterized by higher electron densities and stronger bonds. The transition structure permits both physical and chemical entry of water molecules into it.

Following these discoveries, we decided to study the effects of several short-chain processing additives on the properties of the optimal BDSDA/ODA/MPD [422] copolyimide (see figure). The compositions were prepared by imidizing a mixture of a high-molecular-weight copoly(amic acid) of the BDSDA/ODA/MPD [422] resin with various amic acid additives at a concentration of 5 to 10 percent by weight.

An examination of the saturation moisture contents shows that the free volume in the [422] copolyimide decreases systematically as 5 percent BDSDA/AN, ODA/PA, and MPD/PA are added, respectively. It thus appears that MPD/PA is the most effective short-chain additive for making the [422] copolyimide more compact and, consequently, denser; but doubling the concentration of BDSDA/AN appears to have a disproportionately large effect on free volume in the base polymer. Positron-annihilation results are also consistent with this large reduction in free volume. A concomitant increase in the intensity of the long-lifetime component suggests that most of the free electrons have been engaged in strengthening the electronic bonds between various segments of the molecular chains.

This work was done by Terry L. St. Clair and Jag J. Singh of **Langley Research Center** *and J. Richard Pratt of Planning Research Corp. Further information may be found in NASA TM-89023 [N87-12614],*

BDSDA	4′4′-bis(3,4-dicarboxyphenoxy)diphenylsulfide dianhydride
ODA	4,4′-diaminodiphenyl ether
MPD	1,3-diaminobenzene(m-phenylene diamine)
PA	phthalic anhydride
AN	aniline
BDSDA/AN	BDSDA end-capped with aniline
ODA/PA	ODA end-capped with phthalic anhydride
MPD/PA	MPD end-capped with phthalic anhydride
BDSDA/ODA/MPD	a copolyimide of BDSDA and ODA plus MPD in a molar ratio of 4:2:2, hence [422]

The **Abbreviations Used in the Text** are defined above.

THEORETICAL POLYIMIDE STRUCTURE

BDSDA/4,4-ODA Segment

BDSDA/MPD Segment

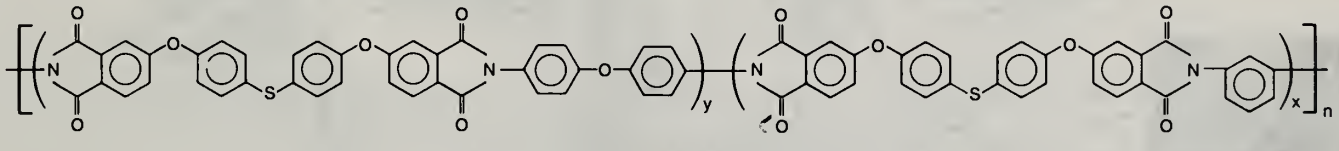

Note: For the 422 copolyimide, y = 2, x = 2 (50-50 copolymer).

The **BDSDA/ODA/MPD Copolyimide** exhibits a decrease in free volume after a small addition of BDSDA end-capped with aniline and of ODA and MPD, both end-capped with phthalic anhydride.

Price Code: A02 "Investigation of the Effects of Short Chain Processing Additives on Polymers."

Copies may be purchased from the National Technical Information Service, Springfield, Virginia 22161, Telephone No. (703) 487-4650. Rush orders may be placed for an extra fee by calling (800) 336-4700.

This invention is owned by NASA, and a patent application has been filed. Inquiries concerning nonexclusive or exclusive license for its commercial development should be addressed to the Patent Counsel, Langley Research Center. Refer to LAR-13679/TN.

Langley Research Ctr.
Technology Utilization Officer: John Samos
Mail Stop 139A
Hampton, VA 23665
(804) 864-2484
Patent Counsel:
George F. Helfrich
Mail Code 279
Hampton, VA 23665
(804) 864-3523

FOR ADDITIONAL INFORMATION: *Contact: Director, Technology Transfer Division, P.O. Box 8757, BWI Airport, MD 21240; (301) 621-0100 Ext. 241*
REFER TO THE NUMBER LISTED AT THE END OF THIS ARTICLE

NASA Tech Brief
National Aeronautics and Space Administration
Ames Research Center, Moffett Field, California

Licensing Opportunity

Alumina-Enhanced Thermal Barrier

Improved fibrous refractory composite material raises the temperature limit.

A rigid, fibrous ceramic tile material called "alumina-enhanced thermal barrier" (AETB) extends the high-temperature capability of insulating materials. Although it is intended primarily for use in the heat shield of the Space Shuttle orbiter, the new material has obvious potential for terrestrial use in kilns, furnaces, heat engines, and other applications in which light weight and high operating temperature are specified.

AETB results from a modification of FRCI, a lightweight aluminoborosilicate (ABS)/silica material developed to replace much of the denser all-silica high-temperature reusable surface insulation (HRSI) originally used on the Space Shuttle. AETB is made from high-purity silica fibers 1 to 3 μm in diameter, alumina fibers 2 to 4 μm in diameter, and ABS fibers 2 to 4 μm in diameter with a nominal composition of 62 percent Al_2O_3, 14 percent B_2O_3, and 24 percent SiO_2 by weight.

The proportions of ABS to silica and of alumina to the ABS/silica combination can be varied to change the properties of the AETB. With an ABS/silica ratio of less than 0.15, the AETB becomes unstable and devitrifies at high temperatures. With an ABS/silica ratio of more than 0.3, the boria from the ABS softens the silica so much that the AETB loses its high-temperature strength and insulating properties. The alumina fibers inhibit shrinkage at high temperatures, but if present at more than 30 percent by weight, they reduce the ability of the AETB to withstand thermal shock.

Tiles of AETB are now being manufactured (see figure) with a composition of 14 percent ABS, 66 percent silica, and 20 percent alumina. The fibers are processed into homogeneous billets 8.5 by 8.5 by 5.5 in. (21.6 by 21.6 by 14.0 cm) and fired at 2,425 °F (1,329 °C) for 90 min to yield rigid tiles having a density of 12 lb/ft^3 (190 kg/m^3). These have 20 percent more tensile strength than that of comparable FRCI tiles of 20 weight percent ABS and equal density. The AETB tiles provide thermal insulation at 2,700 °F (1,480 °C) — more than 300 °F (170 °C) above the maximum operating temperatures of HRSI and FRCI. The thermal conductivity of the AETB is the same as that of the FRCI. The only disadvantage of the AETB over the FRCI appears to be a slight increase in thermal expansion.

This work was done by Marnell Smith, Dan Leiser, and Howard Goldstein of **Ames Research Center.**

Inquiries concerning rights for the commercial use of this invention should be addressed to the Patent Counsel, Ames Research Center. Refer to ARC-12135/TN.

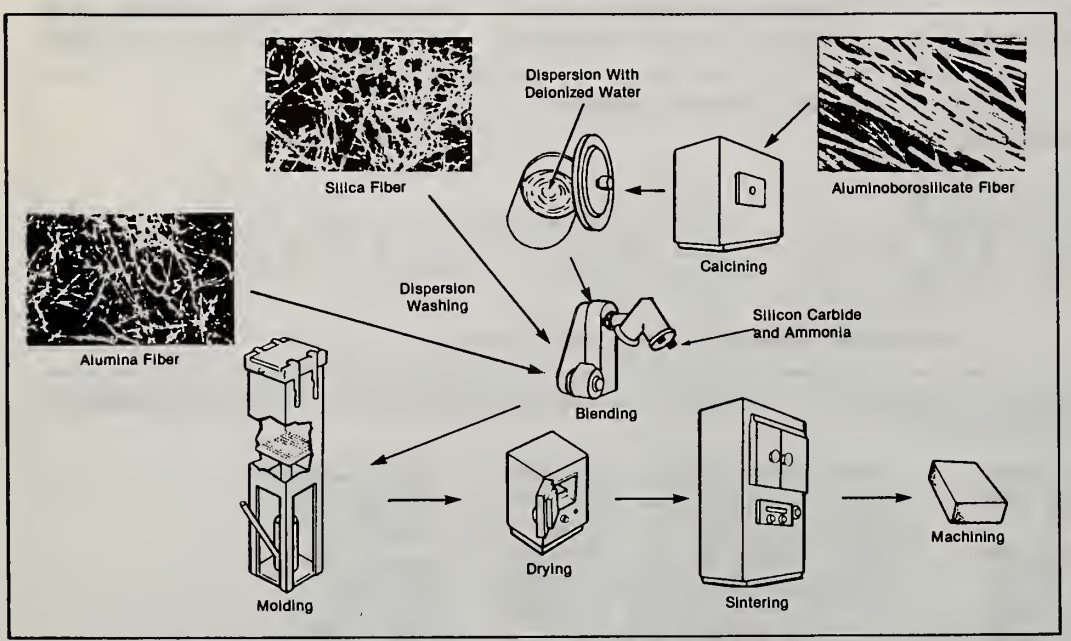

Three Kinds of Ceramic Fibers are blended, molded, and sintered to make refractory tiles.

Ames Research Ctr.
Technology Utilization Officer: Laurance Milov
Mail Code 223-3
Moffett Field, CA 94035
(415) 694-4044
Patent Counsel:
Darrell G. Brekke
Mail Code 200-11
Moffett Field, CA 94035
(415) 694-5104

FOR ADDITIONAL INFORMATION: *Contact: Director, Technology Transfer Division, P.O. Box 8757, BWI Airport, MD 21240; (301) 621-0100 Ext. 241*
REFER TO THE NUMBER LISTED AT THE END OF THIS ARTICLE

NASA Tech Brief
National Aeronautics and Space Administration
Langley Research Center, Hampton, Virginia

Annealing Increases Stability of Iridium Thermocouples

An improved heat treatment also increases ductility.

The temperatures in settling chambers and the total temperatures in high-temperature wind-tunnel facilities have been measured commonly with uncooled thermocouple probes. Platinum/rhodium-alloy thermocouples have been used from 1,300 to 1,800 °C. Temperatures up to 2,000 °C in oxidizing atmospheres can be measured with iridium/rhodium-alloy thermocouples, although these have several disadvantages, including the lack of agreement with standard calibration tables, the lack of agreement between thermocouples from the same lot of wire, changes of calibration with time in service, and susceptibility to breakage after exposure to high temperatures. Consequently, a study of the metallurgy of this type thermocouple was undertaken.

The metallurgical studies were carried out on samples of iridium versus iridium/40-percent rhodium thermocouples in the condition as received from the manufacturer. The metallurgical studies included x-ray, macroscopic, resistance, and metallographic studies. The studies revealed a large amount of internal stress caused by cold-working during manufacturing, as well as a large number of segregations and inhomogeneities. No phase transformations in the alloy were observed at temperatures up to 1,100 °C. The short life of the thermocouple in high-temperature applications was found to be due mainly to the oxidation of iridium and the subsequent volatilization of the iridium oxide.

The thermocouple samples were annealed in a furnace at temperatures from 1,000 to 2,000 °C for intervals up to 1 h to study the effects of heat treatment. At all the annealing temperatures, there was nucleation of the recrystallized grains at different times, with the shorter times at higher temperatures. To prevent possible excessive growth of grains, the wires were heat-treated for 2 h at 1,400 °C after the initial annealing at 1,800 °C and then cooled to room temperature in the furnace. The wire annealed by this procedure was found to be ductile.

The effect of annealing on the stability of thermal electromotive force (emf) was also investigated. The procedure included the annealing of the individual thermocouples in a pyrolytic graphite furnace controlled by an optical pyrometer. Then each thermocouple was inserted in the well of a copper freezing-point standard. A thermal-analysis curve was made on a strip-chart recorder, and simultaneous readings were taken at regular intervals with a nanovoltmeter. This annealing procedure, followed by cooling to room temperature in the furnace, stabilized the thermal emf of the thermocouple to within ±0.02 percent for applications below 1,800 °C.

This work was done by Edward F. Germain, Kamran Daryabeigi, David W. Alderfer, and Robert E. Wright of **Langley Research Center** *and Shaffiq Ahmed of Youngstown State University. Further information may be found in NASA TM-89086 [N87-17018], "A Preliminary Study of Factors Affecting the Calibration Stability of the Iridium versus Iridium-40 Percent Rhodium Thermocouple."*

Copies may be purchased [prepayment required] from the National Technical Information Service, Springfield, Virginia 22161, Telephone No. (703) 487-4650. Rush orders may be placed for an extra fee by calling (800) 336-4700.
LAR-13951/TN

FOR ADDITIONAL INFORMATION: *Contact: Director, Technology Transfer Division, P.O. Box 8757, BWI Airport, MD 21240; (301) 621-0100 Ext. 241*
REFER TO THE NUMBER LISTED AT THE END OF THIS ARTICLE

NASA Tech Brief
National Aeronautics and Space Administration
Lewis Research Center, Cleveland, Ohio

Better PFAE's From Direct Fluorination

The process yields stable and effective lubricants under proper conditions.

New low-molecular-weight perfluoroalkylethers (PFAE's) were synthesized by direct fluorination in an experimental study. The study correlated the viscosity and oxidation characteristics of the PFAE's with their structures to evaluate their suitability as high-temperature lubricants and hydraulic fluids.

PFAE's are generally well suited for these applications because of their thermal and oxidative stabilities, viscosity-vs.-temperature characteristics, elastohydrodynamic film-forming capabilities, boundary-lubricating abilities, and nonflammability. The study was aimed at determining these properties in compounds made by the direct fluorination process.

The direct fluorination process is attractive because it often involves a single-step reaction and uses cheap starting materials. Moreover, it is versatile: it can produce highly branched ethers as well as polyethers containing more than two sequential carbon atoms in the polymer chains. Such molecules cannot be made by conventional techniques.

In a typical direct fluorination process, the liquid to be treated is reacted with an atmosphere that contains fluorine. The products of the reaction are collected in a cold trap, and the desired product is separated from the others by atmospheric distillation.

The study showed that for the best viscometric properties (that is, the least variation of viscosity with temperature), a PFAE should have a low carbon-to-oxygen ratio (see figure) and a low degree of branching. In addition, the more-highly-branched PFAE fluids are less resistant to oxidation than are those containing single pendant trifluoromethyl groups or those containing no branching at all. It is postulated that a single pendant group attached to a carbon atom adjacent to an oxygen atom in a PFAE may stabilize the polymer by sterically protecting the oxygen in the backbone of the molecule.

This work was done by W. R. Jones, Jr., of **Lewis Research Center** *and T. R. Bierschenk of Exfluor Research Corp. Further information may be found in NASA TM-87284 [N86-25475/NSP], Price Code: A02 "The Preparation of New Perfluoroether Fluids Exhibiting Excellent Thermal-Oxidative Stabilities."*

Copies may be purchased from the National Technical Information Service, Springfield, Virginia 22161, Telephone No. (703) 487-4650. Rush orders may be placed for an extra fee by calling (800) 336-4700.
LEW-14613/TN

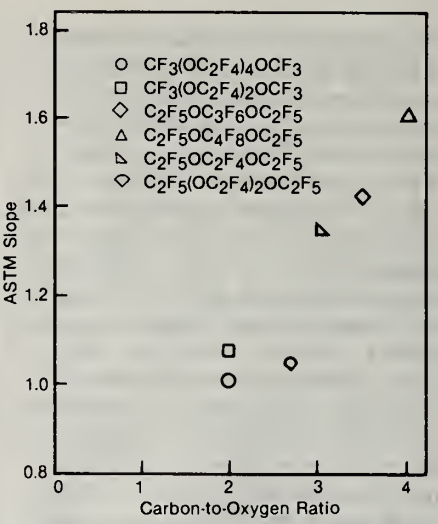

The ASTM Slopes of Unbranched PFAE's Increase with increasing carbon-to-oxygen ratio of PFAE's made by direct fluorination. (The ASTM slope is a measure of the decrease of viscosity with temperature: a lower slope indicates a viscometrically superior lubricant.)

FOR ADDITIONAL INFORMATION: *Contact: Director, Technology Transfer Division, P.O. Box 8757, BWI Airport, MD 21240; (301) 621-0100 Ext. 241*
REFER TO THE NUMBER LISTED AT THE END OF THIS ARTICLE

NASA Tech Brief
National Aeronautics and Space Administration
Marshall Space Flight Center, Alabama

Licensing Opportunity

Calculating Dynamic Shear Moduli of Polymers

A nonlinear mathematical model replaces oversimplified linear and Prony-series models.

An improved nonlinear mathematical model has been developed to fit experimental data on the relaxation of stresses in viscoelastic materials. The model, which was developed specifically to study the shear moduli of rubbery solid rocket propellants, can also be used to characterize polymers in general, other viscoelastic materials, and composites of viscoelastic materials. It can facilitate and improve the accuracy of analysis and numerical simulation of the mechanical behavior of structural components (for example, tires) made of such materials.

Plots of the shear modulus as a function of time have been fitted by such models as piecewise-linear approximations, power laws, and Prony series. These models do not represent the data accurately over the full range of times (see figure) and do not account adequately for the effects of temperature, strain, and rate of strain. The new model provides the flexibility to fit a wide range of experimental data by expressing the shear modulus as a sum of terms, each of which is a product of other terms. One form of the model, which is likely to be used widely, is

$$G = G_{static} + G_{dynamic}$$

where G = the shear modulus.

In a typical case, the static term would be a constant, while the dynamic term would be given by

$$G(t,T,\varepsilon,\dot{\varepsilon})_{dynamic} = M(t)M(T)M(\varepsilon)M(\dot{\varepsilon})$$

where t = time, T = temperature, ε = strain, and $\dot{\varepsilon}$ = rate of strain. Each of the multiplicative terms could have either of two forms:

$$M(X) = C_1\beta_m(X) \text{ or}$$

$$M(X) = C_1\exp[C_2\beta_m(X)]$$

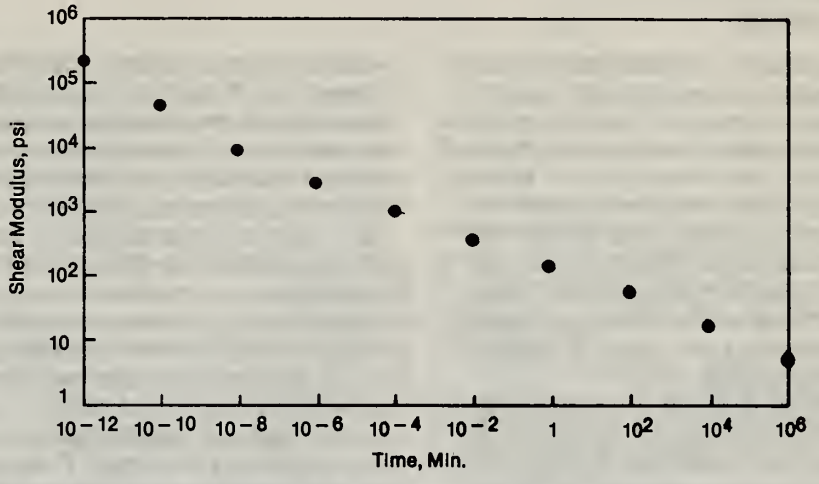

These Experimental Stress-Relaxation Data can be fitted fairly well with a straight line at times greater than 10^{-6} min. However, the data diverge from the line at shorter times, necessitating the use of a different mathematical model.

where

$$\beta_m(X) = \left\{\left[\sum_{i=0}^{m} C_{Ni}(X - X_R)^i\right] \Big/ \left[\sum_{j=0}^{m} C_{Dj}(X_o - X_R)^j\right]\right\}^{P_X}$$

where X_o may equal X or an original value of X; X_R is a reference value of X; and C_{Ni}, C_{Dj}, and P_X are constants. For example, the temperature multiplier might be given by

$$M(T) = C_1\exp\{C_2[-C_3(T-T_R)/(C_4+T-T_R)]^{P_T}\}$$

The further development and verification of the new model depend on detailed and consistent tests of specimens of the material in question.

This work was done by Carleton J. Moore of **Marshall Space Flight Center.**

Inquiries concerning rights for the commercial use of this invention should be addressed to the Patent Counsel, Marshall Space Flight Center Refer to MFS-28340/TN

George C. Marshall Space Flight Center
Technology Utilization Officer: Ismail Akbay
Code AT01
Marshall Space Flight Center,
AL 35812
(205) 544-2223
Patent Counsel:
Leon D. Wofford, Jr.
Mail Code CC01
Marshall Space Flight Center,
AL 35812
(205) 544-0024

FOR ADDITIONAL INFORMATION: *Contact: Director, Technology Transfer Division, P.O. Box 8757, BWI Airport, MD 21240; (301) 621-0100 Ext. 241*
REFER TO THE NUMBER LISTED AT THE END OF THIS ARTICLE

NASA Tech Brief
National Aeronautics and
Space Administration

CdO Pretreatment for Graphite Lubricant Films

Sputtered films decrease friction and increase endurance.

The lubrication of rubbing steel surfaces with graphite can be improved by sputtering cadmium oxide onto the surfaces, according to a report. Previous investigations of surface pretreatments and of the tribological effects of cadmium oxide had prompted speculation as to whether cadmium oxide might enhance the lubricant effect of graphite by increasing the adherence of the graphite to the metal surface or by contributing to the film-forming properties of the graphite.

In the investigation described in the report, sputtered films of cadmium oxide were applied to sandblasted disks of AISI 440C HT stainless steel, as a surface pretreatment for the application of graphite films by rubbing. For comparison, other disks were pretreated by rubbing the sandblasted surfaces with cadmium oxide prior to the rubbing of graphite. For another comparison, mixtures of cadmium oxide and graphite were rubbed into the sandblasted but otherwise nonpretreated surfaces.

The treated disks were tested in a pin-on-disk tribometer, equipped with SAE 1045 steel pins. These tests yielded coefficients of friction, wear lives, and pinwear rates and volumes. The wear tracks on the disks were also examined microscopically and by energy-dispersive x-ray analysis.

The results of the tests showed that sputtered cadmium oxide films and graphite lubrication gave mean endurance (as measured in sliding distance until a coefficient of friction of 0.25 is reached) about 20 times as long and mean pinwear rates about one one-hundredth of those of the same surfaces with graphite lubrication alone but without pretreatment. Pretreatment with cadmium oxide also proved better than the best commercial pretreatment (zinc phosphate), with endurance and pinwear rates increased by a factor of 7 and decreased by a factor of 10, respectively. While the various pretreatments had pronounced effects on endurance, they gave nearly equivalent coefficients of friction.

The disks that were pretreated by rubbing with cadmium oxide exhibited improvements over nonpretreated disks but did not perform as well as those with sputtered cadmium oxide. Lubricating films consisting of mixtures of cadmium oxide and graphite did not perform as well as films of graphite alone on surfaces pretreated with cadmium oxide; such mixtures formed thicker films, which tended to spall from the wear tracks, thereby depleting the surfaces of lubricants. The primary beneficial effect is obtained by the sputtering pretreatment with cadmium oxide, which apparently improves the bond between the metallic substrate and the graphite.

This work was done by Robert L. Fusaro of **Lewis Research Center**. *Further information may be found in NASA TM-87300 [N86-25473], Price Code: A03 "Sputtered Cadmium Oxide as a Surface Pretreatment for Graphite Solid Lubricant Films."*

Copies may be purchased from the National Technical Information Service, Springfield, Virginia 22161, Telephone No. (703) 487-4650. Rush orders may be placed for an extra fee by calling (800) 336-4700.
LEW-14635/TN

FOR ADDITIONAL INFORMATION: *Contact: Director, Technology Transfer Division, P.O. Box 8757, BWI Airport, MD 21240; (301) 621-0100 Ext. 241*
REFER TO THE NUMBER LISTED AT THE END OF THIS ARTICLE

NASA Tech Brief
National Aeronautics and
Space Administration

Effects of Aging on Embrittlement by Hydrogen

Concentration of hydrogen at grain boundaries determines the mode of fracture.

A report discusses a study of grain-boundary fracture of hydrogen-charged nickel under conditions in which the hydrogen is immobile. Thermally-charged nickel specimens were aged at several temperatures for various periods of time to allow hydrogen to diffuse. The specimens were then quenched and tested in liquid nitrogen (at a temperature of 77 K) so that the distribution of hydrogen produced by aging would be maintained.

The study showed that embrittlement is a function of bulk hydrogen concentration and the thermal history of the hydrogen-charged nickel. The bulk concentration and the thermal history apparently control the concentration of segregated hydrogen at grain boundaries and thus govern intergranular fracture.

The test data show that the equilibrium concentration of hydrogen at grain boundaries can be expressed by Fermi-Dirac statistics. The mathematical model of concentration as a function of aging time can be developed from classical diffusion theory.

The binding enthalpy of hydrogen to grain-boundary trapping sites is 11.6 kJ/mole (0.12 eV/atom). The transition from ductile fracture to completely intergranular fracture occurs at hydrogen concentrations from 5 to 15 percent at the grain boundaries. Hydrogen-rich layers about 300 Å thick develop at nickel grain boundaries.

This work was done by D. H. Lassila of **Ames Research Center** *and H. K. Birnbaum of the University of Illinois. Further information may be found in NASA TM-88207 [N86-26416], Price Code: A02 "Hydrogen Embrittlement of Nickel: Modeling of the Effect of Diffusive Segregation of Hydrogen on Intergranular Fracture."*

Copies may be purchased from the National Technical Information Service, Springfield, Virginia 22161, Telephone No. (703) 487-4650. Rush orders may be placed for an extra fee by calling (800) 336-4700.

Inquiries concerning rights for the commercial use of this invention should be addressed to the Patent Counsel, Ames Research Center. Refer to ARC-11762/TN.

FOR ADDITIONAL INFORMATION: *Contact: Director, Technology Transfer Division, P.O. Box 8757, BWI Airport, MD 21240; (301) 621-0100 Ext. 241*
REFER TO THE NUMBER LISTED AT THE END OF THIS ARTICLE

NASA Tech Brief
National Aeronautics and
Space Administration

Degradation of Carbon/Phenolic Composites by NaOH

NaOH degrades both the carbon and the phenolic components of carbon/phenolic laminates.

The effects of the sodium hydroxide contamination level on physical and chemical properties of phenolic resin and carbon/phenolic composites are described in a report. Prior studies focused on the effect of sodium contamination on the carbon fibers in these materials.

As the concentration of sodium hydroxide in one-stage (Borden's SC-1008 or equivalent) phenolic resin is increased, the gel times are reduced, the polymerization onset temperature is lowered (according to differential scanning calorimetry), and the polymerization reaction rate is increased. These results are consistent with the known ability of sodium hydroxide to convert phenol to the more reactive phenolate anion, which perhaps results in an increased incidence of parasubstitution. According to gel-permeation chromatography, the average molecular weight of the polymer decreases, perhaps because of sodium hydroxide-catalyzed breakdown of the oligomers. Finally, the resin viscosity increases with the sodium content.

When resin-impregnated laminated cloths (prepregs) are squeezed in a hot press, the flow of resin out of the prepregs decreases with increasing sodium content. This decrease is consistent with the reduction in gel time caused by the sodium hydroxide. A greater sodium hydroxide concentration also leads to an increase in moisture absorption by the prepreg under ambient conditions and to an increase in the phenol efflux measured during the tests for volatiles.

Thermogravimetric analyses of carbon broad goods and of carbon/phenolic laminates show a striking increase in weight loss with increasing sodium concentration. In the case of the laminates, the weight loss is much greater in the presence of a normal (50 ml/min) airflow than in the absence of an airflow.

Mechanical-property tests showed that an increase in sodium content apparently decreases the compressive modulus and flexural strength and increases the shear strength of the composites. The failure mechanism (shown by optical and scanning-electron microscopy) is related to sodium concentration, and transitions among failure mechanisms are observed in the cases of shear and flexural modes. Results from thermogravimetric analyses indicate that higher levels of sodium may also lead to matrix degradation at lower temperatures.

This work was done by H. M. King, M. L. Semmel, and B. E. Goldberg of **Marshall Space Flight Center** *and Raymond G. Clinton, Jr., of Georgia Institute of Technology for Marshall Space Flight Center. "Investigation of the Effects of NaOH Dopant Level on the Physical and Mechanical Properties of Carbon/Phenolic Composite Material."*
MFS-27099/TN

FOR ADDITIONAL INFORMATION: *Contact: Director, Technology Transfer Division, P.O. Box 8757, BWI Airport, MD 21240; (301) 621-0100 Ext. 241*
REFER TO THE NUMBER LISTED AT THE END OF THIS ARTICLE

NASA Tech Brief
National Aeronautics and Space Administration
NASA's Jet Propulsion Laboratory, Pasadena, California

Orienting Superconductive Crystals for High Current Density

Uniaxial stress would promote rearrangement of oxygen atoms in a favorable direction.

A proposed technique for the controlled distortion of crystal grains in the newly discovered superconductor $YBa_2Cu_3O_{7-x}$ would increase its current-carrying capacity. The technique would help to ensure that the grains in this and other anisotropic materials are all oriented in the same direction so that charge carriers can be transferred readily from one grain to another.

One disadvantage of $YBa_2Cu_3O_{7-x}$ is that its superconductivity is limited to the chains of copper and oxygen atoms that lie along the *b* dimension of the crystal lattice. In a polycrystalline film of the material, superconductivity is therefore confined to tortuous paths between fortuitously oriented adjacent grains, and the current-carrying capacity is therefore low.

$YBa_2Cu_3O_{7-x}$ undergoes a transition in crystalline structure at a temperature of 600 °C. Above this temperature, the *a* and *b* dimensions are identical. As the temperature drops through that value, oxygen atoms rearrange themselves to form the potentially superconductive copper/oxygen chains in the *b* direction. As part of this rearrangement, the *a* dimension shrinks and the *b* dimension expands because of the movement of oxygen atoms from the *a* axis to the *b* axis.

According to the proposed technique, a specimen of $YBa_2Cu_3O_{7-x}$ heated in an oxygen atmosphere would be compressed in one direction as it is slowly cooled below the transition temperature (see figure). Under these conditions, oxygen atoms should tend to rearrange themselves so as to relieve the stress created by the compression. That is, they would tend to form chains with the copper atoms in a direction perpendicular to the direction of compression. Thus, the superconductive *b* axes would all tend to be oriented in the same direction perpendicular to the squeezing direction and would tend to be continuous from one grain to the next.

One technique for compression involves the prior deposition of the $YBa_2Cu_3O_{7-x}$ on a substrate material that has anisotropic contraction. As the substrate is cooled, it contracts more in one direction, thus providing the required uniaxial compression in the material deposited on it. Alternatively, the stress could be induced by mechanically compressing the substrate or by applying an electrostatic field.

This work was done by Paul J. Shlichta of Caltech for **NASA's Jet Propulsion Laboratory**. *NPO-17330/TN*

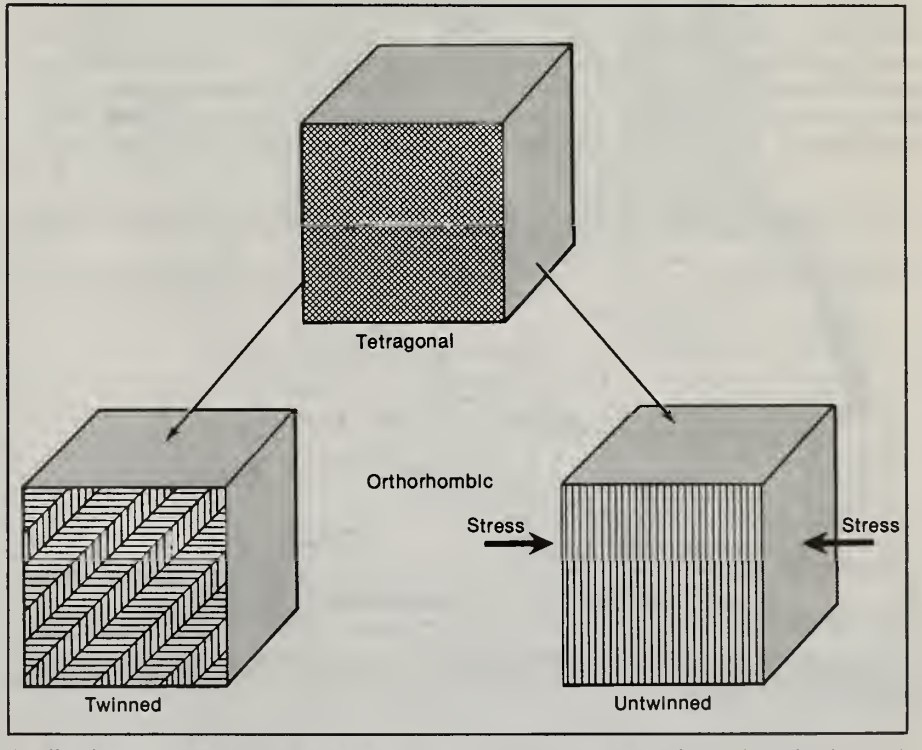

Application of Stress to cooled tetragonal $YBa_2Cu_3O_{7-x}$ prevents formation of twins and yields untwinned orthorhombic crystal.

FOR ADDITIONAL INFORMATION: *Contact: Director, Technology Transfer Division, P.O. Box 8757, BWI Airport, MD 21240; (301) 621-0100 Ext. 241*
REFER TO THE NUMBER LISTED AT THE END OF THIS ARTICLE

NASA Tech Brief
National Aeronautics and Space Administration
NASA's Jet Propulsion Laboratory, Pasadena, California

Licensing Opportunity

Variable-Energy Ion Beams for Modification of Surfaces

Ions at low energy react chemically with silicon without damaging it.

A beam of low-energy negative oxygen ions can be used to grow a layer of silicon dioxide on silicon. This beam is unique both in its purity, as it contains no molecular oxygen or other charged species, and in its low energy, which is insufficient to damage the silicon by physically displacing atoms. It promises to be a useful device to study oxidation of semiconductors and, in certain applications, to replace conventional oxidation processes.

The standard method for growing oxides on silicon requires heating the wafer to temperatures of 800 to 1,100°C in a clean quartz furnace filled with flowing gas. This process can cause thermal stress, which can be damaging to high-density integrated circuitry, thin-layered structures, and other delicate devices. Low-temperature alternatives, particularly those that can be directed onto a specific part of the wafer, have been sought in the form of chemical vapor deposition, laser-assisted oxidation, rapid thermal oxidation, anodic oxidation, and ion implantation of oxygen. All of these solutions only partially address the problem of unintentional damage to the device.

The low-energy ion beam is an optimal growth tool in that atomic oxygen is chemically far more active than molecular oxygen and can be directed onto the surface at low energies insufficient to cause damage. The beam energy and sample temperature can be continuously varied to optimize oxide growth. In initial experiments, a 20-Å thick oxide layer was grown at room temperature in a mattter of minutes, compared to hours or days using other room-temperature oxidizing techniques.

The low-energy growth is accomplished with the help of the ion-beam apparatus shown in the figure. The kinetic energy of the ions in the beam is only 5 eV, the ions are in the ^2P quantum state, and the ion flux density is high, approximately 10^{15} ions/(cm)^{2}s. The apparatus can also generate pure beams of negative hydrogen ions and a variety of negative metal ions. It can therefore be used for hydrogen annealing of silicon and gallium arsenide surfaces and to asist in the growth of diamond films for radiation-resistant semiconductor devices. It will be useful in the modification of the surface oxygen content in superconducting films, in the formation of tunnel junctions, and in the passivation of photosensitive structures such as charge-coupled devices.

This work was done by Ara Chutjian, Michael H. Hecht, and Otto J. Orient of Caltech for **NASA's Jet Propulsion Laboratory**.

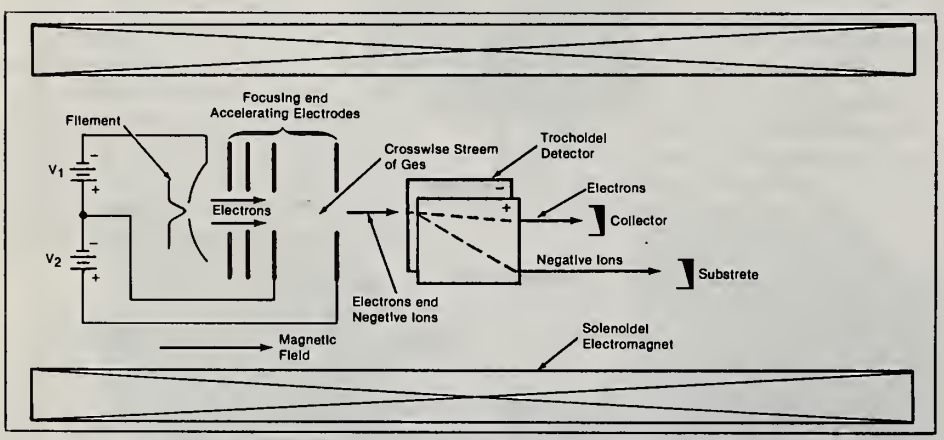

The Ion-Beam Apperetus directs electrons into a crosswise stream of gas, thereby generating a streem of negetive ions. A pair of charged plates separates the ions from the accompanying electrons and diverts the ion beam to its target — a silicon substrate. The diameter of the beam at the target is 0.5 to 0.75 cm.

This invention is owned by NASA, and a patent application has been filed. Inquiries concerning nonexclusive or exclusive license for its commercial development should be addressed to the Patent Counsel, NASA's Resident Office-JPL. Refer to NPO-17498/TN.

Jet Propulsion Lab.
NASA Resident Office
Technology Utilization Officer: Gordon S. Chapman
Mail Stop 180-801
4800 Oak Grove Drive
Pasadena, CA 91109
(818) 354-4849
Patent Counsel: Paul F. McCaul
Mail Code 180-801
4800 Oak Grove Drive
Pasadena, CA 91109
(818) 354-2734
Technology Utilization Mgr. for JPL: Norman L. Chalfin
Mail Stop 156-211
4800 Oak Grove Drive
Pasadena, CA 91109
(818) 354-2240

FOR ADDITIONAL INFORMATION: *Contact: Director, Technology Transfer Division, P.O. Box 8757, BWI Airport, MD 21240; (301) 621-0100 Ext. 241*
REFER TO THE NUMBER LISTED AT THE END OF THIS ARTICLE

NASA Tech Brief
National Aeronautics and Space Administration
Marshall Space Flight Center, Alabama

Measurement of Composition in Transparent Model Alloy

Noninvasive measurements are taken by Fourier-transform infrared spectroscopy.

Fourier-transform infrared spectroscopy (FTIR) has been used to measure the composition as a function of position in cells that contain mixtures of succinonitrile and glycerol. This particular variation of the FTIR technique was developed to enable study of the growth of cells of different solid phase in unidirectional solidification of these organic mixtures, which serve as transparent analogs of opaque monotectic metal alloys. The study of the organic analogs is expected to contribute to understanding of the formation of aligned rods and particles in the directional solidification of the metal alloys.

The organic mixture was confined in each cell between two glass cover plates 2 cm wide and 5 cm long, held 10 to 50 μm apart. The cell was pushed across the gap between a hot and a cold plate to effect directional solidification (see Figure 1). Cells were quenched rapidly at various stages of progress of the solidification front to enable subsequent determination of compositions as functions of position at those stages.

FTIR measurements were taken at a sequence of locations along the cell both before and after unidirectional solidification to reveal the changes that occur during solidification. The FTIR observation area at each location had a diameter of 100 μm. The spectral absorption peak of glycerol at a wave number of 3,359 $(cm)^{-1}$ and that of succinonitrile at 3,096 $(cm)^{-1}$ were selected to obtain the concentration of each constituent at each location (see Figure 2).

The advantage of this FTIR technique is that the redistribution of material caused by solidification can be determined after the fact, to a very fine scale. Unlike in metallographic techniques, this one is nondestructive: it is not necessary to section the specimens or even to open the cells at all. Direct correlations can be made between the FTIR observations and the microstructures visible under microscopes at the same positions. Because the specimens are not destroyed, interesting regions can be rescanned at other wavelengths or different parameters.

One disadvantage is that the glass in the cover plates might not be transparent at a wavelength of interest. This can be over-

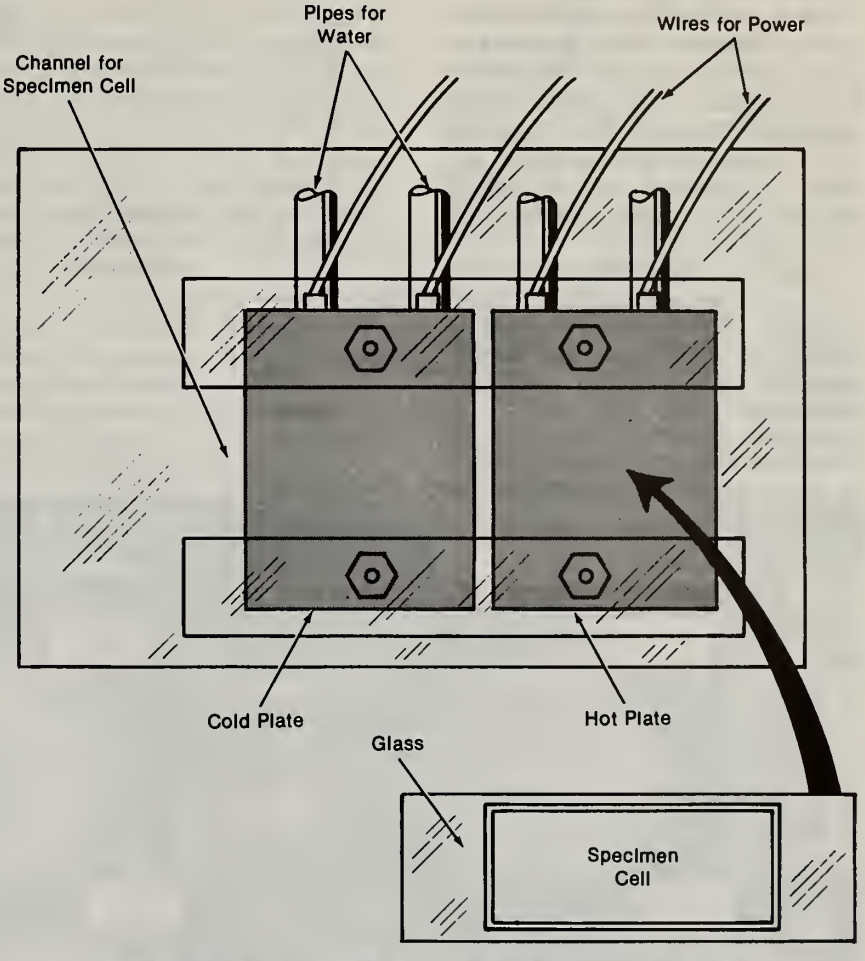

SPECIMEN CELL AND DIRECTIONAL-SOLIDIFICATION APPARATUS

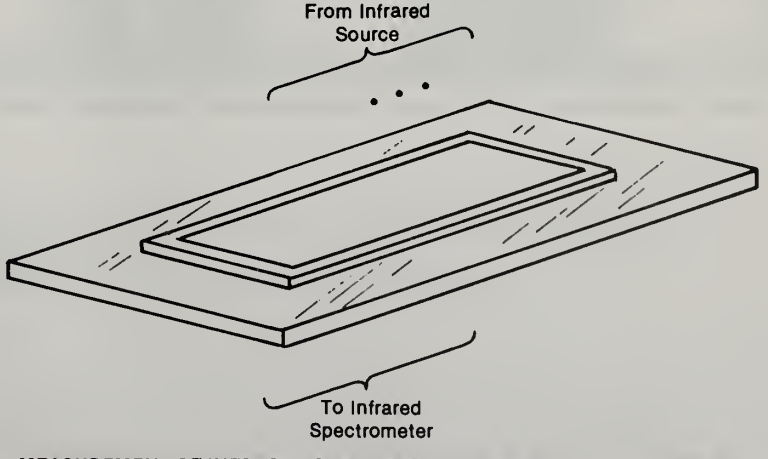

MEASUREMENT OF INFRARED SPECTRA AT SPOTS ALONG THE SPECIMEN

Figure 1. **A Thin Specimen of Succinonitrile/Glycerol Mixture** is probed by FTIR spectroscopy before and after directional solidification.

come by selection of a different glass or wavelength. The use of more than one absorption peak for each compound would increase the sensitivity. If the absorption peaks of impurities are known, the segregation of impurities caused by unidirectional solidification or zone refining could also be measured by this technique.

This work was done by William F. Kaukler, Gretchen L. Perry, and Peter A. Curreri of the University of Alabama for **Marshall Space Flight Center**. *Further information may be found in NASA TM-100317 [N88-15027], Price Code: A03 "Cellular Solidification in a Monotectic System—Center Director's Discretionary Fund Final Report."*

Copies may be purchased from the National Technical Information Service, Springfield, Virginia 22161, Telephone No. (703) 487-4650. Rush orders may be placed for an extra fee by calling (800) 336-4700.

Inquiries concerning rights for the commercial use of this invention should be addressed to the Patent Counsel, Marshall Space Flight Center. Refer to MFS 26079/TN.

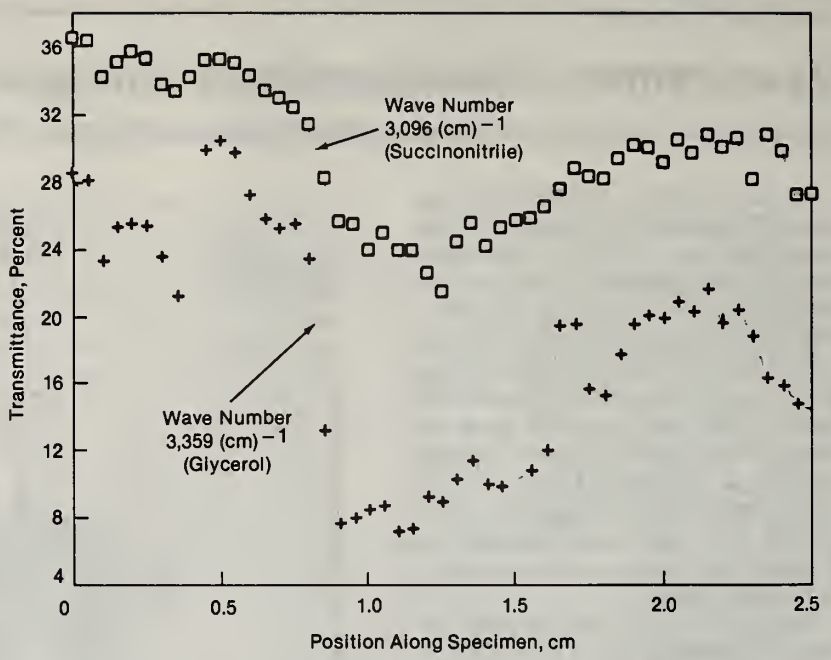

Figure 2. The **Transmittance of a Specimen at Two Wavelengths** as was measured at various positions along a specimen. Because each wavelength lies at a spectral absorption peak of one of the compounds in the specimen, these data can be used to infer the composition of the specimen as a function of position.

FOR ADDITIONAL INFORMATION: *Contact: Director, Technology Transfer Division, P.O. Box 8757, BWI Airport, MD 21240; (301) 621-0100 Ext. 241*

REFER TO THE NUMBER LISTED AT THE END OF THIS ARTICLE

NASA Tech Brief
National Aeronautics and Space Administration
Lewis Research Center, Cleveland, Ohio

Acoustical Imaging of Defects in Ceramics

Ultrasound is superior to x rays in the detection of microporosity.

To date, the strengths of sintered ceramics (e.g., SiC) vary significantly and are about two orders of magnitude below the theoretical strengths. Adding to the problem is the fact that the fracture strengths of identically-produced experimental samples differ as much as 35 percent. These discrepancies are attributed to voids, inclusions, agglomerates, and anomalously large grains. These defects, which cause premature failures, are introduced or formed during the ceramic-manufacturing process. Considerable work has been done already to remove these strength-reducing variations in materials.

Because of their brittle nature, ceramics are extremely sensitive to even slight variations in microstructure. Direct observations have shown the importance of the kinds of defects mentioned above by identifying them as the sites of localized failures. These sites cannot be determined a priori by optical and x-ray methods. It seems plausible that these failure-causing variations do not occur spontaneously in isolation but are the result of the history of variations in processing.

Color images obtained from precise acoustic measurements reveal subtle variations in the porosity fractions and the mean sizes of pores in ceramics (see figure). The velocity and attenuation of ultrasound have been found to be related directly to the density and mean size of the pores, respectively. These variations are unobservable in x-ray analysis.

This work was done by Edward R. Generazio, Don J. Roth, and George Y. Baaklini of **Lewis Research Center**. *Further information may be found in NASA TM-100129 [N88-15257], Price Code: A03 "Imaging Subtle Microstructural Variations in Ceramics with Precision Ultrasonic Velocity and Attenuation Measurements.*

Copies may be purchased from the National Technical Information Service, Springfield, Virginia 22161, Telephone No. (703) 487-4650. Rush orders may be placed for an extra fee by calling (800) 336-4700. *LEW-14592/TN*

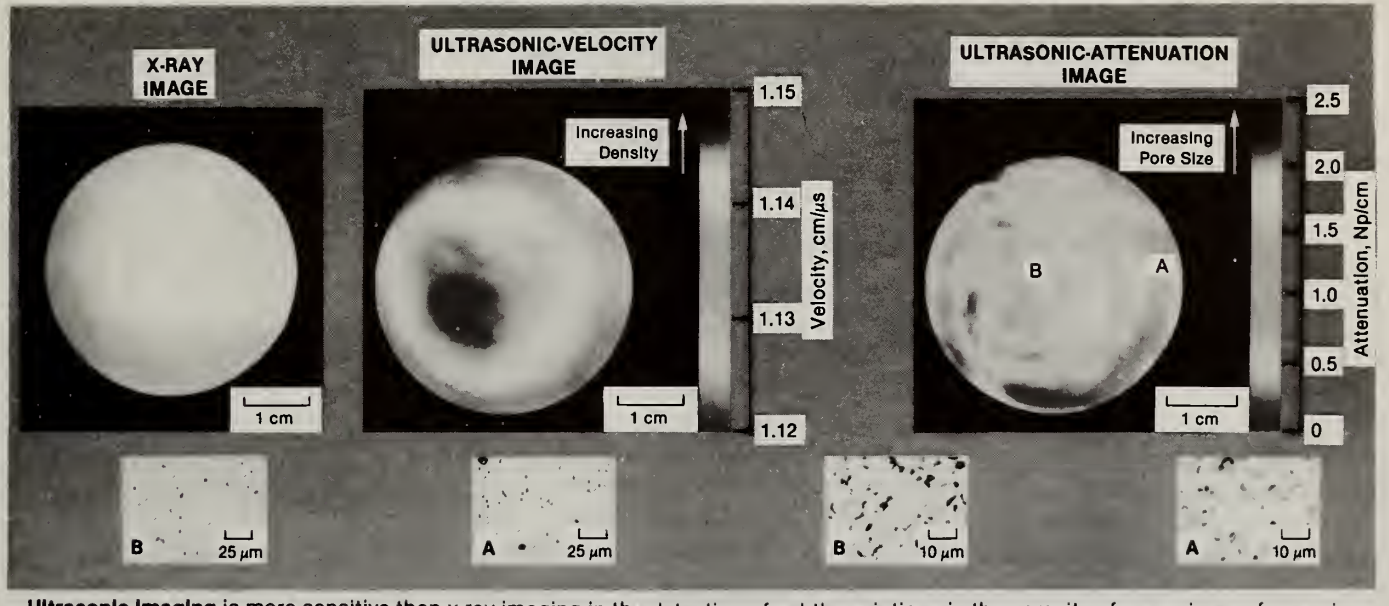

Ultrasonic Imaging is more sensitive than x-ray imaging in the detection of subtle variations in the porosity of a specimen of ceramic.

FOR ADDITIONAL INFORMATION: *Contact: Director, Technology Transfer Division, P.O. Box 8757, BWI Airport, MD 21240; (301) 621-0100 Ext. 241*
REFER TO THE NUMBER LISTED AT THE END OF THIS ARTICLE

Medicine & Biology

0790 Host Immune Response Causes Anemia of Malaria

0791 Navy Combats Hypothermia

0792 Alaskan Coastal Biological Data

0793 National Magnetic Resonance Facility at Madison

0794 Cryopreservation of Murine Germplasm

0795 Institute of Laboratory Animal Resources

0796 MIT Cell Culture Center

0797 University Resource in Laboratory Animal Medicine

0798 Directional Hearing Aid—The approximate directions of sounds are indicated visually. (Licensing Opportunity)

Testing & Instrumentation

0799 New Developments Available to Test Marine Plankton Light Emissions—Test chamber uses an integrating sphere to collect light

Other Items of Interest

0761 Materials Aimed at Improving Pesticide, PCB Analyses

Medicine & Biology

Department of Energy

Technology Application

Lawrence Berkeley Laboratory

Host Immune Response Causes Anemia of Malaria

The severe anemia responsible for death from acute malaria is caused in large part by a protein produced by the host's own immune system, says a team of scientists in the Cell and Molecular Biology Division at Lawrence Berkeley Laboratory (LBL).

Paul Silverman, Associate Laboratory Director for Life Sciences, and staff scientist Kathleen Miller have demonstrated that much of the anemia of malaria can be reversed by giving infected mice an antibody to tumor necrosis factor (TNF), a protein made by macrophages, cells involved in the immune response of humans and animals. Their study appears in the May issue of Infection and Immunity; the research team also included Birgitta Kullgren and Lynn Mahlmann.

"The purpose of TNF is to play a role in protection against disease and in healing," explains Miller, "but if excessive amounts of TNF are produced, you get detrimental effects."

The LBL work has broad implications not only for understanding and treating malaria but also for explaining "chronic disease anemia," a condition associated with cancer and many infectious diseases. Older theories proposed that the cancer cells, parasites, or bacteria secreted toxins that destroyed red blood cells. In the case of malaria, researchers have searched for such a toxin since the disease was discovered in the 1890s.

"It now appears that the anemia results from overstimulation of our own system," says Silverman. "The excitement of this finding is that it helps explain the pathology of a whole series of infectious diseases."

The researchers also showed that administration of TNF to normal, healthy mice results in a reduction of the precursors for red blood cells, indicating that over time the TNF would cause anemia. In organisms infected with malaria, anemia develops very quickly because reduction of precursors is coupled with destruction of red cells by the parasites (numerous studies in the past have shown that this cell destruction alone cannot account for the severity and extent of anemia in malaria).

In another series of studies, the same LBL team, with John Schooley and Karen Smith, showed that a cell-free medium prepared from the spleens of mice infected with malaria inhibits the formation of mouse red blood cells in culture, even when plenty of precursor cells and erythropoietin, the hormone that stimulates red cell development, are present. They determined that the substance blocking red cell development was a large, soluble molecule produced by macrophages.

The researchers now believe that TNF is the most likely candidate for this substance.

FOR ADDITIONAL INFORMATION: Public Information Department, Lawrence Berkeley Laboratory, Berkeley, CA 94720; Telephone (415)486-5771.

Navy Combats Hypothermia

The Navy probably has more personnel near cold water than any other organization in the world. And nature's weapon called hypothermia, arch enemy of naval personnel, claims several lives each year.

Hypothermia occurs when the body's temperature drops, sometimes to the point of unconsciousness. This can occur in less than an hour. Because dependable treatment for hypothermia requires trained medical personnel and nonportable equipment, the victim in the field has little chance of survival.

At the Naval Aerospace Medical Research Laboratory, Pensacola, Florida, a biomedical engineer is experimenting with a portable vest so that naval personnel in remote areas have a better than even chance of winning the battle with hypothermia. The vest, known as the RF Coil Rewarming System, contains wire coils connected to an electric generator. The generator sends radio waves through the coils that penetrate the chest and rewarm the heart. This is a better method than the common treatment of placing the victim in warm water, a procedure that can be dangerous.

The device has been patented, but the inventor says that it will take several more years to perfect. However, once the vest is perfected, it will benefit both military and civilian rescue crews.

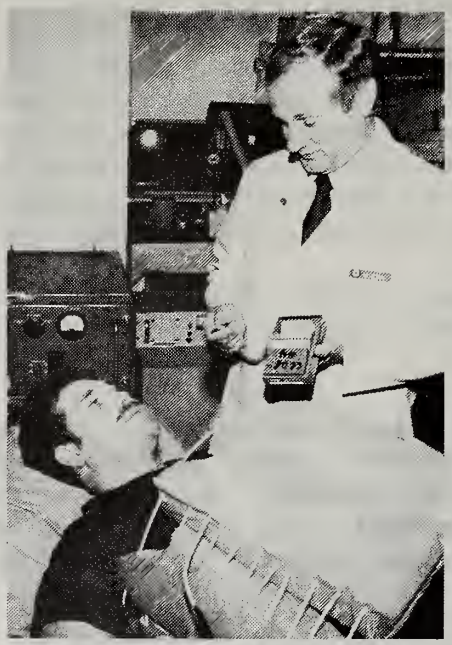

Biomedical engineers test the RF Coil Rewarming System in the effort to treat hypothermia.

For Additional Information:

Backup material on this effort is available from:

Navy Domestic Technology Fact Sheet Reader Reply Service
Code E211
Naval Surface Weapons Center
Dahlgren, VA 22448-5000
(703) 663-8921

Refer to 140305/TN

NOAA Technology Brief

National Oceanic and Atmospheric Administration

National Environmental Satellite, Data, and Information Service
National Oceanographic Data Center

Alaskan Coastal Biological Data

Biological oceanographic data for coastal Alaska are available from NOAA's National Oceanographic Data Center (NODC). The center holds marine biological data on the U.S. outer continental shelf and in other selected areas. Most of these data come from environmental assessment programs conducted to study the effects on the marine environment of human activities like ocean dumping and offshore oil development. Chief among these surveys is the Alaskan Outer Continental Shelf Environmental Assessment Program (OCSEAP), conducted during the 1970's and 1980's.

NODC Master Data Files. NODC's Master Data Files hold numerous individual data submissions from OCSEAP and other programs that undergo quality control procedures and are stored in standard archive formats. Data in the files are available as magnetic tape copies. Subsets of data in NODC's Master Data Files can be selectively retrieved and provided to users. These data can generally be selected either by time period and geographic area or by specific cruise or cruises. The following files, which contain OCSEAP and other data, are available:

1.1 Phytoplankton (F028), 1960-1983, 2,257 stations; 6 Mb.
1.2 Zooplankton (F124), 1965-1983, 15,068 stations; 24 Mb.
1.3 Primary Productivity (F029), 1958-1983, 5,077 stations; 2 Mb.
1.4 Intertidal/Subtidal Organisms and Habitats (F030), 1974-1980, 975 stations; 21 Mb.
1.5 Benthic Organisms (F132), 1957-1984, 26,218 stations; 32 Mb.
1.6 Fish/Shellfish Surveys (F123), 1948-1983, 14,881 stations; 69 Mb.
1.7 Marine Animal Sighting and Census (F127), 1971-1983, 49,518 stations; 10 Mb.

Originator Data Sets. In addition to its Master Data Files, NODC also holds a number of individual OCSEAP and other data sets in originator formats. These data sets typically represent data from completed projects or data compilations subject to special editing, quality control, or analytic procedures. In some cases, data maintained separately in its original form may also be incorporated in whole or in part in the appropriate Master Data Files. Originator Data Sets can be provided to users only as direct one-to-one copies of whole data tapes. Selected subsets cannot be retrieved from these data sets. Data for areas other than coastal Alaska may be present on some tapes.

2.1 Marine Bird Data Sets. Each of these data sets are stored in a separate format, but all are held on a single magnetic tape. Most of these data were collected as part of OCSEAP.
2.1a Marine Bird Specimen and Feeding Studies, 1975-1980, 2,118 stations.
2.1b Marine Bird Sighting, Ship/Aircraft Census, 1974-1982, 32,916 stations.

2.1c Marine Bird Sighting, Land Census, 1975-1980, 7,994 stations.
2.1d Feeding Flock, 1975-1976, 223 stations.
2.1e Migratory Sea Bird Watch, 1977-1978, 12 stations.
2.1f Marine Bird Habitats, 1975-1978, 2,152 stations.
2.2 Marine Mammal Data Sets, 1 tape.
2.2a Marine Mammal Specimen, 1975-1981, 4,467 stations.
2.2c Marine Mammal Sighting 1, 1971-1979, 4,012 stations.
2.3 Pathology Data Sets, 1 tape.
2.3b Fish Pathology, 1975-1980, 948 stations.
2.3c Marine Invertebrate Pathology, 1976-1978, 325 stations.
2.6 Herring Surveys, 1976-1977, 457 stations, 1 tape.

All NODC data products are provided at cost. NODC's standard data files -- as well as available data products, including data inventories -- are described in more detail in the NODC Users Guide. Inquiries and data requests should be directed to:

National Oceanographic Data Center
Users Service Branch
NOAA/NESDIS/E/OC21
Universal Building, Room 412
Washington, D.C. 20235
Telephone: 202/673-5549 (Commercial), FTS 673-5549
Electronic Mail: NODC.WDCA on Omnet/SCIENCEnet (Telemail)
NODC::SERVICES on SPAN

NIH
Research & Technology
Federal Laboratory Resource
U.S. Department of Health and Human Services Public Health Service National Institutes of Health

The National Magnetic Resonance Facility at Madison

The National Magnetic Resonance Facility at the University of Wisconsin, Madison, offers the biomedical and biochemical research community some of the most powerful instruments and sophisticated techniques now available for liquid-phase and in vivo nuclear magnetic resonance spectroscopy.

Nuclear magnetic resonance (NMR), now more popularly recognized for its role in diagnostic medical imaging, has nonetheless been employed continuously since its advent in the late 1940's to obtain basic information about the structure of molecules from the characteristic behavior of atomic nuclei in electromagnetic fields.

The objectives of the core research and development programs at the Madison facility are to improve and extend NMR technologies and to explore new biomedical applications. Core research areas include high-resolution NMR studies of the structure and dynamics of biological polymers, investigations of mechanisms of enzyme action, and noninvasive studies of tissues and living organisms.

NMR has advanced steadily through the application of new techniques made possible by the development of spectrometers boasting powerful superconducting magnets and advanced electronics and through the availability of computer-assisted analysis and graphic modeling of NMR data.

The scientific staff at the facility is actively developing new experimental techniques, spectrometer programming capabilities and probes, and computer software, and is training visiting researchers to take advantage of these new tools.

The facility was established in 1985 with Federal support for equipment and operating expenses from the National Institutes of Health, the National Science Foundation, and the U.S. Department of Agriculture, and with local funding from the University of Wisconsin. It continues to receive support from these sources and operates as a user facility under the Biomedical Research Technology Program of the NIH Division of Research Resources. The facility serves researchers at the University of Wisconsin and at other institutions in the United States and abroad.

The Madison facility currently operates four state-of-the-art Bruker spectrometers, including a 600-megahertz spectrometer for structural studies and a 400-megahertz spectrometer with a wide-bore sample-holder for use with special probes for in vivo spectroscopy. These powerful spectrometers are used in tandem with state-of-the-art computer data stations.

The facility's full-time staff includes director and principal investigator Dr. John Markley, biochemistry professor at the University of Wisconsin; operations director Dr. Milo Westler; instrumentation director Dr. Edward Mooberry; computation director Dr. Prashanth Darba; and administrator James Shurts.

The staff provides hands-on training to all visiting scientists. In addition, scientists may send samples for NMR analysis by staff scientists.

Staff scientists have developed and are refining a number of NMR techniques as well as equipment and computer software. Two-dimensional NMR, an area of rapid development, is a major research focus.

By employing different two-dimensional NMR protocols, researchers can search for three separate kinds of relationships among atoms in a molecule: atoms (usually hydrogens) that are close to one another in space; sets of atoms that make up each chemical unit of a biopolymer (amino acid for a protein); and atoms that shuttle between one structure and another by means of a molecular rearrangement or chemical reaction. These new approaches make NMR the leading technique for studying molecular structure and dynamics in solution. Such problems could be solved only in piecemeal fashion before two-dimensional NMR methods were developed.

"The difference in going from one-dimensional to two-dimensional NMR is analogous to looking across the horizon at distant mountain peaks obscured by peaks in the foreground, and then looking down on the same peaks individually from an airplane," says Dr. Westler.

More refined techniques for programming electromagnetic pulse sequences into more powerful spectrometers are aiding efforts to apply two-dimensional NMR to stable atomic isotopes whose signals are weaker than those of hydrogen-1. Valuable information can now be obtained in experiments using carbon-13 and nitrogen-15, rare isotopes that are naturally far outnumbered by carbon-12, which is nonresonating, and nitrogen-14, which is not amenable to high-resolution studies. Molecules of interest can be multiple-labeled with these rare isotopes and their interactions studied through two-dimensional NMR experiments.

To prepare samples for these experiments, the facility collaborators and users make biolog-

ical macromolecules with multiple labels by feeding labeled nutrients such as carbon dioxide or amino acids to microorganisms. These microorganisms—bacteria, yeast, or photosynthetic cyanobacteria—incorporate the labeled atoms into proteins and other macromolecules.

Staff scientists grow photosynthetic cyanobacteria with specially developed equipment under controlled conditions. Purified labeled proteins, amino acids, and other biomolecules obtained from the cyanobacteria are made available to collaborating projects.

Besides improving experimental approaches, facility scientists are also creating new computer software to analyze data. For example, software programs now enable scientists to better define NMR peaks that rise above uneven interfering background signals and to select peaks of interest for better computer-aided resolution.

Going beyond the generation of NMR data, researchers are developing interactive computer graphics software to convert NMR spectra of proteins into distances between nearby hydrogen atoms. These distances in turn are used to compute models of the three-dimensional solution structures of the proteins.

Facility users are also developing novel NMR probes. A probe is the sample-holder that also acts as an antenna in NMR experiments. Researchers have designed special probes for use in experiments on tissues and living organisms and a perfusion probe that bathes sensitive tissue in oxygen and nutrients during the course of experiments.

By using a probe with a coil wrapped around a frog's leg, a research team from the University of Barcelona, Spain, has noninvasively measured lactate, a product of anaerobic metabolism, in relaxed and contracted muscle.

With the perfusion probe, other researchers have successfully used phosphorus-31 in NMR experiments to monitor adenosine triphosphate (ATP) and phosphorus metabolism in renal glucogenesis, ammoniagenesis, and acidosis in kidney proximal tubule cells. With this perfusion system, proximal cells were studied continuously for more than 12 hours and still remained viable.

The Madison facility recently received a grant from the National Library of Medicine to establish a protein NMR data bank. "The data bank design is intended to be flexible," says Dr. Markley, "capable of expanding to include new techniques, new forms of data, and biopolymers other than proteins. Only through the active cooperation and support of the NMR community can the data bank succeed."

For more information contact:
Dr. Milo Westler
NMRFAM
Department of Biochemistry
420 Henry Mall
University of Wisconsin
Madison, Wisconsin 53706
(608) 263-9599

For Additional Information:

To locate information or professional contacts on this effort, contact:

Research Resources Information Center
1601 Research Boulevard
Rockville, MD 20850
(301) 984-2870

Refer to Volume XIII, No. 5/TN

NIH
Research & Technology
Federal Laboratory Resource
U.S. Department of Health and Human Services Public Health Service National Institutes of Health

Cryopreservation of Murine Germplasm

Principal Investigator:
Larry E. Mobraaten, Ph.D.
Staff Scientist
The Jackson Laboratory
Bar Harbor, Maine 04609
(207) 288-3371 x 235

Resources Provided

- *Reference Services:* The repository contains frozen 8-cell mouse embryos from genetically defined strains of laboratory mice that are maintained at the Jackson Laboratory. Embryos from more than 550 different strains are currently preserved. Breeding pairs of mice are made available when such mice cannot be obtained from conventional breeding sources.
- *Contact Person:* Larry E. Mobraaten, Ph.D., (207) 288-3371 x 235.

Research Emphasis or Application

- *Basic Objectives:* To assure the safe preservation of scientifically valuable strains of laboratory mice by establishing a bank of frozen mouse embryos. At present the program staff is freezing and storing in liquid nitrogen embryos from selected strains of the more than 900 inbred and mutant strains of mice maintained at the Jackson Laboratory. Other objectives are to reduce the necessary number of different stocks or size of colonies maintained by conventional breeding procedures and to retard genetic drift.
- *Current Research:* Freezing of mouse embryos and recovery of liveborn from frozen embryo storage.

NIH
Research & Technology
Federal Laboratory Resource
U.S. Department of Health and Human Services Public Health Service National Institutes of Health

Institute of Laboratory Animal Resources (ILAR)

Principal Investigator:
Thomas L. Wolfle, D.V.M., Ph.D.
Director
Institute of Laboratory Animal Resources
National Academy of Sciences
2101 Constitution Avenue, N.W.
Washington, D.C. 20418
(202) 334-2590

Resources Provided

- *Activities:* ILAR develops guidelines on laboratory animal care and use, and conducts conferences, symposia, and workshops on important laboratory animal problems. ILAR publishes the journal *ILAR News* on a quarterly basis, as well as conference proceedings and special reports prepared by committees of experts. Listings of animal sources are compiled by ILAR staff members and published occasionally. A list of ILAR publications on laboratory animals is available. As a part of the Animal Models and Genetic Stocks Information Exchange Program, ILAR staff members answer direct telephone and mail inquiries on: the existence and location of specific animal models; correct nomenclature to identify animals; and related topics such as facilities, diseases of animals, and relevant publications. ILAR also aids in the relocation of genetic stocks that cannot be maintained at their original sites.
- *Contact Person:* Dorothy D. Greenhouse, Ph.D., (202) 334-2590.

Research Emphasis or Application

- *Basic Objectives:* To develop and make available to the biomedical community scientific and technical information, guidelines, surveys, and directories as a service to improve the availability, quality, and utilization of laboratory animals.

NIH
Research & Technology
Federal Laboratory Resource
U.S. Department of Health and Human Services Public Health Service National Institutes of Health

MIT Cell Culture Center

Principal Investigator:
Phillip A. Sharp, Ph.D.
Massachusetts Institute of Technology
Cell Culture Center
77 Massachusetts Avenue
Building E17, Room 321
Cambridge, Massachusetts 02139
(617) 253-6430

Director:
Donald J. Giard, M.S.

Resources Provided

- The center produces cells and cell products on a large scale as a service to scientists throughout the country who are involved in basic research but lack the facilities or expertise in their own laboratories to produce these materials. An important element of this resource is that the center attempts to customize its services to meet the specific needs of each project. In addition, the center operates a cell sorter laboratory that serves as a facility and resource for flow cytometry and sorting for researchers in the northeastern United States.

Research Emphasis or Application

- The center is currently focusing on new cell production techniques, cell growth in reduced concentrations of serum, cell attachment studies, and bioreactor design.
- *Contact Person:* Donald J. Giard, M.S., director, (617) 253-6430.

NIH
Research & Technology
Federal Laboratory Resource
U.S. Department of Health and Human Services Public Health Service National Institutes of Health

University Resource in Laboratory Animal Medicine

Principal Investigator:
Daniel H. Ringler, D.V.M.
Animal Research Facility
Box 0614
University of Michigan
Ann Arbor, Michigan 48109
(313) 764-0277/0278

Resources Provided

- *Diagnostic Services:* Necropsy examination, histopathology, clinical pathology, parasitology, and bacteriology of laboratory animals. The laboratory has special expertise in pathology of aged rats and mice, pasteurellosis in rabbits, and diseases of amphibians. Diagnostic resources are designed primarily to serve the grantee and affiliated institutions. However, with approval by the principal investigator, they are available for collaboration in investigating laboratory animal disease problems.
- *Contact Persons:* Daniel H. Ringler, D.V.M., or Clarence E. Chrisp, D.V.M., (313) 764-0277/0278.

Research Emphasis or Application

- *Basic Objectives:* To maintain and improve the quality of laboratory animals through control and diagnosis of diseases in the animal colonies at the University of Michigan and affiliated institutions. To conduct research in laboratory animal and experimental medicine. To enhance research training in laboratory animal medicine.
- *Current Research:* Investigation and characterization of spontaneous and iatrogenic diseases of laboratory animals, including study of basic mechanisms of disease caused by such laboratory animal pathogens as *Pasteurella multocida*; prevention of pasteurellosis by vaccination; development of new diagnostic procedures such as an enzyme-linked immunosorbent assay (ELISA) for pasteurellosis in rabbits; recognition and definition of animal models of human disease such as herpesvirus, keratitis, and encephalitis; definition of the spectrum of spontaneous degenerative and neoplastic age-associated lesions in SPF strains or stocks of mice and rats.

NASA Tech Brief
National Aeronautics and Space Administration
Goddard Space Flight Center, Greenbelt, Maryland

Licensing Opportunity

Directional Hearing Aid

The approximate directions of sounds are indicated visually.

A hearing-aid device indicates visually whether a sound is coming from the left, right, back, or front. The device is intended to assist individuals who are deaf in at least one ear and, therefore, unable to discern naturally the directions to sources of sound. The device can thus promote safety in street traffic, on loading docks, and in the presence of sirens, alarms, and other warning sounds.

Figure 1 illustrates a quadraphonic version of the device built into a pair of eyeglasses and a binaural version built into a visor. The quadraphonic version includes four microphones to distinguish left, right, back, and front. The binaural version includes only two microphones to distinguish left and right. Both versions include small batteries, light-emitting-diode displays, and integrated-circuit amplifiers and logic units.

In the binaural version (see Figure 2), the signal from each microphone is amplified and rectified. Each resulting dc signal is fed to an analog-to-digital converter and encoder. The output of each encoder is a 3-bit binary representation of the amplitude of sound in that channel. The encoder outputs are fed to a digital-comparator-and-logic unit to determine which channel contains the louder sound or whether the amplitudes in both channels are equal. The comparator activates a logic unit and a driver in the channel that contains the

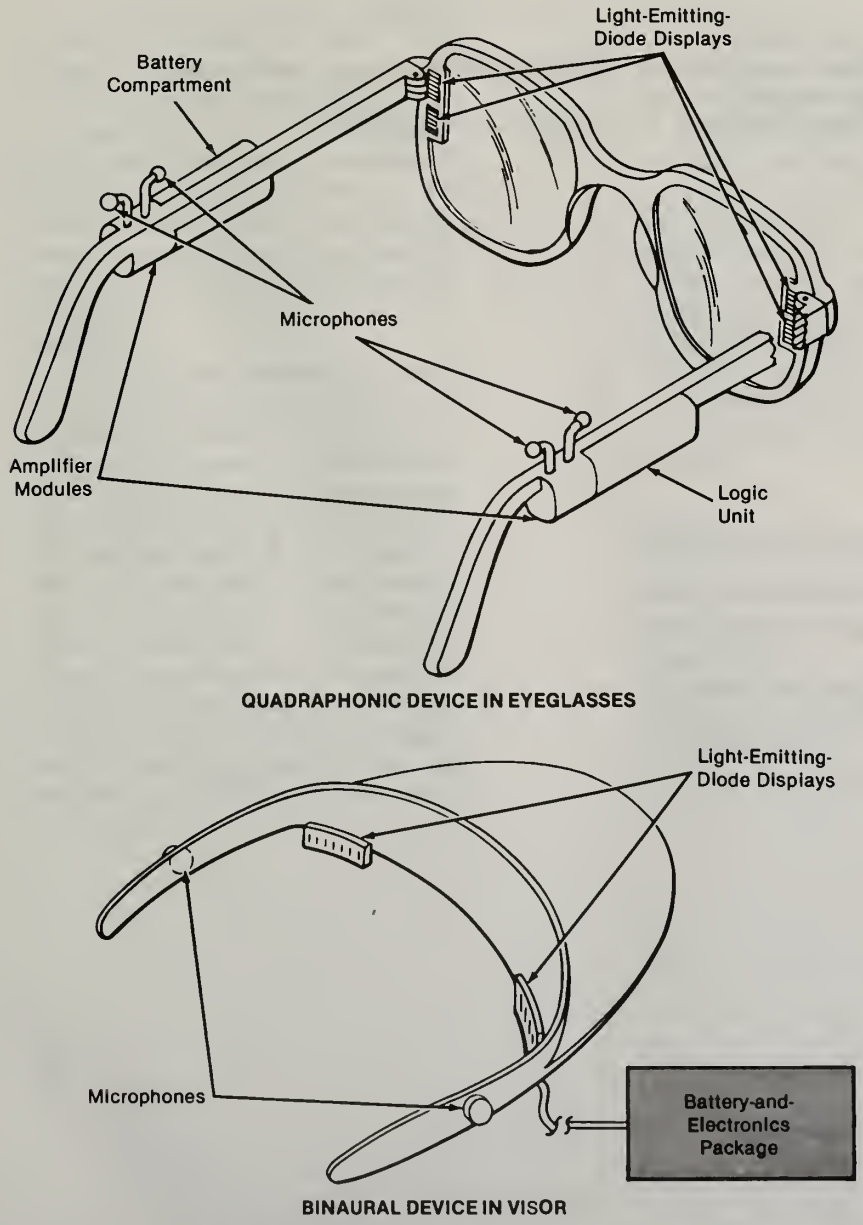

Figure 1. **Visual Displays, Microphones, and Signal-Processing Circuits** can be built into eyeglasses, visors, caps, or other common headgear to indicate the directions of sounds, thanks to the miniaturization of modern integrated-circuit technology.

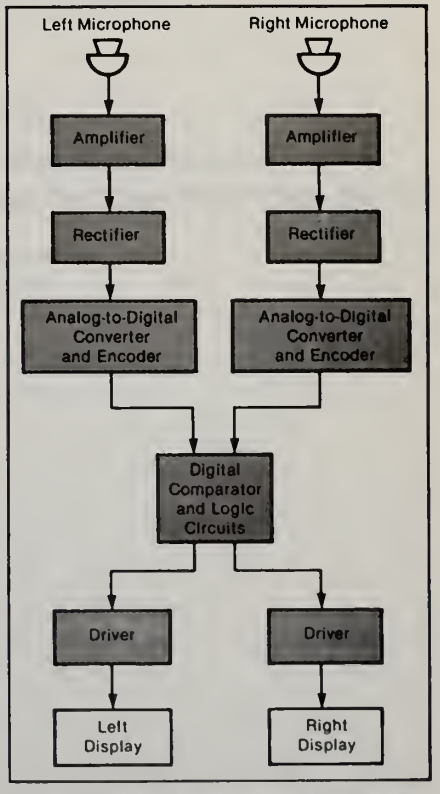

Figure 2. **Sound in Right and Left Channels** is processed, compared, and displayed to indicate the approximate direction of the source of the sound.

louder sound. The logic unit converts the 3-bit binary representation of amplitude to a progressive seven-interval digital representation.

The output of the logic unit controls the driver of the display unit of the channel, which is an array of seven light-emitting diodes. Thus, the display of the right or left channel lights up to indicate which contains the louder sound (thus indicating the approximate direction), and the number of diodes that light up gives an approximate indication of the loudness. If the amplitude is the same in both channels, the comparator activates the displays of both channels, thus indicating that the sound comes from ahead or behind.

The sensing and display portions of the quadraphonic version operate similarly to the corresponding parts of the binaural version. The major difference is that the quadraphonic version has four displays and includes additional comparator and logic circuitry to distinguish between the front and back channels as well as between right and left. Thus, for example, the lighting of the lower left display indicates a sound coming from the left rear, while the lighting of both lower displays indicates a sound coming from behind.

This work was done by M. Jhabvala of **Goddard Space Flight Center** *and H. C. Lin of the University of Maryland.*

This invention is owned by NASA, and a patent application has been filed. Inquiries concerning nonexclusive or exclusive license for its commercial development should be addressed to the Patent Counsel, Goddard Space Flight Center Refer to GSC-13027/TN

FOR ADDITIONAL INFORMATION: *Contact: Director, Technology Transfer Division, P.O. Box 8757, BWI Airport, MD 21240; (301) 621-0100 Ext. 241*

REFER TO THE NUMBER LISTED AT THE END OF THIS ARTICLE

NAVY
Domestic Technology Transfer Fact Sheet

New Developments Available to Test Marine Plankton Light Emissions

Test chamber uses an integrating sphere to collect light

Scientists at the Naval Ocean Systems Center (NOSC), San Diego, California, have developed a test chamber for determining the light emissions of planktonic organisms. The basic instrument has been used extensively since 1981. However, a new instrument can now be used that employs the same basic technique but uses an integrating sphere for light collection.

A light-tight chamber is used that has at least one light port (preferably two) where photomultiplier tubes are connected to the test chamber for detecting and measuring the flash kinetics of marine organisms. A door is pivotally mounted on the chamber so an organism sample holder can be inserted and removed. Then, a vacuum line is connected to the test chamber and to the sample holder through a passageway so that the organism can be excited by drawing off the fluid containing the organism. The light emissions of the sample can be detected and measured by photomultiplier tubes.

Ideally, a third port is added to which another multiplier tube is connected providing a different orientation to the organism in the sample holder. Alternate experiments can be conducted on the organism through the third port. The collected data can help identify which organisms are responsible for the light emissions in the surface waters of the world's oceans.

For Additional Information:

Backup material on this effort is available from:

Navy Domestic Technology Fact Sheet Reader Reply Service
Code E211
Naval Surface Weapons Center
Dahlgren, VA 22448-5000
(703) 663-8921

Refer to 140301/TN

Natural Resources Technology & Engineering

0800 Formula Predicts the Spontaneous Combustion Potential of Bituminous Coals

0801 High-Altitude Turbulence for Supersonic Airplanes—Characteristics and associated meteorological features are discussed.

Other Items of Interest

0799 New Developments Available to Test Marine Plankton Light Emissions—Test chamber uses an integrating sphere to collect light

Technology News

From the Bureau of Mines, United States Department of the Interior

Formula Predicts the Spontaneous Combustion Potential of Bituminous Coals

Objective

To predict the spontaneous combustion potential of bituminous coals using a simple expression based on an easily acquired coal property.

Background

Approximately 20% of underground coal mine fires in the United States since 1978 have been attributed to spontaneous combustion. Spontaneous combustion fires in underground mines are most likely to occur in gob areas and are difficult to detect and to extinguish by direct fire fighting methods. Often, sections of the mine or the entire mine must be sealed for long periods, at a great economic loss to the mine operator, mine employees, and the surrounding community. It is conservatively estimated that the cost of sealing a large mine is about $50 million.

Spontaneous combustion mine fires are expected to increase with the greater consumption of low rank coals, deeper mines, and the introduction of longwall mining methods. In addition, spontaneous combustion continues to be a significant problem in the storage, transport and usage of coal. A reduction of such fires will obviously benefit the entire coal industry.

Many factors contribute to the spontaneous combustion process. One of the most significant is the self-heating tendency of the coal; other factors include temperature, ventilation, geology and mining practices.

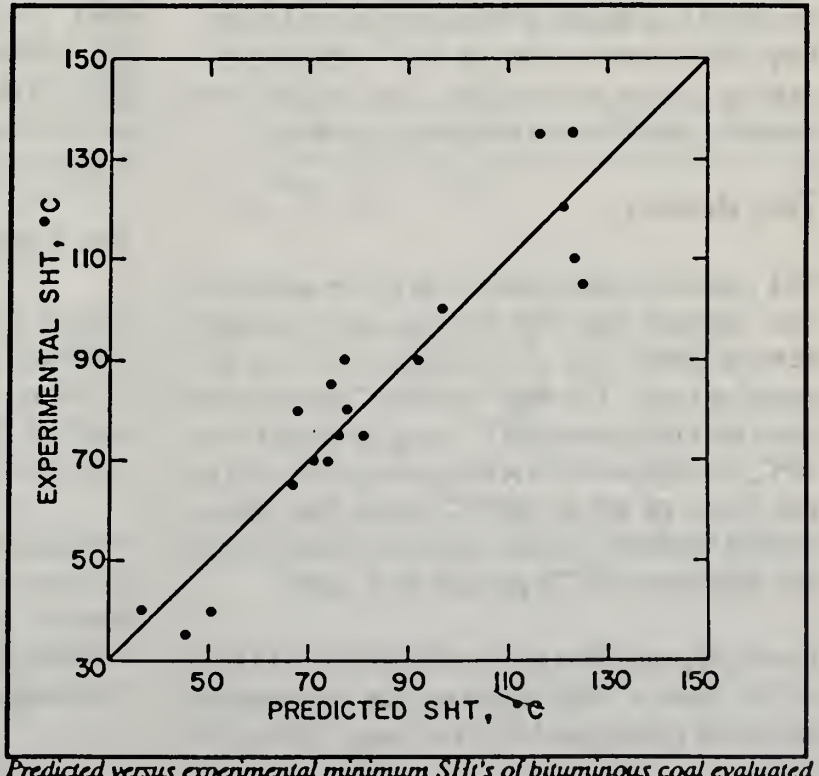

Predicted versus experimental minimum SHt's of bituminous coal evaluated in the adiabatic heating oven.

If a coal has a high self-heating tendency, preventive measures should be applied. In underground mines these include improved fire detection systems, minimizing the amount of coal left in gob areas, controlling the gob ventilation, and sealing worked out sections.

Approach

The Bureau of Mines recently conducted laboratory tests to evaluate the relative spontaneous combustion potential of 19 bituminous coal samples from 14 seams. An adiabatic oven was used to determine each coal's minimum self-heating temperature (SHT), the minimum initial temperature that produced a sustained exothermic (heat producing) reaction, or thermal runaway, under a set of standard conditions. These temperatures were then used to rank the coal's relative self-heating tendency compared to other coals evaluated in the same manner. The lower the minimum SHT, the higher the self-heating potential of the coal.

A statistical analysis of the results was made and a relationship derived that can predict the minimum SHT of a coal as measured in the laboratory. This allows assignment of the relative self-heating risk or potential of a coal without the need for detailed and costly experiments.

Test Results

The results of the experiments in the adiabatic oven agreed with the concept that the self-heating tendencies of coals increases with decreasing rank. The high-volatile C bituminous coals had minimum SHT's ranging from 35° to 70°C, the high-volatile A bituminous coals fell in the range of 65° to 100° C, while the higher ranked medium volatile and low volatile coals had minimum SHT's greater than 100°C.

It was proposed that coals with minimum SHT's < 70° have a high spontaneous combustion potential, those that fall in the range 70° to 100° C have a medium risk, and coals with minimum SHT's > 100° C have a low spontaneous combustion potential when compared with other coals. It must be noted, however, that these were laboratory tests of specific coal samples and are a relative measure of the self-heating tendency of the coal alone without considering other contributing factors associated with the spontaneous combustion process.

A statistical analysis of the data was conducted involving the experimental minimum SHT of the coal and the chemical constituents of the coal such as fixed carbon, ash, oxygen and sulfur, obtained from proximate and ultimate analyses. The resulting expression showed a correlation between the minimum SHT of the coal and its dry ash-free oxygen content:

$$^{SIT}\text{min,°C} = 139.7 - 6.6 \times [0, \text{pct (DAF)}].$$

The resulting line had a correlation coefficient of 0.934 with an average relative error of 10.6 pct.
The expression gives a good prediction of the relative self-heating potential of a bituminous coal. The prediction, which should not be used for subbituminous and lignite coals, is based only on the dry ash-free oxygen content of the coal, a value readily obtained from a standard ultimate analysis.

For More Information

Details of the experimental test procedure and results of this research are described in Bureau of Mines Report of Investigation (RI) 9079 entitled, "Spontaneous Combustion Studies of U.S. Coals."

For additional information about the Bureau's spontaneous combustion research program, contact: Alex C. Smith, U.S. Bureau of Mines, Pittsburgh Research Center, P.O. Box 18070, Pittsburgh, PA 15236, (412) 892-6766.

NASA Tech Brief
National Aeronautics and
Space Administration

High-Altitude Turbulence for Supersonic Airplanes

Characteristics and associated meteorological features are discussed.

A report reviews the accumulated knowledge of atmospheric turbulence at high altitudes. This and related studies are motivated principally by the need to understand and predict the turbulence likely to be encountered by present and future airplanes cruising at supersonic speeds at altitudes ranging from the tropopause up through the stratosphere.

The report begins with a discussion of the characteristics of high-altitude turbulence and the associated meteorological features, with emphasis on data obtained by flight research conducted in XB-70 and YF-12A prototype aircraft. The intensity of turbulence is shown to exhibit predictable relationships with such atmospheric features and quantities as the wind-speed, the temperature structure, and a half dozen assorted parameters derived from meteorological and flight data.

The motion of gravity waves (meaning, in this case, atmospheric waves analogous to waves on the ocean) is involved in a major portion of the turbulence encountered at high altitudes. Turbulence at supersonic-cruise altitudes occurs in patches typically less than 1 km thick, thus suggesting that turbulence is generated in relatively shallow layers of atmospheric structure that are responding to excitation by waves of larger scale, in a manner reminiscent of the breaking of waves on the ocean.

The report gives an example of the numerical simulation of gravity waves to illustrate the potential contribution of such studies to the understanding of atmospheric turbulence. The relatively small dimensions of high-altitude turbulence patches and gusts and their association with underlying wave activity strongly motivate the use of numerical simulation to describe flows at resolutions much finer than are available from upper-air soundings. Moreover, because of the transient nature of waves breaking into turbulence, numerical simulation could potentially augment measurements taken by aircraft to interpret atmospheric structures in regions of strong turbulence.

Henceforth, progress will likely depend on advances in the numerical simulation of gravity waves and comparisons between simulations and observations. This may best be done by collaboration among experts in aircraft measurements, atmospheric observations, mesoscale analysis of the atmosphere, applied forecasting, theoretical atmospheric dynamics, and the formulation of mathematical models of gravity waves. The products of such efforts may include the ability to extend estimates of transient properties of the atmosphere at altitudes below 20 km to altitudes as high as 80 km for use in the design and flight simulation of future advanced aerospace vehicles. In addition, such efforts may enable a more accurate assessment of the feasibility of remote sensors and computer systems aboard airplanes to process measurements into advanced warnings of turbulence.

This work was done by L. J. Ehernberger of Dryden Flight Research Facility for **Ames Research Center**. *Furtherinformation may be found in NASA TM-88285 [N87-23100], Price Code: A02 "High Altitude Turbulence for Supersonic Cruise Vehicles."*

Copies may be purchased from the National Technical Information Service, Springfield, Virginia 22161, Telephone No. (703) 487-4650. Rush orders may be placed for an extra fee by calling (800) 336-4700.
ARC-12149/TN

FOR ADDITIONAL INFORMATION: *Contact: Director, Technology Transfer Division, P.O. Box 8757, BWI Airport, MD 21240; (301) 621-0100 Ext. 241*
REFER TO THE NUMBER LISTED AT THE END OF THIS ARTICLE

Physical Sciences

0802 Heat, Alkali, Convert Crops to Chemicals (Licensing Opportunity)

0803 Cladding for Transversely-Pumped Laser Rod (Licensing Opportunity)

0804 Metal Oxide/Zeolite Combination Absorbs H_2S (Licensing Opportunity)

0805 Theory of a Pyrotechnically Driven Device—Predictions and measurements of operation are presented.

Testing & Instrumentation

0806 Impedance Probe "Fine-Tunes" Electroplating Solutions

0807 Piezoelectric Polymer Forms Inexpensive Accelerometer

0808 Measuring High-Temperature Superconductors

0809 Eight-Channel Spectrometer—Photodetector signals are multiplexed for digitization and recording. (Licensing Opportunity)

0810 Delay-Line Anode for Microchannel-Plate Spectrometer—A zigzag pattern enables the location of incident pulses in two dimensions.

0811 Electron/Ion-Scattering Apparatus—Electron and ion beams are merged, then separated for analysis (Licensing Opportunity)

0812 Keyboard Emulation for Computerized Instrumentation—Experimental parameters can be retrieved or re-entered at will.

0813 Measurement of Molecular Mobilities of Polymers

0814 Modified Technique for Chemisorption Measurements

Other Items of Interest

0738 Lithium Battery (Licensing Opportunity)

0749 Variable-Volume Container—The container expands and contracts according to changes in volume of its solid contents.

0761 Materials Aimed at Improving Pesticide, PCB Analyses

0765 Miniature Centrifugal Compressor—A small machine compresses neon for cooling to temperatures as low as 30K.

0778 Additives Lower Pickup of Moisture by Polyimides—Positron-annihilation tests show increased densities. (Licensing Opportunity)

0781 Better PFAE's from Direct Fluorination—The process yields stable and effective lubricants under proper conditions.

0786 Orientating Superconductive Crystals for High Current Density—Uniaxial stress would promote rearrangement of oxygen atoms in a favorable direction.

0787 Variable-Energy Ion Beams for Modification of Surfaces—Ions at low energy react chemically with silicon without damaging it. (Licensing Opportunity)

Research Technology
Agricultural Research Service
U.S. Department of Agriculture

Licensing Opportunity

Heat, Alkali, Convert Crops to Chemicals

Clothes, detergents, and dozens of other everyday products are made using two versatile chemicals -- glycolic acid and oxalic acid.

Now these compounds can be made from cellulose or starch from the farm, instead of from fossil fuels, using a new process. And although the method might not be economical right now, that may change if the price of oil goes up.

In brief, cornstarch, corn cobs, finely ground wheat straw or rice straw, or similar starch or cellulose source is added to sodium hydroxide (an alkali) that's been mixed with water. The mixture is heated to 464°F in a high-pressure reactor (something like a pressure cooker) for 10 to 40 minutes.

The inky-looking liquid that results has 40 to 45 percent glycolic acid, and 15 to 25 percent oxalic acid -- based on the starting weight of the starch or cellulose. These yields far exceed those from similar methods relying on alkali and heat to produce the acids.

While this research didn't address the final step -- how to extract the useful chemicals from the slurry -- it's expected that a combination of filtration, solvent extraction, and distillation will do the job.

Of the many possible new uses for the process in the future, ARS researchers are especially enthusiastic about converting farm-derived glycolic acid into biodegradable plastic products or into auto antifreeze (ethylene glycol).

For technical information contact John M. Krochta, USDA-ARS Process Chemistry and Engineering, Western Regional Research Center, Albany, CA 94710 (415) 559-5860. Patent Application Serial No. 07/155,442, "Production of High Yields of Glycolic and Oxalic Acids from Polysaccharide-Containing Materials."

For Additional Information:

Inquiries concerning rights for commercial use of this invention should be addressed to:

Office of Federal Patent Licensing
Center for the Utilization of Federal Technology
Room 304, NTIS
Springfield, VA 22161
(703) 487-4738

Refer to Patent Application 07/155,442/TN

NASA Tech Brief
National Aeronautics and Space Administration
NASA's Jet Propulsion Laboratory, Pasadena, California

Licensing Opportunity

Cladding for Transversely-Pumped Laser Rod

Pump power would be coupled in more effectively.

The proposed combination of suitable dimensioning and cladding of a neodymium:yttrium aluminum garnet or similar solid-state laser would provide for the more efficient utilization of transversely-incident pump light from diode lasers. The new design would overcome some of the limitations of longitudinal- and older transverse-pumping concepts and thereby promote operation at higher output powers in the TEM_{00} mode.

The geometry of longitudinal pumping makes it difficult to scale to higher power. Transverse pumping permits the use of multiple diode-laser pumps to increase power, but, in the conventional design, transverse pumping is inefficient because much of the pump power is absorbed near the surface of the gain medium, outside the Gaussian diameter of the TEM_{00} mode (the effective diameter of the laser beam).

The improved laser resonator (see figure) would consist of an inner gain medium surrounded by a cladding that does not absorb at the pump or laser wavelengths and has no gain at the laser wavelength. The index of refraction of the cladding should be close (preferably equal) to that of the gain medium. The gain medium would be wide enough (typically one or more absorption lengths) so that it could absorb most of the pump energy.

One of the principal features of the new concept is that the resonator would be designed to make the Gaussian diameter of the TEM_{00} mode greater than the diameter of the gain medium, so that a significant portion of the laser beam would extend out into the inner portion of the cladding. In addition, the cladding would be made thick enough to make the TEM_{00} mode essentially zero outside the cladding. Thus, the laser beam would still be kept safely within the diameter of the resonator, but the outer portion of the beam could be reached by the pump light.

Because the pump light would be absorbed only by the gain medium and not by the cladding, all of the excitation would take place inside the Gaussian diameter. Thus, the pump power would be extracted efficiently. If the resonator is aligned correctly, it should operate only in the TEM_{00} mode because the overlap between the pump light and the TEM_{00} mode is greater than the overlap between the pump light and any higher-order transverse mode.

While the figure shows a simple round configuration, others are possible. For example, the TEM_{00} could be centered in a slab of gain medium between two slabs of cladding. Also, the laser could be pumped from only one side and a mirror used to reflect light back into the gain medium from the other side.

This work was done by Robert L. Byer and Tso Yee Fan of Stanford University for **NASA's Jet Propulsion Laboratory**.

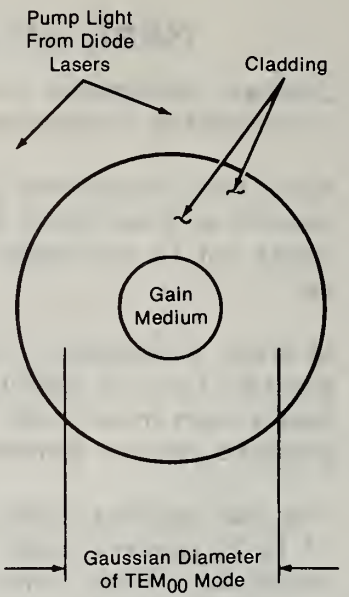

The Improved Laser Resonator Rod for Transverse Pumping would include a central gain medium and a transparent, gainless cladding that has (preferably) the same index of refraction.

This invention is owned by NASA, and a patent application has been filed. Inquiries concerning nonexclusive or exclusive license for its commercial development should be addressed to the Patent Counsel, NASA Resident Office-JPL Refer to NPO-17355/TN

Jet Propulsion Lab.
NASA Resident Office
Technology Utilization Officer: Gordon S. Chapman
Mail Stop 180-801
4800 Oak Grove Drive
Pasadena, CA 91109
(818) 354-4849
Patent Counsel:
Paul F. McCaul
Mail Code 180-801
4800 Oak Grove Drive
Pasadena, CA 91109
(818) 354-2734

Technology Utilization Mgr. for JPL: Norman L. Chaffin
Mail Stop 156-211
4800 Oak Grove Drive
Pasadena, CA 91109
(818) 354-2240

FOR ADDITIONAL INFORMATION: *Contact: Director, Technology Transfer Division, P.O. Box 8757, BWI Airport, MD 21240; (301) 621-0100 Ext. 241*
REFER TO THE NUMBER LISTED AT THE END OF THIS ARTICLE

NASA Tech Brief
National Aeronautics and Space Administration
NASA's Jet Propulsion Laboratory, Pasadena, California

Licensing Opportunity

Metal Oxide/Zeolite Combination Absorbs H_2S

A regenerable absorber cleans up hot gas streams.

Mixed copper and molybdenum oxides supported in the pores of zeolite have been found to remove H_2S from a mixture of gases rich in hydrogen and steam, at temperatures from 256 to 538 °C. Such an absorber of H_2S is needed to clean up gas streams from fuel processors that incorporate high-temperature steam reformers or hydrodesulfurizing units.

Zeolites were chosen as the supporting materials because of their high porosity, rigidity, alumina content, and variety of both composition and form. The zeolite pellets were impregnated with basic cupric carbonate and ammonium molybdate dissolved in concentrated ammonium hydroxide. After drying in an oven at 110 °C, the pellets were impregnated again. This process was repeated 8 to 10 times. The material was then calcined in an oxygen-rich atmosphere in a muffle furnace at 600 °C for 3 hours, yielding zeolite impregnated with $CuO \cdot \frac{1}{3}MoO_3$.

The sorbents were alternately exposed at various temperatures to a flowing sulfidation-gas mixture of $1H_2S/20H_2/25H_2O/54N_2$, then regenerated at a temperature of 600 to 650 °C in a mixture of $70N_2/30$ air (numbers indicate molar percentages). Of the supporting materials tested, the best H_2S-removal performance was shown by 4Å zeolite (see figure). Most of the sulfidation reactions involve the conversion of CuO to Cu_2S; molybdenum sulfides are usually not seen. The sorbent maintains a high capacity for sulfur — in stoichiometric proportion to the copper content — for as many as 12 sulfidation/regeneration cycles.

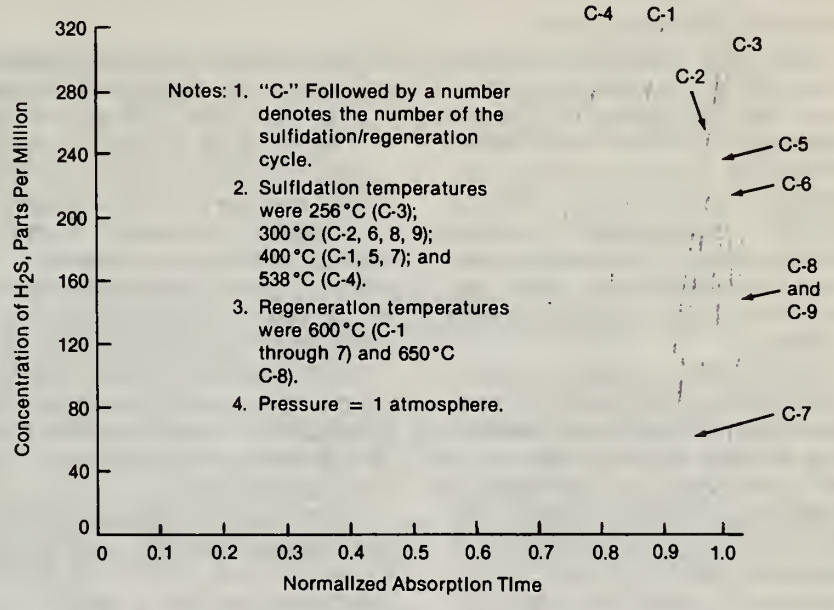

The **Concentration of H_2S** in the gas after passage through the zeolite/$CuO \cdot \frac{1}{3}MoO_3$ sorbent is much lower than the concentration (1 percent) in the entering gas. The normalized absorption time is defined as the time divided by the time that corresponds to the theoretical conversion of all of the CuO to Cu_2S.

This work was done by Gerald E. Voecks and Pramod K. Sharma of Caltech for **NASA's Jet Propulsion Laboratory**.

In accordance with Public Law 96-517, the contractor has elected to retain title to this invention. Inquiries concerning rights for its commercial use should be addressed to

Edward Ansell
Director of Patents and Licensing
Mail Stop 301-6
California Institute of Technology
1201 East California Boulevard
Pasadena, CA 91125

Refer to NPO-17099/TN

FOR ADDITIONAL INFORMATION: *Contact: Director, Technology Transfer Division, P.O. Box 8757, BWI Airport, MD 21240; (301) 621-0100 Ext. 241*

REFER TO THE NUMBER LISTED AT THE END OF THIS ARTICLE

NASA Tech Brief
National Aeronautics and
Space Administration

Theory of a Pyrotechnically Driven Device

Predictions and measurements of operation are presented.

A report presents relations that predict the behavior of a pyrolytically operated device. This mathematical analysis was motivated by the need to evaluate the performances of squib-driven release nuts. The analysis takes into account the most significant of the complicated interrelated processes involved in the operation of pyrotechnically driven devices and as such can aid in their design and in the evaluation of test data.

The gas mixture generated by the pyrotechnic squib is assumed to obey the ideal-gas law, from which a differential equation for the pressure is derived. The rate at which high-pressure gas is generated is assumed to be governed by a reaction-rate model, while the rate of condensation of condensable material is attributed to diffusion to the wall, governed by a simple diffusion-rate model.

The heat load of the wall is a function of heat transfer from the gas, as determined by the temperature difference between the gas and the wall, the exposed wall area, and the heat transfer coefficient of the gas mixture, as well as by radiation from the combustion products. The rate of thermal energy release by the pyrolytic gas generator is taken as the product of the heat of reaction and the rate of reaction. The change of pressure due to the work done on the piston is assumed to be that of an expanding ideal gas. Equations are also introduced to express the rate of change of volume as a function of the speed and the acceleration of the piston, as determined by the pressure, the friction forces, and the inertia of the piston.

All of these relations are combined for the numerical solution, enabling the evaluation of any or all of the physical parameters that affect the operation of the pyrotechnically driven device. These include the rates of combustion, diffusion, and conduction of heat; the area of the combustion chamber; the characteristic diffusion length; the initial volume; the mass of the piston; the static and sliding frictional forces; the travel of the piston before and after release; the ambient temperature during operation; and the ambient temperature and humidity during assembly.

The analysis yields correlations among pressure, piston travel, piston speed, gas temperature, well temperature, and heat load on the wall, as a function of time. For test cases of two types, a locked piston and a piston allowed to travel its full distance, the computed and measured correlations between pressure versus time were in good agreement.

This work was done by Robert Richter of Caltech for **NASA's Jet Propulsion Laboratory.** *"Analysis of the Operation of a Squib Driven Release Nut."*
NPO-17117/TN

FOR ADDITIONAL INFORMATION: *Contact: Director, Technology Transfer Division, P.O. Box 8757, BWI Airport, MD 21240; (301) 621-0100 Ext. 241*
REFER TO THE NUMBER LISTED AT THE END OF THIS ARTICLE

Sandia National Laboratory

Impedance Probe 'Fine-Tunes' Electroplating Solutions

Chemical bath solutions used for electroplating can be "fine-tuned" by using an electronic instrument developed by materials specialists at Sandia National Laboratories, Livermore, California. The same technique could be applied for process control in the manufacture of printed circuit boards.

The new instrument, named the tuned frequency impedance probe, was developed to improve process monitoring and control by ensuring that chemical baths maintain proper amounts of organic additives. Working prototypes of the probe have been built, tested, and used successfully for an electroplating application, but the technology has not yet been transferred for commercial development.

Commercial organic additives are often put into the chemical plating solution to tailor the surface finish and certain mechanical properties of electro deposits, such as brightness, grain size, and throwing power (improved metal distribution over complicated geometric areas). The concentration of the additives needs to be controlled as the plating/manufacturing process proceeds, or product quality can vary and suffer.

During electroplating, the additives are slowly depleted as they are incorporated into electrodeposits, decomposed at the electrodes, absorbed by filters, or otherwise lost. The difficulty of maintaining the additives in the right amounts and adding them at the right times is considerably eased through use of the new probe, since it will continuously monitor the additive concentration.

Former Sandian Joseph C. Farmer (now at Lawrence Livermore National Laboratory) is co-developer of the probe with William D. Bonivert and John T. Hachman, both of Sandia's Joining and Physical Metallurgy Division. Farmer explains its value: "The organic additives in plating baths are present in such small concentrations that is has been very difficult - sometimes impossible - to measure them. It was really an inexact science, almost witchcraft. It became clear several years ago that the physical properties of electrodeposits could be correlated with quality of the bath chemistry. It was obvious that we needed an instrument that could monitor the chemistry closely and continuously."

The Sandia prototype has three wire electrodes. Two of them, the working electrode and the counter electrode, are made from platinum or gold. The third, the reference electrode, is made from the metal that is being deposited (the prototype was copper).

The electrodes can be incorporated in a flow-through electrochemical cell or in a submersible wand. Wires lead from each electrode to a small electronic box that generates two types of wave forms. As the wave forms are generated, the instrument measures the phase shift between the voltage and the current.

"This phase shift is a very sensitive measure of the concentration of organic species on the probe surface," explains Bonivert. "As the organic level goes up and down in the bath, so does the phase shift, and the instrument is designed to put out a voltage that is proportional to the shift."

Sandia expects that a U.S. patent will be issued for the probe soon. Sandia is negotiating with an electronics firm that may license the patent and manufacture the probes for commercial sale.

FOR ADDITIONAL INFORMATION: Public Information Division, Code 3161, Department of Energy, Sandia National Laboratories, Albuquerque, NM 87185-5800; (505) 844-4207. Refer to announcement 24, No. 4.

Technology Application

Sandia National Laboratory

Piezoelectric Polymer Forms Inexpensive Accelerometer

Sandia National Laboratories has completed work on a low-cost accelerometer that can measure and survive changes in velocity generating forces hundreds of thousands of times greater than the force of gravity.

The instrument has been under development since the early 1980s, primarily for use in anti-ship missiles. The accelerometer is extremely sensitive and could be manufactured for $10 or less. Sandia researchers say the device is operational over a wide temperature range, and the design could be modified to meet a variety of applications.

The heart of the accelerometer is a piezoelectric polymer material that generates electrical energy in response to changes in mechanical forces. Sandia developers used an extremely thin film of polyvinylidene fluoride (PVF-2) that had been specially treated to become piezoelectric. Piezoelectric materials generate a current when a mechanical force is applied to them.

The accelerometer is generally installed inside the head of a bolt that has been machined to contain a circular well. The PVF film is cemented to the bottom of the cavity. A weight mass of tungsten carbide is glued to the top of the film. The mass is capped with a special microcircuit that amplifies any charge generated by the film.

A very simple device

In many applications, the tungsten carbide mass can be omitted. In some specific cases, the microcircuit itself can be omitted. In these cases, the PVF-2 would provide sufficient mass and/or signal output to perform the desired function.

In operation, changes in velocity cause the weight mass to squeeze or stretch the piezoelectric film. The film responds by generating voltage, which is picked up and amplified by the microcircuit so the signature of the signal can be analyzed.

"It's a very simple device," said George R. Laguna, acting supervisor of Sandia's Sensor Components Division. "We wanted to make this for five bucks."

The Sandia accelerometer was originally developed to help anti-ship missiles distinguish between the shock of being hit by anti-aircraft fire directed by fast-firing shipboard guns from that of contact with the intended target. Laguna said he believes the characteristic of the signal produced by the accelerometer—both amplitude and timing profile—will make missiles "smart" enough to discriminate between bullets and bulkheads.

Currently no similar device is available for missile applications, Laguna said. Because the design can easily be modified, the accelerometer developed at Sandia might have other applications.

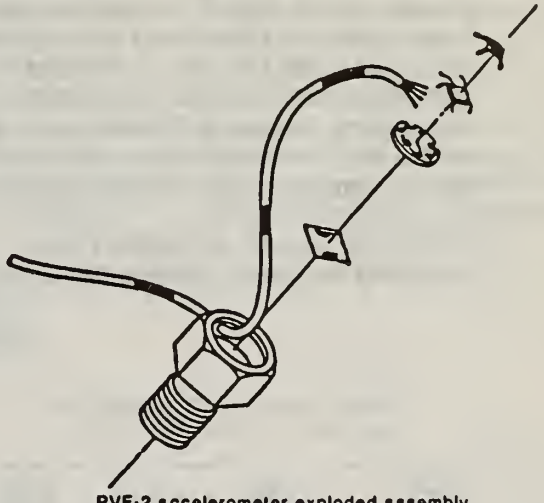

PVF-2 accelerometer exploded assembly.

For example, by changing the type of weight mass, the maximum output of the device could be tailored to specific G (gravity) forces. One idea discussed for the device is using it in automotive airbag systems to help the car distinguish between a collision and a bump in the parking lot.

Not yet in production, the accelerometer has been tested over a range of conditions and is now ready for its primary and secondary uses. The device was developed with funding from a Department of Defense program.

(Elsewhere at Sandia, other scientists are testing PVF-2 materials, that require even more sensitivity in shock stress research. A newly perfected piezoelectric shock sensor, developed in France, has expanded the range of shock stress measurements, they report. The sensor permits study of more intense and shorter duration shock events than previous sensors.) □

FOR ADDITIONAL INFORMATION

Public Information Division,
Code 3161,
Department of Energy,
Sandia National Laboratories,
Albuquerque, NM 87185-5800
(505) 844-4207
Refer to announcement 24, No. 3

NIST Technology Update

National Institute of Standards & Technology
(Formerly the National Bureau of Standards)
U.S. Department of Commerce, Gaithersburg, MD 20899

Measuring High-Temperature Superconductors

NIST researchers have developed a novel apparatus for variable-temperature measurements of high-temperature superconductors. Termed a cryogenic bathysphere, it can rapidly (in 10 minutes) test superconductors over a range of temperatures from 300 to 4 K, or it can be used to stabilize the temperature at a given value. The tiny (three-centimeter-width) device has no moving parts and can be used in compact spaces such as shipping Dewars and small-bore high-field magnets. The apparatus has been tested successfully in liquid helium and liquid nitrogen by measuring the resistance-versus-temperature curves of several superconductors.

FOR ADDITIONAL INFORMATION: A paper describing a prototype device is available from Fred McGehan, Division 360.2, NIST, Boulder, Colo. 80303.

NASA Tech Brief
National Aeronautics and Space Administration

Licensing Opportunity

Marshall Space Flight Center, Alabama

Eight-Channel Spectrometer

Photodetector signals are multiplexed for digitization and recording.

An inexpensive, compact, battery-powered, eight-channel spectrometer (see figure) produces 8-bit digital data in each channel and records the data for subsequent reconstruction in analog form or for transmission to a computer for analysis. The unit is designed for use in the analysis of rocket-exhaust plumes. Modified versions of the spectrometer could be used to analyze combustion in boilers or gas turbines.

The photodetector for each channel is a silicon positive/intrinsic/negative diode operating in the photovoltaic mode. The wavelength range is 185 to 1,150 nm. A lens and a filter of ~10-nm bandwidth at the spectral line of interest are placed in front of each detector. The outputs of the detectors are fed through a multiplexer, which connects each one in turn (at a rate of 10 samples per second) to an electrometer operational amplifier. Each detector is also permanently connected to a feedback resistor and rolloff capacitors so that the output of each can be adjusted and scaled to obtain a nearly-flat spectral response over the wavelength range of interest, with maximum dynamic range.

To obtain net spectral data, the background spectrum is subtracted. Background readings taken previously in the absence of the plume or flame to be analyzed are reconstructed for each channel by a digital-to-analog converter and fed to the noninverting input terminal of a comparator, while the electrometer-amplifier output is fed to the inverting input terminal of the comparator. The output of the comparator, which is the net spectral reading in

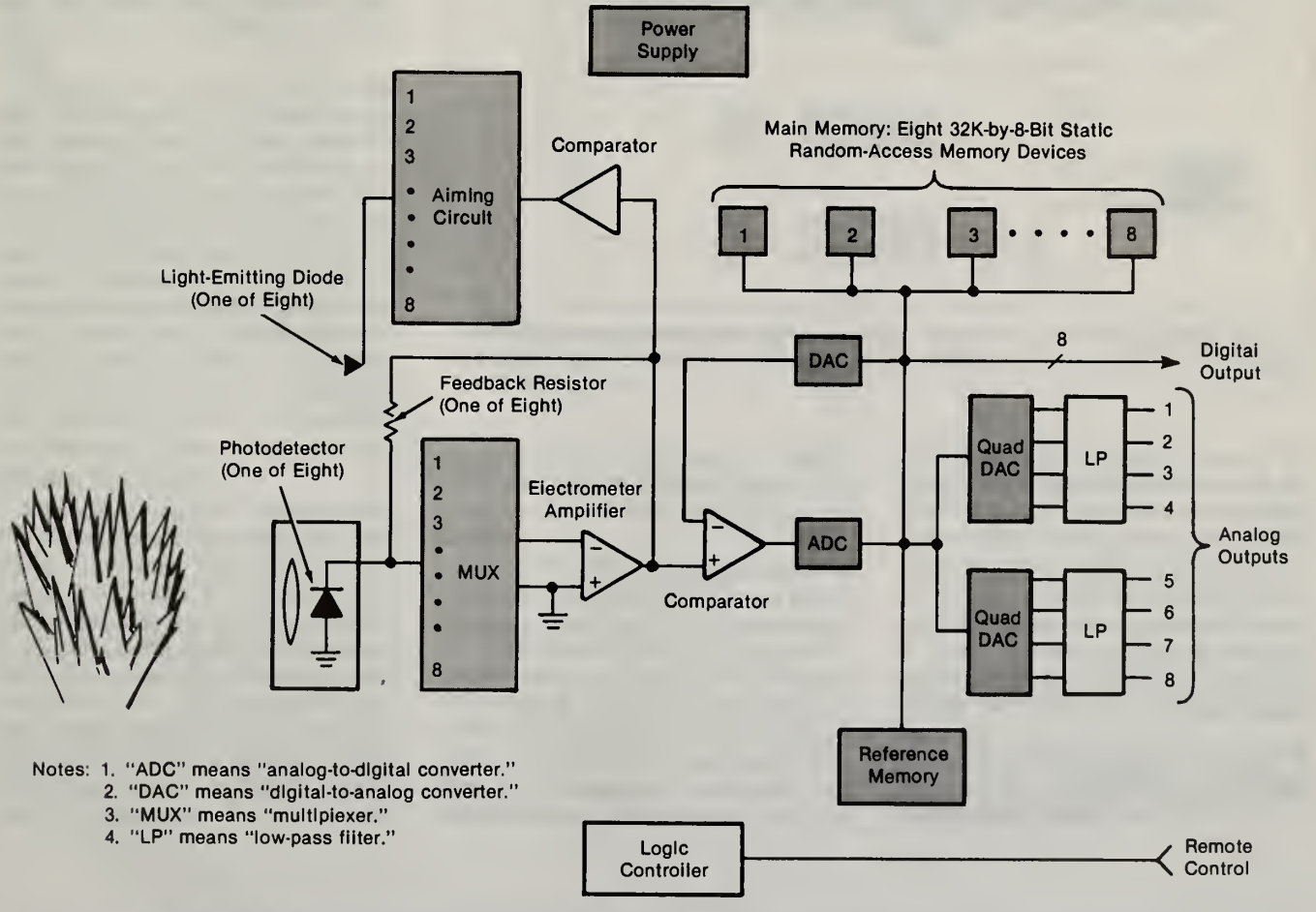

Notes: 1. "ADC" means "analog-to-digital converter."
2. "DAC" means "digital-to-analog converter."
3. "MUX" means "multiplexer."
4. "LP" means "low-pass filter."

The **Eight-Channel Spectrometer** digitizes and stores spectral readings during a test as long as 27 minutes. The recorded spectrum as a function of time can be read out digitally or "played back" in analog form.

one channel, is digitized. The readings from each channel are stored in the main memory in a static random-access-memory device devoted to that channel. The memory holds 27 minutes' worth of spectral readings.

An aiming circuit is used to align the spectrometer with a lamp or other artificial source of light placed temporarily at the test position. This circuit converts the reading in each channel to the output of one of eight light-emitting diodes. When the spectrometer is aligned, these diodes light up with equal brightness.

For analog output or playback of data, the digital data from the main memory are fed through two quad digital-to-analog converters, each of which reconstructs the readings in four channels. The output in each channel can be used to drive a strip-chart recorder or other display or recording device.

This work was done by Steven W. Huston and Milton C. Hensley of Rockwell International Corp. for **Marshall Space Flight Center**.

Inquiries concerning rights for the commercial use of this invention should be addressed to the Patent Counsel, Marshall Space Flight Center Refer to MFS-29421/TN

FOR ADDITIONAL INFORMATION: *Contact: Director, Technology Transfer Division, P.O. Box 8757, BWI Airport, MD 21240; (301) 621-0100 Ext. 241*

REFER TO THE NUMBER LISTED AT THE END OF THIS ARTICLE

NASA Tech Brief
National Aeronautics and Space Administration
Marshall Space Flight Center, Alabama

Delay-Line Anode for Microchannel-Plate Spectrometer

A zigzag pattern enables the location of incident pulses in two dimensions.

A developmental photon-counting readout system for a microchannel-plate spectrometer includes a delay line and timing circuit to measure the wavelength coordinate and a wedge/wedge charge-division system to measure the orthogonal spatial coordinate. The charge-sensing element of this system is a planar anode made of strip-line material featuring a zigzag electrode pattern on the front face and a ground plane on the rear face. This system should prove advantageous for portable two-dimensional spectrometers that have large image planes and for which the design requirements include simplicity, reliability, low power consumption, and low mass.

The anode plane is placed near and parallel to the rear plane of the microchannel-plate detector. When a photon strikes the front plane of the detector, electrons are emitted from the rear plane, and they travel to the adjacent areas on the anode. Because the voltage and current pulses caused by the deposition of the electron charges travel along the zigzag anode strip line at known speed, the difference between the times of arrival of the pulses at the two ends of the line can be used to find the *x* coordinate of point of impingement. The difference in time is measured by a start/stop time counter.

The width of the bunch of electrons from one photon is several times the pitch of the zigzag. To ensure that about half the charge is deposited on the delay line, the width of the delay line is made one-quarter of the pitch of the zigzag. The remaining half of the charge falls on the interdigitating wedge electrodes; the portion that falls on each wedge depends on the width of the wedge at the point of impingement, which varies linearly with the *y* coordinate of the point of impingement. Thus, the *y* coordinate of the photon can be determined by circuits that measure the ratio between the charges deposited on the wedge electrodes.

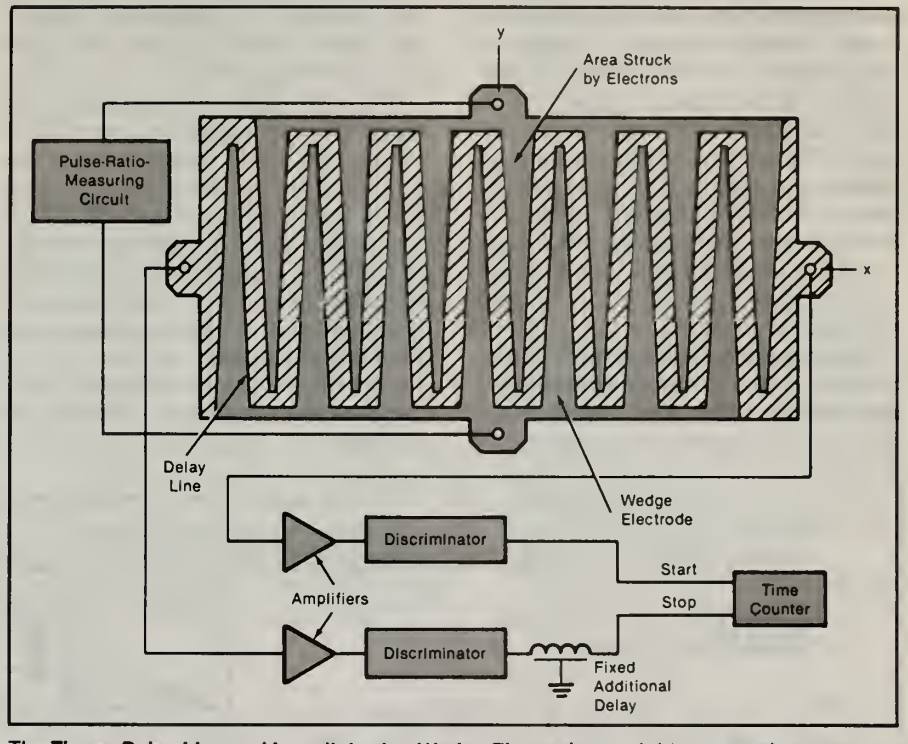

The Zigzag Delay-Line and Interdigitating Wedge Electrodes are laid out together on an anode plane. Time- and charge-ratio-measuring circuits determine the location of an impinging bunch of electrons.

When the system is fully developed, the time- and ratio-measuring circuits should be able to determine the *x,y* coordinates of the centroid of impinging charge with a spatial resolution much finer than the pitch of the zigzag. A design that achieves such performance will have to take into account such considerations as matching of strip-line output impedances, attenuation and dispersion of pulses in the delay line, interactions between the delay line and the wedge electrodes, timing errors due to rise times of pulses, thermal noise, shot noise, and spurious signals at the fundamental frequency of the zigzag. In an experimental version that included a zigzag of 1-mm pitch, illumination with ultraviolet light through a 25-μm pinhole produced a Gaussian distribution in the *x* coordinate of detected photon events with 70 μm full width at half maximum.

This work was done by M. Lampton of the University of California for **Marshall Space Flight Center**. *MFS-26073/TN*

FOR ADDITIONAL INFORMATION: *Contact: Director, Technology Transfer Division, P.O. Box 8757, BWI Airport, MD 21240; (301) 621-0100 Ext. 241*
REFER TO THE NUMBER LISTED AT THE END OF THIS ARTICLE

NASA Tech Brief
National Aeronautics and Space Administration
NASA's Jet Propulsion Laboratory, Pasadena, California

Licensing Opportunity

Electron/Ion-Scattering Apparatus

Electron and ion beams are merged, then separated for analysis.

An apparatus measures cross sections and energies for inelastic scattering of low-energy electrons from positive or negative ions. Previous scattering techniques have involved angle-by-angle sequences of measurements in which only about 1 percent of the scattered electrons could be measured at each setting. In the new apparatus, most of the electrons scattered inelastically over a wide range of angles are measured simultaneously, with a consequent increase in the signal-to-noise ratio by a factor of about 10^4.

As shown in the figure, a beam of electrons and a beam of ions are aimed along a low-intensity magnetic field between a pair of electric-field plates. The crossed electric and magnetic fields hardly affect the ions but cause the electrons to drift toward the ions by trochoidal motion.

The uniform magnetic field causes the beams to remain merged in a region about 20 cm long, where they interact. At the other end of the interaction region, the beams are separated by a second set of electric-field plates. The drift angles of the electrons (or, equivalently, the positions at which the electrons strike a detector plane) depend in part on the energies left after the inelastic collisions with the ions.

Two sets of microchannel-plate, position-sensitive detectors are used to measure the electron scattering signal as a function of position (or energy loss). One set, in the forward direction, measures the signal from electrons scattered in the forward direction (scattering angles from 0° to 90°); while the second set, in the backward direction, measures the electron signals from scattering in the angular range from 90° to 180°. The scattering cross section as a function of the electron energy loss is then obtained, in part, from the incident electron and ion-beam currents and the scattered currents as measured by signals at the forward and back microchannel plates.

Rotatable vanes containing small holes are used to measure the overlap of the electron and ion beams in four planes, yielding an approximate three-dimensional representation of the degree of overlap. With modifications, the apparatus can also be used for measurements of excitation cross sections in neutral atoms, molecules, radicals, and excited states of atoms and molecules.

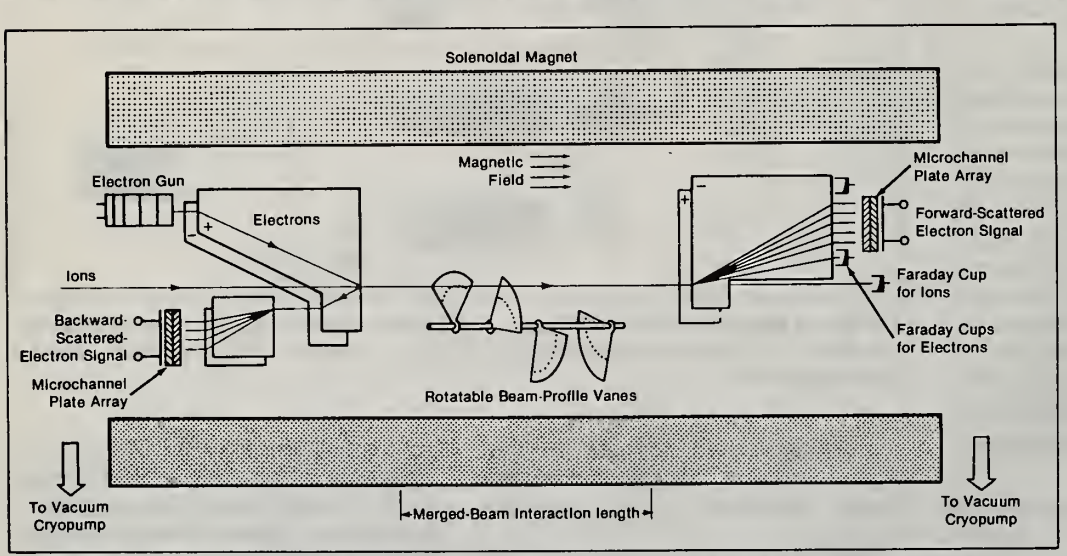

This **Merged-Beam, Trochoidal-Analysis** apparatus measures cross sections for inelastic scattering of electrons by ions.

Jet Propulsion Lab.
NASA Resident Office
Technology Utilization Officer: Gordon S. Chapman
Mail Stop 180-801
4800 Oak Grove Drive
Pasadena, CA 91109
(818) 354-4849
Patent Counsel: Paul F. McCaul
Mail Code 180-801
4800 Oak Grove Drive
Pasadena, CA 91109
(818) 354-2734
Technology Utilization Mgr. for JPL: Norman L. Chalfin
Mail Stop 156-211
4800 Oak Grove Drive
Pasadena, CA 91109
(818) 354-2240

This work was done by Ara Chutjian of Caltech for **NASA's Jet Propulsion Laboratory.**

This invention is owned by NASA, and a patent application has been filed. Inquiries concerning nonexclusive or exclusive license for its commercial development should be addressed to the Patent Counsel, NASA Resident Office-JPL Refer to NPO-16789/TN

FOR ADDITIONAL INFORMATION: *Contact: Director, Technology Transfer Division, P.O. Box 8757, BWI Airport, MD 21240; (301) 621-0100 Ext. 241*
REFER TO THE NUMBER LISTED AT THE END OF THIS ARTICLE

NASA Tech Brief
National Aeronautics and Space Administration
Lewis Research Center, Cleveland, Ohio

Keyboard Emulation for Computerized Instrumentation

Experimental parameters can be retrieved or re-entered at will.

Most new scientific instruments contain microprocessor controllers. While such instruments are exceptionally versatile and simple to operate as stand-alone devices, they are often difficult to modify for incorporation into hierarchical systems with general-purpose laboratory minicomputers or microcomputers. If a communication port is included in the instrument, it often does not provide the same degree of flexibility as that of manual operation.

There are many options for making interfaces with such instruments, depending on the intelligence level at which communication takes place. A keyboard emulator has an interface at the same level as that of manual keyboard entry. Since communication and control take place at the high intelligence level in the instrument, all the instrument circuitry is fully utilized. Little knowledge of the instrument circuitry is necessary, since the only task the interface performs is key closure. All existing logic and error checking is still performed by the instrument, minimizing the workload of the laboratory microcomputer. Timing constraints for interface operation are minimal at the keyboard entry level.

A keyboard emulator interface increases the capabilities of the instrument in three ways. First, the system now has the ability to store permanently a large number of experimental parameters, which can be retrieved and re-entered at will. Second, the clock in the instrument can be synchronized with the clock in the laboratory computer, so that the entire experiment occurs during the same reference time frame. Finally, communication feedback loops can be established, and experimental parameters can be automatically adjusted in response to the measurements.

Designing a keyboard emulator interface for an instrument with discrete switches could be very difficult. However, the advent of transistor/transistor logic (TTL)-based microprocessor-controlled instrumentation has spawned keypad arrays as convenient, efficient means of entering parameters. These arrays can encode a large number of keys using only eight bits of code. It is fairly simple to build a keypad emulator to simulate a keystroke in one of these arrays. The keyboard emulator interface allows the pulse to travel an alternate pathway that mimics the keystroke. An 8-bit parallel input/output port is sufficient for operation.

Using this approach, a microprocessor-based high-performance liquid chromatography (HPLC) solvent-delivery system was connected to a laboratory microcomputer. The computer synchronized and sequenced the entire HPLC experiment, including solvent delivery, valve control for column switching and backflushing, data acquisition, and data processing.

This work was done by P. M. Wiegand and S. R. Crouch of Michigan State University for **Lewis Research Center**.
LEW-14180/TN

FOR ADDITIONAL INFORMATION: *Contact: Director, Technology Transfer Division, P.O. Box 8757, BWI Airport, MD 21240; (301) 621-0100 Ext. 241*
REFER TO THE NUMBER LISTED AT THE END OF THIS ARTICLE

NASA Tech Brief
National Aeronautics and Space Administration
NASA's Jet Propulsion Laboratory, Pasadena, California

Measurement of Molecular Mobilities of Polymers

Time-resolved electron-spin resonance (ESR) offers 667 times the sensitivity of conventional ESR.

A new molecular-probe technique is used to measure the molecular mobility of a polymer. The method is based on the use of time-resolved electron-spin resonance (ESR) spectroscopy to monitor the decay of transient nutation amplitudes from photoexcited triplet states of probe molecules with which the polymer is doped. The higher the molecular mobility of the polymer matrix, the faster the nutation amplitudes of the probe molecules decay.

It has been hypothesized that in polymer matrices, microscopic molecular mobilities are directly related to macroscopic mechanical properties. For example, the aging processes of polymers, which include cross-linking between polymer chains caused by ultraviolet radiation and the collapse of free volumes by isothermal relaxation processes, reduce molecular mobilities.

In the new technique, the probe molecules are first excited to their singlet states by a 5-ns laser pulse. Their manifold of triplet states then becomes populated through intersystem crossing, but, because of selection rules, only one or two of the triplet levels are populated, resulting in spin polarization. Because the triplet spins are created in a relatively short time, they have a high degree of coherence immediately following the laser pulse.

As time goes on, relaxation processes cause the coherence of the spins to decrease. One important relaxation process is the motion of the probe molecules caused by interaction with the surrounding polymer matrix. The higher the molecular mobility of the polymer, the faster the coherence and the related transient nutation amplitudes decrease. The transient nutation amplitude is a measure of the evolution of the ensemble average of the magnetic moment of the coherent spins.

By detecting the photoexcited states of the probe molecules, the time-resolved ESR technique achieves much higher sensitivity than the conventional ESR method, which detects the small population differences that exist under Boltzmann equilibrium conditions. The fractional population difference immediately after population of the triplet state is nearly 1.0, whereas the Boltzmann equilibrium value at room temperature is approximately 0.0015. Thus, the sensitivity of the time-resolved detection method is approximately $1.0/0.0015 \approx 667$ times that of the conventional method.

With phenazine as the probe, the new technique has been used to measure the differences in the molecular mobilities of polymethylmethacrylate samples of different average molecular weights. The differences in mobilities were correlated with the glass-transition temperatures of the samples.

This work was done by Soon Sam Kim and Fun-Dow Tsay of Caltech for **NASA's Jet Propulsion Laboratory**. *NPO-17216/TN*

FOR ADDITIONAL INFORMATION: *Contact: Director, Technology Transfer Division, P.O. Box 8757, BWI Airport, MD 21240; (301) 621-0100 Ext. 241*
REFER TO THE NUMBER LISTED AT THE END OF THIS ARTICLE

NASA Tech Brief
National Aeronautics and Space Administration
Langley Research Center, Hampton, Virginia

Modified Technique for Chemisorption Measurements

A greater number of smaller adsorbate volumes yields more-accurate measurements.

It is frequently desirable to measure the amount of a particular gas, or adsorbate, that will chemisorb, or adsorb with chemical bonding, on a sample of some solid material. Usually, a known volume of adsorbate gas is passed through the sample to be tested, and the amount of this gas that leaves the sample is measured. Although pure adsorbate gas may be used, the adsorbate is often contained in an inert carrier like helium. When the concentration of adsorbate gas leaving the sample is very nearly equal to its initial concentration, the measurement is terminated. The amount of adsorbate chemisorbed is measured as the total amount put into the sample minus the total amount that leaves the sample. The size of the adsorbate sample volume is usually selected so that only a few samples are required to complete this measurement.

In measurements of the chemisorption of CO on a Pt/SnO_2 catalyst it has been observed that if small numbers of relatively large volumes of adsorbate gas are passed through the sample, very little removal of CO is detected. Therefore, it appears in these cases as if little or no CO has been chemisorbed on Pt/SnO_2.

However, if much smaller volumes of adsorbate gas are used, the small amount of CO that is removed is readily detected, and chemisorption can be seen clearly to have occurred. If the catalyst sample is exposed to repeated injections of adsorbate (e.g., 50 or more times), the cumulative removal of CO is found to be significant. Thus, it was found possible to measure quantitatively the chemisorption of CO on Pt/SnO_2 by means of a large number of small injections of CO, whereas the traditional use of a few fairly large volumes of gas erroneously indicated that little or no chemisorption had occurred.

This technique of using a large number of small volumes of adsorbate gas to measure chemisorption should be applicable to many gas/material combinations other than CO on Pt/SnO_2. The volume used should be chosen so that at least 10 percent of the adsorbate gas is removed during each exposure.

This work was done by David R. Schryer of **Langley Research Center** *and Kenneth G. Brown and Jacqueline Schryer of Old Dominion Research Foundation. No further documentation is available.*
LAR-13725/TN

FOR ADDITIONAL INFORMATION: *Contact: Director, Technology Transfer Division, P.O. Box 8757, BWI Airport, MD 21240; (301) 621-0100 Ext. 241*
REFER TO THE NUMBER LISTED AT THE END OF THIS ARTICLE

Transportation & Components

0815 Tire Footprint Affects Hydroplaning on Wet Pavement—Higher aspect ratio of the tire footprint requires slower speed for safer driving on wet roads.

0816 Low-Cost Vertical Accelerometer for Aircraft—Self-aligning feature eliminates the need for costly attitude-rate sensors.

Software

0817 Computing Flutter Boundaries—This program calculates aeroelastic responses of mistuned airfoils.

Testing & Instrumentation

0818 Using EMATs For Rail Car Wheel Inspection

Other Items of Interest

0750 Filmless X-Ray Inspection Methods—Speeds Aircraft Inspection Onboard Carriers

0755 Flight Balance for Skin-Friction Measurements—The force of a tangential airstream is determined by a null-position servomechanism. (Licensing Opportunity)

NASA Tech Brief
National Aeronautics and Space Administration
Langley Research Center, Hampton, Virginia

Tire Footprint Affects Hydroplaning on Wet Pavement

Higher aspect ratio of the tire footprint requires slower speed for safer driving on wet roads.

Recent investigations of tire hydroplaning at highway speeds reveal that, in addition to the inflation pressure, the tire-footprint aspect ratio (FAR), defined as the width divided by the length of the tire surface in contact with the pavement, significantly influences the speed at which dynamic hydroplaning begins. Various tire tests were conducted on flooded surfaces through a range of speeds, inflation pressures, and vertical loads using tires mounted on the instrumented tire-testing vehicle shown in the figure. Tests were conducted at constant speeds on ASTM E-501 grooved and E-524 smooth automotive tires. A com-

INSTRUMENTED TIRE-TESTING VEHICLE

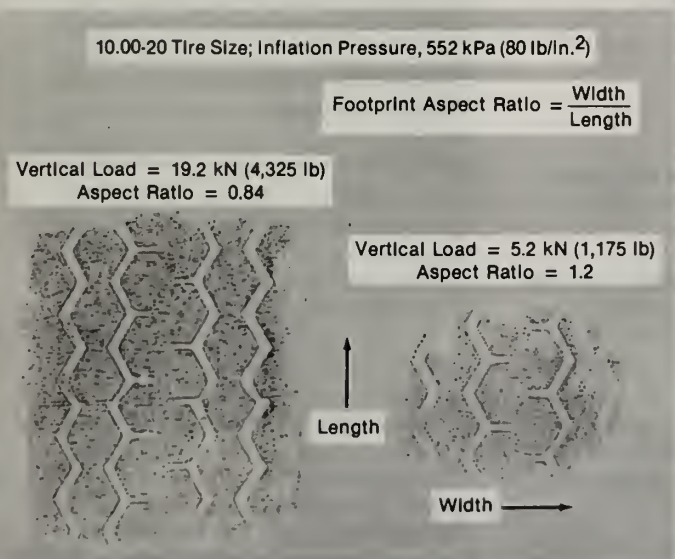
10.00-20 Tire Size; Inflation Pressure, 552 kPa (80 lb/in.^{2})
Footprint Aspect Ratio = Width / Length
Vertical Load = 19.2 kN (4,325 lb)
Aspect Ratio = 0.84
Vertical Load = 5.2 kN (1,175 lb)
Aspect Ratio = 1.2
Length
Width

TRUCK-TIRE FOOTPRINTS

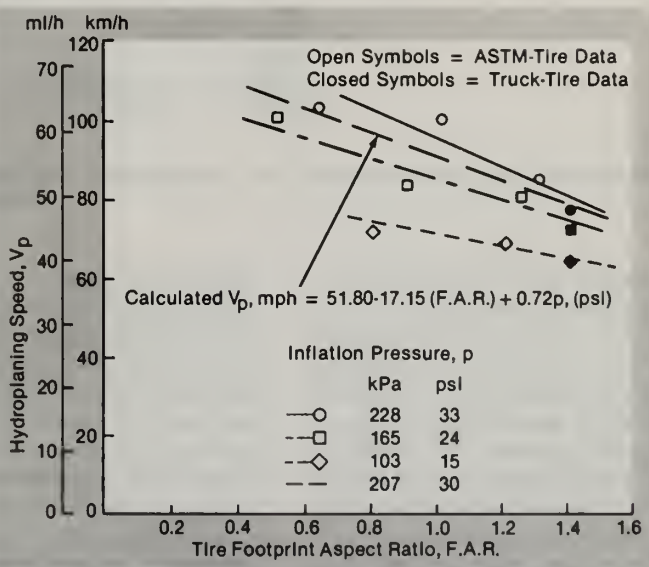

VARIATION OF TIRE-HYDROPLANING SPEED WITH FOOTPRINT ASPECT RATIO

HIGHWAY-VEHICLE TIRE-HYDROPLANING-SPEED STUDY

Automotive-Tire-Footprint Aspect Ratio is a significant factor in the hydroplaning of the tire, as indicated by the results of tests on a highway vehicle.

bination of different tire-inflation pressures and vertical loads produced a large range of FAR's for evaluation under free and yawed rolling-test conditions. Tire speeds and forces developed during the tests of up to 65 mi/h (105 km/h) were monitored on the flooded test surface to identify the development of hydroplaning.

The study was focused on automotive tires because the FAR's of automotive tires vary more than those of aircraft tires. Although footprint widths of automotive tires remain nearly constant, their lengths, and therefore the FAR's, vary significantly under different loading conditions — the greater the load, the smaller the FAR. Footprints of aircraft tires vary with the loading in both dimensions, resulting in a relatively small range of FAR's.

An empirical equation has been formulated to predict highway speeds at which hydroplaning begins for different FAR's. The equation reveals that hydroplaning begins at lower speeds with increasing FAR's, whereas previous studies indicated that hydroplaning was solely a function of tire-inflation pressure. During wet weather, therefore, drivers of lightly loaded vehicles are riding on increased FAR's and should be particularly alert to prevent hydroplaning at lower speeds.

Additional tests are planned to refine and substantiate further the dependence of the hydroplaning of tires upon the FAR's. These tests will evaluate an expanded range of the FAR's and enable the assessment of such other parameters as the net bearing pressure and the construction of the tire on the tire-hydroplaning-initiation speed.

This work was done by Thomas J. Yager of **Langley Research Center**. *For further information, Circle 69 on the TSP Request Card.*
LAR-13683

FOR ADDITIONAL INFORMATION: *Contact: Director, Technology Transfer Division, P.O. Box 8757, BWI Airport, MD 21240; (301) 621-0100 Ext. 241*
REFER TO THE NUMBER LISTED AT THE END OF THIS ARTICLE

NASA Tech Brief
National Aeronautics and Space Administration
Ames Research Center, Moffett Field, California

Low-Cost Vertical Accelerometer for Aircraft

Self-aligning feature eliminates the need for costly attitude-rate sensors.

A proposed self-aligning device would measure the vertical acceleration of an aircraft but would cost only a small fraction of the price of a full inertial navigation system. In essence, the device would consist of an accelerometer mounted vertically on the inner gimbal of an artificial horizon.

Such a vertical accelerometer could prove to be an effective aid to Global Positioning System (GPS) navigation receivers in general-aviation aircraft and helicopters. GPS receivers tend to be least accurate in the vertical direction, whereas the accuracy requirements for aircraft approach and landing are most stringent in the vertical direction. The low-cost vertical accelerometer could be used to improve on the vertical accuracy and the reliability of the GPS receiver alone. The vertical accelerometer could also be used to improve the altitude accuracy for aircraft that would otherwise be equipped with only a baro-altimeter for altitude measurement.

Commercial and military aircraft will soon use navigation systems that combine a GPS receiver with a full inertial navigation system (INS). The heart of an INS is the inertial measurement unit (IMU), an expensive, high-precision electromechanical device that tracks the attitude and trajectory of the aircraft. An IMU requires high-speed mechanical gyroscopes in nearly-perfect mechanical balance or, alternatively, sophisticated ring-laser or fiber-optic attitude-rate sensors. The IMU has stringent performance requirements because it provides all three components of the acceleration of the aircraft. However, the two horizontal components are substantially more difficult to determine accurately than is the vertical component because the errors affecting them are much sensitive to misalignment of the IMU in the gravitational field. The proposed vertical accelerometer is intended for low-cost applications in which the vertical component alone will suffice.

An artificial horizon is a low-cost vertical-reference device in common use on general-aviation aircraft for indicating to the pilot the attitude of the aircraft. It consists of a two-degree-of-freedom gyroscope with a small mass imbalance on the spin axis (see figure). The mass imbalance acts as a pendulum to keep the gyroscope aligned with the local vertical during steady flight, while the gyroscope inhibits the pendulum from swinging during horizontal aircraft acceleration. The accelerometer, which would be mounted to the inner gimbal of the gyroscope, would be designed as an integral part of the mass distribution of the gyroscope assembly. Any type of accelerometer may be used, consistent with the cost, packaging, and performance requirements of the particular application.

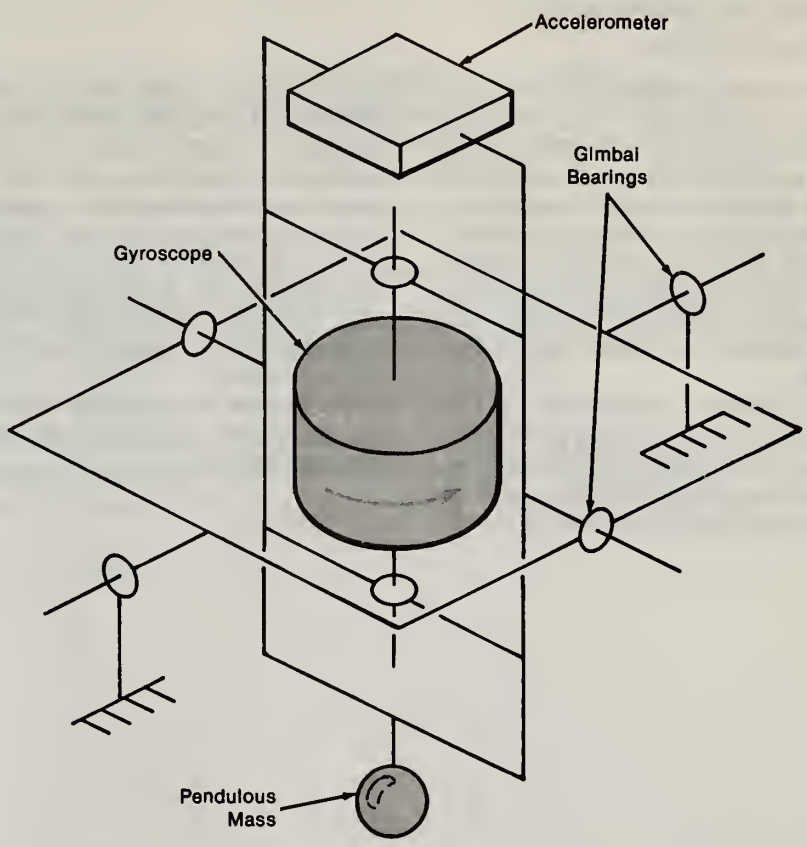

A Pendulous Mass and a Gyroscope in an artificial horizon tend to align an accelerometer in the vertical direction.

The magnitude of the mass imbalance of the gyroscope inner gimbal involves a tradeoff between steady-state accuracy and transient performance. It must be large enough to counteract disturbances reasonably quickly but not so large that it is unduly disturbed by horizontal acceleration. This applies to any artificial horizon but is of greater concern with the vertical accelerometer attached. An interesting approach, which may or may not prove to be worthwhile in practice, involves using the GPS measurements (if available) to compensate for the misalignment of the vertical accelerometer during and shortly after a horizontal acceleration maneuver. If the key parameters of the artificial horizon assembly are known, the deviation from vertical may be modeled as a function of the vehicle acceleration time history, as determined by the GPS system, and then compensated for in software.

This work was done by Russell A. Paielli of **Ames Research Center**.
ARC-11870/TN

FOR ADDITIONAL INFORMATION: *Contact: Director, Technology Transfer Division, P.O. Box 8757, BWI Airport, MD 21240; (301) 621-0100 Ext. 241*
REFER TO THE NUMBER LISTED AT THE END OF THIS ARTICLE

Computing Flutter Boundaries

This program calculates aeroelastic responses of mistuned airfoils.

The MISER2 computer program calculates the flutter boundaries and aeroelastic response of a cascade of arbitrarily mistuned airfoils. This program is based on a typical section formulation incorporating incompressible, subsonic and supersonic cascade, unsteady aerodynamic theories. Each blade is modeled as a two-degree-of-freedom oscillator that has inertial coupling between the bending and torsional motions.

It is possible to consider any type of mistuning; for example, blade-to-blade variations of the uncoupled bending and torsional frequencies of the blade, damping ratios, mass ratios, elastic axes, and positions of centers of gravity. Both the tuned and mistuned, uncoupled bending and torsion cases, in addition to the tuned, coupled bending and torsion case, can be treated as special cases of this program.

This program now operates on the NASA Lewis Research Center IBM 370/333 computer with time-sharing system (TSS). The source code is written in FORTRAN 4. Subroutine calls are made to the IMSL package.

This program was written by Robert E. Kielb and Krishna Rao V. Kaza of **Lewis Research Center**.

LEW-14380/TN

FOR ADDITIONAL INFORMATION

CONTACT:
COSMIC®
112 Barrow Hall
University of Georgia
Athens, GA 30602
(404) 542-3265

NIST Technology Update

National Institute of Standards & Technology
(Formerly the National Bureau of Standards)
U.S. Department of Commerce, Gaithersburg, MD 20899

Using EMATs For Rail Car Wheel Inspection

For several years NIST, at the request of the Federal Railroad Administration, has studied ultrasonic detection of cracks in the treads and residual tensile stresses in the rims of steel railroad wheels. These defects are two main causes of wheel failure, with catastrophic consequences to personnel, rolling stock, tracks, and schedules. NIST's research program has concentrated on using electromagnetic-acoustic transducers (EMATs) for the nondestructive evaluation of wheels. These non-contact devices are more reliable and easier to automate than conventional transducers. Two instruments under development at NIST should be an improvement on the visual inspection methods now used, which have unacceptably high error rates. One instrument can detect cracks as the wheels roll by, enabling more frequent and thorough inspections than is now feasible; the second performs quantitative stress determination while the wheel remains on the axle.

FOR ADDITIONAL INFORMATION: A collection of seven papers published over the past 2 years, Report No. 18: Ultrasonic Railroad Wheel Inspection Using EMATS (NISTIR 88-3906), is available from the National Technical Information Service, Springfield VA 22161; (703)487-4600.

NTIS order number: PB 89-189229/NAC
Price code: A05

U.S. DEPARTMENT OF COMMERCE
National Technical Information Service
Springfield, VA 22161

NTIS ORDER FORM

Use this form ONLY to order reports designated as available from NTIS.

TELEPHONE ORDERS (703) 487-4650 FAX (Telecopier) (703) 321-8547 TELEX 89-9405

For Subscription Questions
(703) 487-4630

For Tracing an Order
(703) 487-4660

Editorial Questions
(703) 487-4805

Postage:
NTIS uses First Class Delivery, or equivalent service, on all shipping. For information about one day RUSH ordering, call (800) 336-4700 or (703) 487-4700.

NTIS PRICE SCHEDULE *

This schedule converts into actual prices the price codes cited in those Tech Notes having a report available from NTIS.

Microfiche	
A01	$6.95
Paper copy	
A02	10.95
A03	13.95
A04 through A05	15.95
A06 through A09	21.95
A10 through A13	28.95
A14 through A17	36.95
A18 through A21	42.95
A22 through A25	49.95
A99	Call for price

These prices are for customers in United States, Canada, and Mexico. Other addresses should write for the price listing, number PR-360-4.

Prices effective January 1, 1989

† Billing Service: There is a $7.50 charge for this service. It is restricted to customers in the United States, Canada, and Mexico. A late payment charge will be applied to all billings more than 30 days overdue.

If your address lable on this Tech Notes is NOT correct, call the NTIS Subscriptions Department on (703) 487-4630.

1 ADDRESS INFORMATION

Last Name .....

Title .....

Company/Organization .....

Address .....

.....

City/State/ZIP .....

Telephone Number .....

2 METHOD OF PAYMENT

☐ Charge my NTIS Deposit Account .... – .....

☐ Check/Money order enclosed payable to NTIS for $ .....

☐ Please bill **ADD $7.50 per order** (see below for restrictions)†

Purchase order number .....

Charge my ☐ American Express ☐ VISA ☐ MasterCard

Account Number. ..... Exp. .....

Signature .....
(Required to validate order)

3 ORDER SELECTION (Use only for reports stated as available from NTIS)

NTIS Order Number	*Price**	*Quantity*	*Total Price*
...../NAC	.....	.....	.....
...../NAC	.....	.....	.....
...../NAC	.....	.....	.....
...../NAC	.....	.....	.....
...../NAC	.....	.....	.....
		Handling fee	$3.00
		Total	.....

U.S. DEPARTMENT OF COMMERCE
National Technical Information Service
Springfield, VA 22161

NTIS ORDER FORM

Use this form ONLY to order reports designated as available from NTIS.

TELEPHONE ORDERS (703) 487-4650 FAX (Telecopier) (703) 321-8547 TELEX 89-9405

For Subscription Questions
(703) 487-4630

For Tracing an Order
(703) 487-4660

Editorial Questions
(703) 487-4805

Postage:
NTIS uses First Class Delivery, or equivalent service, on all shipping. For information about one day RUSH ordering, call (800) 336-4700 or (703) 487-4700.

NTIS PRICE SCHEDULE *

This schedule converts into actual prices the price codes cited in those Tech Notes having a report available from NTIS.

Microfiche	
A01	$6.95
Paper copy	
A02	10.95
A03	13.95
A04 through A05	15.95
A06 through A09	21.95
A10 through A13	28.95
A14 through A17	36.95
A18 through A21	42.95
A22 through A25	49.95
A99	Call for price

These prices are for customers in United States, Canada, and Mexico. Other addresses should write for the price listing, number PR-360-4.

Prices effective January 1, 1989

† Billing Service: There is a $7.50 charge for this service. It is restricted to customers in the United States, Canada, and Mexico. A late payment charge will be applied to all billings more than 30 days overdue.

If your address lable on this Tech Notes is NOT correct, call the NTIS Subscriptions Department on (703) 487-4630.

1 ADDRESS INFORMATION

Last Name .....

Title .....

Company/Organization .....

Address .....

.....

City/State/ZIP .....

Telephone Number .....

2 METHOD OF PAYMENT

☐ Charge my NTIS Deposit Account .... – .....

☐ Check/Money order enclosed payable to NTIS for $ .....

☐ Please bill **ADD $7.50 per order** (see below for restrictions)†

Purchase order number .....

Charge my ☐ American Express ☐ VISA ☐ MasterCard

Account Number. ..... Exp. .....

Signature .....
(Required to validate order)

3 ORDER SELECTION (Use only for reports stated as available from NTIS)

NTIS Order Number	*Price**	*Quantity*	*Total Price*
/NAC			
/NAC			
/NAC			
/NAC			
/NAC			
Handling fee	$3.00		
Total			

- Agriculture & Food
- Computers
- Electrotechnology
- Energy
- Engineering
- Environmental Science & Technology
- Manufacturing, Machinery, & Tools
- Materials
- Medicine & Biology
- Natural Resources Technology & Engineering
- Physical Sciences
- Transportation & Components

Route To:

PENN STATE UNIVERSITY LIBRARIES
A000072010129

PARTMENT OF COMMERCE
l Technical Information Service
l, Va. 22161

BUSINESS
Private Use, $300

AN EQUAL OPPORTUNITY EMPLOYER

BULK RATE
POSTAGE & FEES PAID
NTIS
Permit No. G-292